SUBSTRATE-COMPETITIVE INHIBITORS OF C-SRC KINASE

by

Meghan Elizabeth Breen

A dissertation submitted in partial fulfillment
of the requirements for the degree of
Doctor of Philosophy
(Medicinal Chemistry)
in the University of Michigan
2014

Doctoral Committee:

Assistant Professor Matthew B. Soellner, Chair
Professor George A. Garcia
Professor Anna K. Mapp
Professor Henry I. Mosberg

© Meghan Elizabeth Breen 2014

DEDICATION

To Mom, Dad, and Sarah

ACKNOWLEDGEMENTS

First and foremost, I would like to thank my advisor Prof. Matthew Soellner for his guidance over the past six years. I have grown so much as a scientist under your mentorship, and I am truly grateful. I would also like to thank my dissertation committee members Profs. George Garcia, Anna Mapp, and Hank Mosberg for their helpful discussions and suggestions as I progressed through my projects. Thanks also to Profs. Sylvie Garneau-Tsodikova and Garry Dotson for previously serving on my committee. I am also thankful for teaching mentorship from Dr. Mustapha Beleh.

Thanks also to all the members of the Soellner lab I have overlapped with: Christel Fox, Michael Steffy, Dr. Sonali Kurup, Dr. Peter Barker, Dr. Steven Bremmer, Dr. Kristoffer Brandvold, Dr. Shana Santos, Sameer Phadke, Frank Kwarcinski, Kristin Ko, Taylor Johnson, Michael Agius, Eric Lachacz, and Omar Beleh. I've had a great time working with and learning from all of you. I would especially like to acknowledge Mike S., Chris, Sonali, Kris, Kristin, Frank, and Eric, all of whom made contributions to the work presented here.

I am also thankful for all of the fantastic people I've met in the Department of Medicinal Chemistry. I was very fortunate to matriculate with a wonderful cohort of students, especially Drs. Fardohkt Abulwerdi, Solymar Negretti, and Kamali Sripathi who have been a great support system over our time here. Thank you also to Drs. Jessica Anand, Jessica Bell, and Beth Kuspitz for your advice before all of the major grad school milestones and always convincing me that it would all be fine. Finally, thank you to Lizzie Rowland-Fisher for your friendship and support, especially during this stressful final year.

I would also like to acknowledge the people and organizations that provided financial support during my graduate studies. The work described here was funded by NIH grant R01GM088546, the University of Michigan College of Pharmacy, and a

Rackham graduate student research grant. I am also grateful for financial support provided by the University of Michigan Pharmacological Sciences Training Program, the American Foundation for Pharmaceutical Education, a Sheila B. Cresswell Fellowship, and a Lyons Fellowship.

I never would have ended up at the University of Michigan without the support of many friends and mentors along the way. Thank you to Mr. Kenneth Gattung for being a great teacher and first sparking my interest in chemistry back in high school. At Eastern Illinois University, I was very fortunate to find wonderful mentors in Profs. Kraig Wheeler, Edward Treadwell, and Bonnie Irwin. Your guidance helped me to grow as both a scientist and a person. Thanks also to the amazing friends I made at EIU, especially Michelle Bruggeman, Kim Cagle, Sarah Cain, Sarah Frevert, and Amanda Steber, for your continued friendship and support.

Finally, I am so very grateful for the unwavering support of my wonderful family throughout this journey. Thank you Mom, Dad, and Sarah for never doubting that I could do this. Thanks also to my extended family and the people who might as well be family: the Breens, the Elliotts, the O'Briens, and Jennifer McCollum. Thank you for your love and encouragement. I'm so lucky that you were always interested in knowing what I was doing in the lab, and that you always insisted that I give you "the full explanation, not the dumbed down one" of my research. I love you all, and I truly can't thank you enough.

TABLE OF CONTENTS

DEDICATION ii

ACKNOWLEDGEMENTS iii

LIST OF TABLES viii

LIST OF FIGURES ix

LIST OF SCHEMES xi

LIST OF APPENDICES xiv

ABSTRACT xvi

CHAPTER

I. Discovery of Small Molecule Substrate-Competitive Inhibitors of Protein Kinases: Screening Approaches and Challenges 1

Abstract 1

Introduction 1

Activity Based Biochemical Screens 6

Competitive Binding Screens 9

NMR Screening 14

Conclusions 18

References 19

II. Peptidic Inhibitors of c-Src Kinase for Pharmacophore Identification 24

Abstract 24

Introduction 24

Evaluation of Peptides with Natural Amino Acid Pharmacophores 27

Evaluation of Peptides with Substituted Phenylalanine Pharmacophores 30

Evaluation of Literature Peptides 34

Conclusions 37

Materials and Methods 38

References 45

III. A Substrate Activity Screening Method for Tyrosine Kinases 48

Abstract 48

Introduction 48

Step 1: Identification of Small Molecule Substrates 50

Step 2: Conversion of Substrates to Inhibitors 54

Step 3: Inhibitor Optimization 56

Binding Mode Analysis 59

In Cellulo Evaluation 62

Synergy Studies 64

Conclusions 65

Materials and Methods 66

References 82

IV. Progress Towards Non-Peptidic Bisubstrate Kinase Inhibitors 87

Abstract 87

Introduction 87

Evaluation of First Generation Inhibitors 91

Evaluation of Second Generation Inhibitors 95

Conclusions 96

Materials and Methods 98

References 108

V. Conclusions 110

Abstract 110

Discovery of Substrate-Competitive Kinase Inhibitors 110

Peptidic Inhibitors of c-Src Kinase for Pharmacophore Identification 111

Substrate Activity Screening for Protein Tyrosine Kinases 113

Progress Towards Nonpeptidic Bisubstrate Kinase Inhibitors 114

Conclusions 115

References 117

APPENDICES 119

LIST OF TABLES

TABLE

2.1	Peptides with the general structure Ac-AIXAA-NH_2, where X is a natural amino acid, were evaluated for c-Src and c-Abl inhibition using the pyrene assay.	29
2.2	Peptides with the general structure Ac-AIXAA-NH_2, where X is a substituted phenylalanine derivative, were evaluated for c-Src and c-Abl inhibition using the pyrene assay.	31
2.3	Comparison of reported IC_{50} values for peptidic inhibitors of c-Src with values obtained using the pyrene assay.	36
3.1	Comparison of IC_{50} values obtained under standard conditions to values obtained under low ATP conditions or high substrate conditions.	55
3.2	Inhibition of Src family kinases by inhibitor 3.12 and PP2 was determined using the pyrene fluorescence assay. The selectivity for c-Src over each kinase is given in parentheses.	59
B.1	Evaluation of a library of small molecule phenols as substrates of c-Src.	158
B.2	Kinetic parameters for phenolic substrates of c-Src. Select compounds were also evaluated as substrates of Hck and c-Abl.	171

LIST OF FIGURES

FIGURE

1.1	Crystal structure of the catalytic domain of Lck (PDB 1QPC). Highlighted are the N-terminal lobe (bright green), the C-terminal lobe (bright blue), the hinge region (orange), the phosphate binding loop (olive), the activation loop (dark blue), and the gatekeeper residue (red).	2
1.2	Comparison of the ATP and substrate binding sites for (A) the tyrosine kinase IRK (PDB 1IR3) and (B) the serine/threonine kinase Akt (PBD 1O6K). ATP-competitive ligands are shown in green and substrate-competitive ligands are shown in orange.	4
1.3	Crystal structure of IRK bound to an ATP analogue (green) and a peptidic substrate mimic (orange), with residues within 20 Å of the ATP binding site highlighted in cyan (PDB 1IR3).	15
3.1	Analytical HPLC traces confirmed phosphorylation of a small molecule substrate by Src. A) Trace of substrate 3.2, (B) trace of a known standard of the corresponding phosphate of substrate 3.2, and (C) trace of the reaction after incubating 3.2 with c-Src and ATP.	52
3.2	Lineweaver-Burk analysis of inhibitor 3.12. Initial velocity was measured using the pyrene fluorescence assay in the presence of variable concentrations of 3.12. A) Double reciprocal plot of initial velocity vs. "substrate 3" concentration. B) Double reciprocal plot of initial velocity vs. ATP concentration.	60
3.3	Induced fit docking of inhibitor 3.12 with c-Src. A) Inhibitor 3.12 binds in the substrate binding site. B) The model predicts a cation-π interaction between Arg388 and 3.12.	61
3.4	Activation of (A) c-Src dependent and (B) c-Src independent signaling pathways in the presence of 3.12 and PP2 was evaluated in SK-BR-3 cells using an AlphaScreen assay.	63

3.5 Synergy studies of combinations of substrate-competitive inhibitor 3.12 with ATP-competitive inhibitors PP2 or PP5. IC_{35} concentrations were dosed individually and in combination. The red line indicates the predicted additivity of 3.12 + PP2. 64

LIST OF SCHEMES

SCHEME

1.1	Biased activity assays use high concentrations of ATP to encourage formation of the ATP-bound state. This discourages the binding of weak to moderate ATP-competitive inhibitors.	7
1.2	Competitive binding assays can be used to identify substrate-competitive inhibitors via net displacement of a substrate-competitive probe. Substrate-noncompetitive ligands will not displace the probe.	10
1.3	In competitive binding assays using bisubstrate probes, both substrate-competitive and ATP-competitive ligands will displace the probe.	11
1.4	Bisubstrate probes for competitive binding assays.	12
1.5	Spin-labeled ATP-competitive probes for NMR screening.	16
2.1	A nucleoside disphosphate kinase (NDPK) coupled assay was used for the analysis of kinase substrates.	26
2.2	A library of peptides was prepared based on the c-Src and c-Abl substrate peptide 2.1. The library had the general structure Ac-AIXAA-NH_2, where X was natural amino acids and substituted phenylalanine derivatives.	27
2.3	A continuous fluorescence-based assay utilizing a fluorescent peptide substrate reporter (Ac-EEEIYGE(Dap-pyrene)EA-NH_2) was used to evaluate c-Src and c-Abl inhibition.	28
2.4	Structures of reported potent peptidic inhibitors of c-Src (2.48-2.50) and two analogues (2.51 and 2.52).	35
2.5	Fmoc-based solid phase peptide synthesis.	39
3.1	Proposed SAS methodology for protein tyrosine kinases.	49

3.2	The ADP-Glo assay kit was used to evaluate small molecules as potential kinase substrates. Image adapted from Promega.	50
3.3	Small molecule substrates of c-Src kinase identified using the ADP-Glo sassay. The compounds were also evaluated as substrates of Hck and c-Abl. None of the compounds were found to be substrates for c-Abl (K_M > 1 mM).	51
3.4	Conversion of a small molecule kinase substrate scaffold into kinase inhibitors. Inhibitors were evaluated against c-Src, Hck, and c-Abl using the pyrene fluorescence assay.	54
3.5	Optimized substrate-competitive inhibitors of c-Src kinase. Compounds were evaluated against c-Src, Hck, and c-Abl using the pyrene fluorescence assay.	57
3.6	ATP-competitive inhibitors of c-Src.	58
3.7	Synthesis of compound 3.7.	67
3.8	Synthesis of compound 3.8.	68
3.9	Synthesis of compound 3.9.	70
3.10	Synthesis of compound 3.10.	70
3.11	Synthesis of compound 3.11.	71
3.12	Synthesis of compound 3.12.	72
4.1	A peptidic bisubstrate inhibitor of c-Src.	89
4.2	A modular approach for the preparation of nonpeptidic bisubstrate inhibitors.	90
4.3	Nonpeptidic bisubstrate inhibitors containing a substrate scaffold identified through SAS.	91
4.4	Nonpeptidic bisubstrate inhibitors containing an optimized substrate scaffold.	92
4.5	Analogues of the nonpeptidic bisubstrate inhibitor 4.9 containing the unoptimized diphenylamine scaffold and a quinoline scaffold identified through SAS.	93

4.6 The nonpeptidic bisubstrate inhibitor 4.9 separated into its ATP-competitive (4.13) and substrate-competitive (4.14) components. 94

4.7 Nonpeptidic bisubstrate inhibitors which retain a hydroxyl group in the substrate scaffold. 96

4.8 Synthesis of compound 4.19. 98

4.9 Synthesis of substrate scaffolds attached to an azide linker. 100

4.10 Synthesis of phenol substrates attached to azido linkers. 102

4.11 Synthesis of 1,4-disubstituted-1,2,3-triazoles. 103

4.12 Synthesis of 1,5-disubstituted-1,2,3-triazoles. 105

LIST OF APPENDICES

APPENDIX

A. Analytical Data for Chapter II 119

Analytical Data for Determination of K_i for Peptidic Inhibitors 120

Analytical Data for Determination of Peptide Substrate "Substrate 3" K_M 144

B. Analytical Data and Supplemental Information for Chapter III 145

Spectral Data for Compounds 3.7-3.12 146

Gas Chromatography Traces of Compounds 3.7-3.12 155

Analytical Data and Supplemental Information for Biochemical Substrate Identification Assays 158

Analytical Data and Supplemental Information for Determination of K_M for Phenolic Substrates 171

Analytical Data for Determination of K_i for Inhibitors 177

Analytical Data for Determination of Peptide Substrate "Substrate 3" K_M 188

Analytical Data for Determination of ATP K_M 189

Analytical Data for Determination of Inhibitor IC_{50} at Variable ATP and Peptide Substrate Concentration 190

Analytical Data for Lineweaver-Burk Analysis of Compound 3.12 192

Analytical Data for Combination Studies of Compound 3.12 with PP2 and PP5 193

Analytical Data for Inhibition of c-Src Autophosphorylation 194

Analytical Data for Cancer Cell Growth Inhibition Assays 194

C. Analytical Data for Chapter IV 195

Spectral Data (^{1}H NMR) for Compounds 4.2-4.34 196

Analytical Data for Determination of IC_{50} for Bisubstrate Inhibitors 222

Analytical Data for Determination of IC_{50} for Inhibitors Under High "Substrate 3" Conditions 224

ABSTRACT

Protein kinases are key mediators of cellular signal transduction and are heavily studied drug targets. Greater than 99% of reported kinase inhibitors act through the same mechanism of competing for binding to the highly conserved ATP pocket. Although ATP-competitive inhibitors have experienced clinical success, the disadvantages associated with them has resulted in significant interest in the discovery of inhibitors that target regions outside of the ATP binding pocket, such as the protein substrate binding site. However, the identification of compounds that can inhibit the kinase-substrate protein-protein interaction has proven challenging, especially for small molecules. To address this problem, we developed screening methodology that can identify small molecule substrate-competitive inhibitors using the tyrosine kinase c-Src as a model system.

Studies began with the preparation of a library of peptidic inhibitors to evaluate tyrosine pharmacophores and generate probes for a competitive binding assay. No peptides with potency suitable for probe development were identified, however important structure activity relationships were gleaned for tyrosine pharmacophores. In a second study, a substrate activity screening (SAS) method for tyrosine kinases was developed. Using an assay that monitors ADP production, the first small molecule substrates for any protein kinase were identified. By applying knowledge gained from the previous pharmacophore study, a small molecule substrate (K_M = 122 μM) was then successfully converted into a substrate-competitive, ATP-noncompetitive inhibitor (K_i = 16 μM). The lead inhibitor has improved selectivity compared to an ATP-competitive inhibitor commonly used as a c-Src probe, and has cellular efficacy similar to FDA approved ATP-competitive kinase inhibitors (SK-BR-3 GI_{50} = 14 μM). This SAS method is the only general screening technique for the selective identification of substrate-competitive kinase inhibitors and should be applicable to any tyrosine kinase of interest. In a final

study, substrates identified through SAS were applied to the design of nonpeptidic bisubstrate inhibitors. As a whole, the work presented has demonstrated the importance of retaining hydrogen bonding interactions made by the substrate hydroxyl group in order to generate potent inhibitors. Results from this work should advance the discovery of new small molecule substrate-competitive inhibitors through both screening and rational design.

CHAPTER I

Discovery of Small Molecule Substrate-Competitive Inhibitors of Protein Kinases: Screening Approaches and Challenges

Abstract

Protein kinases are important mediators of cellular communication and attractive drug targets for many diseases. Although success has been achieved with developing ATP-competitive kinase inhibitors, the disadvantages of ATP-competitive inhibitors has led to an increased interest in targeting sites outside of the ATP binding pocket. Kinase inhibitors with substrate-competitive, ATP-noncompetitive binding modes are promising due to the possibility of increased selectivity and better agreement between biochemical and *in vivo* potency. However, the difficulty of identifying these types of inhibitors using high throughput screens has resulted in significantly fewer small molecule substrate-competitive inhibitors being reported. This review examines reported screening approaches that can identify small molecule substrate-competitive kinase inhibitors, including biased activity assays, competitive binding assays, and NMR screening with ATP-competitive probes, and discusses the challenges when utilizing these methods.

Introduction

Protein kinases catalyze the transfer of the gamma-phosphate of ATP to a serine, threonine, or tyrosine residue of a substrate protein or peptide. The human kinome includes 518 kinases and accounts for nearly 2% of the human genome.[1] It is estimated that collectively the 518 human kinases can phosphorylate up to one-third of intracellular proteins to generate up to 20,000 distinct phosphoproteins.[2] Phosphorylation of a substrate protein by a protein kinase is an important signal transduction mechanism within the cell and can yield diverse responses, including activation or deactivation of an enzyme, recruitment of adaptor proteins, and changes in cellular localization.[3-6] Through

their involvement in many critical signaling pathways, kinases control processes such as cell growth, apoptosis, motility, angiogenesis, metabolism, and inflammation.[7-12]

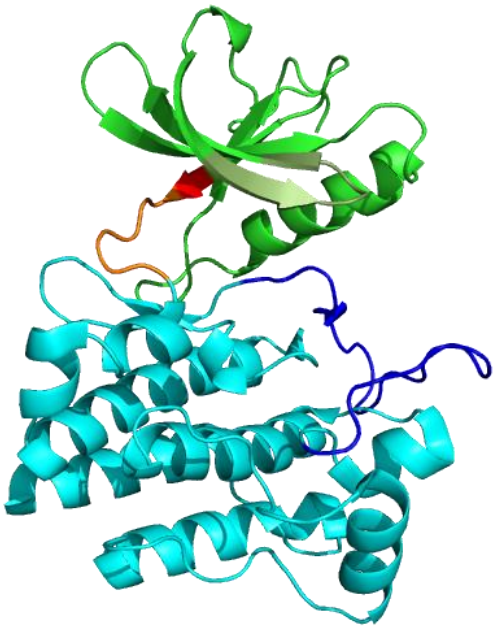

Figure 1.1. Crystal structure of the catalytic domain of Lck (PDB 1QPC). Highlighted are the N-terminal lobe (bright green), the C-terminal lobe (bright blue), the hinge region (orange), the phosphate binding loop (olive), the activation loop (dark blue), and the gatekeeper residue (red).

Illustrated in **Figure 1.1** is the conserved structure of the kinase catalytic domain which consists of N-terminal and C-terminal lobes connected by a short loop termed the hinge region.[13-14] The smaller N-terminal lobe is composed of five anti-parallel β strands and one α helix, and the larger C-terminal lobe is composed of eight α helices and four β strands. The region between the N-terminal and C-terminal lobes and the hinge region forms a deep hydrophobic cleft that contains the ATP-binding site. ATP makes several key hydrogen bonds to the backbone of the hinge region which facilitate binding within the pocket. Additionally, the phosphate binding loop forms the ceiling of the ATP binding site and clamps down over the phosphate groups to orient them for catalysis. The protein substrate binding site is located within the C-terminal lobe. Also located in the C-

terminal lobe is the activation loop. Many kinases are phosphorylated within this loop, which then undergoes a conformational change to activate the kinase and allow access to the substrate binding site. In addition to the catalytic domain, kinases may contain other regulatory domains which vary across the kinome and have diverse roles including modulating catalytic activity, recruiting substrates, controlling localization, and serving as scaffolding sites for other proteins.[15-17]

Due to the key roles of kinases in critical signaling pathways, the dysregulation of kinase activity has been linked to over 400 diseases including many cancers, autoimmune disorders, inflammation, and diabetes.[18-20] As a result, kinases are highly studied drug targets and constitute the largest drug target class after GPCRs.[21] The first kinase inhibitor received FDA approval in 2001, and currently over 20 kinase inhibitors have been approved, mostly for use in oncology. Although there are two binding sites within the catalytic domain of kinases, greater than 99% of reported kinase inhibitors, including all of the currently approved kinase-targeting drugs for oncology, inhibit kinase activity via competition for the ATP binding site.[22] The heavy focus on ATP-competitive inhibitors can be largely attributed to the relative ease with which these inhibitors were identified, initially through the design of adenosine analogues and later using techniques such as high throughput screening (HTS) and structure based drug design. The success of these approaches is directly related to the well-defined structure of the ATP binding pocket, which makes it well-suited for binding small molecules.[13] Conversely, the substrate binding site is a shallow, open surface in order to facilitate the kinase-substrate protein-protein interaction.[23] The differences between these two binding sites are demonstrated in **Figure 1.2**, which shows the structures of the tyrosine kinase IRK and the serine/threonine kinase Akt crystalized with ATP mimics bound to the ATP binding pocket and peptidic ligands bound to the substrate site. In both structures, the ATP mimic nestles deeply into the ATP cleft; in contrast, the peptide substrate mimic sits in a much shallower, solvent exposed cleft.

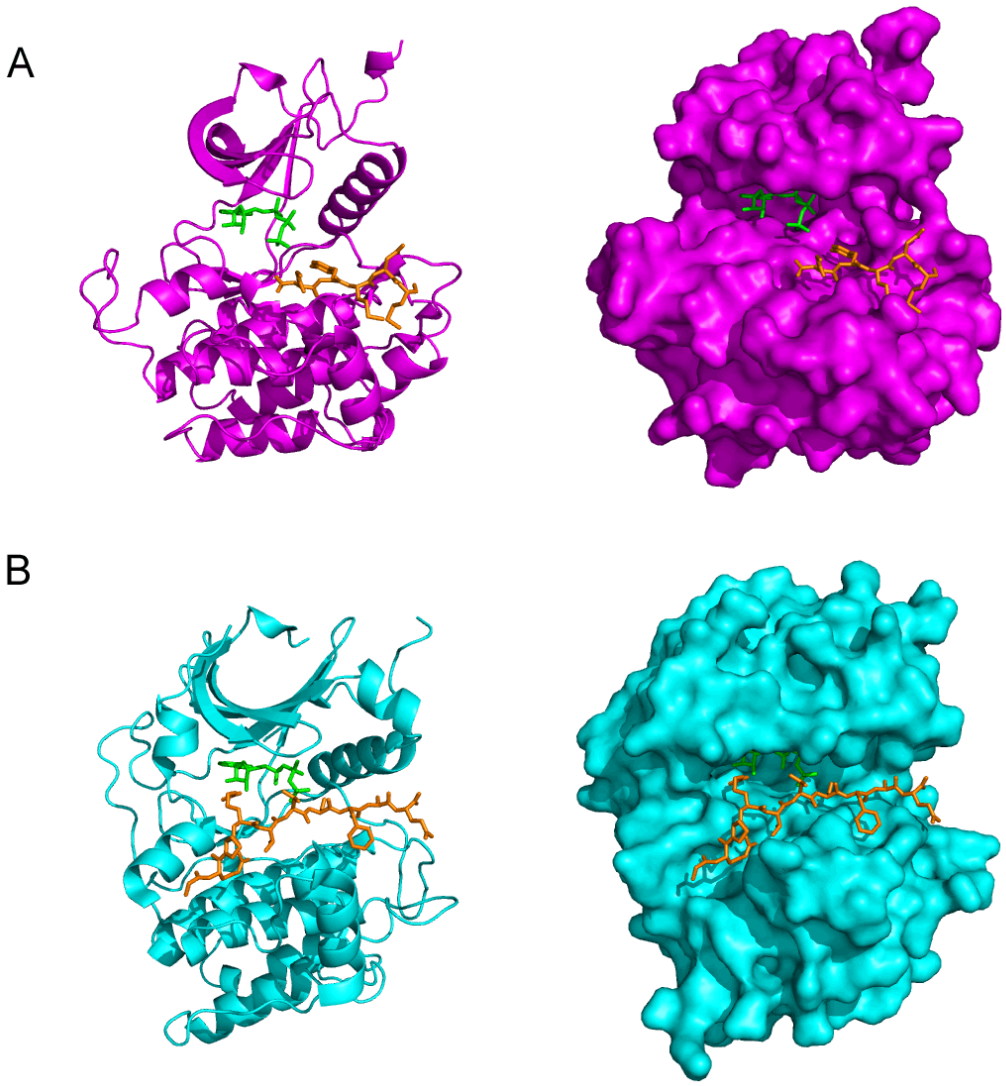

Figure 1.2. Comparison of the ATP and substrate binding sites for (A) the tyrosine kinase IRK (PDB 1IR3) and (B) the serine/threonine kinase Akt (PBD 1O6K). ATP-competitive ligands are shown in green and substrate-competitive ligands are shown in orange.

Although many ATP-competitive kinase inhibitors have been described and several have proved successful in the clinic, there are drawbacks to these inhibitors that should be considered. First, the kinase ATP pocket is highly conserved across the kinome leading to poor selectivity of most ATP-competitive kinase inhibitors.[24-26] Off-target binding can result in additional toxicity of these compounds in the clinic and also prevents the use of most ATP-competitive inhibitors as biological probes. In addition to

selectivity concerns, ATP-competitive inhibitors must contend with intracellular ATP levels that are typically in the millimolar range, while the ATP K_M values for most kinases are in the low micromolar range. As a result of this, there is usually poor agreement between biochemical and cellular potency for ATP-competitive inhibitors, and a high affinity compound (typically nanomolar to picomolar) is required in order to see activity *in vivo*.[24, 27] Finally, the rapid and common development of ATP pocket mutations, such as mutations of the "gatekeeper" residue that regulates access to a back hydrophobic pocket within the ATP site, confer resistance to ATP-competitive inhibitors.[28-29] Due to these considerations, increased attention has been placed on developing inhibitors that target the protein substrate binding site. Unlike the ATP binding site, the substrate binding site is less conserved between different kinases, thus offering the chance for improved selectivity. Additionally, because kinase substrates are typically present at or below their K_M value *in vivo*, a high biochemical affinity is not always required to yield *in vivo* activity.[30]

Despite the potential benefits and the considerable effort put towards identifying substrate-competitive inhibitors, thus far their development has seen only limited success. The majority of reported substrate-competitive inhibitors are peptides which were either rationally designed from peptidic substrates or discovered from screens of combinatorial libraries generated using one-bead-one-compound techniques or phage display.[31-33] Due to their peptidic nature, these inhibitors typically have poor cellular permeability and stability, and these features make them undesirable for use as biological probes or therapeutics. While the development of small molecule substrate-competitive inhibitors would address the problems associated with the peptidic inhibitors, the discovery of such inhibitors has proved incredibly challenging. As discussed, traditional HTS approaches have rarely yielded substrate-competitive inhibitors. This is a consequence of the lack of a well-defined pocket in the substrate site, as well as the fact that HTS libraries are often highly biased towards small, flat, heterocyclic molecules that are more likely to function as ATP-mimics than as peptidomimetics.[34]

In the last decade, reports of small molecule ATP-noncompetitive inhibitors (both substrate-competitive inhibitors and allosteric inhibitors) have increased. These inhibitors have been identified using a wide variety of methods ranging from high

throughput screens to rational design and virtual screening. Although approaches utilizing structural data have been successful in identifying substrate-competitive inhibitors for several kinases, these methods are not readily applicable to any target of interest. Currently less than 15 kinases have been crystalized with a ligand bound to the substrate site, and over 300 kinases have no structural data available.[35] As new drug targets continue to be discovered from the greater than 50% of the kinome that is largely uncharacterized, screening methods that do not require structural data and can be widely utilized will continue to be important drug discovery tools.[36-37] This review will survey screening approaches that can be applied across the kinome for the discovery of substrate-competitive inhibitors, with a focus on the identification of small molecule inhibitors. The benefits and challenges inherent to each of these methods will also be discussed.

Activity Based Biochemical Screens

Activity based assays have long been the first choice for kinase inhibitor HTS.[38] As discussed, these approaches have traditionally been more likely to discover ATP competitive inhibitors, and the identification of substrate-competitive inhibitors from an activity based HTS was usually serendipitous. However, several groups have recently reported activity-based screens in which the assay conditions were modified to promote the identification of ATP-noncompetitive inhibitors. This was generally accomplished by encouraging formation of the enzyme-ATP complex, which was predicted to favor the binding of ATP-noncompetitive ligands and discourage the binding of weak and modest ATP-competitive inhibitors (**Scheme 1.1**). While this approach aims to reduce the number of ATP-competitive hits, it can also bias towards the identification of highly potent ATP-competitive inhibitors.

Liu and colleagues reported a biased activity assay for the identification of ATP-noncompetitive inhibitors of LRRK2.[39] Knowledge of the kinetic mechanism and the kinetic parameters for LRRK2, coupled with mechanistic simulations, enabled determination of initial concentrations of ATP and PLK-peptide substrate which would bias towards formation of the enzyme-ATP complex. A time resolved Forster resonance energy transfer (TR-FRET) assay performed under these conditions was used quantify

phosphorylation of the PLK-peptide substrate in the presence of potential inhibitors. From a screen of 63,400 compounds, 21 hits with IC_{50} <10 μM were identified. The lead compound from the screen is an allosteric inhibitor, as analysis of its effects on the ATP and substrate kinetic parameters suggested that it is noncompetitive with both ATP and peptide substrate.

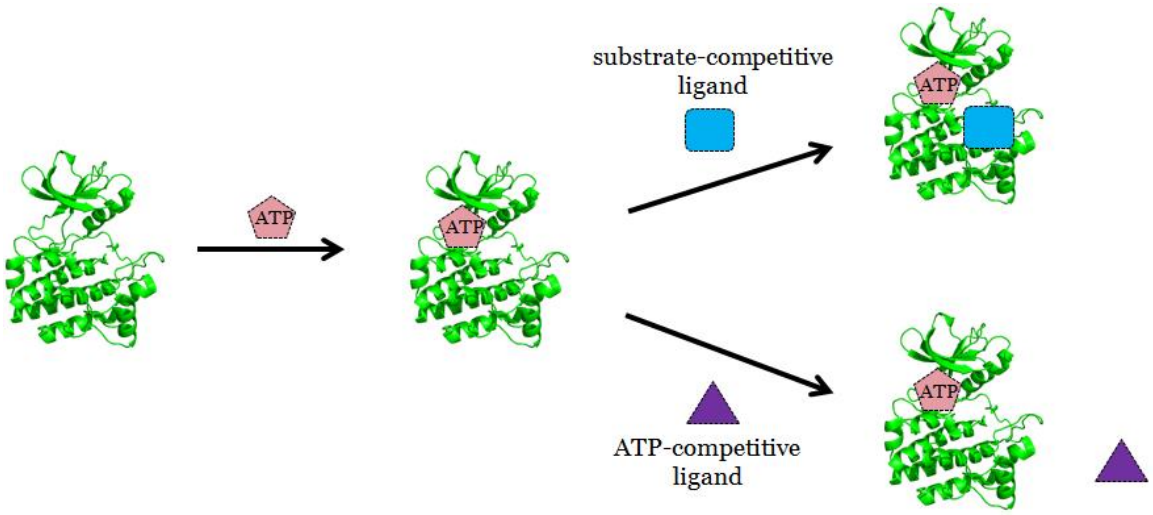

Scheme 1.1. Biased activity assays use high concentrations of ATP to encourage formation of the ATP-bound state. This discourages the binding of weak to moderate ATP-competitive inhibitors.

A similar approach was taken by Lo and coworkers to screen for ATP-noncompetitive inhibitors of CDK4.[40] It was predicted that increasing the concentration of ATP in the assay to 12-fold above its apparent K_M value would bias towards the enzyme-ATP complex. As mentioned earlier, because the assay format also would allow for highly potent ATP-competitive inhibitors to be identified, the IC_{50} values for initial hits were determined at ATP concentrations equal to K_M and 12-fold greater than K_M. From a screen of 250,000 compounds, three compounds were identified with potencies that were relatively insensitive to ATP concentration, suggesting that they are ATP-noncompetitive inhibitors. Additional analysis of the most potent hit (IC_{50} = 2.4 μM) in the presence of increasing concentrations of substrate demonstrated that potency was also insensitive to substrate concentration. Surprisingly, although the lead compound appears

to be an allosteric inhibitor of CDK4, it was found to be an ATP-competitive of the tyrosine kinase Lck.

Our lab has also modified the conditions of an activity-based assay to favor the discovery of ATP-noncompetitive inhibitors of c-Src by increasing the concentration of ATP.[41] In one screen, the ATP concentration was increased to 10-fold above its K_M value and fragment libraries were screened. Although several hits were identified, the lead compound was found to be an ATP-competitive inhibitor. We then tried to further bias the assay conditions by increasing the ATP concentration to 50-fold higher than K_M and screening against the c-Src T338M gatekeeper mutant. Because gatekeeper mutations are known to cause resistance to ATP-competitive inhibitors, we hypothesized that this would also favor the discovery of ATP-noncompetitive inhibitors. Several hits were identified from this screen, and Lineweaver-Burk analysis suggests that the lead inhibitor is ATP-noncompetitive and substrate-noncompetitive.

These examples highlight that although activity based assays can be biased towards identifying ATP-noncompetitive inhibitors, the discovery of substrate-competitive inhibitors from such assays remains elusive. Assay conditions that favor the identification of substrate-competitive inhibitors will also favor the identification of allosteric inhibitors that bind at neither the ATP nor the substrate sites. Additionally, while these modifications discourage ligands with weak to moderate affinity for the ATP site, they can also promote the identification of potent ATP-competitive inhibitors. As a result of this, further analysis of each hit will be required in order to determine the binding mode. Overall, it appears that assays monitoring enzyme inhibition will continue to be a poor choice for the identification of substrate-competitive kinase inhibitors.

In contrast to assays which monitor inhibition of enzymatic activity, the Ellman lab has developed a screening approach termed substrate activity screening (SAS) that instead identifies molecules that serve as substrates of an enzyme.[42-47] The identified substrates can then be optimized and later converted into inhibitors by replacement of the reactive functionality. A benefit of the SAS method is that because it identifies substrates of an enzyme the hits which are converted into inhibitors should inherently be substrate-competitive inhibitors. The Ellman lab has previously described SAS methodology for several proteases and phosphatases, and a group from Novartis recently reported the

application of SAS to the discovery of peptidic substrate-competitive inhibitors of c-Src.[48] In the SAS method for kinases, optimized peptidic substrates of c-Src were identified, and then the reactive tyrosine residue was modified to prevent the phosphotransfer reaction, thereby converting the substrate into an inhibitor. The described SAS method is similar to the approach that was previously applied to the discovery of peptidic substrate-competitive inhibitors, in which the phosphorylatable residue in a known peptidic substrate was replaced to generate a peptidic inhibitor. As it currently stands, the SAS method will not be widely useful for the development of substrate-competitive kinase inhibitors since the peptidic nature of the inhibitors will limit their use as a biological probes and potential therapeutics; however, the development of a non-peptidic SAS method for kinases would enable the identification of small molecule substrate-competitive inhibitors.

Competitive Binding Screens

Although activity-based screens generally have not identified substrate-competitive kinase inhibitors, binding assays appear better poised for success. Binding assays can be used to either directly detect binding of a ligand to the target, or to indirectly detect binding through competitive displacement of a probe. Direct binding assays using surface plasmon resonanace (SPR) and affinity selection mass spectrometry (ASMS) have been used to discover ATP-noncompetitive ligands for kinase targets; however, these methods are non-biased and ligands can bind to all exposed sites on the protein.[49-51] As such, these screens are similar to activity based screens in that they will be far more likely to identify ATP-competitive ligands, and extensive additional analysis is required to determine the binding mode of each hit. In contrast, using a competitive-binding assay will allow for identifying ligands that bind to a specific site on the target. A general scheme demonstrating how competitive binding assays can be used to identify substrate-competitive inhibitors is shown in **Scheme 1.2**. These assays rely on the net displacement of a probe to measure ligand binding, and therefore using a substrate-competitive probe should enable the exclusive identification of substrate-competitive inhibitors. The net displacement of the probe from the target can be evaluated by multiple methods, including fluorescence-based techniques such as fluorescence

polarization (FP) and Forster resonance energy transfer (FRET) and biophysical techniques such as SPR.

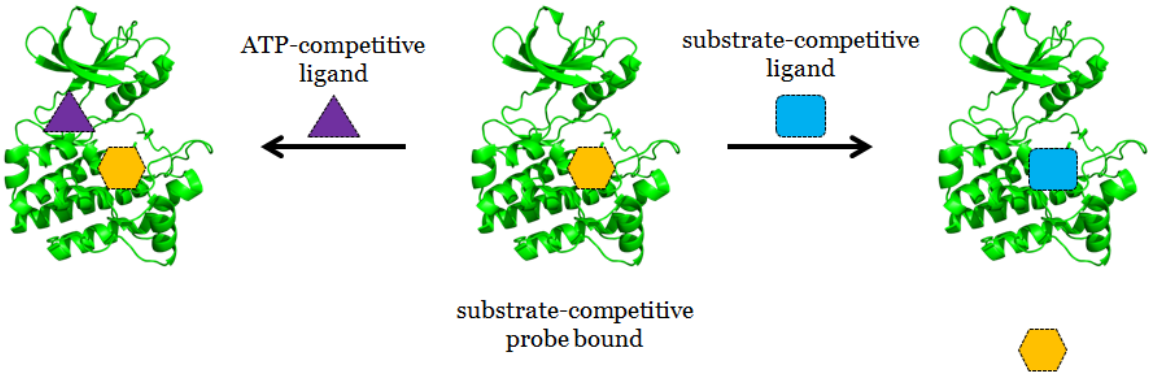

Scheme 1.2. Competitive binding assays can be used to identify substrate-competitive inhibitors via net displacement of a substrate-competitive probe. Substrate-noncompetitive ligands will not displace the probe.

Stebbins and colleagues have reported using a time resolved fluorescence (TRF) assay to screen a 30,000 member library for small molecule, substrate-competitive inhibitors of JNK.[52] This screen used a dissociation enhanced lanthanide fluoro-immuno assay (DELFIA) platform to evaluate compounds for their ability to disrupt the interaction between JNK and a peptidic probe based on JNK-interacting protein 1 (biotin-$(CH_2)_6$-KRPKRPTTLNLF, **1.1**). Probe **1.1** was immobilized via a streptavidin-biotin interaction, and dissociation of the GST-JNK and probe complex was evaluated using an anti-GST europium antibody. The lead compound identified from the screen was confirmed to inhibit JNK activity (IC_{50} = 280 nM), and Lineweaver-Burk analysis demonstrated that it is competitive with the JNK substrate ATF2. Further evidence that the lead inhibitor binds to the JIP1 interaction site was provided through modeling, mutagenesis, and NMR studies.

Interestingly, fluorescently labeled substrate peptide analogues that could be used in competitive binding assays to identify substrate-competitive inhibitors have been developed but were not used for this purpose. For example, Saldanha and coworkers used a substrate-competitive probe in a ligand-regulated competition (LiReC) screen to identify compounds that modulate the interactions between the catalytic and regulatory

domains of PKA, and Tsuganezawa and colleagues used substrate-competitive probes in a fluorescent correlation spectroscopy (FCS) assay to identify ATP-competitive inhibitors of Pim-1 that also make interactions with residues known to be important for substrate binding.[53-54] While these probes could be used in FP, FRET, or FCS screens for substrate-competitive inhibitors of PKA or Pim-1, this application has not been reported.

The limited development of competitive-binding screens using substrate-competitive probes, despite their promise for identifying exclusively substrate-competitive inhibitors, may be a direct result of the assay design requirements.[55] Ideally, the substrate-competitive probe used should have high affinity for the target in order to ensure that a high fraction of the probe is bound without requiring large quantities of enzyme. Most reported substrate-competitive ligands are peptides with modest affinity that do not fulfill this requirement. One way to address the modest potency of many substrate-competitive ligands is to develop bisubstrate ligands.[56] These compounds contain a substrate-competitive ligand (usually a peptide) linked to an ATP-competitive ligand. The bisubstrate compound usually has greatly increased potency relative to the peptide alone, which makes them more amenable for use as probes. As illustrated in **Scheme 1.3**, bisubstrate probes will be displaced by both substrate-competitive and ATP-competitive inhibitors. There have been several reports of the use of bisubstrate probes in the development of competitive-binding assays for kinase targets that can identify and characterize both ATP-competitive and substrate-competitive inhibitors (**Scheme 1.4**).

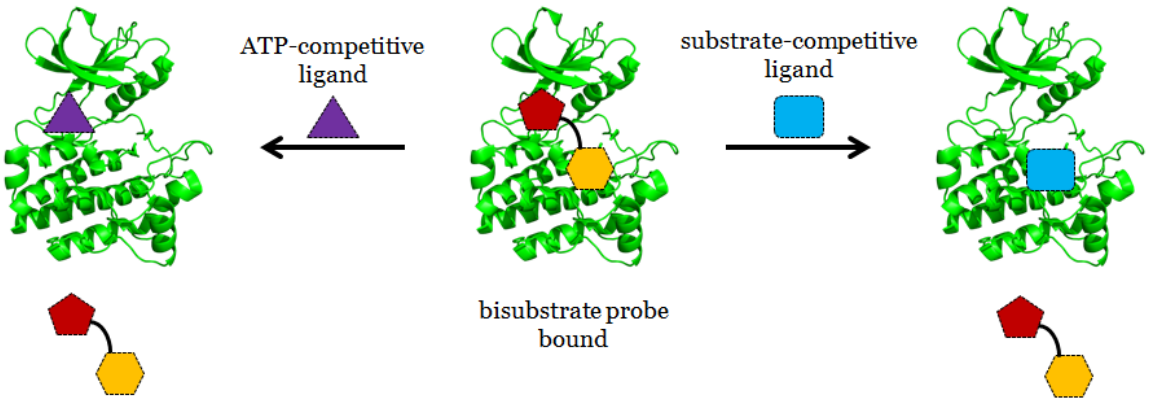

Scheme 1.3. In competitive binding assays using bisubstrate probes, both substrate-competitive and ATP-competitive ligands will displace the probe.

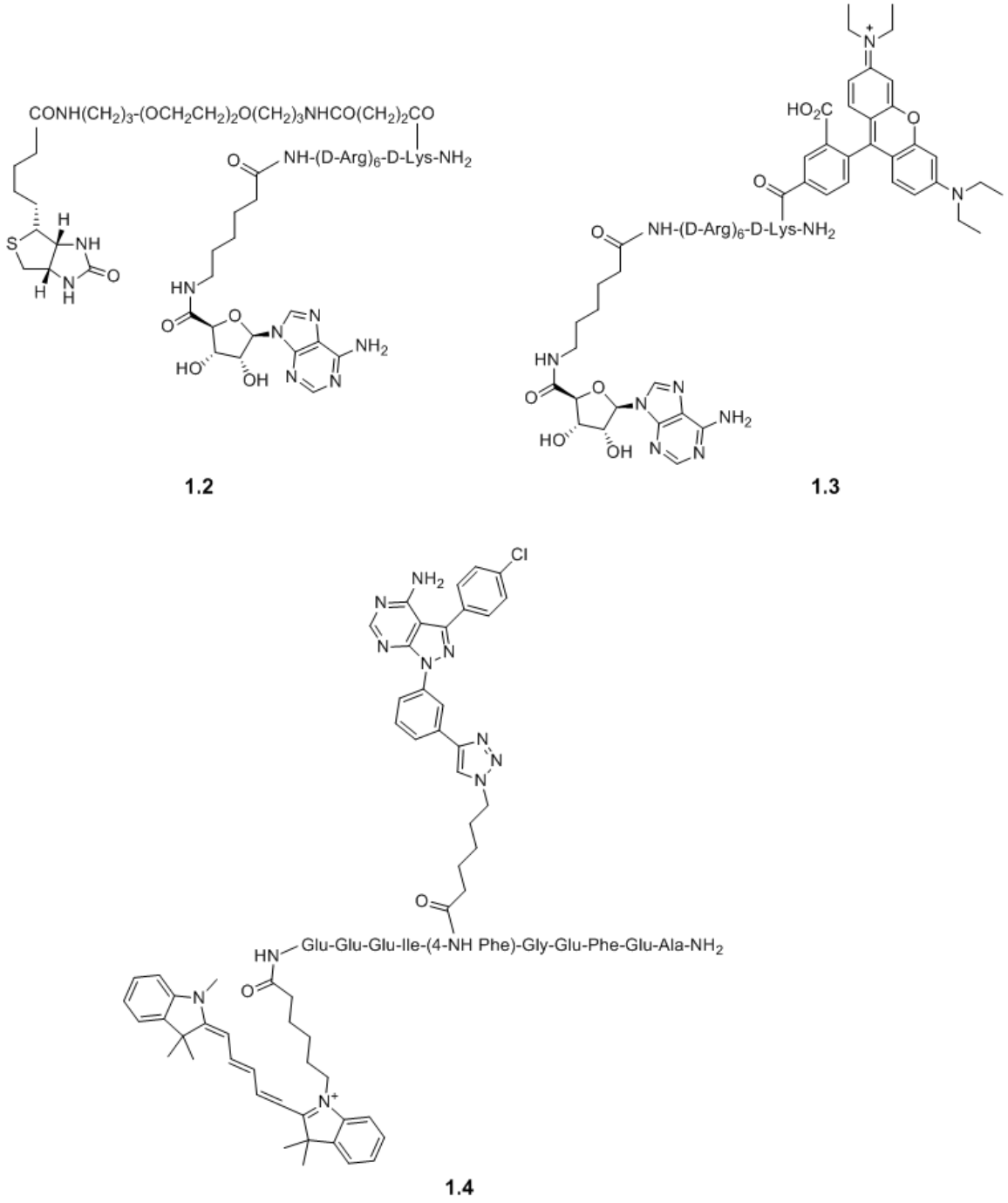

Scheme 1.4. Bisubstrate probes for competitive binding assays.

The Uri group has developed several bisubstrate inhibitors, termed ARCs, by linking adenosine to arginine rich peptides, and they have begun using these ARCs as probes to develop competitive binding assays. A SPR competitive-binding assay for the determination of the affinities of ATP-competitive and substrate-competitive ligands of

PKA was developed by immobilizing an ARC via a streptavidin-biotin complex.[57] The immobilized probe **1.2** had excellent affinity for PKA (K_d = 16 nM), and the SPR assay was able to detect displacement of the bisubstrate probe by the binding of ATP-competitive inhibitors, other ARCs, and protein substrates of PKA. The K_d values for the known inhibitors characterized with this assay were in good agreement with reported values.

The same group has also developed an FP method utilizing a bisubstrate probe based on an ARC for the characterization of ligands of PKA and ROCK.[58] The FP probe **1.3** was generated by labeling the N-terminus of the peptidic portion of the ARC with the fluorescent tag TAMRA. The probe had excellent affinity for PKA (K_d = 480 pM), and displacement of the probe from PKA was observed with ATP-competitive inhibitors, other ARCs, and protein substrates of PKA. The probe is also reported to be a ligand for ROCK (K_d = 3.6 nM), but displacement of the probe by a substrate-competitive ligand for ROCK was not evaluated. In both cases, the K_d values for inhibitors obtained using the FP assay were in good agreement with literature reports.

Our lab has also developed a bisubstrate TR-FRET tracer that can identify substrate-competitive inhibitors.[59] A bisubstrate inhibitor of c-Src, composed of an analogue of the ATP-competitive inhibitor PP2 and an optimal c-Src peptide ligand, was fluorescently labeled with Cy5 at the N-terminal of the peptide to generate tracer **1.4**. Similar to what was seen with the ARC probes, this probe has excellent affinity for c-Src with K_d = 6 nM. In a TR-FRET assay with c-Src, displacement of the tracer by known ATP-competitive and substrate-competitive ligands could be detected, and the K_d values obtained for the ligands using this assay were in good agreement with literature values.

These examples demonstrate that a variety of competitive binding assay formats can be used with bisubstrate probes to recognize substrate-competitive ligands, but thus far screens for substrate-competitive inhibitors using these methods have not been reported. Although bisubstrate probes hold promise for the identification of substrate-competitive inhibitors, a complication of using bisubstrate probes instead of purely substrate-competitive probes is that ATP-competitive inhibitors will be identified as well. Therefore, a counter screen against an ATP-competitive probe should be performed to rule out compounds which displace the bisubstrate probe by competing for binding to the

ATP site. A further complication that could arise during counter screening is that recent work by Lebakken and coworkers has shown that ligands binding outside the ATP site, including substrate-competitive inhibitors, can sometimes displace ATP-competitive TR-FRET tracers by causing perturbations within the ATP binding pocket.[60] This raises the possibility that substrate-competitive inhibitors identified from a competitive binding assay using a bisubstrate probe may be ruled out as ATP-competitive inhibitors during counter screening. Due to these issues, the use of a substrate-competitive probe instead of a bisubstrate probe would be preferable when available.

A remaining issue with both substrate-competitive and bisubstrate probes is that they are not likely to bind to a large number of kinases due to the less conserved nature of the substrate binding site. This means that while in general competitive binding assays could be applied to any kinase of interest, a single probe cannot be used for all (or even most) kinases and new probes will need to be developed in order to access different subsets of targets. This will be most challenging for new kinase targets; however, while the development of substrate-competitive probes may not be initially feasible for new targets since high potency substrate-competitive ligands will likely not yet be known, a bisubstrate approach may be possible. Many services offering broad kinase inhibitor profiling screens include kinases whose functions are currently unknown in their panels, and published datasets of kinase inhibitor selectivity show that a potent ATP-competitive inhibitor can be identified for most kinases. This data could aid in the development of bisubstrate probes for competitive-binding assays with new targets.

NMR Screening

NMR screening has become a popular screening method due to its ability to detect even weakly binding fragments, but while NMR screens against kinase targets have been successful in identifying ATP-competitive fragments, the propensity of the ligands to bind within the better defined ATP-pocket has stalled the discovery of substrate-competitive inhibitors.[61] Recently, however, some success in identify ATP-noncompetitive ligands has been achieved by utilizing paramagnetic spin-labeled ATP-competitive probes (**Scheme 1.5**). In these experiments, NMR spectra of a compound with the kinase of interest are obtained both in the presence and in the absence of the

spin-labeled probe. The spin-label will increase the relaxation time of nearby protons, and thus compounds which bind simultaneously near the probe can be identified by observing a paramagnetic relaxation enhancement (PRE) in the NMR spectrum.[62] When using an ATP-competitive spin-labeled probe, other ATP-competitive ligands will not be identified since these compounds cannot bind at the same time as the probe. The probes are sensitive to ligands binding up to 25 Å away from the spin label, a distance which includes the substrate binding site (**Figure 1.3**).

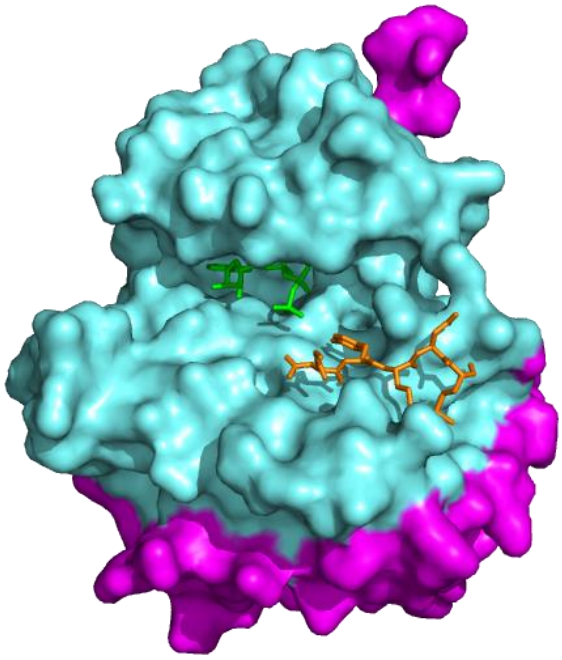

Figure 1.3. Crystal structure of IRK bound to an ATP analogue (green) and a peptidic substrate mimic (orange), with residues within 20 Å of the ATP binding site highlighted in cyan (PDB 1IR3).

In 2005, McCoy and coworkers reported the use of manganese-chelated ATP as a paramagnetic probe for identifying ATP-noncompetitive ligands.[63] The authors demonstrated that the probe could detect the binding of a known ATP-noncompetitive inhibitor of MEK1, but no new ligands were reported. Although this probe should bind to any kinase of interest, ATP (and therefore the probe) has micromolar affinity for many kinases. Due to the modest affinity, a large excess of the probe may be required in order

saturate the kinase and obtain the maximum signal, but this could also result in nonspecific binding of probe. Furthermore, Mn^{2+} can also bind nonspecifically to proteins. To ensure that only ligands binding within 25 Å of the ATP binding site are identified, it is noted that the probe should have good affinity (low micromolar to nanomolar), and if the buffer used contains manganese the concentration of Mn^{2+} should be less than 100 µM.

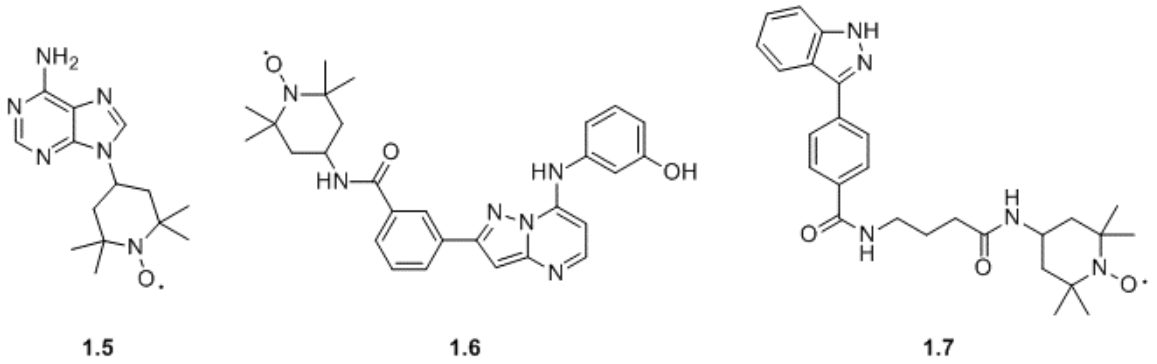

1.5 **1.6** **1.7**

Scheme 1.5. Spin-labeled ATP-competitive probes for NMR screening.

At the same time, Jahnke and coworkers reported the TEMPO-labeled adenine analogue **1.5**.[64] While an example NMR spectrum for the identification of an ATP-noncompetitive ligand (ligand and kinase not disclosed) and recommendations for confirming hits are outlined, no new ligands were reported. The close structural resemblance of probe **1.5** to ATP should allow it to bind to most kinases. However, similar the ATP-manganese chelate probe, the interaction between probe **1.5** and many kinases will be weak, and a large quantity of the probe may be required. As mentioned previously, this can lead to nonspecific binding, and, in fact, the authors report that the probe does bind nonspecifically to some kinases.

To remedy the low affinity and nonspecific binding of previous probes, research groups have begun modifying potent ATP-competitive inhibitors with spin labels. Moy and coworkers have developed the spin-labeled probe **1.6** based on an ATP-competitive inhibitor that was reported to bind potently to several kinases.[65] Profiling of probe **1.6**

against a panel of nineteen kinases showed that it bound eight kinases with an IC_{50} value less than 40 nM. However, of the other eleven kinases examine nine had IC_{50} > 50 μM, suggesting that **1.6** cannot be widely applied to any kinase of interest. The ability of **1.6** to identify compounds binding outside the ATP pocket was confirmed by detecting the binding of a previously reported weak substrate-competitive c-Src inhibitor. While a full scale screen was not reported using this probe, the authors were able to identify the binding of the fragment *N*-phenylanthranilic acid to Lck. The binding site for this fragment has not been conclusively determined, but the weak PRE signal and modeling of the probe in complex with Lck predicted that it binds in a pocket adjacent to the ATP binding site and the substrate binding site.

To bias screening towards identifying substrate-competitive ligands, Vazquez and coworkers used structural data to develop probe **1.7** for JNK.[66] Probe **1.7** is based on a known ATP-competitive inhibitor and was designed so that the TEMPO spin label would sit at the edge of the JIP1 interaction site. Because the PRE is proportional to the distance between the probe and the proton, ligands binding to the JIP1 interaction site would experience the stronger PRE than ligands further away outside of the JIP1 interaction site. The probe was able to identify the binding of two peptides based on JIP1, and the binding orientation of each ligand was deduced from the differences in the PRE for each residue in the peptide. The affinity of one of these peptides was too weak for it to be identified as an inhibitor using an activity-based assay, which demonstrates the power of NMR screening for detecting even weakly binding ligands. Probe **1.7** was also used by Stebbins and coworkers to confirm that their small molecule substrate-competitive JNK inhibitor identified from a competitive binding assay bound to the JIP1 interaction site.[52] Although this probe has not yet been used to identify small molecule ligands, this strategy of situating the spin-label at the edge of the substrate-binding site should enable better identification of substrate-competitive ligands over allosteric ligands.

Large screens utilizing spin-labeled ATP-competitive probes have not yet been reported, and it is important to remember that these probes will identify any ligand that binds within 25 Å of the spin-label. As such, they will not exclusively identify substrate-competitive inhibitors, and after a screen using one of these probes additional

experiments may be required to determine if the ligand binds to the substrate site or an allosteric site. This could be minimized by carefully designing the probe so that it places the spin label as close as possible to the substrate-binding site, but this will require structural data.

Similar to competitive binding assays, the affinity and selectivity of the spin-labeled probes will also complicate their use. Probes based on ATP or adenine will bind to most if not all kinases, but their weak affinity and nonspecific binding will limit their use. Conversely, designing probes based on potent ATP-competitive inhibitors such as **1.6** and **1.7** will minimize nonspecific binding, but these probes will not bind to the full kinome. This means that the development of new probes will be required for some targets of interest, but as discussed previously selectivity datasets show that potent ATP-competitive inhibitors can be found for most kinases, even kinases whose functions are currently unknown.

Conclusions

Despite the interest in using small molecule substrate-competitive kinase inhibitors as biological probes and therapeutics, only a small fraction of reported kinase inhibitors fall into this category. This can largely be attributed to the fact that traditionally HTS monitoring inhibition of enzyme activity were used to discover kinase inhibitors, and these screens are highly biased towards the identification of ATP-competitive inhibitors. Recently, however, reports of the discovery of ATP-noncompetitive inhibitors identified using a variety of approaches has increased. Although some of these approaches required structural data and are not readily applicable to all targets, other approaches including biased activity assays, competitive binding assays, and NMR screening using ATP-competitive probes can be even when there is only limited knowledge about the target to begin with. These approaches will continue to be useful tools for the continuing discovery of new substrate-competitive kinase inhibitors.

When considering using one of these methods for a screen to identify small molecule substrate-competitive kinase inhibitors, there are advantages and disadvantages that should be carefully taken into account. Biased activity assays may facilitate the use

of assays that are already established in-house, but the conditions can also select for the identification of potent ATP-competitive inhibitors as well as allosteric inhibitors. NMR screening using ATP-competitive paramagnetic probes eliminates the identification of ATP-competitive compounds, but may still identify allosteric ligands. If structural data is available, this can aid in developing a probe with the spin-label positioned near the substrate binding site, which can bias towards the identification of substrate-competitive inhibitors. A direct binding assay monitoring net displacement of a substrate-competitive probe should enable the exclusive identification of substrate-competitive inhibitors; however, the development of such probes has been hindered by the modest potency of most substrate-competitive ligands. While bisubstrate probes overcome this obstacle, additional screening will be required to eliminate hits that displaced the probe due to competition at the ATP site. An additional complication for methods utilizing probes is that although these methods can be applied to any kinase, a single probe is not likely to bind potently to the entire kinome, and therefore the development of a new probe may be required in order to screen the target of interest.

Overall, these methods will aid in the identification of new small molecule substrate-competitive inhibitors, but their shortcomings demonstrate that there is still a continuing need to improve current screening methods as well as develop new methods. Ideally, a screening method would not require structural knowledge of the target, would not require the development of multiple probes for different targets, and would exclusively identify substrate-competitive inhibitors. A screening method such as this would be of great value for advancing the discovery of new substrate-competitive inhibitors, especially because a significant portion of the kinome remains unexplored.

References

1. Manning, G.; Whyte, D. B.; Martinez, R.; Hunter, T.; Sudarsanam, S., The Protein Kinase Complement of the Human Genome. *Science* **2002,** *298* (5600), 1912-1934.
2. Johnson, S. A.; Hunter, T., Kinomics: methods for deciphering the kinome. *Nat Meth* **2005,** *2* (1), 17-25.
3. Ryšlavá, H.; Doubnerová, V.; Kavan, D.; Vaněk, O., Effect of posttranslational modifications on enzyme function and assembly. *Journal of Proteomics* **2013,** *92* (0), 80-109.

4. Pawson, T.; Scott, J. D., Protein phosphorylation in signaling – 50 years and counting. *Trends in Biochemical Sciences* **2005,** *30* (6), 286-290.
5. Graves, J. D.; Krebs, E. G., Protein Phosphorylation and Signal Transduction. *Pharmacology & Therapeutics* **1999,** *82* (2–3), 111-121.
6. Hunter, T., Protein kinases and phosphatases: The Yin and Yang of protein phosphorylation and signaling. *Cell* **1995,** *80* (2), 225-236.
7. Dhanasekaran, D. N.; Reddy, E. P., JNK signaling in apoptosis. *Oncogene* **2008,** *27* (48), 6245-6251.
8. Manning, B. D.; Cantley, L. C., AKT/PKB Signaling: Navigating Downstream. *Cell* **2007,** *129* (7), 1261-1274.
9. Olsson, A.-K.; Dimberg, A.; Kreuger, J.; Claesson-Welsh, L., VEGF receptor signalling ? in control of vascular function. *Nat Rev Mol Cell Biol* **2006,** *7* (5), 359-371.
10. Mitra, S. K.; Hanson, D. A.; Schlaepfer, D. D., Focal adhesion kinase: in command and control of cell motility. *Nat Rev Mol Cell Biol* **2005,** *6* (1), 56-68.
11. Zarubin, T.; Han, J., Activation and signaling of the p38 MAP kinase pathway. *Cell Res* **2005,** *15* (1), 11-18.
12. Birchmeier, C.; Birchmeier, W.; Gherardi, E.; Vande Woude, G. F., Met, metastasis, motility and more. *Nat Rev Mol Cell Biol* **2003,** *4* (12), 915-925.
13. Hubbard, S. R.; Till, J. H., Protein Tyrosine Kinase Structure and Function. *Annual Review of Biochemistry* **2000,** *69* (1), 373-398.
14. Hanks, S. K.; Hunter, T., Protein kinases 6. The eukaryotic protein kinase superfamily: kinase (catalytic) domain structure and classification. *The FASEB Journal* **1995,** *9* (8), 576-96.
15. Deshmukh, K.; Anamika, K.; Srinivasan, N., Evolution of domain combinations in protein kinases and its implications for functional diversity. *Progress in Biophysics and Molecular Biology* **2010,** *102* (1), 1-15.
16. Endicott, J. A.; Noble, M. E. M.; Johnson, L. N., The Structural Basis for Control of Eukaryotic Protein Kinases. *Annual Review of Biochemistry* **2012,** *81* (1), 587-613.
17. Dohlman, H. G., A Scaffold Makes the Switch. *Sci. Signal.* **2008,** *1* (42), pe46-.
18. Blume-Jensen, P.; Hunter, T., Oncogenic kinase signalling. *Nature* **2001,** *411* (6835), 355-365.
19. Kumar, S.; Boehm, J.; Lee, J. C., p38 MAP kinases: key signalling molecules as therapeutic targets for inflammatory diseases. *Nat Rev Drug Discov* **2003,** *2* (9), 717-726.
20. Evans, J. L.; Goldfine, I. D.; Maddux, B. A.; Grodsky, G. M., Oxidative Stress and Stress-Activated Signaling Pathways: A Unifying Hypothesis of Type 2 Diabetes. *Endocrine Reviews* **2002,** *23* (5), 599-622.
21. Cohen, P., Protein kinases - the major drug targets of the twenty-first century? *Nat Rev Drug Discov* **2002,** *1* (4), 309-315.
22. Zhang, J.; Yang, P. L.; Gray, N. S., Targeting cancer with small molecule kinase inhibitors. *Nat Rev Cancer* **2009,** *9* (1), 28-39.
23. Bose, R.; Holbert, M. A.; Pickin, K. A.; Cole, P. A., Protein tyrosine kinase-substrate interactions. *Curr. Opin. Struct. Biol.* **2006,** *16* (6), 668-675.
24. Knight, Z. A.; Shokat, K. M., Features of Selective Kinase Inhibitors. *Chemistry & Biology* **2005,** *12* (6), 621-637.
25. Vulpetti, A.; Bosotti, R., Sequence and structural analysis of kinase ATP pocket residues. *Il Farmaco* **2004,** *59* (10), 759-765.

26. Davis, M. I.; Hunt, J. P.; Herrgard, S.; Ciceri, P.; Wodicka, L. M.; Pallares, G.; Hocker, M.; Treiber, D. K.; Zarrinkar, P. P., Comprehensive analysis of kinase inhibitor selectivity. *Nat. Biotechnol.* **2011,** *29* (11), 1046-U124.
27. Scapin, G., Protein Kinase Inhibition: Different Approaches to Selective Inhibitor Design *Current Drug Targets* **2006,** *7* (11), 1443-1454.
28. Krishnamurty, R.; Maly, D. J., Biochemical Mechanisms of Resistance to Small-Molecule Protein Kinase Inhibitors. *ACS Chem. Biol.* **2010,** *5* (1), 121-138.
29. Daub, H.; Specht, K.; Ullrich, A., Strategies to overcome resistance to targeted protein kinase inhibitors. *Nat Rev Drug Discov* **2004,** *3* (12), 1001-1010.
30. Lawrence, D. S.; Niu, J., Protein Kinase Inhibitors: The Tyrosine-Specific Protein Kinases. *Pharmacology & Therapeutics* **1998,** *77* (2), 81-114.
31. Bidwell, G. L.; Raucher, D., Therapeutic peptides for cancer therapy. Part I – peptide inhibitors of signal transduction cascades. *Expert Opinion on Drug Delivery* **2009,** *6* (10), 1033-1047.
32. Eldar-Finkelman, H.; Eisenstein, M., Peptide Inhibitors Targeting Protein Kinases *Current Pharmaceutical Design* **2009,** *15* (21), 2463-2470.
33. Bogoyevitch, M. A.; Barr, R. K.; Ketterman, A. J., Peptide inhibitors of protein kinases—discovery, characterisation and use. *Biochimica et Biophysica Acta (BBA) - Proteins and Proteomics* **2005,** *1754* (1–2), 79-99.
34. Akritopoulou-Zanze, I.; Hajduk, P. J., Kinase-targeted libraries: The design and synthesis of novel, potent, and selective kinase inhibitors. *Drug Discovery Today* **2009,** *14* (5–6), 291-297.
35. Structural Genomics Consortium, Progress in protein kinase structural biology. http://www.thesgc.org/scientists/resources/kinases.
36. Fedorov, O.; Muller, S.; Knapp, S., The (un)targeted cancer kinome. *Nat Chem Biol* **2010,** *6* (3), 166-169.
37. Manning, B. D., Challenges and Opportunities in Defining the Essential Cancer Kinome. *Sci. Signal.* **2009,** *2* (63), pe15-.
38. von Ahsen, O.; Bömer, U., High-Throughput Screening for Kinase Inhibitors. *ChemBioChem* **2005,** *6* (3), 481-490.
39. Liu, M.; Poulose, S.; Schuman, E.; Zaitsev, A. D.; Dobson, B.; Auerbach, K.; Seyb, K.; Cuny, G. D.; Glicksman, M. A.; Stein, R. L.; Yue, Z., Development of a mechanism-based high-throughput screen assay for leucine-rich repeat kinase 2—Discovery of LRRK2 inhibitors. *Analytical Biochemistry* **2010,** *404* (2), 186-192.
40. Lo, M.-C.; Ngo, R.; Dai, K.; Li, C.; Liang, L.; Lee, J.; Emkey, R.; Eksterowicz, J.; Ventura, M.; Young, S. W.; Xiao, S.-H., Development of a time-resolved fluorescence resonance energy transfer assay for cyclin-dependent kinase 4 and identification of its ATP-noncompetitive inhibitors. *Analytical Biochemistry* **2012,** *421* (2), 368-377.
41. Steffey, M. E., unpublished data, 2012.
42. Baguley, T. D.; Xu, H.-C.; Chatterjee, M.; Nairn, A. C.; Lombroso, P. J.; Ellman, J. A., Substrate-Based Fragment Identification for the Development of Selective, Nonpeptidic Inhibitors of Striatal-Enriched Protein Tyrosine Phosphatase. *J. Med. Chem.* **2013,** *56* (19), 7636-7650.
43. Leyva, M. J.; DeGiacomo, F.; Kaltenbach, L. S.; Holcomb, J.; Zhang, N.; Gafni, J.; Park, H.; Lo, D. C.; Salvesen, G. S.; Ellerby, L. M.; Ellman, J. A., Identification and

Evaluation of Small Molecule Pan-Caspase Inhibitors in Huntington's Disease Models. *Chemistry & Biology* **2010,** *17* (11), 1189-1200.
44. Brak, K.; Doyle, P. S.; McKerrow, J. H.; Ellman, J. A., Identification of a New Class of Nonpeptidic Inhibitors of Cruzain. *J. Am. Chem. Soc.* **2008,** *130* (20), 6404-6410.
45. Soellner, M. B.; Rawls, K. A.; Grundner, C.; Alber, T.; Ellman, J. A., Fragment-based substrate activity screening method for the identification of potent inhibitors of the Mycobacterium tuberculosis phosphatase PtpB. *J. Am. Chem. Soc.* **2007,** *129* (31), 9613-9615.
46. Patterson, A. W.; Wood, W. J. L.; Hornsby, M.; Lesley, S.; Spraggon, G.; Ellman, J. A., Identification of Selective, Nonpeptidic Nitrile Inhibitors of Cathepsin S Using the Substrate Activity Screening Method. *J. Med. Chem.* **2006,** *49* (21), 6298-6307.
47. Wood, W. J. L.; Patterson, A. W.; Tsuruoka, H.; Jain, R. K.; Ellman, J. A., Substrate activity screening: A fragment-based method for the rapid identification of nonpeptidic protease inhibitors. *J. Am. Chem. Soc.* **2005,** *127* (44), 15521-15527.
48. Chapelat, J.; Berst, F.; Marzinzik, A. L.; Moebitz, H.; Drueckes, P.; Trappe, J.; Fabbro, D.; Seebach, D., The Substrate-Activity-Screening methodology applied to receptor tyrosine kinases: A proof-of-concept study. *Eur. J. Med. Chem.* **2012,** *57*, 1-9.
49. Comess, K. M.; Sun, C.; Abad-Zapatero, C.; Goedken, E. R.; Gum, R. J.; Borhani, D. W.; Argiriadi, M.; Groebe, D. R.; Jia, Y.; Clampit, J. E.; Haasch, D. L.; Smith, H. T.; Wang, S.; Song, D.; Coen, M. L.; Cloutier, T. E.; Tang, H.; Cheng, X.; Quinn, C.; Liu, B.; Xin, Z.; Liu, G.; Fry, E. H.; Stoll, V.; Ng, T. I.; Banach, D.; Marcotte, D.; Burns, D. J.; Calderwood, D. J.; Hajduk, P. J., Discovery and Characterization of Non-ATP Site Inhibitors of the Mitogen Activated Protein (MAP) Kinases. *ACS Chem. Biol.* **2010,** *6* (3), 234-244.
50. Ashwell, M. A.; Lapierre, J.-M.; Brassard, C.; Bresciano, K.; Bull, C.; Cornell-Kennon, S.; Eathiraj, S.; France, D. S.; Hall, T.; Hill, J.; Kelleher, E.; Khanapurkar, S.; Kizer, D.; Koerner, S.; Link, J.; Liu, Y.; Makhija, S.; Moussa, M.; Namdev, N.; Nguyen, K.; Nicewonger, R.; Palma, R.; Szwaya, J.; Tandon, M.; Uppalapati, U.; Vensel, D.; Volak, L. P.; Volckova, E.; Westlund, N.; Wu, H.; Yang, R.-Y.; Chan, T. C. K., Discovery and Optimization of a Series of 3-(3-Phenyl-3H-imidazo[4,5-b]pyridin-2-yl)pyridin-2-amines: Orally Bioavailable, Selective, and Potent ATP-Independent Akt Inhibitors. *J. Med. Chem.* **2012,** *55* (11), 5291-5310.
51. Navratilova, I.; Macdonald, G.; Robinson, C.; Hughes, S.; Mathias, J.; Phillips, C.; Cook, A., Biosensor-Based Approach to the Identification of Protein Kinase Ligands with Dual-Site Modes of Action. *Journal of Biomolecular Screening* **2012,** *17* (2), 183-193.
52. Stebbins, J. L.; De, S. K.; Machleidt, T.; Becattini, B.; Vazquez, J.; Kuntzen, C.; Chen, L.-H.; Cellitti, J. F.; Riel-Mehan, M.; Emdadi, A.; Solinas, G.; Karin, M.; Pellecchia, M., Identification of a new JNK inhibitor targeting the JNK-JIP interaction site. *Proceedings of the National Academy of Sciences* **2008,** *105* (43), 16809-16813.
53. Saldanha, S. A.; Kaler, G.; Cottam, H. B.; Abagyan, R.; Taylor, S. S., Assay Principle for Modulators of Protein−Protein Interactions and Its Application to Non-ATP-Competitive Ligands Targeting Protein Kinase A. *Analytical Chemistry* **2006,** *78* (24), 8265-8272.

54. Tsuganezawa, K.; Watanabe, H.; Parker, L.; Yuki, H.; Taruya, S.; Nakagawa, Y.; Kamei, D.; Mori, M.; Ogawa, N.; Tomabechi, Y.; Handa, N.; Honma, T.; Yokoyama, S.; Kojima, H.; Okabe, T.; Nagano, T.; Tanaka, A., A Novel Pim-1 Kinase Inhibitor Targeting Residues That Bind the Substrate Peptide. *Journal of Molecular Biology* **2012,** *417* (3), 240-252.
55. Zettner, A., Principles of Competitive Binding Assays (Saturation Analyses). I. Equilibrium Techniques. *Clinical Chemistry* **1973,** *19* (7), 699-705.
56. Gower, C. M.; Chang, M. E. K.; Maly, D. J., Bivalent inhibitors of protein kinases. *Critical Reviews in Biochemistry and Molecular Biology* **2014,** *49* (2), 102-115.
57. Viht, K.; Schweinsberg, S.; Lust, M.; Vaasa, A.; Raidaru, G.; Lavogina, D.; Uri, A.; Herberg, F. W., Surface-plasmon-resonance-based biosensor with immobilized bisubstrate analog inhibitor for the determination of affinities of ATP- and protein-competitive ligands of cAMP-dependent protein kinase. *Analytical Biochemistry* **2007,** *362* (2), 268-277.
58. Vaasa, A.; Viil, I.; Enkvist, E.; Viht, K.; Raidaru, G.; Lavogina, D.; Uri, A., High-affinity bisubstrate probe for fluorescence anisotropy binding/displacement assays with protein kinases PKA and ROCK. *Analytical Biochemistry* **2009,** *385* (1), 85-93.
59. Brandvold, K. R.; Soellner, M. B., manuscript in preparation. 2014.
60. Lebakken, C. S.; Reichling, L. J.; Ellefson, J. M.; Riddle, S. M., Detection of Allosteric Kinase Inhibitors by Displacement of Active Site Probes. *Journal of Biomolecular Screening* **2012,** *17* (6), 813-821.
61. Pellecchia, M.; Bertini, I.; Cowburn, D.; Dalvit, C.; Giralt, E.; Jahnke, W.; James, T. L.; Homans, S. W.; Kessler, H.; Luchinat, C.; Meyer, B.; Oschkinat, H.; Peng, J.; Schwalbe, H.; Siegal, G., Perspectives on NMR in drug discovery: a technique comes of age. *Nat Rev Drug Discov* **2008,** *7* (9), 738-745.
62. Jahnke, W.; Perez, L. B.; Paris, C. G.; Strauss, A.; Fendrich, G.; Nalin, C. M., Second-Site NMR Screening with a Spin-Labeled First Ligand. *J. Am. Chem. Soc.* **2000,** *122* (30), 7394-7395.
63. McCoy, M. A.; Senior, M. M.; Wyss, D. F., Screening of Protein Kinases by ATP-STD NMR Spectroscopy. *J. Am. Chem. Soc.* **2005,** *127* (22), 7978-7979.
64. Jahnke, W.; Blommers, M. J. J.; Fernández, C.; Zwingelstein, C.; Amstutz, R., Strategies for the NMR-Based Identification and Optimization of Allosteric Protein Kinase Inhibitors. *ChemBioChem* **2005,** *6* (9), 1607-1610.
65. Moy, F. J.; Lee, A.; Gavrin, L. K.; Xu, Z. B.; Sievers, A.; Kieras, E.; Stochaj, W.; Mosyak, L.; McKew, J.; Tsao, D. H. H., Novel Synthesis and Structural Characterization of a High-Affinity Paramagnetic Kinase Probe for the Identification of Non-ATP Site Binders by Nuclear Magnetic Resonance. *J. Med. Chem.* **2009,** *53* (3), 1238-1249.
66. Vazquez, J.; De, S. K.; Chen, L.-H.; Riel-Mehan, M.; Emdadi, A.; Cellitti, J.; Stebbins, J. L.; Rega, M. F.; Pellecchia, M., Development of Paramagnetic Probes for Molecular Recognition Studies in Protein Kinases. *J. Med. Chem.* **2008,** *51* (12), 3460-3465.

CHAPTER II

Peptidic Inhibitors of c-Src Kinase for Pharmacophore Identification

Abstract

This study evaluated three libraries of peptides to (1) identify new tyrosine pharmacophores for c-Src kinase and (2) discover potent peptidic inhibitors of c-Src that could be used in fluorescence polarization assay development. While several pharmacophores have been reported for peptidic tyrosine kinase inhibitors, an extensive study of tyrosine pharmacophores including substitutions at the *ortho*, *meta*, and *para* positions of phenylalanine has never been conducted. Peptides based on known c-Src and c-Abl substrates with the structure Ac-AIXAA-NH_2 were prepared and evaluated as c-Src inhibitors. Although no potent inhibitors were identified, analysis of this library demonstrates that both an increase in hydrophobic surface area and a decrease in the electron density within the phenylalanine ring are necessary for c-Src inhibition. Additionally, three peptides reported in the literature to be potent inhibitors of c-Src were evaluated and found to be generally poor inhibitors in our hands. Overall, no peptides were identified with suitable potency for use as FP probes, highlighting the difficulty in developing highly potent peptidic inhibitors.

Introduction

Many of the first reported substrate-competitive protein kinase inhibitors were peptidic inhibitors.[1-2] While combinatorial libraries have been used to screen large peptides inhibitor libraries, most peptidic inhibitors are based on known kinase substrates which were modified to generate peptidic inhibitors. Early inhibitors replaced the phosphorylatable residue with phenylalanine (for tyrosine kinase substrates) or alanine (for serine/threonine kinase substrates), but these inhibitors often suffered from poor potency. This has prompted the examination of other pharmacophores, with the largest focus on tyrosine pharmacophores.[3-10] The most extensive examination of

pharmacophores for tyrosine kinases was performed by Niu and Lawrence who evaluated 20 peptides with *para*-substituted phenethylamines as c-Src inhibitors.[9] However, despite identifying several pharmacophores with modest improvement over phenylalanine, the corresponding peptides still have poor potency.

The aim of the current study was to identify new tyrosine pharmacophores for c-Src using a library of peptidic inhibitors. Any potent peptidic inhibitors discovered could then be fluorescently labeled and used in the development of a fluorescence polarization (FP) competitive binding assay to screen for small molecule substrate-competitive inhibitors of c-Src. In addition to generating peptidic probes, we hypothesized that newly identified pharmacophores could also be applied later to the design of small molecule substrate-competitive inhibitors (see **Chapter III**). While Niu and Lawrence examined 20 pharmacophores for c-Src, their study was limited to only *para*-substituted pharmacophores (with the exception of pentafluorophenylalanine).[9] We wanted to examine additional substitutions at the *para* position, as well as *meta* and *ortho* substitutions that could potentially be combined in order to increase potency. Herein is reported the design and evaluation of a library of peptides containing diverse tyrosine replacements as inhibitors of c-Src.

We chose to use the eukaryotic protein tyrosine kinase c-Src as a model kinase in all of the studies presented in this dissertation as it is well characterized, expresses well in *E. coli*, and is a validated target in multiple cancers.[11-14] c-Src is composed of a catalytic domain, which has the characteristic kinase fold and contains the kinase active site, and two regulatory domains (SH2 and SH3), which modulate kinase activity and have scaffolding roles.[15] All three domains of c-Src have been targeted for inhibitor development, although most focus has been placed on the ATP binding site.[16-18] Throughout this work, the selectivity of inhibitors for c-Src over c-Abl kinase will be used as a selectivity benchmark. Although it is not a member of the Src family, c-Abl shares 68% similarity with c-Src across the catalytic domain, and this high similarity has made the development of c-Src inhibitors that do not also inhibit c-Abl challenging.[19-20]

The peptide library was designed around known c-Src and c-Abl substrates. Peptides based on the v-Src autophosphorylation site with the structure LIEDAXYAARG (where X is varied) have been shown to be substrates for c-Src and c-Abl.[21] The

synthetic peptide (EAIYAAPFAKKK) has also been shown to be an optimal substrate for c-Abl.[22] On the basis of the shared elements of these peptides near the reactive tyrosine (-AXYAA-), we hypothesized that the truncated sequence Ac-AIYAA-NH_2 (**2.1**) would be a substrate for both c-Src and c-Abl. This peptide would serve as the starting point for the design of the library would enable us to determine if the pharmacophores increased the selectivity for c-Src over c-Abl.

Ac-AIYAA-NH_2 (**2.1**) was evaluated as a substrate of c-Src and c-Abl using a nucleoside disphosphate kinase (NDPK) coupled assay.[23] This assay utilizes NDPK that has been labeled with an environmentally sensitive coumarin fluorophore near the active site. As shown in **Scheme 2.1**, ADP is generated as a byproduct of kinase activity and is bound by the fluorescently-labeled, phosphorylated NDPK (NDPK-P). Transfer of the phosphate group from NDPK-P to ADP changes the local environment around the fluorophore and results in decreased fluorescence. Thus, the amount of kinase activity can be extrapolated from the change in fluorescence intensity.

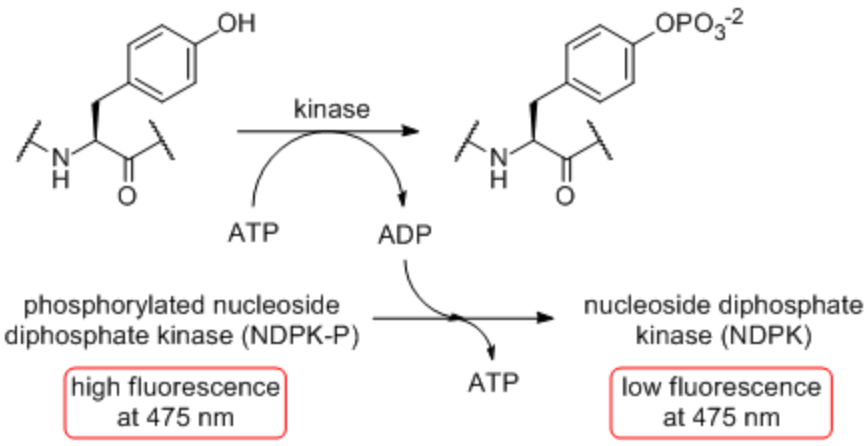

Scheme 2.1. A nucleoside disphosphate kinase (NDPK) coupled assay was used for the analysis of kinase substrates.

The truncated sequence Ac-AIYAA-NH_2 (**2.1**) was found to have K_M = 57 μM for c-Src and K_M = 97 μM for c-Abl (data provided by Dr. Sonali Kurup). It should be noted, however, that it has previously been shown that K_M values for kinase substrates greatly

overestimates the affinity of the peptide for the substrate binding site ($K_M < K_d$), and thus the K_d values for this peptide with c-Src and c-Abl are likely in the mid-micromolar range.[24-25] Using peptide **2.1** as a starting point, two peptide libraries were designed for evaluation as c-Src and c-Abl inhibitors (**Scheme 2.2**). In the first library, the reactive tyrosine residue was replaced with other natural amino acids, including D-amino acids. In the second library, the reactive tyrosine was replaced with substituted phenylalanine residues. All peptides were prepared using standard Fmoc-based solid phase peptide synthesis methods and purified by reverse phase HPLC.[26]

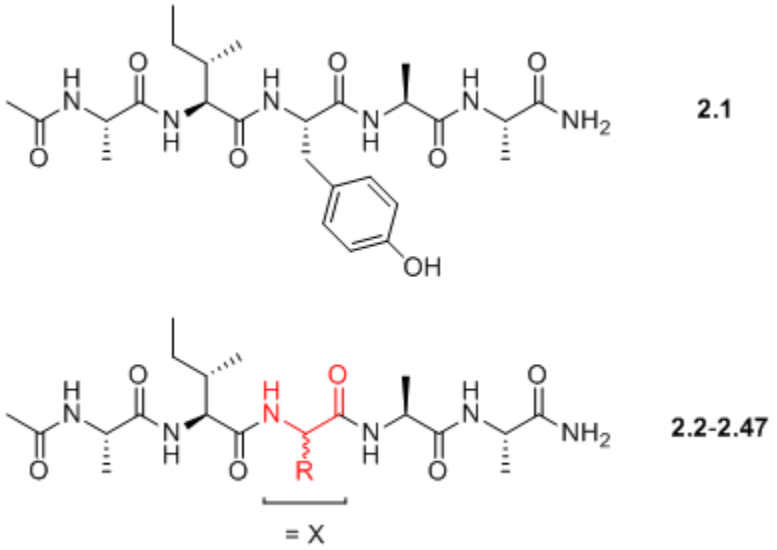

Scheme 2.2. A library of peptides was prepared based on the c-Src and c-Abl substrate peptide **2.1**. The library had the general structure Ac-AIXAA-NH_2, where X was natural amino acids and substituted phenylalanine derivatives.

Evaluation of Peptides with Natural Amino Acid Pharmacophores

The peptidic inhibitors in this study were evaluated using a previously reported continuous fluorescence assay utilizing a fluorescent peptide substrate reporter.[27] In this assay, a peptide substrate is modified to include a pyrene fluorophore at the Y+2 position. As shown in **Scheme 2.3**, a π-stacking interaction between the tyrosine side chain and pyrene results in low fluorescence at 405 nm. However, when the tyrosine residue is phosphorylated by a kinase this stacking interaction is disrupted and pyrene fluorescence

at 405 nm is increased. By measuring the increase in fluorescence over time the amount of kinase activity can be determined. The reporter peptide Ac-EEEIYGE(Dap-pyrene)EA-NH_2 was used in the evaluation of the peptidic inhibitors against both c-Src and c-Abl. This assay was preferred over the NDPK coupled assay used for substrate analysis because it enables direct observation of kinase activity and requires fewer materials.

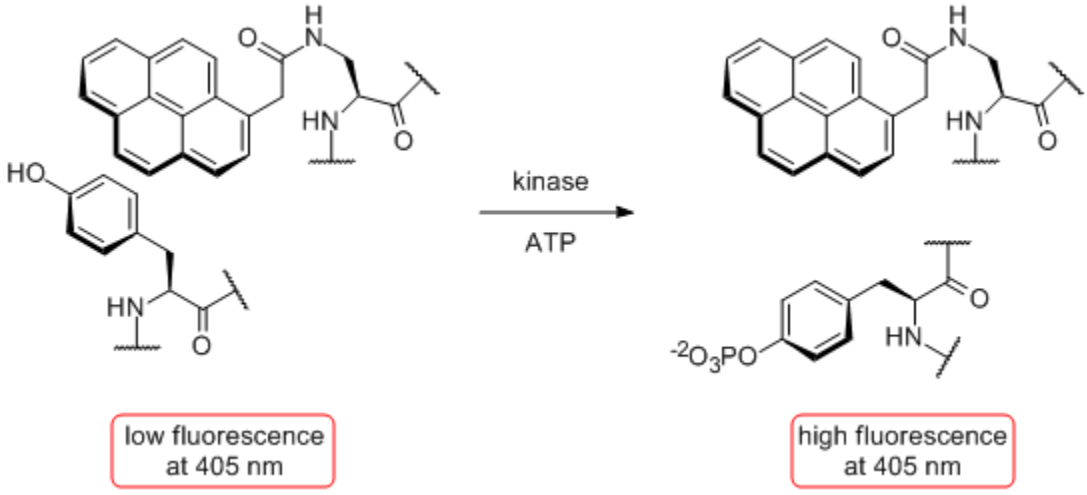

Scheme 2.3. A continuous fluorescence-based assay utilizing a fluorescent peptide substrate reporter (Ac-EEEIYGE(Dap-pyrene)EA-NH_2) was used to evaluate c-Src and c-Abl inhibition.

The K_i values for the first peptide library are shown in **Table 2.1**. The substrate peptide **2.1** was not able to effectively prevent the phosphorylation of the pyrene reporter peptide (K_i > 1000 μM). Changing the stereochemistry of the peptide did not increase binding and gave poor inhibitors (K_i > 1000 μM) as was seen with the D-tyrosine peptide (**2.2**) and the retro-inverse peptide (**2.3**). Removal of the hydroxyl group to give the phenylalanine peptide (**2.4**) or removal of the phenol to give the alanine peptide (**2.5**) also yielded poor inhibitors (K_i > 1000 μM). This is consistent with previous literature reports and was not unexpected since the tyrosine hydroxyl group is thought to make important hydrogen bonding interactions within the substrate binding site.[28] The loss of these hydrogen bond interactions coupled with the fact that the inhibitors are based on a

substrate with likely modest affinity results in the poor potency observed for these inhibitors.

Table 2.1. Peptides with the general structure Ac-AIXAA-NH_2, where X is a natural amino acid, were evaluated for c-Src and c-Abl inhibition using the pyrene assay.

		K_i (μM)	
	Ac-AI(X)AA-NH_2, X =	**c-Src**	**c-Abl**
2.1	Tyr	>1000	NT[a]
2.2	D-Tyr	>1000	>1000
2.3	D-Tyr, retro-inverso peptide	>1000	NT
2.4	Phe	950 ± 55	>500
2.5	Ala	>1000	>1000
2.6	Trp	>1000	>1000
2.7	His	218 ± 44	>1000

[a] Not tested

We also explored replacing tyrosine with other aromatic amino acids. Both peptides **2.6** and **2.7** contain amines that could mimic the hydrogen bonding of the tyrosine phenol. We found that the tryptophan peptide (**2.6**) was a poor inhibitor (K_i > 1000 μM) and the histidine peptide (**2.7**) had K_i = 218 μM. This suggests that the tyrosine may bind in a smaller pocket which does not accommodate binding of the larger tryptophan indole ring. Conversely, the histidine imidazole ring is closer in size to the tyrosine phenol, and therefore it can fit in the tyrosine binding site and possibly retain some of the hydrogen bonding interactions made by the tyrosine phenol. Interestingly, the histidine peptide also showed selectivity for c-Src over c-Abl. Although the histidine peptide was the most potent inhibitor found in the first library, it was not potent enough for use in future assay development. Ideally, a low micromolar or nanomolar probe is required for a fluorescence polarization assay in order to avoid the use of large (micromolar) quantities of enzyme.[29]

Evaluation of Peptides with Substituted Phenylalanine Pharmacophores

Although no inhibitors with low micromolar potency were found in the first library, it was hypothesized that substituted phenylalanine residues could make additional interactions within the substrate binding pocket to give more potent inhibitors. While previous studies have examined a small number of *para*-substituted phenylalanine derivatives as c-Src inhibitors, pharmacophores mono-substituted at the *ortho* or *meta* positions have not been explored. In addition to identifying more potent peptidic inhibitors, substituted phenylalanine pharmacophores could later be applied to the design of small molecule substrate-competitive inhibitors. A library of forty peptides containing substituted phenylalanine derivatives in place of the reactive tyrosine residue was evaluated using the pyrene peptide assay and the results are summarized in **Table 2.2**.

Of the *ortho*-substituted peptides (**2.8**-**2.12**), the best inhibitor was the *ortho*-fluoro peptide (**2.11**) with K_i = 433 μM. The increase in potency relative to the phenylalanine peptide (**2.4**) may be due to the increased hydrophobic surface area making greater interactions with a hydrophobic pocket.[30] This pocket is likely small, as potency decreases as the hydrophobic substituent increases in size with the *ortho*-methyl peptide (**2.8**) having K_i > 500 μM, the *ortho*-chloro peptide (**2.12**) having K_i = 845 μM, and the *ortho*-trifluoromethyl peptide (**2.9**) having K_i > 1000 μM. When the *meta*-substituted peptides (**2.13**-**2.17**) were evaluated none were found to be potent inhibitors of c-Src (all K_i > 1000 μM), suggesting that no additional interactions can be made with the substrate pocket at this location. To our knowledge, this is the first study to explore tyrosine pharmacophores mono-substituted at the *ortho* and *meta* positions. Although no beneficial substitutions at the *meta* position were identified, analysis of *ortho* substitutions suggests an *ortho*-fluorine substituent could be combined with an optimal *para* substituent to increase c-Src inhibitory potency.

Table 2.2. Peptides with the general structure Ac-AIXAA-NH_2, where X is a substituted phenylalanine derivative, were evaluated for c-Src and c-Abl inhibition using the pyrene assay.

		K_i (μM)	
	Ac-AI(X)AA-NH_2, X =	**c-Src**	**c-Abl**
2.8	2-CH_3 Phe	>500	>1000
2.9	2-CF_3 Phe	>1000	NT[a]
2.10	2-OCH_3 Phe	>1000	NT
2.11	2-F Phe	433 ± 48	>1000
2.12	2-Cl Phe	845 ± 186	>1000
2.13	3-CH_3 Phe	>1000	NT
2.14	3-CF_3 Phe	>1000	NT
2.15	3-OCH_3 Phe	>1000	NT
2.16	3-F Phe	>1000	NT
2.17	3-Cl Phe	>1000	NT
2.18	4-CH_3 Phe	>500	>1000
2.19	4-CF_3 Phe	862 ± 159	>1000
2.20	4-OCH_3 Phe	>1000	NT
2.21	4-OCH_2CH_3 Phe	>1000	NT
2.22	4-$OCHCH_2$ Phe	>1000	NT
2.23	4-OPh Phe	>1000	NT
2.24	4-OBn Phe	783 ± 156	>1000
2.25	4-Bz Phe	429 ± 91	>1000
2.26	4-CO_2H Phe	>1000	NT
2.27	4-CN Phe	>1000	NT
2.28	4-N_3 Phe	831 ± 199	>1000
2.29	4-NH_2 Phe	>1000	NT
2.30	4-CH_2NH_2 Phe	>1000	NT
2.31	4-SO_2NH_2 Phe	>1000	NT
2.32	4-guanido Phe	>1000	NT
2.33	4-F Phe	>500	NT
2.34	4-Cl Phe	446 ± 70	>1000
2.35	4-Br Phe	392 ± 97	>500
2.36	4-I Phe	242 ± 31	827 ± 81
2.37	4-NO_2 Phe	>1000	NT
2.38	3,4-OCH_3 Phe	>1000	NT
2.39	3-NO_2, 4-OAc Phe	789 ± 102	>1000
2.40	3,4-F Phe	379 ± 68	>500
2.41	3,5-F Phe	545 ± 37	912 ± 267
2.42	3,4,5-F Phe	>1000	NT
2.43	2,3,4,5,6-F Phe	205 ± 56	>250
2.44	1-naphthyl Ala	>1000	NT
2.45	2-naphthyl Ala	>1000	NT
2.46	4-Ph Phe	>1000	NT
2.47	3-pyridyl Ala	>1000	NT

[a] Not tested

Analysis of the *para*-substituted peptides revealed some trends that had not been previously observed in smaller *para*-substituted libraries. Similar to previous studies, we found that the *para*-methyl, *para*-trifluoromethyl, and *para*-methoxy peptides (**2.18**-**2.20**) were weak inhibitors of c-Src.[4, 9] We also evaluated *para*-ethoxy (**2.21**) and *para*-allyloxy (**2.22**) peptides and found that consistent with our results for the *para*-methoxy peptide (**2.20**) these peptides were also poor c-Src inhibitors (K_i > 1000 μM). Additionally, previously unexplored aryl ethers (**2.23** and **2.24**) were examined since these could provide additional opportunities for functionalization to improve potency. Like the alkyl ethers, the aryl ethers were also found to be weak c-Src inhibitors. The small increase in potency relative to phenylalanine observed with the *para*-benzyloxy peptide (**2.24**, K_i = 783 μM) is likely due to the benzyl ring beginning to reach the edge of the ATP pocket and making weak interactions there. A related peptide with *para*-benzoylphenylalanine (**2.25**) was one of the better peptides in the library (K_i = 429 μM), but it should be noted that this could be due to covalent inactivation of the enzyme. *Para*-benzoylphenylalanine is often used as a photoaffinity label and is activated at approximately 350 nm.[31] The pyrene reporter peptide assay used to evaluate the peptidic inhibitors uses an excitation wavelength of 340 nm. A *para*-carboxy substituted phenylalanine (**2.26**), which we hypothesized could possibly retain interactions made by the tyrosine hydroxyl group, was a poor inhibitor of c-Src (K_i > 1000 μM). Finally, a *para*-cyano peptide (**2.27**) did not inhibit c-Src (K_i > 1000 μM), and a *para*-azido peptide (**2.28**) showed only weak inhibition (K_i = 831 μM).

While our results for *para*-alkyl and *para*-ether substituents were in good agreement with previous studies, we did see discrepancies with other pharmacophores that have been described by Niu and Lawrence.[9] While our results agree with their report that substitutions containing primary amines (**2.29** and **2.30**) are poor c-Src inhibitors, we found that *para*-sulfonamide (**2.31**) and *para*-guanido (**2.32**) peptides were also poor inhibitors of c-Src (K_i > 1000 μM), despite being previously reported as two of their best pharmacophores for c-Src. Furthermore, Niu and Lawrence's pharmacophore evaluation showed that peptides with *para*-halogen substituted phenylalanines were worse inhibitors of c-Src compared to phenylalanine.[9] We observed the opposite trend and found inhibitor potency increased with increasing halogen size (**2.33**-**2.36**). The *para*-fluoro peptide

(**2.34**) was a poor inhibitor of c-Src (K_i > 500 μM), but the *para*-iodo peptide (**2.36**) was one of the most potent peptides with K_i = 242 μM. Although some of our results differ from previous reports, these peptides are in good agreement with the long held belief that the area surrounding the tyrosine binding site is largely hydrophobic.

In addition to examining monosubstituted phenylalanine analogues, we also evaluated phenylalanine analogues with multiple substituents. Overall, the best results were observed when the phenylalanine derivative contained multiple fluorines. Peptides di-substituted with non-halogen groups (**2.38** and **2.39**) were poor inhibitors of c-Src, but peptides di-substituted with fluorine (**2.40** and **2.41**) were modest inhibitors (K_i = 379 μM and K_i = 549 μM, respectively). It is interesting that the 3,5-difluoro peptide (**2.41**) was a modest inhibitor, since all of the peptides in the *meta* mono-substituted library were poor inhibitors. Furthermore, the fluorine tri-substituted peptide (**2.42**) was not an inhibitor of c-Src (K_i > 1000 μM), but the pentafluoro peptide (**2.43**) was the most potent peptide in the library (K_i = 205 μM). The pentafluorophenylalanine pharmacophore was previously evaluated by Niu and Lawrence and also generated one of the best peptides in their library.[9]

Finally, we evaluated adding rings to phenylalanine (**2.44**-**2.46**) as this could give further opportunities for optimization by functionalizing the additional rings. Unfortunately, none of the modifications were found to increase c-Src potency (K_i > 1000 μM). The 1-naphthylalanine (**2.44**) and 2-naphthylalanine (**2.45**) peptides are in good agreement with data from the tryptophan peptide and the *ortho* and *meta* substituted peptides, and the poor potency of these peptides confirms that the tyrosine binding site cannot accommodate larger substituents at the *ortho* and *meta* positions. However, it was surprising that the *para*-phenyl peptide (**2.46**) was not an inhibitor of c-Src since peptides with large *para*-halogen substituents (**2.35** and **2.36**) were among the best peptides in the library, suggesting that there is room at the *para* position to accommodate a phenyl ring. Combined with the data from the ether substituted peptides and the multiply fluorine-substituted peptides, it appears that both an increase in hydrophobic surface area and a decrease in the electron density within the phenylalanine ring are needed for increased potency relative to phenylalanine. This hypothesis is supported by the 3-pyridylalanine

peptide (**2.47**). Although this is an electron poor ring system, it does not have increased hydrophobic surface area and thus is a poor inhibitor (K_i > 1000 μM).

Fifteen of the peptides, including all of the peptides found to be c-Src inhibitors with K_i < 1000 μM, were also evaluated with c-Abl (**Table 2.2**). In general, none of the peptides tested were found to be potent inhibitors of c-Abl, and all of the peptides tested were less potent against c-Abl compared to c-Src. Only peptides containing halogen substitutions (**2.35** and **2.36**) had c-Abl K_i < 1000 μM, and no peptides with *ortho* or *meta* mono-substitution had c-Abl K_i < 1000 μM. Low solubility prevented the accurate evaluation of the pentafluorophenylalanine pharmacophore (**2.43**) with c-Abl. As was seen with c-Src, the results suggest that the area surrounding the tyrosine binding site is largely hydrophobic. Unfortunately, it is difficult to make comparisons and define what characteristics contribute to selectivity for c-Src over c-Abl because we do not know the K_d values for the starting peptide substrate and we could not accurately measure the K_i value for the phenylalanine peptide with c-Abl. The difference in pharmacophore potency between c-Src and c-Abl could be due to the substituents on the tyrosine pharmacophore making different interactions with the two binding sites, or could be due to the peptide scaffold having disparate affinity for c-Src versus c-Abl.

Evaluation of Literature Peptides

Although no peptides in the two libraries were found to have the desired low micromolar potency, several linear peptides have been reported in the literature as c-Src inhibitors with low micromolar to nanomolar potencies (**Scheme 2.4**). The peptide MIYKYYF (**2.48**) was developed by Kamath and coworkers based on the substrate peptide YIYGSFK and was reported to have c-Src IC_{50} = 6 μM in a radiometric assay.[32] Kumar and coworkers used the same c-Src substrate as a starting point and reported the peptide Ac-CIYK(4-NO_2 Phe)Y (**2.49**), which is the most potent linear peptidic inhibitor of c-Src reported with IC_{50} = 0.53 μM in a radiometric assay.[33] Finally, Hah and coworkers explored adding groups to both the N-terminus and an amino acid side chain within the optimal c-Src substrate EEEIYGEFEA-NH_2 to develop the peptide (Ba)-EEEIFGEF(Dap-Hna)-NH$(CH_2)_2$SH (**2.50**).[34] This peptide had c-Src IC_{50} = 2 μM in an ELISA-based assay.

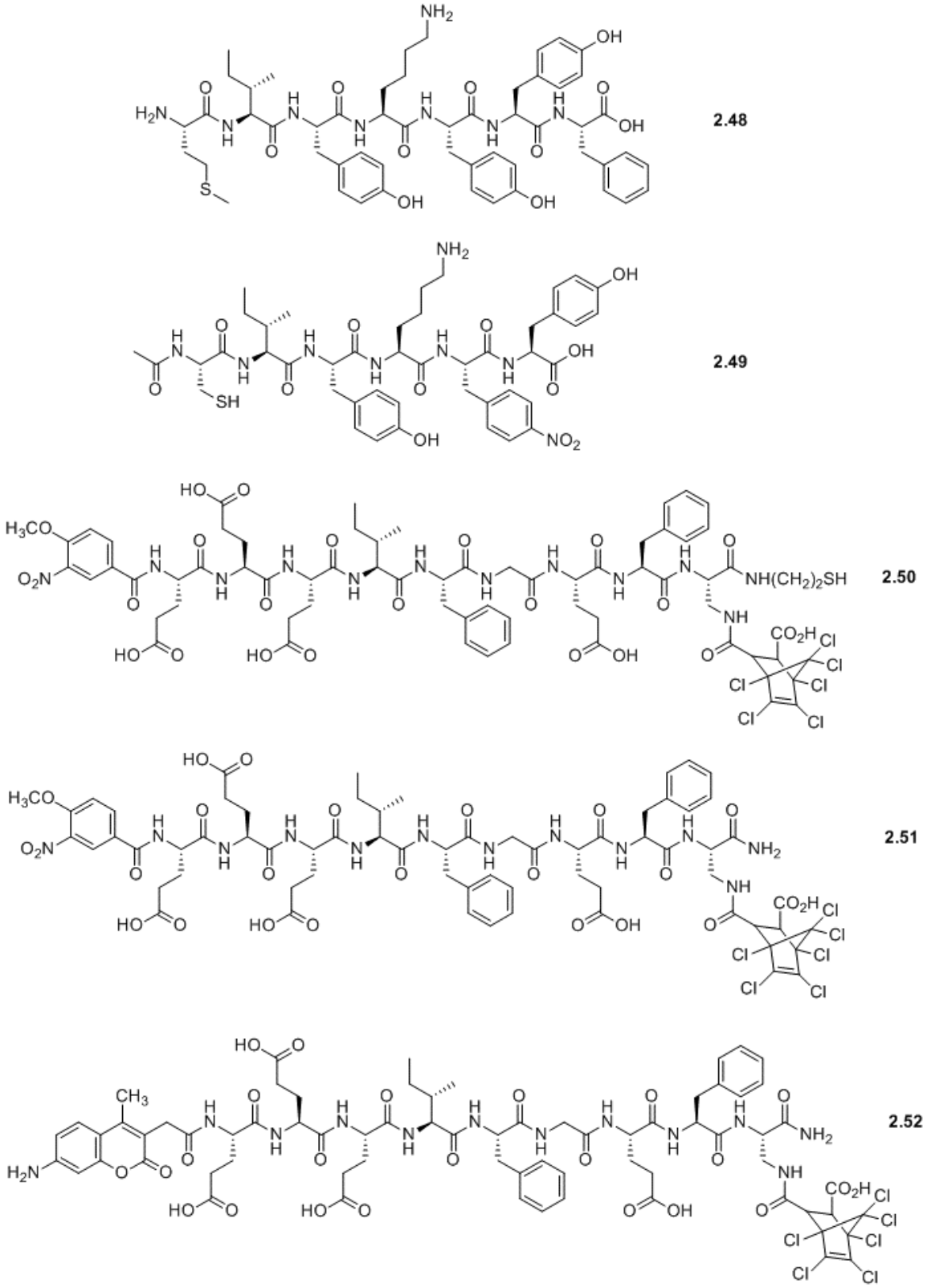

Scheme 2.4. Structures of reported potent peptidic inhibitors of c-Src (**2.48**-**2.50**) and two analogues (**2.51** and **2.52**).

The poor potency of our peptide library caused us to question the veracity of these reported inhibitors, especially considering that two of the inhibitors do not modify the reactive hydroxyl group and peptide **2.50** replaces the reactive tyrosine with phenylalanine. We decided to re-evaluate these peptides using the pyrene peptide assay to confirm their reported potencies. If these literature peptides were still potent inhibitors in our assay they could be fluorescently-labeled and used in future assay development. Peptides **2.48**, **2.49**, and **2.51** (prepared as an analogue of peptide **2.50** for synthetic ease) were prepared and evaluated in the pyrene peptide assay.

Table 2.3. Comparison of reported IC_{50} values for peptidic inhibitors of c-Src with values obtained using the pyrene assay.

	Reported c-Src IC_{50} (μM)	**Pyrene Peptide Assay c-Src K_i (μM)**	**Substrate Used in Assay for Reported Value**
2.48	6	>1000	YIYGSFK
2.49	0.53	>1000	polE_4Y
2.50	1.9 ± 0.3	NT[a]	biotinyl-(aminohexanoic acid)$_2$-AEEEIYGEF-NH_2
2.51	NA[b]	70 ± 16	NA
2.52	NA	49 (n = 2)	NA

[a] Not tested
[b] Not applicable, analogue prepared for current study

The results from analysis of the literature peptides are shown in **Table 2.3**. Overall, poor agreement was observed between our assay and the reported IC_{50} values. Peptides **2.48** and **2.49** were not c-Src inhibitors in our hands. Furthermore, although c-Src inhibition was observed for analogue peptide **2.51** (K_i = 70 μM) it was significantly less potent than the literature peptide **2.50** (IC_{50} = 1.9 μM).[34] It has previously been reported that c-Src inhibition by the peptide CIYKYY, which peptide **2.49** is an analogue of, is dependent on the peptide substrate used in the assay.[33] A similar phenomenon could be occurring in our assay and may be responsible for the discrepancies from the literature values. It is worth noting that the peptide substrate used in the reported analysis of peptide **2.50** is the most similar to the pyrene peptide substrate used in our assays, and

the best agreement with the literature value was seen with our analogue peptide **2.51**. Because peptide **2.51** was the most potent inhibitor peptide identified from our studies, an AMCA-labeled derivative (**2.52**) was also evaluated and found to have K_i = 49 μM. Although a small increase in potency was observed relative to the parent peptide **2.51**, peptide **2.52** is still not potent enough for the development of an FP assay.

Conclusions

This study evaluated three libraries of peptides in order to identify new tyrosine pharmacophores for c-Src kinase and to discover potent peptidic inhibitors of c-Src that could be used in FP assay development. Two libraries of peptides were prepared based on the c-Src and c-Abl substrate Ac-AIYAA-NH_2, and the third library was composed of peptides (or analogues thereof) reported to be potent inhibitors of c-Src.

The initial library of peptides incorporating natural amino acid pharmacophores was in good agreement with previously reported trends.[1-2] In general, poor inhibition was observed upon replacement of the reactive tyrosine residue. Although the histidine peptide (**2.7**) showed improvement relative to the phenylalanine pharmacophore, only modest c-Src inhibition (K_i = 218 μM) was observed. Due to the poor potency of these peptides, we then turned our attention towards identifying substituted phenylalanine pharmacophores.

While peptidic inhibitors of c-Src using substituted phenylalanine pharmacophores have been previously reported, the pharmacophores were generally limited to those with *para* mono-substitutions.[4, 9] In the current study we have expanded the substituents explored at the *para* position as well as the effects of substitutions at the *ortho* and *meta* positions. Although no mono-substitutions at the *meta* position were found to increase potency, an *ortho*-fluorine group (**2.11**) increased potency and could later be combined with optimal *para* substituents to increase potency. The best *para* substituents were halogens, and inhibitor potency increased with increasing halogen size. The best c-Src inhibition was produced by pentafluoro-phenylalanine (**2.43**, K_i = 205 μM). Because other substitutions that only increased hydrophobicity or only decreased electron density were poor inhibitors, we hypothesize that pharmacophores must both increase the

hydrophobic surface area and decrease the electron density within the phenylalanine ring in order to produce c-Src inhibition.

Although pharmacophores that increased c-Src potency relative to phenylalanine were identified, none of the peptides had the desired low micromolar potency necessary for developing an FP probe. This prompted us to re-examine three peptides reported in the literature to be potent inhibitors of c-Src. In our hands, only one of these peptides (**2.51**) was a c-Src inhibitor, and it was found to be significantly less potent than reported (K_i = 70 μM).[34] An AMCA-labeled analogue of this peptide (**2.52**) was also evaluated and found to have slightly increased potency, but was still at least one order of magnitude less potent than required for FP assay development.

Taken together, these peptide libraries have reaffirmed long-held beliefs about the substrate binding site as well as given new insight into the design of future pharmacophores. It has long been thought that the tyrosine hydroxyl group makes important hydrogen bonding contacts within the substrate binding site. Although peptidic substrates have been identified with low micromolar K_M values, the K_d values for kinase substrates are thought to likely be in the low hundreds of micromolar range. The loss of the hydrogen bonding contacts made by the tyrosine hydroxyl group would further decrease the binding affinity of peptidic inhibitors. Combined with our pharmacophore analysis, this suggests that an ideal pharmacophore would maintain these hydrogen bonding contacts, have increased hydrophobic surface area, and have decreased electron density. The development of such a pharmacophore may enable the design of peptidic inhibitors with the low micromolar potency required for FP assay development.

Materials and Methods

General Synthetic Methods

Unless otherwise noted, all reagents were obtained via commercial sources and used without further purification. Mass spectrometry (MS) was performed using a Waters MicromassZQ or MicromassLCT mass spectrometer. High resolution mass spectrometry (HRMS) was carried out by the University of Michigan Mass Spectrometry Facility (J. Windak, director).

Synthesis of Ac-AIXAA-NH_2 Peptides

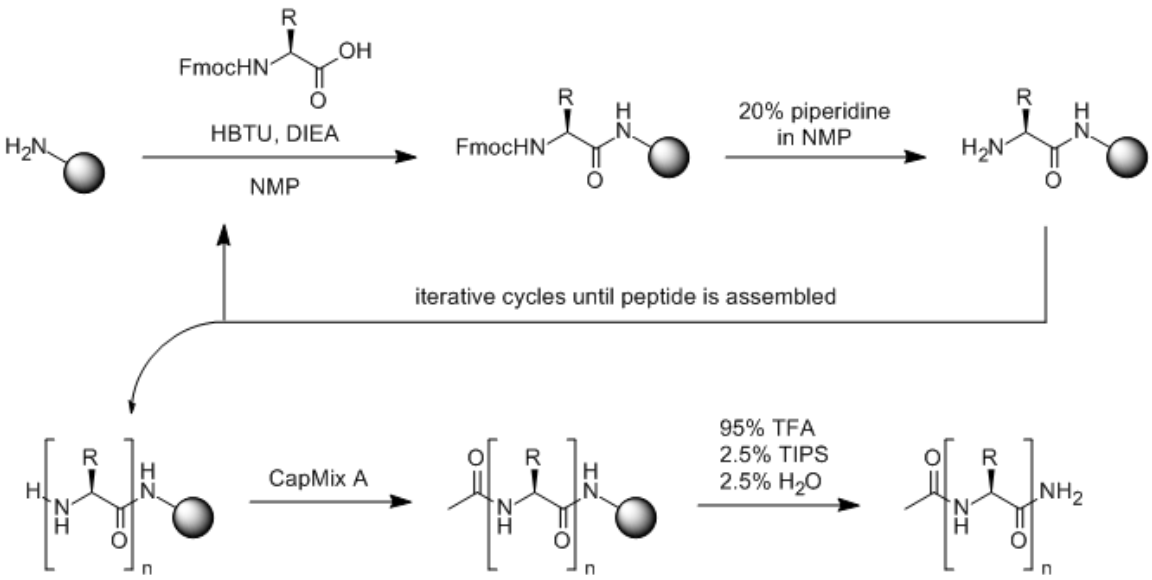

Scheme 2.5. Fmoc-based solid phase peptide synthesis.

General Solid Phase Peptide Synthesis Protocol. Peptides were prepared on resin following standard procedures for Fmoc solid phase peptide synthesis.[26] Fmoc-protected Rink amide resin (1 eq.) was swelled in NMP and deprotected by gently shaking in 20% piperidine in NMP for 20 minutes at room temperature. The deprotection solution was drained and the resin was washed three times with NMP. A solution containing the desired amino acid (5 eq.), HBTU (5 eq.), and DIEA (5 eq.) was added to the resin and the mixture was gently shaken at room temperature for 20 minutes. The resin was drained and washed three times with NMP. Iterative cycles of deprotection and amino acid coupling were repeated until the desired peptide sequence was completed, and then the N-terminus was acetylated following removal of the N-terminal protecting group. An excess of CapMix A solution (10% acetic anhydride, 10% 2,6-lutidine, 80% THF) was added to the resin, and the mixture was gently shaken at room temperature for 20 minutes. The solution was drained and the resin was washed three times with NMP and three times with DCM. The peptides were cleaved from the resin by treatment with a 95% TFA, 2.5% TIPS, and 2.5% H_2O solution. The mixture was gently stirred for 1-2h at room temperature, and then the solution was drained and concentrated under reduced

pressure. Peptides were purified by reverse phase HPLC using a 5 → 95% ACN in H_2O (+0.1% TFA) gradient. Assistance with peptide synthesis and purification was provided by Dr. Sonali Kurup and Chenxi Shen.

Ac-AIYAA-NH_2 (**2.1**). HRMS-ESI (*m*/*z*): $[M+Na]^+$ calcd for $C_{26}H_{40}N_6O_7$, 571.2856; found 571.2848.

Ac-AIyAA-NH_2 (**2.2**). HRMS-ESI (*m*/*z*): $[M+Na]^+$ calcd for $C_{26}H_{40}N_6O_7$, 571.2856; found 571.2848.

Ac-aayia-NH_2 (**2.3**). MS-ESI (*m*/*z*): $[M+Na]^+$ calcd for $C_{26}H_{40}N_6O_7$, 571.3; found 571.1.

Ac-AIFAA-NH_2 (**2.4**). HRMS-ESI (*m*/*z*): $[M+Na]^+$ calcd for $C_{26}H_{40}N_6O_6$, 555.2907; found 555.2902.

Ac-AIAAA-NH_2 (**2.5**). HRMS-ESI (*m*/*z*): $[M+Na]^+$ calcd for $C_{20}H_{36}N_6O_6$, 479.2594; found 479.2586.

Ac-AIWAA-NH_2 (**2.6**). MS-ESI (*m*/*z*): $[M+Na]^+$ calcd for $C_{28}H_{41}N_7O_6$, 594.3; found 594.1.

Ac-AIHAA-NH_2 (**2.7**). MS-ESI (*m*/*z*): $[M+H]^+$ calcd for $C_{23}H_{38}N_8O_6$, 522.3; found 521.2.

Ac-AI(2-CH_3 Phe)AA-NH_2 (**2.8**). HRMS-ESI (*m*/*z*): $[M+Na]^+$ calcd for $C_{27}H_{42}N_6O_6$, 569.3064; found 569.3051.

Ac-AI(2-CF_3 Phe)AA-NH_2 (**2.9**). HRMS-ESI (*m*/*z*): $[M+Na]^+$ calcd for $C_{27}H_{39}F_3N_6O_6$, 623.2781; found 623.2786.

Ac-AI(2-OCH_3 Phe)AA-NH_2 (**2.10**). HRMS-ESI (*m*/*z*): $[M+Na]^+$ calcd for $C_{27}H_{42}N_6O_7$, 585.3013; found 585.3022.

Ac-AI(2-F Phe)AA-NH_2 (**2.11**). HRMS-ESI (*m*/*z*): $[M+Na]^+$ calcd for $C_{26}H_{39}FN_6O_6$, 573.2813; found 573.2823.

Ac-AI(2-Cl Phe)AA-NH_2 (**2.12**). HRMS-ESI (*m*/*z*): $[M+Na]^+$ calcd for $C_{26}H_{39}ClN_6O_6$, 589.2517; found 589.2522.

Ac-AI(3-CH_3 Phe)AA-NH_2 (**2.13**). HRMS-ESI (*m*/*z*): $[M+Na]^+$ calcd for $C_{27}H_{42}N_6O_6$, 569.3064; found 569.3059.

Ac-AI(3-CF_3 Phe)AA-NH_2 (**2.14**). HRMS-ESI (*m*/*z*): $[M+Na]^+$ calcd for $C_{27}H_{39}F_3N_6O_6$, 623.2781; found 623.2781.

Ac-AI(3-OCH_3 Phe)AA-NH_2 (**2.15**). HRMS-ESI (*m*/*z*): $[M+Na]^+$ calcd for $C_{27}H_{42}N_6O_7$, 585.3013; found 585.3021.

Ac-AI(3-F Phe)AA-NH_2 (**2.16**). HRMS-ESI (*m*/*z*): $[M+Na]^+$ calcd for $C_{26}H_{39}FN_6O_6$, 573.2813; found 573.2817.

Ac-AI(3-Cl Phe)AA-NH_2 (**2.17**). HRMS-ESI (*m*/*z*): $[M+Na]^+$ calcd for $C_{26}H_{39}ClN_6O_6$, 589.2517; found 589.2519.

Ac-AI(4-CH_3 Phe)AA-NH_2 (**2.18**). HRMS-ESI (*m*/*z*): $[M+Na]^+$ calcd for $C_{27}H_{42}N_6O_6$, 569.3064; found 569.3053.

Ac-AI(4-CF_3 Phe)AA-NH_2 (**2.19**). HRMS-ESI (*m*/*z*): $[M+Na]^+$ calcd for $C_{27}H_{39}F_3N_6O_6$, 623.2781; found 623.2782.

Ac-AI(4-OCH_3 Phe)AA-NH_2 (**2.20**). HRMS-ESI (*m*/*z*): $[M+Na]^+$ calcd for $C_{27}H_{42}N_6O_7$, 585.3013; found 585.3015.

Ac-AI(4-OCH_2CH_3 Phe)AA-NH_2 (**2.21**). HRMS-ESI (*m*/*z*): $[M+Na]^+$ calcd for $C_{28}H_{44}N_6O_7$, 599.3169; found 599.3167.

Ac-AI(4-$OCHCH_2$)AA-NH_2 (**2.22**). HRMS-ESI (*m*/*z*): $[M+Na]^+$ calcd for $C_{28}H_{42}N_6O_7$, 611.3169; found 611.3193.

Ac-AI(4-OPh Phe)AA-NH_2 (**2.23**). HRMS-ESI (*m*/*z*): $[M+Na]^+$ calcd for $C_{32}H_{44}N_6O_7$, 647.3169; found 647.3162.

Ac-AI(4-OBn Phe)AA-NH_2 (**2.24**). HRMS-ESI (*m*/*z*): $[M+Na]^+$ calcd for $C_{33}H_{46}N_6O_7$, 661.3326; found 661.3333.

Ac-AI(4-Bz Phe)AA-NH_2 (**2.25**). HRMS-ESI (*m*/*z*): $[M+Na]^+$ calcd for $C_{33}H_{44}N_6O_7$, 659.3169; found 659.3159.

Ac-AI(4-CO_2H Phe)AA-NH_2 (**2.26**). HRMS-ESI (*m*/*z*): $[M+Na]^+$ calcd for $C_{27}H_{40}N_6O_8$, 599.2805; found 599.2802.

Ac-AI(4-CN Phe)AA-NH_2 (**2.27**). HRMS-ESI (*m*/*z*): $[M+Na]^+$ calcd for $C_{27}H_{39}N_7O_6$, 580.2860; found 580.2858.

Ac-AI(4-N_3 Phe)AA-NH_2 (**2.28**). HRMS-ESI (*m*/*z*): $[M+Na]^+$ calcd for $C_{26}H_{39}N_9O_6$, 596.2921; found 596.2932.

Ac-AI(4-NH_2 Phe)AA-NH_2 (**2.29**). HRMS-ESI (*m*/*z*): $[M+Na]^+$ calcd for $C_{26}H_{41}N_7O_6$, 570.3016; found 570.3000.

Ac-AI(4-CH_2NH_2 Phe)AA-NH_2 (**2.30**). HRMS-ESI (*m*/*z*): $[M+Na]^+$ calcd for $C_{27}H_{43}N_7O_6$, 584.3173; found 584.3163.

Ac-AI(4-SO_2NH_2 Phe)AA-NH_2 (**2.31**). HRMS-ESI (*m*/*z*): $[M+Na]^+$ calcd for $C_{26}H_{41}N_7O_8S$, 634.2635; found 634.2658.

Ac-AI(4-guanido Phe)AA-NH_2 (**2.32**). HRMS-ESI (*m*/*z*): $[M+Na]^+$ calcd for $C_{27}H_{43}N_9O_6$, 612.3234; found 612.3226.

Ac-AI(4-F Phe)AA-NH_2 (**2.33**). HRMS-ESI (*m*/*z*): $[M+ Na]^+$ calcd for $C_{26}H_{39}FN_6O_6$, 573.2813; found 573.2809.

Ac-AI(4-Cl Phe)AA-NH_2 (**2.34**). HRMS-ESI (*m*/*z*): $[M+Na]^+$ calcd for $C_{26}H_{39}ClN_6O_6$, 589.2517; found 589.2518.

Ac-AI(4-Br Phe)AA-NH_2 (**2.35**). HRMS-ESI (*m*/*z*): $[M+Na]^+$ calcd for $C_{26}H_{39}BrN_6O_6$, 633.2012; found 633.2012.

Ac-AI(4-I Phe)AA-NH_2 (**2.36**). HRMS-ESI (*m*/*z*): $[M+Na]^+$ calcd for $C_{26}H_{39}IN_6O_6$, 681.1874; found 681.1874.

Ac-AI(4-NO_2 Phe)AA-NH_2 (**2.37**). HRMS-ESI (*m*/*z*): $[M+Na]^+$ calcd for $C_{26}H_{39}N_7O_8$, 600.2758; found 600.2753.

Ac-AI(3,4-OCH_3 Phe)AA-NH_2 (**2.38**). HRMS-ESI (*m*/*z*): $[M+Na]^+$ calcd for $C_{28}H_{44}N_6O_8$, 615.3118; found 615.3119.

Ac-AI(3-NO_2, 4-OAc Phe)AA-NH_2 (**2.39**). MS-ESI (*m*/*z*): $[M+Na]^+$ calcd for $C_{28}H_{41}N_7O_{10}$, 658.3; found 658.0.

Ac-AI(3,4-F Phe)AA-NH_2 (**2.40**). HRMS-ESI (*m*/*z*): $[M+Na]^+$ calcd for $C_{26}H_{38}F_2N_6O_6$, 591.2719; found 591.2722.

Ac-AI(3,5-F Phe)AA-NH_2 (**2.41**). HRMS-ESI (*m*/*z*): $[M+Na]^+$ calcd for $C_{26}H_{38}F_2N_6O_6$, 591.2719; found 591.2719.

Ac-AI(3,4,5-F Phe)AA-NH_2 (**2.42**). HRMS-ESI (*m*/*z*): $[M+Na]^+$ calcd for $C_{26}H_{37}F_3N_6O_6$, 609.2624; found 609.2623.

Ac-AI(2,3,4,5,6-F Phe)AA-NH_2 (**2.43**). HRMS-ESI (*m*/*z*): $[M+Na]^+$ calcd for $C_{26}H_{35}F_5N_6O_6$, 645.2436; found 645.2430.

Ac-AI(1-naphthyl Ala)AA-NH_2 (**2.44**). HRMS-ESI (*m*/*z*): $[M+Na]^+$ calcd for $C_{30}H_{42}N_6O_6$, 605.3064; found 605.3084.

Ac-AI(2-naphthyl Ala)AA-NH_2 (**2.45**). HRMS-ESI (*m*/*z*): $[M+Na]^+$ calcd for $C_{30}H_{42}N_6O_6$, 605.3064; found 605.3057.

Ac-AI(4-Ph Phe)AA-NH_2 (**2.46**). HRMS-ESI (*m*/*z*): $[M+Na]^+$ calcd for $C_{32}H_{44}N_6O_6$, 631.3220; found 631.3239.

Ac-AI(3-pyridyl Ala)AA-NH_2 (**2.47**). HRMS-ESI (*m*/*z*): $[M+Na]^+$ calcd for $C_{25}H_{39}N_7O_6$, 556.260; found 556.2849.

Synthesis of Literature Peptides

MIYKYYF (**2.48**). Peptide **2.48** was prepared as previously described.[32] MS-ESI (*m*/*z*): $[M+H]^+$ calcd for $C_{53}H_{70}N_8O_{11}S$, 1027.5; found 1027.1.

Ac-CIYK(4-NO_2 Phe)F (**2.49**). Peptide **2.49** was prepared as previously described.[33] MS-ESI (*m*/*z*): $[M+H]^+$ calcd for $C_{44}H_{58}N_8O_{12}S$, 923.4; found 923.0.

(Ba)-EEEIFGEF(Dap-Hna)-NH_2 (**2.51**). Peptide **2.51** was prepared as previously described using Rink amide resin in place of TentaGel resin.[34] MS-ESI (*m*/*z*): $[M+Na]^+$ calcd for $C_{66}H_{76}Cl_6N_{12}O_{24}$, 1655.3; found 1656.9.

(AMCA)-EEEIFGEF(Dap-Hna)-NH_2 (**2.52**). Peptide **2.52** was prepared in the same manner as peptide **2.51** by replacing Ba (4-methoxy-3-nitrobenzoic acid) with AMCA. MS-ESI (*m*/*z*): $[M+2Na]^{2+}$ calcd for $C_{70}H_{80}Cl_6N_{12}O_{23}$, 857.2; found 856.3.

General Biochemical Methods

Black, opaque-bottom 96 well plates were used for fluorescence assays and were purchased from Nunc. c-Src, c-Abl, and NDPK were expressed in *E. coli* using previously published procedures.[13] IDCC-NDPK-P was prepared as previously described.[23] Data was obtained using a Molecular Devices SpectraMax M5 plate reader. Curve fitting was performed using GraphPad Prism 4 software unless otherwise noted.

Determination of Peptide Substrate 2.1 K_M

A coupled continuous fluorescence assay was used to determine K_M for peptide substrate **2.1**.[23] Reaction volumes of 40 μL were used in 96-well plates. To each well was added 4 μL of 10X buffer, 20 μL H_2O, 2 μL of the substrate dilution (typically 20, 10, 5, 2.5, 1.25, 0.625, and 0.313 mM in DMSO), 4 μL of IDCC-NDPK-P (12.5 μM), and 4 μL of the appropriate kinase (1.2 μM for c-Src or 0.6 μM for c-Abl). The contents were incubated for 5 minutes at room temperature, and then the kinase reaction was initiated

by the addition of 4 μL of ATP (1 mM in water) and reaction progress was immediately monitored at 475 nm (ex. 436 nm) for 10 minutes. Reactions had final concentrations of 100 μM ATP, 100mM Tris buffer (pH 8), 10 mM $MgCl_2$, and 120 nM c-Src or 60 nM c-Abl. The initial rate data collected was used for determination of K_M values, which were obtained directly from nonlinear regression of substrate-velocity curves. The K_M values for **2.1** were determined using at least 3 independent experiments which were averaged to give an average K_M value ± standard deviation. Data for peptide **2.1** was provided by Dr. Sonali Kurup.

Determination of Inhibitor K_i

A continuous fluorescence assay was used to determine K_i.[27] Reaction volumes of 100 μL were used in 96-well plates. 85 μL of enzyme in buffer mix was added to each well followed by 2.5 μL of the appropriate inhibitor dilution (typically 40, 20, 10, 5, 2.5, 1.25, 0.625, and 0.313 mM in DMSO) and 2.5 μL of a substrate peptide solution ("compound 3" as described in Wang *et al.*, 1.8 mM in DMSO). The reaction was initiated with 10 μL of ATP (10 mM in water), and reaction progress was immediately monitored at 405 nm (ex. 340 nm) for 10 minutes. Reactions had final concentrations of 1 mM ATP, 45 μM "substrate 3" peptide, 100 μM Na_3VO_4, 100mM Tris buffer (pH 8), 10 mM $MgCl_2$, and 0.01% Triton X-100. c-Src kinase domain assays had a final concentration of 30 nM enzyme and c-Abl kinase domain assays had a final concentration of 300 nM enzyme.

The initial rate data collected was used for determination of K_i values. For K_i determination, the IC_{50} values were obtained directly from nonlinear regression of substrate-velocity curves in the presence of various concentrations of the inhibitor and converted to K_i values using the Cheng-Prusoff equation. The K_M values used for "substrate 3" were determined as described below (see "Determination of Peptide Substrate "Substrate 3" K_M"). The K_i value for each peptide was determined using at least 3 independent experiments which were averaged to give an average K_i value ± standard deviation. For analytical data see **Appendix A**.

Determination of Peptide Substrate "Substrate 3" K_M

The previously described continuous fluorescence assay was used to determine K_M for "substrate 3" described in Wang *et al*.[27] Reaction volumes of 100 µL were used in 96-well plates. 85 µL of enzyme in buffer mix was added to each well followed by 2.5 µL of the appropriate dilution of "substrate 3" (typically 20, 10, 5, 2.5, 1.25, 0.625, 0.31, 0.16, 0.078, and 0 mM in DMSO) and 2.5 µL of DMSO. The reaction was initiated with 10 µL of ATP (10 mM in water), and reaction progress was immediately monitored at 405 nm (ex. 340 nm) for 10 minutes. Reactions had final concentrations of 1 mM ATP, 100 µM Na_3VO_4, 100mM Tris buffer (pH 8), 10 mM $MgCl_2$, and 0.01% Triton X-100. c-Src reactions had a final concentration of 30 nM enzyme, and c-Abl reactions had a final concentration of 300 nM enzyme.

The initial rate data collected was used for determination of K_M values, which were obtained directly from nonlinear regression of substrate-velocity curves. The "substrate 3" K_M values were determined using at least 3 independent experiments which were averaged to give an average K_M value ± standard deviation. Representative substrate velocity curves for "substrate 3" with c-Src kinase domain and c-Abl kinase domain are shown in **Appendix A**.

References

1. Eldar-Finkelman, H.; Eisenstein, M., Peptide Inhibitors Targeting Protein Kinases *Current Pharmaceutical Design* **2009,** *15* (21), 2463-2470.
2. Bogoyevitch, M. A.; Barr, R. K.; Ketterman, A. J., Peptide inhibitors of protein kinases—discovery, characterisation and use. *Biochimica et Biophysica Acta (BBA) - Proteins and Proteomics* **2005,** *1754* (1–2), 79-99.
3. Wong, T. W.; Goldberg, A. R., Kinetics and mechanism of angiotensin phosphorylation by the transforming gene product of Rous sarcoma virus. *J. Biol. Chem.* **1984,** *259* (5), 3127-3131.
4. Shoelson, S. E.; White, M. F.; Kahn, C. R., Nonphosphorylatable substrate analogs selectively block autophosphorylation and activation of the insulin receptor, epidermal growth factor receptor, and pp60v-src kinases. *J. Biol. Chem.* **1989,** *264* (14), 7831-7836.
5. Yuan, C. J.; Jakes, S.; Elliott, S.; Graves, D. J., A rationale for the design of an inhibitor of tyrosyl kinase. *J. Biol. Chem.* **1990,** *265* (27), 16205-16209.
6. Fry, D. W.; McMichael, A.; Singh, J.; Dobrusin, E. M.; McNamara, D. J., Design of a potent peptide inhibitor of the epidermal growth factor receptor tyrosine kinase utilizing sequences based on the natural phosphorylation sites of phospholipase C-γ1. *Peptides* **1994,** *15* (6), 951-957.

7. Cole, P. A.; Grace, M. R.; Phillips, R. S.; Burn, P.; Walsh, C. T., The Role of the Catalytic Base in the Protein Tyrosine Kinase Csk. *J. Biol. Chem.* **1995,** *270* (38), 22105-22108.
8. Kim, M. H.; Lai, J. H.; Hangauer, D. G., Tetrapeptide tyrosine kinase inhibitors. *International Journal of Peptide and Protein Research* **1994,** *44* (5), 457-465.
9. Niu, J.; Lawrence, D. S., Nonphosphorylatable Tyrosine Surrogates: Implications for Protein Kinase Inhibitor Design. *J. Biol. Chem.* **1997,** *272* (3), 1493-1499.
10. Niu, J.; Lawrence, D. S., l-Dopa: A Powerful Nonphosphorylatable Tyrosine Mimetic for pp60c-src. *J. Am. Chem. Soc.* **1997,** *119* (16), 3844-3845.
11. Martin, G. S., The hunting of the Src. *Nat. Rev. Mol. Cell Biol.* **2001,** *2* (6), 467-475.
12. Thomas, S. M.; Brugge, J. S., Cellular functions regulated by Src family kinases. *Annu. Rev. Cell Dev. Biol.* **1997,** *13*, 513-609.
13. Seeliger, M. A.; Young, M.; Henderson, M. N.; Pellicena, P.; King, D. S.; Falick, A. M.; Kuriyan, J., High yield bacterial expression of active c-Abl and c-Src tyrosine kinases. *Protein Science* **2005,** *14* (12), 3135-3139.
14. Kim, L. C.; Song, L.; Haura, E. B., Src kinases as therapeutic targets for cancer. *Nat Rev Clin Oncol* **2009,** *6* (10), 587-595.
15. Sicheri, F.; Kuriyan, J., Structures of Src-family tyrosine kinases. *Curr. Opin. Struct. Biol.* **1997,** *7* (6), 777-785.
16. Trevino, J. G.; Summy, J. M.; Gallick, G. E., Src Inhibitors as Potential Therapeutic Agents for Human Cancers. *Mini Reviews in Medicinal Chemistry* **2006,** *6* (6), 681-687.
17. Chong, Y.-P.; Ia, K. K.; Mulhern, T. D.; Cheng, H.-C., Endogenous and synthetic inhibitors of the Src-family protein tyrosine kinases. *Biochimica et Biophysica Acta (BBA) - Proteins and Proteomics* **2005,** *1754* (1–2), 210-220.
18. Sawyer, T.; Boyce, B.; Dalgarno, D.; Iuliucci, J., Src inhibitors: genomics to therapeutics. *Expert Opinion on Investigational Drugs* **2001,** *10* (7), 1327-1344.
19. Colicelli, J., ABL Tyrosine Kinases: Evolution of Function, Regulation, and Specificity. *Sci. Signal.* **2010,** *3* (139), re6-.
20. Musumeci, F.; Schenone, S.; Brullo, C.; Botta, M., An update on dual Src/Abl inhibitors. *Future Med. Chem.* **2012,** *4* (6), 799-822.
21. Till, J. H.; Annan, R. S.; Carr, S. A.; Miller, W. T., Use of synthetic peptide libraries and phosphopeptide-selective mass spectrometry to probe protein kinase substrate specificity. *J. Biol. Chem.* **1994,** *269* (10), 7423-7428.
22. Songyang, Z.; Carraway, K. L.; Eck, M. J.; Harrison, S. C.; Feldman, R. A.; Mohammadi, M.; Schlessinger, J.; Hubbard, S. R.; Smith, D. P.; Eng, C.; Lorenzo, M. J.; Ponder, B. A. J.; Mayer, B. J.; Cantley, L. C., Catalytic specificity of protein-tyrosine kinases is critical for selective signalling. *Nature* **1995,** *373* (6514), 536-539.
23. Brune, M.; Corrie, J. E. T.; Webb, M. R., A Fluorescent Sensor of the Phosphorylation State of Nucleoside Diphosphate Kinase and Its Use To Monitor Nucleoside Diphosphate Concentrations in Real Time†. *Biochemistry* **2001,** *40* (16), 5087-5094.
24. Adams, J. A.; Taylor, S. S., Energetic limits of phosphotransfer in the catalytic subunit of cAMP-dependent protein kinase as measured by viscosity experiments. *Biochemistry* **1992,** *31* (36), 8516-8522.

25. Wang, C.; Lee, T. R.; Lawrence, D. S.; Adams, J. A., Rate-Determining Steps for Tyrosine Phosphorylation by the Kinase Domain of v-fps†. *Biochemistry* **1996,** *35* (5), 1533-1539.
26. Amblard, M.; Fehrentz, J.-A.; Martinez, J.; Subra, G., Methods and protocols of modern solid phase peptide synthesis. *Mol Biotechnol* **2006,** *33* (3), 239-254.
27. Wang, Q.; Cahill, S. M.; Blumenstein, M.; Lawrence, D. S., Self-Reporting Fluorescent Substrates of Protein Tyrosine Kinases. *J. Am. Chem. Soc.* **2006,** *128* (6), 1808-1809.
28. Hubbard, S. R., *Crystal structure of the activated insulin receptor tyrosine kinase in complex with peptide substrate and ATP analog*. 1997; Vol. 16, p 5572-5581.
29. Zettner, A., Principles of Competitive Binding Assays (Saturation Analyses). I. Equilibrium Techniques. *Clinical Chemistry* **1973,** *19* (7), 699-705.
30. Gao, J.; Qiao, S.; Whitesides, G. M., Increasing Binding Constants of Ligands to Carbonic Anhydrase by Using "Greasy Tails". *J. Med. Chem.* **1995,** *38* (13), 2292-2301.
31. Dorman, G.; Prestwich, G. D., Benzophenone Photophores in Biochemistry. *Biochemistry* **1994,** *33* (19), 5661-5673.
32. Kamath, J. R.; Liu, R.; Enstrom, A. M.; Lou, Q.; Lam, K. S., Development and characterization of potent and specific peptide inhibitors of p60c-src protein tyrosine kinase using pseudosubstrate-based inhibitor design approach. *The Journal of Peptide Research* **2003,** *62* (6), 260-268.
33. Kumar, A.; Ye, G.; Wang, Y.; Lin, X.; Sun, G.; Parang, K., Synthesis and Structure−Activity Relationships of Linear and Conformationally Constrained Peptide Analogues of CIYKYY as Src Tyrosine Kinase Inhibitors. *J. Med. Chem.* **2006,** *49* (11), 3395-3401.
34. Hah, J.-M.; Sharma, V.; Li, H.; Lawrence, D. S., Acquisition of a “Group A”-Selective Src Kinase Inhibitor via a Global Targeting Strategy. *J. Am. Chem. Soc.* **2006,** *128* (18), 5996-5997.

CHAPTER III

A Substrate Activity Screening Method for Tyrosine Kinases

Abstract

Despite the interest in substrate-competitive kinase inhibitors, few screening methods exist that can identify small molecule substrate-competitive inhibitors. This chapter details the development of a substrate activity screening method for the identification of substrate-competitive tyrosine kinase inhibitors. Using this methodology, we have identified the first small molecule substrate-competitive inhibitor of c-Src with activity in both biochemical and cellular assays. Analysis of the lead compound *in cellulo* revealed that substrate-competitive inhibitors possess unique properties such as cellular potency equivalent to biochemical potency, an enhanced selectivity profile, and synergy with ATP-competitive inhibitors. The described substrate activity screening methodology is the first general method that can exclusively identify small molecule substrate-competitive kinase inhibitors and should be applicable to any tyrosine kinase of interest.

Introduction

In spite of the interest in substrate-competitive kinase inhibitors, there are far fewer substrate-competitive inhibitors reported compared to ATP-competitive inhibitors, and the majority of substrate-competitive inhibitors are peptides.[1-3] These inhibitors often have poor potency as well as poor permeability and stability due to their peptidic nature, and this makes them unsuitable for use *in vivo*.[4] Even fewer small molecule substrate-competitive inhibitors have been reported, a fact that is largely attributed to the difficulty associated with identifying substrate-competitive inhibitors from high throughput screens.[5-6] Unlike the ATP binding site, which is located in a deep hydrophobic cleft, the substrate binding site is a shallow, solvent exposed surface that facilitates protein-protein interactions. The differences in these two binding sites make the ATP site far more

amenable to the binding of small molecules, and as a result of this traditional high throughput screens rarely identify small molecule substrate-competitive inhibitors. A limited number of screening methods have been reported that can identify substrate-competitive inhibitors, but all of these methods suffer from significant drawbacks (see **Chapter I**). Thus, we aimed to develop a general screening method that could be applied to any tyrosine kinase of interest for the discovery of small molecule substrate-competitive inhibitors.

Substrate activity screening (SAS) is a screening method pioneered by the Ellman lab that identifies substrates of an enzyme instead of inhibitors.[7] The reactive portion of the identified substrate is then modified to convert the substrate into an inhibitor. Because the enzyme is not inhibited, SAS allows for the identification of even very weakly binding substrates due to enzyme turnover and subsequent signal amplification. Additionally, because substrate binding and product formation is monitored by the assay instead of enzyme inhibition false negatives from nonspecific interactions are eliminated. The Ellman lab has previously used SAS to discover small molecule inhibitors of several proteases and phosphatases.[7-12] Although there are previous reports of peptide substrates converted into peptide inhibitors, nonpeptidic substrates have not been reported for any protein kinase.[13-17]

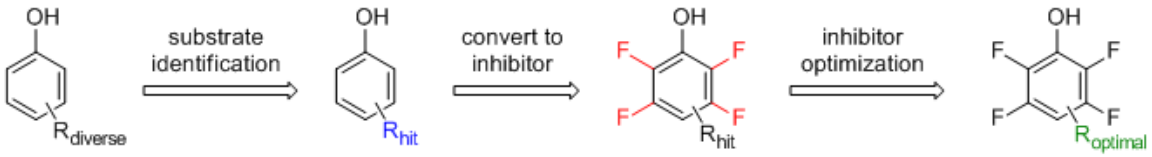

Scheme 3.1. Proposed SAS methodology for protein tyrosine kinases.

We thought SAS would be an excellent strategy for the identification of small molecule substrate-competitive inhibitors of tyrosine kinases because small molecule substrates converted into inhibitors should inherently be substrate-competitive. The proposed methodology is outlined in **Scheme 3.1**. A library of small molecule phenols will serve as tyrosine surrogates and will be screened to identify compounds that can be

phosphorylated by a kinase. The identified substrates will then be converted to inhibitor either by replacement of the reactive hydroxyl group or by modifying the reactivity of the hydroxyl group. Finally, the inhibitor will be optimized to give a lead substrate-competitive inhibitor. For the development of SAS for tyrosine kinases, c-Src kinase was used as a model kinase.[18-19]

Step 1: Identification of Small Molecule Substrates

The development of SAS for tyrosine kinases began with the identification of small molecule substrates of c-Src kinase. We hypothesized that small molecules would be poor kinase substrates compared to peptidic substrates, meaning a highly sensitive assay would be needed to identify leads. The ADP-Glo kinase assay was selected due to its ability to detect low levels of kinase activity, and to be run at high levels of ATP, which would discourage the small molecules from binding to the ATP pocket. As shown in **Scheme 3.2**, this multistep endpoint assay links kinase activity to luciferase activity.[20] First, the kinase reaction is performed, and if the small molecule is a substrate of the kinase then ADP will be produced as a byproduct of the kinase reaction. After sequestration of the remaining unreacted ATP, the ADP byproduct is converted back to ATP which is then used to fuel a luciferase reaction. The amount of luminescence can then be correlated to the amount of kinase activity. In addition to having the required sensitivity for the identification of small molecule substrates, this assay enables the SAS methodology to be readily adapted to any tyrosine kinase of interest since ADP is the byproduct of all kinase reactions.

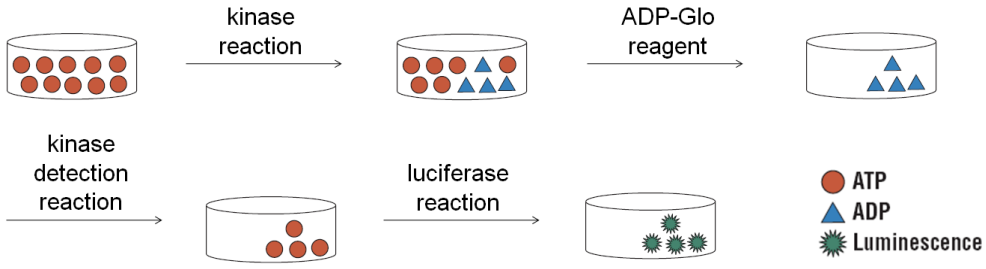

Scheme 3.2. The ADP-Glo assay kit was used to evaluate small molecules as potential kinase substrates. Image adapted from Promega.[20]

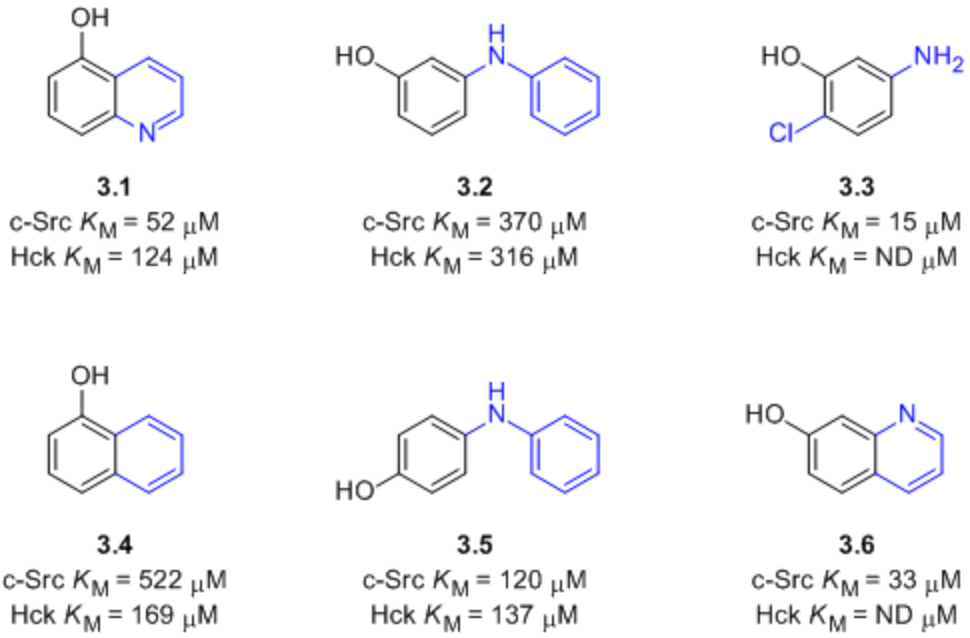

Scheme 3.3. Small molecule substrates of c-Src kinase identified using the ADP-Glo sassay. The compounds were also evaluated as substrates of Hck and c-Abl. None of the compounds were found to be substrates for c-Abl (K_M > 1 mM).

A library of 88 diverse small molecule phenols was assembled to serve as tyrosine mimics (see **Appendix B**, **Table B.1** for structures). The known c-Src substrate peptide Ac-AIYAA-NH_2 was also included in the screen as a positive control.[21] The phenol library was initially screened at 100 μM in the presence of 1 mM ATP and 100 nM c-Src. The amount of ADP produced as a byproduct of kinase activity was evaluated using an ADP-Glo assay kit (assays performed by Michael Steffey). In addition to the peptide substrate control, nine small molecule substrates of c-Src were identified that produced >2.5% ADP after a 30 minute reaction in the ADP-Glo screen (assays performed by Michael Steffey). Percent ADP for all compounds screened can be found in Appendix B and the six most interesting substrates are shown in **Scheme 3.3**. To confirm that the observed ADP formation was due to phosphorylation of the small molecule phenols one of the reactions was analyzed by reverse phase analytical HPLC. As shown in **Figure 3.1**, the phosphate of substrate **3.2** was unambiguously identified by comparison to a known standard, proving that the small molecules are phosphorylated by c-Src. K_M values were also obtained for the identified substrates and ranged from 15-522 μM. This

data demonstrates that small molecules can serve as competent substrates for a protein kinase, and in fact, several of the small molecule substrates have K_M values lower than that for the peptidic c-Src substrate Ac-AIYAA-NH_2 (K_M = 60 μM). It is noteworthy that these are the first non-peptidic substrates reported for any protein kinase.

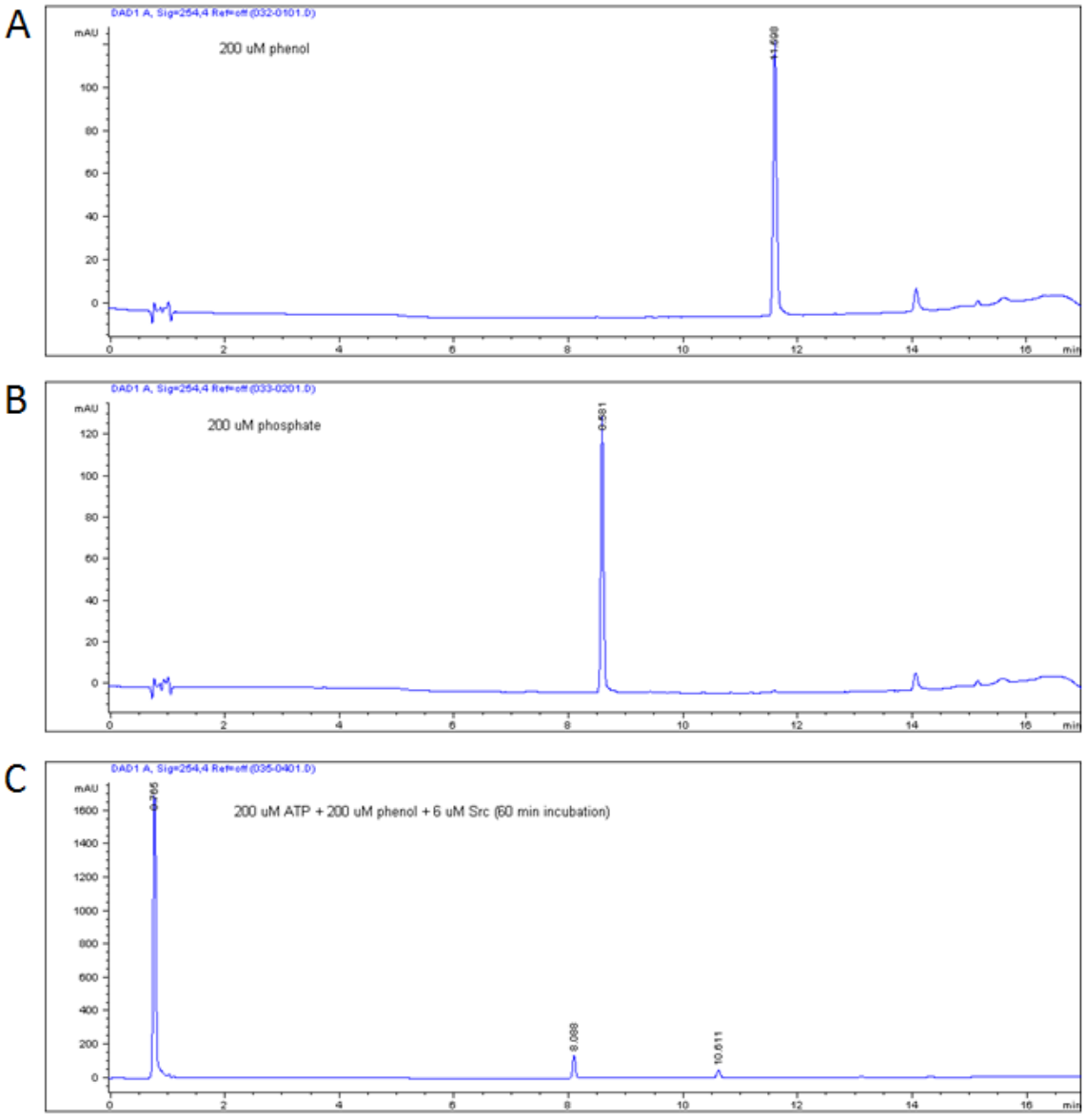

Figure 3.1. Analytical HPLC traces confirmed phosphorylation of a small molecule substrate by Src. A) Trace of substrate **3.2**, (B) trace of a known standard of the corresponding phosphate of substrate **3.2**, and (C) trace of the reaction after incubating **3.2** with c-Src and ATP.

From the identified small molecule c-Src substrates some initial SAR trends were observed. Several of the substrates (**3.1**, **3.2**, **3.4**, **3.5** and **3.6**) are bicyclic structures, although this is not surprising since these ring systems are privileged scaffolds that are known to have binding affinity for proteins.[22] Additionally, most of the substrates contain a nitrogen at a position *meta* or *para* to the hydroxyl group. This nitrogen can be a primary or secondary sp^3 nitrogen or a sp^2 nitrogen. When comparing similar quinoline and naphthalene substrates **3.1** and **3.4** (K_M = 52 μM and 522 μM, respectively) an order of magnitude decrease in potency is observed when the nitrogen is removed. Furthermore, while two diphenylamines isomers (**3.2** and **3.5**) were identified as substrates, a corresponding diphenylmethane scaffold (**P-S58**) was not identified as a substrate in the initial screen. Taken together this suggests that the nitrogen may be making important interactions within the substrate binding site, likely by acting as a hydrogen bond acceptor for a nearby residue.

To gain further insight to the selectivity of the substrate site K_M values were determined for the c-Src substrates with the highly similar kinases Hck and c-Abl (**Scheme 3.3** and **Appendix B**, **Table B.2**). Hck is a member of the Src subfamily of protein tyrosine kinases and has 85% sequence similarity to c-Src across the kinase domain.[23] c-Abl is not a member of the Src family but still has 70% sequence similarity to c-Src across the kinase domain, and the high degree of similarity between c-Src and c-Abl has made it very difficult to design inhibitors of c-Src that do not also inhibit c-Abl.[24-25] All of the c-Src substrates tested were found to also be Hck substrates with similar potencies, and this result was expected since members of the same kinase subfamily share many similar substrates. The best selectivity was observed with substrate **3.1** which was 2.4-fold selective for c-Src over Hck. Interestingly, the selectivity is reversed in the corresponding **3.4** which is 3.1-fold selective for Hck over Src. Promisingly, none of the c-Src substrates were found to be substrates for c-Abl (K_M > 1000 μM). This supports that despite having high overall similarity and nearly identical ATP binding sites homologous kinases have divergent substrate binding preferences. It has previously been shown with peptidic substrates that c-Src and c-Abl have divergent substrate binding preferences, and these results demonstrate that these preferences hold even with small molecule substrates. This also supports the hypothesis

that substrate-competitive kinase inhibitors will show increased selectivity relative to ATP-competitive inhibitors.

Step 2: Conversion of Substrates to Inhibitors

After identifying small molecule substrates of c-Src, the next step was to convert the substrates into inhibitors. This could be accomplished by either replacement of the reactive hydroxyl group or by altering the reactivity of the hydroxyl group. A library of peptides based on the known c-Src substrate Ac-AIYAA-NH_2 in which the reactive tyrosine was replaced by a nonphosphorylatable residue was prepared and evaluated for c-Src inhibition (see **Chapter II**). All of the peptides were poor inhibitors (all K_i > 100 μM) likely due to the loss of hydrogen bonding interactions made by the tyrosine hydroxyl group in the active site. Because of the smaller size of the substrates and therefore limited interactions that could be made with the substrate binding site, it was hypothesized that retaining this hydrogen bonding interaction would be critical for the binding of small molecule inhibitors. Therefore, modifications that would retain similar hydrogen bonding interactions while preventing phosphotransfer were explored.

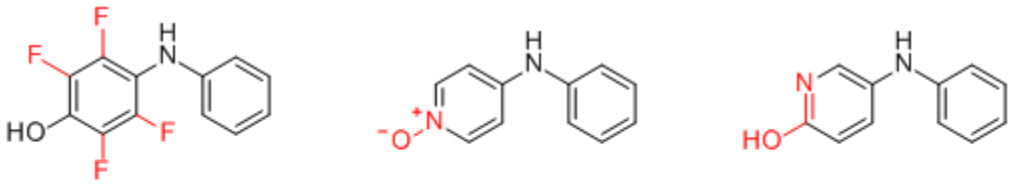

3.7
c-Src K_i = 257 ± 28 μM
Hck K_i = 1015 ± 165 μM
c-Abl K_i > 1170 μM

3.8
c-Src K_i = 478 ± 82 μM
Hck K_i = 517 ± 32 μM
c-Abl K_i > 1170 μM

3.9
c-Src K_i = 552 ± 9 μM
Hck K_i = 318 ± 17 μM
c-Abl K_i = 1046 ± 176 μM

Scheme 3.4. Conversion of a small molecule kinase substrate scaffold into kinase inhibitors. Inhibitors were evaluated against c-Src, Hck, and c-Abl using the pyrene fluorescence assay.

Graves and coworkers have previously shown that incorporation of tetrafluorotyrosine in place of tyrosine converted a peptidic substrate of IRK into an IRK inhibitor.[17, 26] This modification deactivates the tyrosine residue for phosphotransfer but

enables key interaction made by the hydroxyl group to be retained. To test if this strategy could also be applied to small molecule inhibitors of c-Src a tetrafluorinated analogue of substrate **3.5** was prepared (**Scheme 3.4**). Substrate **3.5** was chosen based on its potency and the synthetic feasibility of the fluorinated analogue as well as other analogues. Fluorinated inhibitor **3.7** was evaluated using the pyrene peptide fluorescence assay previously described (see **Chapter II**) and found to have K_i = 257 μM.[27] It was further hypothesized that pyridine N-oxide and hydroxypyridine may also serve as nonphosphorylatable phenol mimics. Inhibitors **3.8** and **3.9** were found to be less potent inhibitors of c-Src with K_i = 478 μM and K_i = 552 μM, respectively (**Scheme 3.4**). The potency of the 3 pharmacophores examined are consistent with results from the library of peptidic inhibitors, where the best c-Src inhibition was observed with pharmacophores that both increased the hydrophobic surface area and decreased the electron density within the phenyl ring (see **Chapter II**). When evaluated in the ADP Glo assay, inhibitors **3.8**, **3.9**, and **3.12** (an optimized analogue of **3.7**) were not phosphorylated by c-Src (assays performed by Michael Steffey).

Table 3.1. Comparison of IC_{50} values obtained under standard conditions to values obtained under low ATP conditions or high substrate conditions.

	c-Src IC_{50} (μM)		
	Standard Conditions (45 μM peptide substrate, 1 mM ATP)	Low ATP Conditions (45 μM peptide substrate, 100 μM ATP)	High Substrate Conditions (500 μM peptide substrate, 1 mM ATP)
3.7	436 ± 60 μM	253 ± 37 μM	>2000 μM
3.8	830 ± 143 μM	444 ± 59 μM	1520 ± 440 μM
3.9	958 ± 16 μM	665 ± 97 μM	1742 ± 614 μM

To determine if conversion from substrate to inhibitor was changing the binding mode of the scaffold each inhibitor was evaluated under conditions where the concentration of either ATP or peptide substrate had been changed (**Table 3.1**). The IC_{50} value for each inhibitor decreased approximately 2-fold or less when the concentration of ATP was decreased tenfold from 1 mM to 100 μM. Similarly, when the concentration of

peptide substrate was increased 10-fold from 45 μM to 500 μM the IC_{50} values of all three inhibitors decreased approximately 2-fold or greater. Notably, although the potency of inhibitor **3.7** decreased 2-fold when ATP concentration was decreased, the IC_{50} potency decreased ≥5-fold when peptide substrate was increased. Taken together this suggested that the inhibitors were not binding exclusively to the ATP-binding site and that the inhibitors are substrate-competitive.

Additionally, the three inhibitors were evaluated against Hck and c-Abl to assess selectivity of the inhibitors (**Scheme 3.4**). None of the inhibitors were potent inhibitors of c-Abl as would be expected since the starting scaffold was not a substrate for c-Abl. Unexpectedly, despite the similar K_M values for substrate **3.5** with c-Src and Hck (K_M = 120 μM and 137 μM, respectively) the inhibitors show different potencies against Hck compared to c-Src. The hydroxypyridine inhibitor **3.9** was the least potent inhibitor against c-Src but is the most potent inhibitor against Hck (K_i = 318 μM). Additionally, although **3.8** and **3.9** have similar potencies for c-Src and Hck, inhibitor **3.7** is 3.9-fold selective for c-Src over Hck. These data suggest that the optimal pharmacophore is likely different for each kinase. While it will require additional compound synthesis, the divergent pharmacophore preference will afford the opportunity to refine the selectivity of an inhibitor.

Step 3: Inhibitor Optimization

The tetrafluorophenol **3.7** was chosen for further optimization based on its c-Src potency and selectivity, and a focused library of twelve analogues of inhibitor **3.7** was prepared and evaluated using the pyrene peptide fluorescence assay. Three inhibitors were found to have improved potency relative to the parent compound (**Scheme 3.5**, see **Appendix B** for full library details). Addition of an *ortho*-methyl group in inhibitor **3.10** gave a 2.0-fold increase in potency (K_i = 127 μM) and addition of a *para*-phenyl group in inhibitor **3.11** gave a 3.2-fold increase in potency (K_i = 80 μM). Remarkably, replacement of the phenyl ring with a 1-naphthyl ring improved potency to 16 μM, a 16.1-fold increase. The potency of **3.12** is on par with other small molecule protein-protein interaction inhibitors.[28] Inhibitor **3.12** was also evaluated against the full construct of c-Src containing its regulatory domains (c-Src 3D) and had K_i = 36 μM.

When tested with phosphorylated c-Src kinase domain (pY416) and c-Src kinase domain containing the gatekeeper T338M mutation, a modest decrease in potency was observed (K_i = 73 μM and 75 μM, respectively). Because both phosphorylation at Y416 and the gatekeeper mutation render the kinase in the active form, the decreased potency of **3.12** against these constructs suggests that it may be binding to an inactive conformation of the kinase.

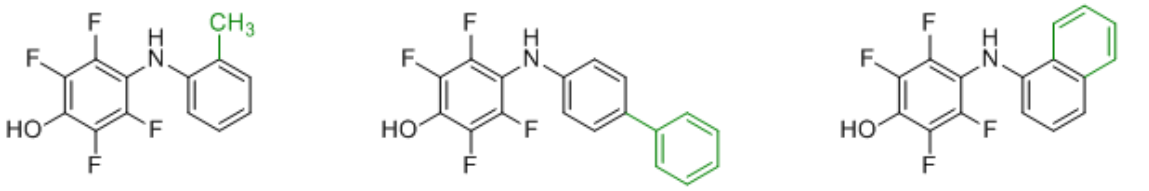

3.10
c-Src K_i = 127 ± 11 μM
Hck K_i > 1080 μM
c-Abl K_i > 1170 μM

3.11
c-Src K_i = 80 ± 6 μM
Hck K_i = 149 ± 6 μM
c-Abl K_i = 549 ± 138 μM

3.12
c-Src K_i = 16 ± 1 μM
Hck K_i = 325 ± 30 μM
c-Abl K_i = 1065 ± 385 μM
c-Src 3D K_i = 36 ± 5 μM
c-Src T338M K_i = 75 ± 15 μM

Scheme 3.5. Optimized substrate-competitive inhibitors of c-Src kinase. Compounds were evaluated against c-Src, Hck, and c-Abl using the pyrene fluorescence assay.

As was done previously, the three analogues were evaluated against Hck and c-Abl to determine selectivity. All three analogues saw improvements in selectivity for c-Src over c-Abl relative to the parent compound, although a smaller increase in selectivity was observed with inhibitor **3.11** due to the >2-fold increase in Abl potency. With Hck, **3.10** and **3.12** show increased selectivity relative to the parent compound while **3.11** shows decreased selectivity. Like what was seen with c-Abl, the decrease in c-Src selectivity over Hck for **3.11** (1.9-fold selective) is due to an increase in Hck potency. Inhibitor **3.11** saw a 6.8-fold increase in potency for Hck while only increasing potency 3.2-fold for c-Src. The increase in potency for the biphenyl analogue with all three kinases is likely due to the fact that biphenyl is a privileged scaffold that is known to bind to a large number of proteins. The 1-naphthyl analogue **3.12** showed the best selectivity overall, with 20.3-fold selectivity for c-Src over Hck and 66.6-fold selectivity for c-Src

over c-Abl. Due to its superior potency and selectivity, inhibitor **3.12** was chosen as the lead inhibitor for further characterization.

While determining the selectivity of the lead inhibitor **3.12** across the kinome is desirable, current profiling methods cannot perform this analysis with substrate-competitive inhibitors. All commercially available profiling services measure selectivity by evaluating displacement of an ATP-competitive probe, and this will not occur with a substrate-competitive inhibitor.[29-30] Profiling a substrate-competitive inhibitor against a wide panel of kinases would require developing assay conditions for each kinase tested, which is beyond the resources of our laboratory. Due to these limitations, we instead chose to profile **3.12** against all of the Src family kinases. These experiments would give additional insight into the selectivity of the lead compound since it is expected that substrate-competitive inhibitors will have the least selectivity against members of the same subfamily. For comparison, the ATP-competitive inhibitor **PP2** (**Scheme 3.6**) was also evaluated against the Src family kinases. **PP2** was reported as a c-Src selective inhibitor and is often used as a c-Src selective probe in cell biology experiments, although recent evidence shows that **PP2** has poor selectivity across the kinome.[31-32]

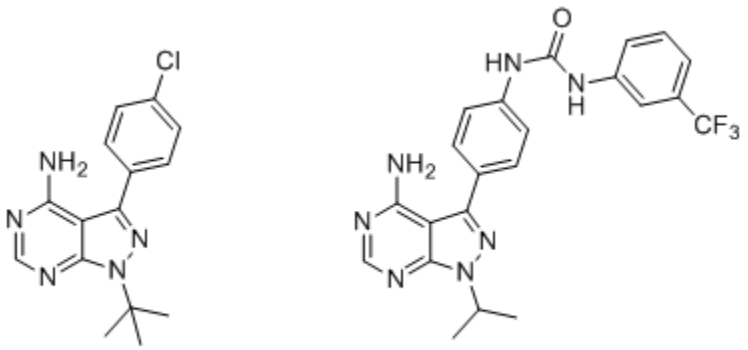

Scheme 3.6. ATP-competitive inhibitors of c-Src.

As seen in **Table 3.2**, inhibitor **3.12** has the best selectivity against Hck and has at least 3.2-fold selectivity against all of the Src family kinases. Impressively, **3.12** has 5.1-fold selectivity for c-Src over Yes despite the fact that Yes has 95% sequence similarity

and 90% sequence identity with c-Src over the kinase domain.[19] Inhibitor **3.12** represents one of the most selective inhibitors for c-Src over Yes reported to date, and only one ATP-competitive inhibitor has been reported with better selectivity.[31, 33] In contrast, poor selectivity is observed for the ATP-competitive inhibitor **PP2** across the Src family. While **PP2** also has the best selectivity against Hck, the selectivity is much lower (1.8-fold). Additionally, **PP2** has equivalent or better potency with six members of the Src family (Yes, Frk, Lck, Fyn, Lyn, and Fgr) than with c-Src. Overall, the average selectivity for inhibitor **3.12** across the Src family is 6.8, while the average selectivity for **PP2** is 0.8. This highlights the improved selectivity that can be achieved with substrate-competitive inhibitors compared to ATP-competitive inhibitors, even against highly similar kinases.

Table 3.2. Inhibition of Src family kinases by inhibitor **3.12** and **PP2** was determined using the pyrene fluorescence assay. The selectivity for c-Src over each kinase is given in parentheses.

	c-Src K_i (selectivity ratio)	
	3.12	**PP2**
c-Src	16 μM	45 nM
Hck	325 μM (20.3)	88 nM (2.0)
Frk	83 μM (5.2)	20 nM (0.4)
Yes	82 μM (5.1)	46 nM (1.0)
Lck	63 μM (3.9)	9 nM (0.2)
Fyn	61 μM (3.8)	20 nM (0.4)
Lyn	60 μM (3.8)	16 nM (0.4)
Blk	52 μM (3.3)	67 nM (1.5)
Fgr	51 μM (3.2)	25 nM (0.6)
Average Selectivity	6.1	0.8

Binding Mode Analysis

Inhibitors identified from SAS should inherently be substrate-competitive inhibitors, however because multiple binding sites exist on the kinase extensive biochemical evaluation was carried out to confirm the binding mode of inhibitor **3.12**.

Initially, the effect of varying ATP or peptide substrate concentration on the potency of **3.12** (IC_{50} = 27 μM) was examined. As expected, the IC_{50} value was independent of ATP concentration and decreasing the ATP concentration 10-fold to 100 μM did not significantly change the IC_{50} value (IC_{50} = 44 μM). However, the IC_{50} value was highly sensitive to peptide substrate concentration, and a 10-fold increase in peptide substrate concentration resulted in a >20-fold decreased in the IC_{50} value (IC_{50} = 577 μM).

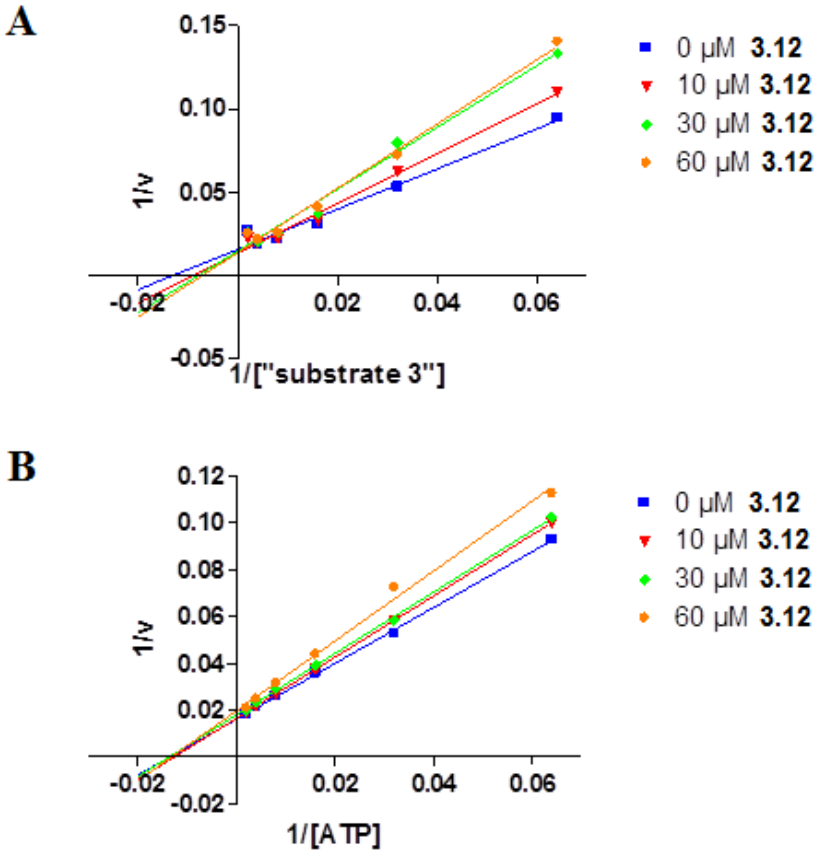

Figure 3.2. Lineweaver-Burk analysis of inhibitor **3.12**. Initial velocity was measured using the pyrene fluorescence assay in the presence of variable concentrations of **3.12**. A) Double reciprocal plot of initial velocity vs. "substrate 3" concentration. B) Double reciprocal plot of initial velocity vs. ATP concentration.

Lineweaver-Burk analysis was then performed to further confirm the binding mode (**Figure 3.2**). A double reciprocal plot of initial velocity against peptide substrate

concentration in the presence of varying concentrations of inhibitor **3.12** clearly shows intersection on the Y-axis, indicating that inhibitor **3.12** is substrate-competitive. Conversely, a double reciprocal plot of initial velocity against ATP concentration in the presence of various concentrations of inhibitor **3.12** intersects on the X-axis, indicating that inhibitor **3.12** is ATP-noncompetitive. Additionally, global fit analysis was performed to fit the K_M and V_{max} data for peptide substrate and ATP to competitive, noncompetitive, and uncompetitive models (see **Appendix B**). The global fit analysis agreed with the Lineweaver-Burk analysis that inhibitor **3.12** is substrate-competitive (R^2 = 0.993) and ATP-noncompetitive (R^2 = 0.999).

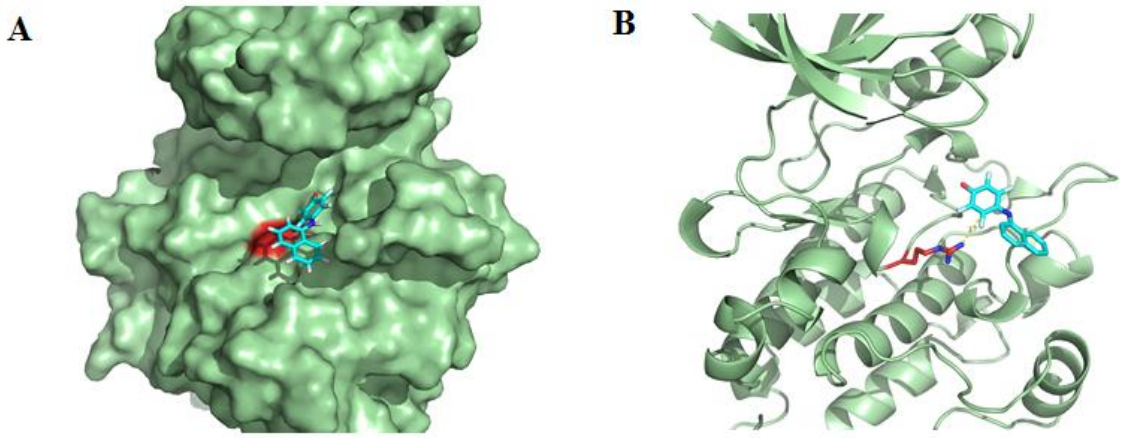

Figure 3.3. Induced fit docking of inhibitor **3.12** with c-Src. A) Inhibitor **3.12** binds in the substrate binding site. B) The model predicts a cation-π interaction between Arg388 and **3.12**.

To gain further insight into the binding mode of inhibitor **3.12**, induced-fit docking was used to flexibly dock **3.12** into c-Src (modeling performed by Dr. Matthew Soellner).[34] As shown in **Figure 3.3**, the inhibitor clearly binds in the substrate binding site, and a cation-π interaction is predicted between **3.12** and an arginine residue (Arg388) in the substrate binding site. Because this arginine residue is replaced by an alanine in c-Abl and Arg365 in c-Abl replaces Ala390 in c-Src, inhibitor **3.12** was evaluated with a R388A/A390R c-Src mutant. This mutant was found to be catalytically competent, and as predicted by the model inhibitor **3.12** was only a weak inhibitor of this

mutant (K_i = 184 μM). Taken together, the biochemical and modeling data offers strong support that kinase inhibitors identified through SAS have the desired substrate-competitive, ATP-noncompetitive binding mode.

In Cellulo Evaluation

Inhibitor **3.12** was also evaluated *in cellulo* (assays performed by Michael Steffey and Eric Lachacz unless otherwise noted). Initially, the inhibition of c-Src autophosphorylation was examined using an enzyme-linked immunosorbent assay (ELISA)-based assay (assays performed by Proquinase GmbH). Inhibitor **3.12** prevented c-Src autophosphorylation in MEF cells with IC_{50} = 15 μM. This is in excellent agreement with the biochemical potency (K_i = 16 μM) and proves that **3.12** is cell permeable. This was compared to **PP2**, which despite having biochemical K_i = 45 nM has a c-Src autophosphorylation IC_{50} of 2.2 μM.[31] This supports a long-standing hypothesis that unlike ATP-competitive inhibitors, which lose potency *in vivo* due to high intracellular ATP levels, substrate-competitive inhibitors will see less difference between biochemical and cellular potency due to kinase substrates being present at levels near or below their K_M values. The 44-fold decrease in potency that was observed here for **PP2** *in cellulo* is consistent with a cellular ATP concentration of approximately 5 mM.

Growth inhibition of cancer cell lines was also evaluated. Inhibitor **3.12** prevented the growth of SK-BR-3 breast cancer cells and HT-29 colorectal adenocarcinoma cells with GI_{50} = 15 μM and 37 μM, respectively. Both of these cell lines have previously been shown to be c-Src growth dependent.[31, 35] Despite its modest biochemical potency, inhibitor **3.12** is significantly more potent against these cell lines than **PP2** (SK-BR-3 GI_{50} >100 μM and HT-29 GI_{50} = 48 μM).[31] Notably, the SK-BR-3 antiproliferative effects of **3.12** are similar to the most potent ATP-competitive c-Src inhibitors known, including the FDA-approved inhibitors dasatinib and bosutinib.[36-37] Additionally, inhibitor **3.12** did not significantly inhibit the growth of MCF7 and T47D breast cancer (GI_{50} > 100 μM). MCF7 and T47D cells are c-Src growth independent, and thus the inability of **3.12** to prevent the growth of these cells suggests that **3.12** is still acting as a selective c-Src inhibitor *in cellulo*.

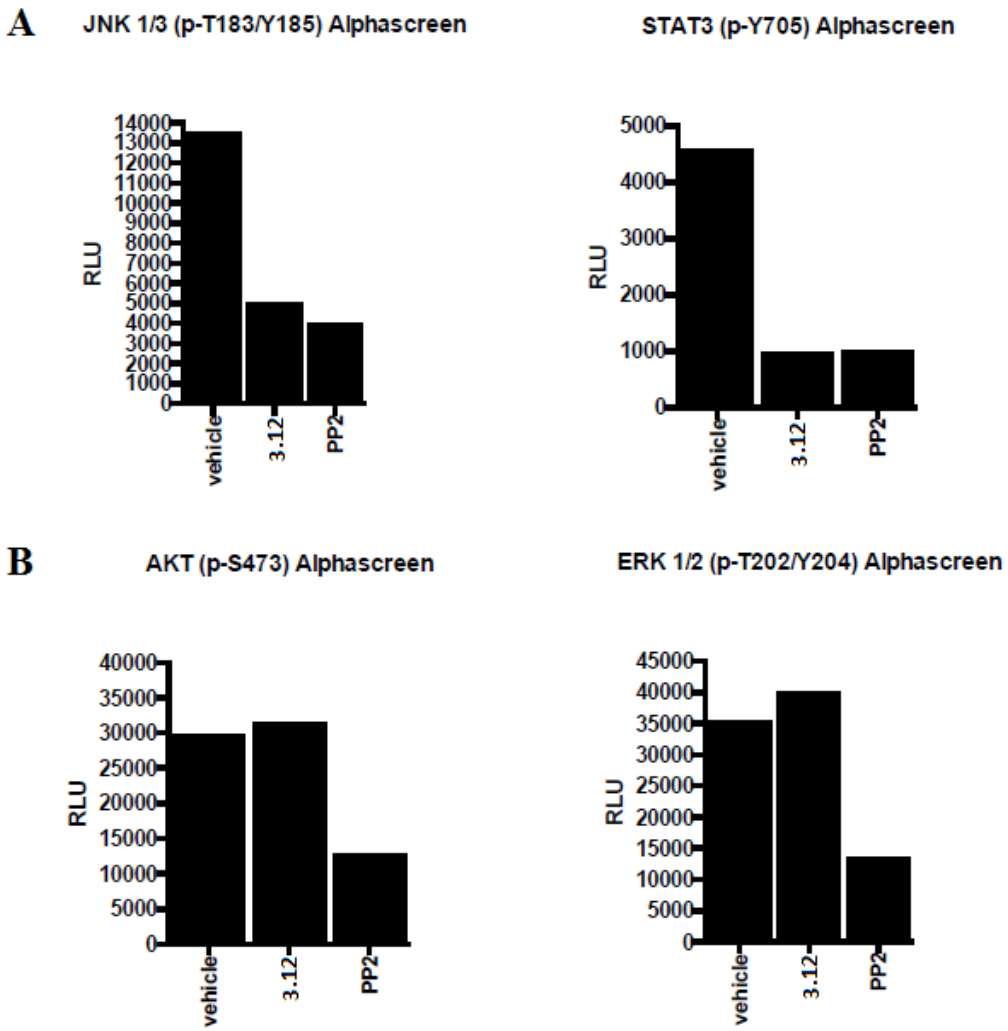

Figure 3.4. Activation of (A) c-Src dependent and (B) c-Src independent signaling pathways in the presence of **3.12** and **PP2** was evaluated in SK-BR-3 cells using an AlphaScreen assay.

To further probe the selectivity of inhibitor **3.12** *in cellulo*, the activation of c-Src dependent and independent signaling pathways was examined in SK-BR-3 cells using an AlphaScreen assay. As seen in **Figure 3.4**, inhibitor **3.12** was able to decrease activation of the c-Src dependent Jnk and STAT3 pathways to levels similar to those observed in the presence of **PP2**, but it did not decrease the activation of the c-Src independent Akt and Erk pathways.[38-39] In contrast, **PP2** decreased all four signaling pathways. Together with the cell growth inhibition studies these results offer strong evidence that **3.12** is highly selective for c-Src over other kinases.

Synergy Studies

As a final study, c-Src inhibition by combinations of inhibitor **3.12** and ATP-competitive inhibitors was examined. Because they share different binding sites, it is possible that substrate-competitive and ATP-competitive inhibitors could bind at the same time to give additive or even synergistic (hyper-additive) inhibition. Synergy between two compounds binding to different sites on the same target has been shown in other systems such as antibiotics targeting the eubacterial large ribosomal subunit and inhibitors of HIV reverse transcriptase.[40-43] Previous studies have also shown synergistic inhibition of cell growth when substrate-competitive or allosteric kinase inhibitors were dosed with an ATP-competitive kinase inhibitor, but because these studies were performed *in cellulo* using nonselective inhibitors the hyper-additivity observed could be due to inhibition of off-target kinases.[44-45] As such, the current study was performed biochemically to ensure that any additive or synergistic effects were due exclusively to binding to c-Src.

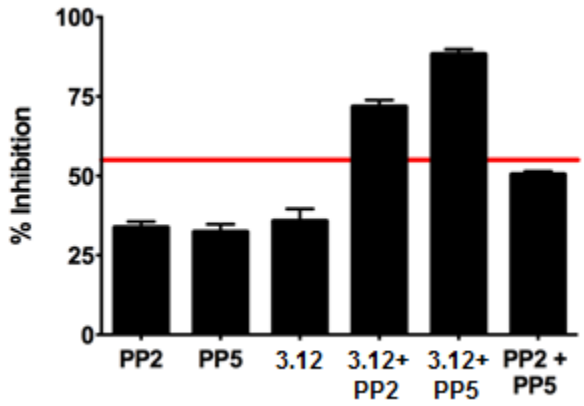

Figure 3.5. Synergy studies of combinations of substrate-competitive inhibitor **3.12** with ATP-competitive inhibitors **PP2** or **PP5**. IC_{35} concentrations were dosed individually and in combination. The red line indicates the predicted additivity of **3.12** + **PP2**.

The inhibition of c-Src in the presence of IC_{35} doses of inhibitor **3.12** with either **PP2** or **PP5** was evaluated using the pyrene peptide fluorescence assay. **PP2** and **PP5** are both pyrazolopyrimidine ATP-competitive inhibitors of c-Src that target the active

(DFG-in) and inactive (DFG-out) conformations, respectively.[32, 46] The threshold for synergistic inhibition was calculated using the Bliss equation.[47] As seen in **Figure 3.5**, inhibitor **3.12** shows synergistic inhibition of c-Src with both ATP-competitive inhibitors, although greater synergy is observed with **PP5**. Taken together with the previously observed decrease in the potency of inhibitor **3.12** with pY416 c-Src and T338M c-Src, this suggests that inhibitor **3.12** prefers to bind to an inactive-type conformation. As a control, combination of **PP2** and **PP5** was examined and only additivity was observed as expected for two compounds sharing the same binding site. Overall, these results unambiguously demonstrate for the first time synergy between a substrate-competitive inhibitor and ATP-competitive inhibitors.

Conclusions

The development of small molecule substrate-competitive kinase inhibitors has been impeded by the lack of general screening methods that can exclusively identify substrate-competitive inhibitors. To develop a general screening method for the identification of substrate-competitive tyrosine kinase inhibitors, we have applied the SAS method developed by the Ellman lab to the tyrosine kinase c-Src. Because SAS methods identify of substrates of an enzyme that are later converted into inhibitors, we hypothesized this method would be well suited for the discovery of substrate-competitive kinase inhibitors.

Using an ADP detection assay, we have reported the first small molecule substrates of protein kinases. By utilizing pharmacophore SAR gleaned from our peptidic inhibitor studies, we then successfully converted one of the small molecule c-Src substrates into a series of c-Src inhibitors. Optimization of one of these inhibitors generated our lead inhibitor **3.12** with c-Src K_i = 16 μM. Extensive kinetics analysis, modeling, and mutagenesis studies support that **3.12** has a substrate-competitive, ATP-noncompetitive binding mode as originally hypothesized. In contrast to the ATP-competitive c-Src inhibitor **PP2**, the lead inhibitor **3.12** shows excellent selectivity against highly similar kinases. Inhibitor **3.12** is over 66-fold selective for c-Src over c-Abl, and has an average selectivity of 6.1 across the Src family of kinases. Additionally, inhibitor **3.12** is active *in cellulo* and inhibits the growth of c-Src dependent cancer cell lines with low micromolar

GI_{50} values comparable to some of the most potent FDA-approved ATP-competitive inhibitors. Cellular evaluation of **3.12** also demonstrated the improved features of substrate-competitive inhibitors compared to ATP-competitive inhibitors *in cellulo*, including cellular potency that more closely resembles biochemical potency and improved selectivity. Inhibitor **3.12** is one of only a few substrate-competitive kinase inhibitors with activity in both biochemical and cellular assays and is the only such inhibitor of c-Src.[14] Finally, we have conclusively demonstrated for the first time that a substrate-competitive kinase inhibitor can be combined with ATP-competitive inhibitors to produce synergistic inhibition.

Taken together, these results clearly demonstrate the potential of this SAS method for the discovery of small molecule substrate-competitive inhibitors that can serve as improved biological probes compared to ATP-competitive inhibitors. While other methods have been reported for the discovery of substrate-competitive kinase inhibitors (see **Chapter I**), our SAS method is the only general screening method for the exclusive identification small molecule substrate-competitive kinase inhibitors. By utilizing a screen that identifies ADP, the byproduct of any kinase reaction, the described SAS method should be applicable to any tyrosine kinase of interest. Furthermore, the SAS method could likely be applied to other non-tyrosine kinases. There is evidence that some serine/threonine kinases can also phosphorylate tyrosine, which could allow for the use of the method as outlined.[48-49] Additionally, the method could potentially be modified for non-tyrosine kinases by altering the library composition and pharmacophores utilized. We anticipate that our SAS method will enable the rapid discovery of substrate-competitive kinase inhibitors against additional targets which will serve as important biological probes for studying kinase activity or even potential therapeutics.

Materials and Methods

General Synthetic Methods

Unless otherwise noted, all reagents were obtained via commercial sources and used without further purification. ^{1}H, ^{13}C, and ^{19}F NMR spectra were measured with a

Varian MR400 or Inova 500 spectrometer. Mass spectrometry (HRMS) was carried out by the University of Michigan Mass Spectrometry Facility (J. Windak, director).

Synthetic Protocols

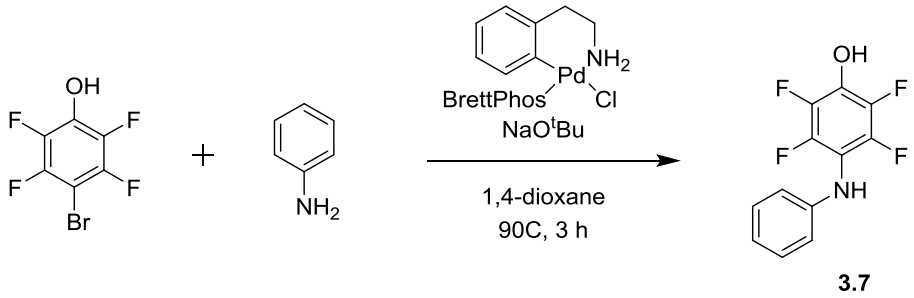

Scheme 3.7. Synthesis of compound **3.7**.

2,3,5,6-tetrafluoro-4-(phenylamino)phenol (**3.7**). Compound **3.7** was prepared in a manner similar to that described by Maiti and Buchwald.[50] To an oven-dried 4 mL conical vial was added 4-bromo-2,3,5,6-tetrafluorophenol (123 mg, 0.5 mmol), aniline (55 μL, 0.6 mmol), sodium tert-butoxide (120 mg, 1.25 mmol), and BrettPhos palladacycle (0.8 mg, 0.001 mmol). The vial was flushed with N_2, then 1 mL anhydrous 1,4-dioxane was added. The reaction was stirred at 90 C for 3 h. After cooling to RT, the reaction was poured into a 10% aqueous citric acid solution (30 mL) and extracted with EtOAc (4 x 20 mL). The organic extracts were dried over $MgSO_4$ and the solvent was removed under reduced pressure. Purification by automated silica gel chromatography using a 6 → 60% EtOAc in hexanes gradient afforded **3.7** as a pale yellow crystalline solid (36 mg, 28% yield). ^{1}H NMR (400 MHz, $CDCl_3$) δ 7.28 – 7.14 (m, 2H), 6.96 – 6.86 (m, 1H), 6.74 (m, 2H), 5.51 (s, 1H), 5.23 (s, 1H). ^{19}F NMR (400 MHz, $CDCl_3$) δ -149.9 (dd, *J* = 23.7 Hz, 7.2 Hz, 2F), -163.8 (dd, *J* = 23.7 Hz, 7.2 Hz, 2F). HRMS-ESI (*m*/*z*): $[M+H]^+$ calcd for $C_{12}H_7F_4NO$, 258.0537; found 258.0533.

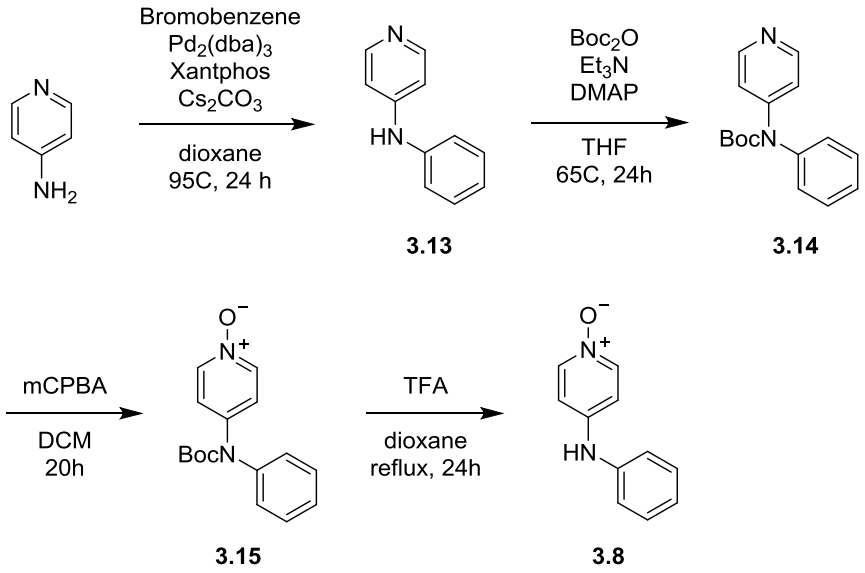

Scheme 3.8. Synthesis of compound **3.8**.

N-phenylpyridin-4-amine (**3.13**). To an oven-dried vial was added 4-aminopyridine (113 mg, 1.2 mmol), bromobenzene (106 µL, 1.0 mmol), Cs_2CO_3 (814 mg, 2.5 mmol), Xantphos (58 mg, 0.1 mmol), and $Pd_2(dba)_3$ (46 mg, 0.05 mmol). The vial was flushed with N_2 for 5 min, then anhydrous 1,4-dioxane (4 mL) was added and the reaction was stirred at 95 C for 24 h. The reaction was cooled to room temperature, diluted with H_2O (30 mL), and extracted with EtOAc (3x20 mL). The combined organic extracts were dried over $MgSO_4$, filtered, and the solvent was removed under reduced pressure. Purification by automated silica gel chromatography using a 0 → 10% MeOH in DCM gradient afforded **3.13** as a light yellow solid (133 mg, 78% yield). ^{1}H NMR (500 MHz, $CDCl_3$) δ 8.28 – 8.23 (m, 2H), 7.39 – 7.31 (m, 2H), 7.21 – 7.08 (m, 3H), 6.83 – 6.77 (m, 2H), 6.14 (s, 1H). ^{13}C NMR (125 MHz, $CDCl_3$) δ 150.83, 149.91, 139.50, 129.52, 124.12, 121.63, 109.41. HRMS-ESI (*m*/*z*): $[M+H]^+$ calcd for $C_{11}H_{10}N_2$, 171.0917; found 171.0916.

Tert-butylphenyl(pyridin-4-yl)carbamate (**3.14**). In a 25 mL roundbottom flask, **3.13** (100 mg, 0.59 mmol) was dissolved in 6 mL anhydrous THF. TEA (160 µL, 1.2 mmol) was added followed by DMAP (0.7 mg, 0.006 mmol) and Boc_2O (154 mg, 0.71 mmol). The reaction was stirred at room temperature overnight then at 65 C for 24 h. The

reaction was cooled to room temperature, diluted with H_2O (30 mL) and extracted with EtOAc (3x15 mL). The combined organic extracts were dried over $MgSO_4$, filtered, and the solvent was removed under reduced pressure. Purification by automated silica gel chromatography using a 10 → 80% EtOAc in hexanes gradient afforded **3.14** as a white solid (52 mg, 32% yield). ^{1}H NMR (500 MHz, $CDCl_3$) δ 8.43 – 8.38 (m, 2H), 7.43 – 7.35 (m, 2H), 7.35 – 7.27 (m, 1H), 7.18 – 7.10 (m, 4H), 1.42 (s, 9H). ^{13}C NMR (125 MHz, $CDCl_3$) δ 152.83, 150.11, 150.04, 140.99, 129.38, 128.30, 127.42, 117.78, 82.30, 28.04. HRMS-ESI (*m*/*z*): $[M+H]^+$ calcd for $C_{16}H_{18}N_2O_2$, 271.1441; found 271.1443.

4-((tert-butoxycarbonyl)(phenyl)amino)pyridine 1-oxide (**3.15**). **3.14** (41 mg, 0.15 mmol) was dissolved in 5 mL DCM then mCPBA (104 mg, 0.6 mmol) was added. The reaction was stirred at room temperature for 20 h. The reaction was diluted with 10 mL DCM and washed with 1 N NaOH (15 mL), and the organic layer was dried over MgSO4, filtered, and the solvent was removed under reduced pressure. Purification by automated silica gel chromatography using a 0 → 7% MeOH in DCM gradient afforded **3.15** as a light yellow glass (38 mg, 89% yield). ^{1}H NMR (500 MHz, $CDCl_3$) δ 8.07 – 8.00 (m, 2H), 7.45 – 7.37 (m, 2H), 7.37 – 7.30 (m, 1H), 7.20 – 7.11 (m, 4H), 1.40 (s, 9H). ^{13}C NMR (125 MHz, $CDCl_3$) δ 152.40, 141.55, 140.25, 138.70, 129.61, 127.98, 127.80, 119.80, 82.82, 27.91. HRMS-ESI (*m*/*z*): $[M+H]^+$ calcd for $C_{16}H_{18}N_2O_3$, 287.1390; found 287.1393.

4-(phenylamino)pyridine 1-oxide (**3.8**). In a dry 10 mL round bottom flask **3.15** (30 mg, 0.10 mmol) was dissolved in 4 mL DCM then TFA (2 mmol) was added. The reaction was stirred at reflux for 24 h, then the solvent was removed under reduced pressure. Purification by automated silica gel chromatography using a 0 → 7% MeOH in DCM gradient afforded **3.8** as a light brown solid (8 mg, 41% yield). ^{1}H NMR (500 MHz, DMSO-d_6) δ 9.08 (s, 1H), 8.01 – 7.95 (m, 2H), 7.35 (t, J = 7.8 Hz, 2H), 7.16 (d, J = 7.9 Hz, 2H), 7.04 (t, J = 7.4 Hz, 1H), 6.98 – 6.91 (m, 2H). ^{13}C NMR (125 MHz, DMSO-d_6) δ 143.83, 140.00, 139.14, 129.54, 123.05, 119.99, 111.01. HRMS-ESI (*m*/*z*): $[M+H]^+$ calcd for $C_{11}H_{10}N_2O$, 187.0866; found 187.0866.

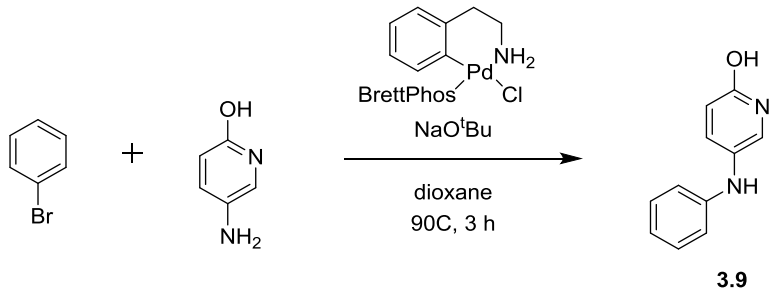

Scheme **3.9**. Synthesis of compound **3.9**.

5-(phenylamino)pyridin-2(1H)-one (**3.9**). Compound **3.9** was prepared in a manner similar to that described by Maiti and Buchwald.[50] To an oven-dried 4 mL conical vial was added bromobenzene (53 μL, 0.5 mmol), 5-amino-2-hydroxypyridine (66 mg, 0.6 mmol), sodium tert-butoxide (120 mg, 1.25 mmol), and BrettPhos palladacycle (0.8 mg, 0.001 mmol). The vial was flushed with N_2, then 1 mL anhydrous 1,4-dioxane was added. The reaction was stirred at 90 C for 3 h. After cooling to RT, the reaction was poured into water (30 mL) and extracted with EtOAc (3 x 15 mL). The organic extracts were dried over $MgSO_4$ and the solvent was removed under reduced pressure. The crude product was dissolved in DMSO (2 mL) and purified by reverse-phase HPLC using a 5 → 95% acetonitrile in water gradient. Lyophilization afforded **3.9** as a pale brown solid (30 mg, 32% yield). ^{1}H NMR (400 MHz, DMSO-d_6) δ 11.27 (s, 1H), 7.41 (s, 1H), 7.34 (dd, J = 9.6, 3.0 Hz, 1H), 7.19 – 7.07 (m, 3H), 6.71 – 6.61 (m, 3H), 6.36 (dd, J = 9.5, 0.7 Hz, 1H). ^{13}C NMR (125 MHz, DMSO-d_6) δ 159.89, 145.83, 139.90, 129.28, 127.54, 124.89, 118.90, 118.46, 114.31. HRMS-ESI (m/z): $[M+H]^+$ calcd for $C_{11}H_{10}N_2O$, 187.0866; found 187.0865.

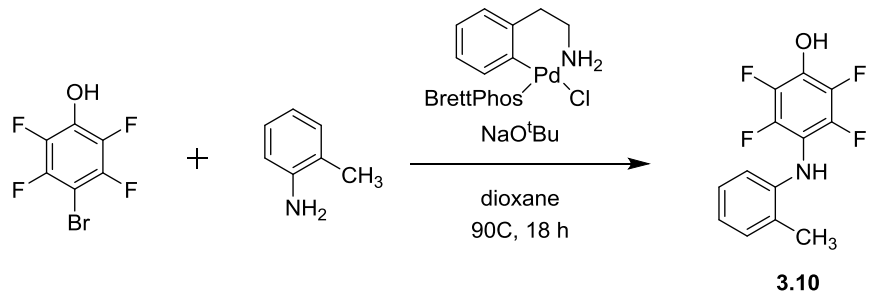

Scheme 3.10. Synthesis of compound **3.10**.

2,3,5,6-tetrafluoro-4-(o-tolylamino)phenol (**3.10**). Compound **3.10** was prepared in a manner similar to that described by Maiti and Buchwald.[50] To an oven-dried 4 mL conical vial was added 4-bromo-2,3,5,6-tetrafluorophenol (123 mg, 0.5 mmol), *o*-toluidine (64 µL, 0.6 mmol), sodium tert-butoxide (120 mg, 1.25 mmol), and BrettPhos palladacycle (0.8 mg, 0.001 mmol). The vial was flushed with N_2, then 1 mL anhydrous 1,4-dioxane was added. The reaction was stirred at 90 C for 18 h. After cooling to RT, the reaction was poured into a 10% aqueous citric acid solution (15 mL) and extracted with EtOAc (3 x 10 mL). The organic extracts were dried over $MgSO_4$ and the solvent was removed under reduced pressure. Purification by automated silica gel chromatography using a 6 → 50% EtOAc in hexanes gradient afforded **3.10** as purple crystalline solid (80 mg, 59% yield). ^{1}H NMR (400 MHz, $CDCl_3$) δ 7.20 – 7.03 (m, 2H), 6.86 (td, *J* = 7.4, 1.2 Hz, 1H), 6.55 (dq, *J* = 8.1, 1.9 Hz, 1H), 4.95 (s, 1H), 2.31 (s, 3H). ^{19}F NMR (400 MHz, $CDCl_3$) δ -150.6 (dd, *J* = 22.6 Hz, 6.6 Hz, 2F), -163.8 (dd, *J* = 22.6 Hz, 6.6 Hz, 2F). HRMS-ESI (*m*/*z*): $[M+H]^+$ calcd for $C_{13}H_9F_4NO$, 272.0693; found 272.0690.

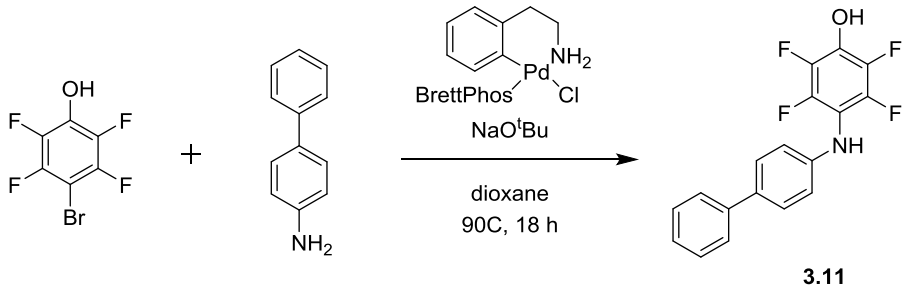

3.11

Scheme 3.11. Synthesis of compound **3.11**.

4-([1,1'-biphenyl]-4-ylamino)-2,3,5,6-tetrafluorophenol (**3.11**). Compound **3.11** was prepared in a manner similar to that described by Maiti and Buchwald.[50] To an oven-dried 4 mL conical vial was added 4-bromo-2,3,5,6-tetrafluorophenol (123 mg, 0.5 mmol), [1,1'-biphenyl]-4-amine (102 mg, 0.6 mmol), sodium tert-butoxide (120 mg, 1.25 mmol), and BrettPhos palladacycle (0.8 mg, 0.001 mmol). The vial was flushed with N_2, then 1 mL anhydrous 1,4-dioxane was added. The reaction was stirred at 90 C for 18 h.

After cooling to RT, the reaction was poured into a 10% aqueous citric acid solution (15 mL) and extracted with EtOAc (3 x 10 mL). The organic extracts were dried over $MgSO_4$ and the solvent was removed under reduced pressure. Purification by automated silica gel chromatography using a 6 → 50% EtOAc in hexanes gradient afforded **3.11** as purple crystalline solid (105 mg, 63% yield). ^{1}H NMR (500 MHz, $CDCl_3$) δ 7.56 – 7.44 (m, 4H), 7.43 – 7.35 (m, 2H), 7.32 – 7.22 (m, 1H), 6.84 – 6.77 (m, 2H), 5.76 (s, 1H), 5.31 (s, 1H). ^{19}F NMR (400 MHz, $CDCl_3$) δ -149.8 (dd, *J* = 23.2 Hz, 7.6 Hz, 2F), -163.6 (dd, *J* = 23.2 Hz, 7.6 Hz, 2F). HRMS-ESI (*m*/*z*): $[M+H]^+$ calcd for $C_{16}H_9F_4NO$, 308.0693; found 308.0689.

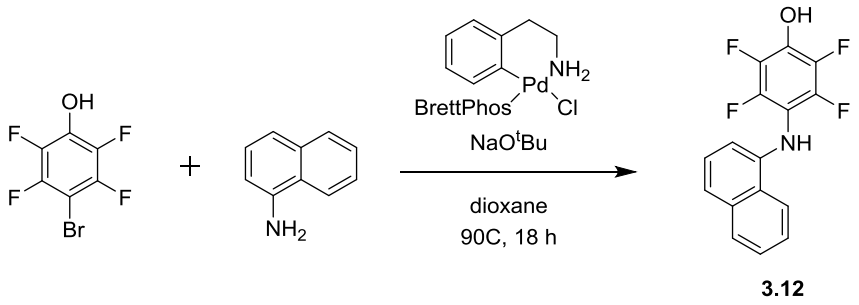

3.12

Scheme **3.12**. Synthesis of compound **3.12**.

2,3,5,6-tetrafluoro-4-(naphthalen-1-ylamino)phenol (**3.12**). Compound **3.12** was prepared in a manner similar to that described by Maiti and Buchwald.[50] To an oven-dried 4 mL conical vial was added 4-bromo-2,3,5,6-tetrafluorophenol (123 mg, 0.5 mmol), naphthalen-1-amine (86 mg, 0.6 mmol), sodium tert-butoxide (120 mg, 1.25 mmol), and BrettPhos palladacycle (0.8 mg, 0.001 mmol). The vial was flushed with N_2, then 1 mL anhydrous 1,4-dioxane was added. The reaction was stirred at 90 C for 18 h. After cooling to RT, the reaction was poured into a 10% aqueous citric acid solution (15 mL) and extracted with EtOAc (3 x 10 mL). The organic extracts were dried over $MgSO_4$ and the solvent was removed under reduced pressure. The crude product was dissolved in DMSO (2 mL) and purified by reverse-phase HPLC using a 5 → 95% acetonitrile in water gradient. Lyophilization afforded **3.12** as pale purple solid (12 mg, 8% yield). ^{1}H NMR (400 MHz, $CDCl_3$) δ 8.05 (m, 1H), 7.89 – 7.80 (m, 1H), 7.58 – 7.45

(m, 3H), 7.36 – 7.21 (m, 2H), 6.73 – 6.65 (m, 1H), 5.65 (s, 1H). ^{19}F NMR (400 MHz, $CDCl_3$) δ -151.0 (dd, *J* = 23.0 Hz, 5.8 Hz, 2F), -163.5 (dd, *J* = 23.0 Hz, 5.8 Hz, 2F). HRMS-ESI (*m*/*z*): $[M+H]^+$ calcd for $C_{18}H_{11}F_4NO$, 334.0850; found 334.0848.

Spectral Data for Compounds

Spectral data (^{1}H, ^{13}C and ^{19}F NMR) for compounds **3.7**-**3.15** is shown in Appendix B.

Gas Chromatography Analysis of Compounds

Gas chromatography was carried out using a Shimadzu GC 2010 containing a Shimadzu SHRX5 (crossbound 5% diphenyl–95% dimethyl polysiloxane; 15 m, 0.25 mm ID, 0.25μm df) column. Traces for compounds **3.7**-**3.12** are shown in Appendix B.

Biochemical Substrate Identification Assays

Substrate identification assays were performed by Michael Steffey using an ADP-Glo™ assay kit (Promega). Compounds were solubilized in 100% DMSO to 0.2M then subsequently diluted into ADP-Glo Kinase buffer (40 mM Tris pH 7.5, 20 mM $MgCl_2$, 0.1 mg/mL bovine serum albumin) to a working stock concentration of 167 μM (1.7% DMSO). 3 μL of the compound solution was added to the wells of a 384-well PerkinElmer Optiplate followed by the addition of 2 μL of kinase/ATP mix (250 nM c-Src, 250 μM ATP in ADP-Glo Kinase buffer). The plate was then sealed and pulse-spun in a tabletop centrifuge for 10 seconds to thoroughly mix the well contents. The final concentrations in the well were: 100 μM compound (1.0% DMSO), 100 nM c-Src, and 100 μM ATP. The peptide substrate (Ac-AIYAA-NH_2) was used as a control substrate to verify kinase activity.[2] Blank wells containing the reaction mixture without substrate were included as well. The kinase reaction was allowed to proceed at room temperature for 30 minutes after which the reaction was stopped by the addition of 5 μL/well of ADP-Glo Reagent (Promega). The contents were mixed by centrifugation as above and an additional room temperature 40 minute incubation was followed per the Promega protocol. 10 μL/well of Kinase Detection Reagent (Promega) was added to each well, the plate was spun as described to mix the contents, and an additional 30 minute room temperature incubation was performed per the Promega protocol. Luminescence was read in a Biotek Synergy 4 multimode plate reader and the percent ADP formed in the

well was calculated against a standard curve using a ratio of ATP/ADP as described in the Promega protocol under the same incubation conditions as the kinase reaction. Each data point was determined with $n \geq 2$ and the percent ADP formed is given as the mean ± standard error.

The ATP/ADP calibration curve, structures for the phenol library, and percent ADP formed for each compound can be found in **Appendix B**.

Determination of K_M for Phenolic Substrates

The K_M values for the phenolic substrates were determined by Michael Steffey using an ADP-Glo™ assay kit (Promega). The compounds were supplied as 100% DMSO solutions at 200 mM and were diluted to 2.5 mM into ADP-Glo buffer (40 mM Tris, pH 7.5, 20 mM $MgCl_2$, 0.1 mg/ml BSA, 0.1 mM Na_3VO_4, 0.01% Triton X-100). 1:1 dilutions were done in ADP-Glo buffer containing 1.25% DMSO and 2 μl of the solutions (in triplicate) were then added to wells of a 384-well PerkinElmer Optiplate. The kinase and ATP solution was prepared in ADP-Glo buffer to 2.5X the final concentrations desired in the assay and 3 μl was added to the wells containing the compound. The final concentrations used in the assay were: ATP = 100 μM, Src and Hck = 30 nM, Abl = 150 nM. The solutions were mixed in the plate by a brief centrifugation and allowed to incubate for 30 minutes at room temperature. 5 μl of ADP-Glo Reagent was added to each well and mixed by a brief centrifugation to terminate the kinase reaction. The plate was then incubated an additional 40 minutes at room temperature. The luciferase signal was generated by adding 10 μl per well of Kinase Detection Reagent and mixing by a brief centrifugation and incubation for 30 minutes at room temperature. Luminescence was measured in a Biotek Synergy 4 multimode plate reader. ATP conversion was determined against a standard curve of ATP/ADP using the ADP-Glo workup conditions listed above. K_M values were obtained directly from nonlinear regression of substrate-velocity curves. Curve fitting was done using Graphpad Prism 4 software using nonlinear curve fitting parameters. Each data point was determined in triplicate and is shown as the mean ± standard error.

The K_M curves for substrates **P-S1** – **P-S9** with c-Src kinase domain are shown in **Appendix B**. Inhibitor **3.12** was also evaluated as a c-Src substrate and the K_M curve is

shown in **Appendix B**. K_M curves for **P-S1**, **P-S2**, **P-S5**, and **P-S8** with Hck kinase domain are also shown in **Appendix B**.

HPLC Analysis of Substrate Phosphorylation

The phosphorylation of phenol **P-S2** by c-Src was monitored by analytical reverse phase HPLC (Zorbax Eclipse Plus C18 4.6 x 75 mm, 3.5 μm column) using an acetonitrile in water (+0.1% TFA) gradient (5% ACN for 3 min, then 5→70% ACN over 10 min). The enzymatic reaction had a final concentration 200 μM **P-S2**, 200 μM ATP, 6 μM c-Src, 100 mM Tris buffer (pH 8), and 10 mM $MgCl_2$. The phosphate **P-S2-phos** was prepared as described by Soellner *et al* and used as a known standard for comparison.[3] HPLC traces for **P-S2**, **P-S2-phos**, and **P-S2** + **ATP** + **Src** are shown in **Appendix B**.

General Biochemical Methods

Black, opaque-bottom 96 well plates were used for fluorescence assays and were purchased from Nunc. c-Src, c-Abl, Yes, and Hck were expressed in *E. coli* by Christel Fox and Frank Kwarcinski using previously published procedures.[51] Chicken c-Src numbering is used unless otherwise noted. Blk, Fgr, Frk, Fyn A, Lck, and Lyn A were purchased from SignalChem. Data was obtained using a Molecular Devices SpectraMax M5 plate reader or Biotek Synergy 4 plate reader. Curve fitting was performed using GraphPad Prism 4 software unless otherwise noted.

Determination of Inhibitor K_i

A continuous fluorescence assay was used to determine K_i.[27] Reaction volumes of 100 μL were used in 96-well plates. 85 μL of enzyme in buffer mix was added to each well followed by 2.5 μL of the appropriate inhibitor dilution (typically 80, 40, 20, 10, 5, 2.5, 1.25, 0.625 mM in DMSO) and 2.5 μL of a substrate peptide solution ("compound 3" as described in Wang *et al.*, typically 1.8 mM in DMSO). The reaction was initiated with 10 μL of ATP (10 mM in water), and reaction progress was immediately monitored at 405 nm (ex. 340 nm) for 10 minutes. Reactions had final concentrations of 1 mM ATP, 100 μM Na_3VO_4, 100mM Tris buffer (pH 8), 10 mM $MgCl_2$, and 0.01% Triton X-100. Final concentrations of enzyme and "substrate 3" for each kinase are as follows: c-Src kinase domain, 3 domain (3D) c-Src, phosphorylated (pY416) c-Src kinase domain,

double mutant R388A/A390R c-Src kinase domain, Hck kinase domain assays, and Yes kinase domain reactions had a final concentration of 30 nM enzyme and 45 μM peptide substrate. T338M c-Src kinase domain reactions had a final concentration of 30 nM enzyme and 20 μM peptide substrate. c-Abl kinase domain reactions had a final concentration of 120 nM enzyme and 120 μM peptide substrate. 3D Blk reactions had a final concentration of 30 nM enzyme and 85 μM peptide substrate. 3D Fgr reactions had a final concentration of 30 nM enzyme and 54 μM peptide substrate. 3D Frk reactions had a final concentration of 30 nM enzyme and 165 μM peptide substrate. 3D Fyn A reactions had a final concentration of 30 nM enzyme and 69 μM peptide substrate. 3D Lck reactions had a final concentration of 30 nM enzyme and 96 μM peptide substrate. 3D Lyn A reactions had a final concentration of 30 nM enzyme and 140 μM peptide substrate. The initial rate data collected was used for determination of K_i values. For K_i determination, the IC_{50} values were obtained directly from nonlinear regression of substrate-velocity curves in the presence of various concentrations of the inhibitor and converted to K_i values using the Cheng-Prusoff equation. The K_M values used for "substrate 3" were obtained from Wang *et al* or were determined as described below (see "Determination of Peptide Substrate "Substrate 3" K_M").[27]

For biochemical evaluation of **PP2**, the protocol above was followed with modifications to the ATP concentration. c-Src, Blk, Fgr, Frk, Fyn A, Lck, and Lyn A reactions had a final concentration of 300 μM ATP. c-Abl and Hck reactions had a final concentration of 100 μM ATP, and Yes reactions had a final concentration of 500 μM ATP. The K_M values used for ATP were obtained from Carna Biosciences or were determined as described below (see "Determination of ATP K_M").[52]

Each inhibitor K_i value was determined using at least 3 independent experiments (unless otherwise noted) which were averaged to give an average K_i value ± standard deviation. A representative curve is shown in **Appendix B** for inhibitors **3.7-3.12** and **PP2** with c-Src kinase domain, Hck kinase domain, and c-Abl kinase domain. For inhibitor **3.12** additional representative curves are shown in **Appendix B** for Yes kinase domain, 3 domain (3D) c-Src, phosphorylated (pY416) c-Src kinase domain, T338M c-Src kinase domain, double mutant R388A/A390R c-Src kinase domain, 3D Blk, 3D Fgr, 3D Frk, 3D Fyn A, 3D Lck, and 3D Lyn A. For PP2, additional representative curves are

shown in **Appendix B** for Yes kinase domain, 3D Blk, 3D Fgr, 3D Frk, 3D Fyn A, 3D Lck, and 3D Lyn A.

Determination of Peptide Substrate "Substrate 3" K_M

The previously described continuous fluorescence assay was used to determine K_M for "substrate 3" described in Wang *et al*.[27] Reaction volumes of 100 µL were used in 96-well plates. 85 µL of enzyme in buffer mix was added to each well followed by 2.5 µL of the appropriate dilution of "substrate 3" (typically 20, 10, 5, 2.5, 1.25, 0.625, 0.31, 0.16, 0.078, and 0 mM in DMSO) and 2.5 µL of DMSO. The reaction was initiated with 10 µL of ATP (10 mM in water), and reaction progress was immediately monitored at 405 nm (ex. 340 nm) for 10 minutes. Reactions had final concentrations of 1 mM ATP, 100 µM Na_3VO_4, 100mM Tris buffer (pH 8), 10 mM $MgCl_2$, and 0.01% Triton X-100. c-Src, Hck, Yes, Blk, and Frk reactions had a final concentration of 30 nM enzyme, and c-Abl reactions had a final concentration of 120 nM enzyme. The initial rate data collected was used for determination of K_M values, which were obtained directly from nonlinear regression of substrate-velocity curves.

The "substrate 3" K_M values were determined using at least 3 independent experiments which were averaged to give an average K_M value ± standard deviation. A representative curve is shown in **Appendix B** for "substrate 3" with c-Src kinase domain, 3-domain (3D) c-Src, phosphorylated (pY416) c-Src kinase domain, T338M c-Src kinase domain, double mutant R388A/A390R c-Src kinase domain, Hck kinase domain, Yes kinase domain, 3D Blk, 3D Frk, and c-Abl kinase domain.[7] For "substrate 3" with Fgr, Fyn A, Lck, and Lyn A the K_M values reported in Wang *et al*. were used.[5]

Determination of ATP K_M

The previously described continuous fluorescence assay was used to determine K_M for ATP described in Wang *et al*.[27] Reaction volumes of 100 µL were used in 96-well plates. 85 µL of enzyme in buffer mix was added to each well followed by 2.5 µL of "substrate 3" (1.8 mM in DMSO) and 2.5 µL of DMSO. The reaction was initiated with 10 µL of ATP (typically 10, 5, 2.5, 1.25, 0.63, 0.31, 0.16, 0.078, 0.039, and 0 mM in water), and reaction progress was immediately monitored at 405 nm (ex. 340 nm) for 10 minutes. Reactions had final concentrations of 45 µM "substrate 3", 100 µM Na_3VO_4,

100mM Tris buffer (pH 8), 10 mM $MgCl_2$, and 0.01% Triton X-100. c-Src, Hck, and Yes reactions had a final concentration of 30 nM enzyme, and c-Abl reactions had a final concentration of 120 nM enzyme. The initial rate data collected was used for determination of K_M values, which were obtained directly from nonlinear regression of substrate-velocity curves.

The ATP K_M values were determined using at least 3 independent experiments which were averaged to give an average K_M value ± standard deviation. A representative curve is shown in **Appendix B** for ATP with c-Abl kinase domain, Hck kinase domain, and Yes kinase domain. For analytical data for ATP with c-Src kinase domain see Kwarcinski *et al*.[53] For ATP with Blk, Fgr, Frk, Fyn A, Lck, and Lyn A the K_M values reported by Carna Biosciences were used.[52]

Determination of Inhibitor IC_{50} at Variable ATP and Peptide Substrate Concentration

The continuous fluorescence assay described previously was used to determine IC_{50} for inhibitors at higher "substrate 3" concentration and at lower ATP concentration with c-Src.[27] For higher "substrate 3" conditions the reactions had final concentrations of 30 nM c-Src, 500 μM "substrate 3", 1 mM ATP, 100 μM Na_3VO_4, 100mM Tris buffer (pH 8), 10 mM $MgCl_2$, and 0.01% Triton X-100. For lower ATP conditions the reactions had final concentrations of 30 nM c-Src, 45 μM "substrate 3", 100 μM ATP, 100 μM Na_3VO_4, 100mM Tris buffer (pH 8), 10 mM $MgCl_2$, and 0.01% Triton X-100. The initial rate data collected was used for determination of IC_{50} values, which were obtained directly from nonlinear regression of substrate-velocity curves in the presence of various concentrations of the inhibitor. The IC_{50} value for inhibitors under each set of conditions was determined using at least 3 independent experiments which were averaged to give an average IC_{50} ± standard deviation. Representative curves for compound **3.12** under each set of conditions is shown in **Appendix B**.

Lineweaver-Burk Analysis of Compound 3.12

The continuous fluorescence assay previously described was used to determine initial velocities for ATP and "substrate 3" (as described in Wang *et al*) with c-Src in the presence of compound **3.12**.[27]

For "substrate 3", reaction volumes of 100 µL were used in 96-well plates. 85 µL of enzyme in buffer mix was added to each well followed by 2.5 µL of the appropriate dilution of "substrate 3" (typically 20, 10, 5, 2.5, 1.25, 0.625, 0.31, 0.16, 0.078, and 0 mM in DMSO) and 2.5 µL of compound **3.12** (0.4, 1.2, or 2.4 mM in DMSO). The reaction was initiated with 10 µL of ATP (5 mM in water), and reaction progress was immediately monitored at 405 nm (ex. 340 nm) for 10 minutes. Reactions had final concentrations of 30 nM c-Src, 500 µM ATP, 100 µM Na_3VO_4, 100 mM Tris buffer (pH 8), 10 mM $MgCl_2$, and 0.01% Triton X-100. The kinetic values (K_M and V_{max}) were obtained directly from nonlinear regression of substrate-velocity curves.

For ATP, reaction volumes of 100 µL were used in 96-well plates. 85 µL of enzyme in buffer mix was added to each well followed by 10 µL of the appropriate dilution of ATP (typically 5, 2.5, 1.25, 0.625, 0.31, 0.16, 0.078, 0.039, 0.020, and 0 mM in water) and 2.5 µL of compound **3.12** (0.4, 1.2, or 2.4 mM in DMSO). The reaction was initiated with 2.5 µL of "substrate 3" (1.8 mM in DMSO), and reaction progress was immediately monitored at 405 nm (ex. 340 nm) for 10 minutes. Reactions had final concentrations of 30 nM c-Src, 45 µM "substrate 3", 100 µM Na_3VO_4, 100 mM Tris buffer (pH 8), 10 mM $MgCl_2$, and 0.01% Triton X-100. The kinetic values (K_M and V_{max}) were obtained directly from nonlinear regression of substrate-velocity curves.

The initial velocities for "substrate 3" or ATP in the presence of inhibitor **3.12** were determined (n = 4), and the average velocities were used to generate substrate-velocity curves. Lineweaver-Burk plots were generated by plotting the reciprocal of the average initial rates as a function of 1/["substrate 3"] or 1/[ATP] and performing linear regression. Additionally, global fit analysis was performed using GraphPad Prism 5 for each data set to determine R^2 for competitive, noncompetitive, and uncompetitive fits. The substrate-velocity curves for "substrate 3" and ATP are shown in **Appendix B**. R^2 values from global fit analysis for "substrate 3" and ATP are also shown in **Appendix B**.

Combination Studies of Compound 3.12 with PP2 and PP5

Before proceeding with combination studies the IC_{35} values for compound **3.12**, **PP2**, and **PP5** were estimated from dose-response curves. The previously described continuous fluorescence assay was used to obtain dose-response curves for **3.12**, **PP2**, and **PP5** with c-Src under the following final conditions: 30 nM c-Src, 45 µM "substrate

3", 300 μM ATP, 100 μM Na_3VO_4, 100mM Tris buffer (pH 8), 10 mM $MgCl_2$, and 0.01% Triton X-100.[27] The initial rate data collected was used for determination of IC_{50} values, which were obtained directly from nonlinear regression of substrate-velocity curves in the presence of various concentrations of the inhibitor. Each inhibitor IC_{50} value was determined using at least 3 independent experiments which were averaged to give an average IC_{50} ± standard deviation. A representative curve for each inhibitor under these conditions with c-Src is shown in **Appendix B**.

To determine if additive or synergistic effects occurred when compound **3.12** was combined with ATP-competitive inhibitors, single point assays of the inhibitors at IC_{35} (20 μM inhibitor **3.12**, 100 nM **PP2**, and 50 nM **PP5**) were carried out under the conditions described above. Initial velocity was measured for **3.12**, **PP2**, and **PP5** alone as well as for combinations of **12** + **PP2**, **12** + **PP5**, and **PP2** + **PP5**. The ratio of the initial velocity in the presence of inhibitor(s) and the initial velocity in the presence of no inhibitor (DMSO control) was used to calculate percent activity remaining, and percent inhibition was calculated as 100 - percent activity remaining. The percent inhibition for each inhibitor or combination of inhibitors was determined using at least 6 independent experiments which were averaged to give an average percent inhibition ± standard deviation. The predicted additivity was determined using the Bliss equation [predicted additivity = (eA + eB) – (eA * eB)].[47]

Induced Fit Molecular Docking of Compound 3.12

Induced fit docking (IFD) was performed by Dr. Matthew Soellner. The IFD workflow from the Schrödinger Suite Programs was used to flexibly dock compound **3.12** into 4 c-Src structures (PDB IDs 1YI6, 1Y57, 2BDF, and 2SRC).[34] Prime, also from the Schrödinger Suite Programs, was used to build in the activation loop of 2BDF using 3DQW as the template applying default parameters. Default parameters were used for the IFD and the docking score/glide gscore along with visual inspection was used to determine if a binding pose was reasonable.

Production of c-Src R388A/A390R Mutant

The c-Src R388A/A390R mutant was prepared by Christel Fox. Chicken c-Src kinase domain in pET28a, modified with a TEV protease cleavable N-terminal 6x-His

tag, was prepared as previously reported.[51] The desired mutations were added to this plasmid using iterative rounds of mutagenesis using the Agilent QuikChange II kit. The plasmid was transformed by electroporation into Bl21DE3 electrocompetent cells containing YopH in pCDFDuet-1. Cell growth, expression, and protein purification were performed using modified literature protocols for expression of wild-type c-Src kinase domain.[51]

Inhibition of c-Src Autophosphorylation

c-Src autophosphorylation assays were performed by ProQinase GmbH (Freiburg, Germany). Murine embryonal fibroblast (MEF) cells were used that express a high level of exogenously introduced full-length Src. The high Src expression level results in a constitutive tyrosine autophosphorylation of Src at Tyr416. MEF-SRC cells were plated in DMEM supplemented with 10% FCS in multiwell cell culture plates. Compound incubation was done in serum-free medium. Quantification of Src phosphorylation was assessed in 96-well plates via ELISA using a phospho-Src specific antibody and a secondary detection antibody. Raw data were converted into percent phosphorylation and the IC_{50} value was determined using nonlinear regression. Each concentration had n = 2 data points. The dose-response curve for compound **3.12** is shown in **Appendix B**. For analytical data for **PP2**, see Brandvold *et al*.[31]

Cancer Cell Growth Inhibition Assays

Growth inhibition assays were performed by Michael Steffey and Eric Lachacz. SK-BR-3 (ATCC® HTB-30™), MCF7 (ATCC® HTB-22™), T47D (ATCC® HTB-133™), and HT-29 (ATCC® HTB-38™) cells were grown and maintained using complete growth media (DMEM for SK-BR-3, MCF7, and T47D and McCoy's 5a Modified Medium for HT-29, supplemented with 10% fetal bovine serum) in a 37 C, 5% CO_2, humidified air incubator. Cells were then plated into 96 well plates in complete growth media (100 μL/well) at a concentration of 5000 cells per well and allowed to attach overnight. The cells were dosed with compound at 1% DMSO in media then cultured for 72 hours prior to addition of 10 μL/well of Cell Proliferation Agent WST-1 (Roche) for SK-BR-3 and HT-29 cells. The absorbance at 450 and 630 nm was read on a Biotek Synergy 4 multimode reader after incubation for 1 h at 37C. Life Technologies CyQUANT direct

cell proliferation assay was used for MCF7 and T47D. This general procedure was followed for all cell lines with the following differences: Prior to dosing the SK-BR-3 cells the complete growth media was removed by aspiration and replaced with compound at 1% DMSO in base media, 0.5% fetal bovine serum, and 60 ng/mL epidermal growth factor in DMEM (100 μL/well). HT-29, MCF7, and T47D cells were dosed by addition of 1 μL of 100X compound in 100% DMSO to complete growth media.

The raw $\Delta(A_{450}-A_{630})$ data were converted into percent of the average of the vehicle treated wells for each cell line and the IC_{50} value was determined using nonlinear regression. The dose-response curve for each cell line with compound **3.12** is shown in **Appendix B**.

Cell Signalling Assays

AlphaScreen SureFire assay kit (Perkin Elmers) was used to determine phosphorylation of Akt, JNK1/3, STAT3, and ERK1/2. SK-BR-3 cells (ATCC) were plated in 96-well plates at a density of 1.0-2.0 x 10^4 cells per well. The cells were grown to 80-90% confluency prior to overnight serum starvation in DMEM, 0.1% BSA. The serum free media was then removed and replaced with DMEM containing 10 μM compound **3.12** or **PP2** in 1% DMSO. The cells were incubated for 60 min prior to the addition of EGF (Sigma Aldrich). After incubation, the media was removed and 50 μL AlphaScreen Lysis Buffer (Perkin Elmers) was added to each well. The lysates were analyzed using the using the AlphaScreen SureFire assay kit according to the manufacturer's protocol. The average relative luminesce in the presence of each inhibitor (or vehicle) is shown (n = 3).

References

1. Chahrour, O.; Cairns, D.; Omran, Z., Small Molecule Kinase Inhibitors as Anti-Cancer Therapeutics *Mini-Reviews in Medicinal Chemistry* **2012,** *12* (5), 399-411.
2. Eldar-Finkelman, H.; Eisenstein, M., Peptide Inhibitors Targeting Protein Kinases *Current Pharmaceutical Design* **2009,** *15* (21), 2463-2470.
3. Bogoyevitch, M. A.; Barr, R. K.; Ketterman, A. J., Peptide inhibitors of protein kinases—discovery, characterisation and use. *Biochimica et Biophysica Acta (BBA) - Proteins and Proteomics* **2005,** *1754* (1–2), 79-99.
4. Bidwell, G. L.; Raucher, D., Therapeutic peptides for cancer therapy. Part I – peptide inhibitors of signal transduction cascades. *Expert Opinion on Drug Delivery* **2009,** *6* (10), 1033-1047.

5. Gavrin, L. K.; Saiah, E., Approaches to discover non-ATP site kinase inhibitors. *MedChemComm* **2013,** *4* (1), 41-51.
6. Han, K.-C.; Kim, S. Y.; Yang, E. G., Recent Advances in Designing Substrate-Competitive Protein Kinase Inhibitors *Current Pharmaceutical Design* **2012,** *18* (20), 2875-2882.
7. Wood, W. J. L.; Patterson, A. W.; Tsuruoka, H.; Jain, R. K.; Ellman, J. A., Substrate activity screening: A fragment-based method for the rapid identification of nonpeptidic protease inhibitors. *J. Am. Chem. Soc.* **2005,** *127* (44), 15521-15527.
8. Baguley, T. D.; Xu, H.-C.; Chatterjee, M.; Nairn, A. C.; Lombroso, P. J.; Ellman, J. A., Substrate-Based Fragment Identification for the Development of Selective, Nonpeptidic Inhibitors of Striatal-Enriched Protein Tyrosine Phosphatase. *J. Med. Chem.* **2013,** *56* (19), 7636-7650.
9. Leyva, M. J.; DeGiacomo, F.; Kaltenbach, L. S.; Holcomb, J.; Zhang, N.; Gafni, J.; Park, H.; Lo, D. C.; Salvesen, G. S.; Ellerby, L. M.; Ellman, J. A., Identification and Evaluation of Small Molecule Pan-Caspase Inhibitors in Huntington's Disease Models. *Chemistry & Biology* **2010,** *17* (11), 1189-1200.
10. Brak, K.; Doyle, P. S.; McKerrow, J. H.; Ellman, J. A., Identification of a New Class of Nonpeptidic Inhibitors of Cruzain. *J. Am. Chem. Soc.* **2008,** *130* (20), 6404-6410.
11. Soellner, M. B.; Rawls, K. A.; Grundner, C.; Alber, T.; Ellman, J. A., Fragment-based substrate activity screening method for the identification of potent inhibitors of the Mycobacterium tuberculosis phosphatase PtpB. *J. Am. Chem. Soc.* **2007,** *129* (31), 9613-9615.
12. Patterson, A. W.; Wood, W. J. L.; Hornsby, M.; Lesley, S.; Spraggon, G.; Ellman, J. A., Identification of Selective, Nonpeptidic Nitrile Inhibitors of Cathepsin S Using the Substrate Activity Screening Method. *J. Med. Chem.* **2006,** *49* (21), 6298-6307.
13. Chapelat, J.; Berst, F.; Marzinzik, A. L.; Moebitz, H.; Drueckes, P.; Trappe, J.; Fabbro, D.; Seebach, D., The Substrate-Activity-Screening methodology applied to receptor tyrosine kinases: A proof-of-concept study. *Eur. J. Med. Chem.* **2012,** *57*, 1-9.
14. Ye, G. F.; Tiwari, R.; Parang, K., Development of Src tyrosine kinase substrate binding site inhibitors. *Curr. Opin. Investig. Drugs* **2008,** *9* (6), 605-613.
15. Al-Obeidi, F. A.; Wu, J. J.; Lam, K. S., Protein tyrosine kinases: Structure, substrate specificity, and drug discovery. *Biopolymers* **1998,** *47* (3), 197-223.
16. Niu, J.; Lawrence, D. S., Nonphosphorylatable Tyrosine Surrogates: Implications for Protein Kinase Inhibitor Design. *J. Biol. Chem.* **1997,** *272* (3), 1493-1499.
17. Yuan, C. J.; Jakes, S.; Elliott, S.; Graves, D. J., A rationale for the design of an inhibitor of tyrosyl kinase. *J. Biol. Chem.* **1990,** *265* (27), 16205-16209.
18. Martin, G. S., The hunting of the Src. *Nat. Rev. Mol. Cell Biol.* **2001,** *2* (6), 467-475.
19. Thomas, S. M.; Brugge, J. S., Cellular functions regulated by Src family kinases. *Annu. Rev. Cell Dev. Biol.* **1997,** *13*, 513-609.
20. Zegzouti, H.; Zdanovskaia, M.; Hsiao, K.; Goueli, S. A., ADP-Glo: A Bioluminescent and Homogeneous ADP Monitoring Assay for Kinases. *Assay Drug Dev. Technol.* **2009,** *7* (6), 560-572.
21. Songyang, Z.; Carraway, K. L.; Eck, M. J.; Harrison, S. C.; Feldman, R. A.; Mohammadi, M.; Schlessinger, J.; Hubbard, S. R.; Smith, D. P.; Eng, C.; Lorenzo, M. J.;

Ponder, B. A. J.; Mayer, B. J.; Cantley, L. C., Catalytic specificity of protein-tyrosine kinases is critical for selective signalling. *Nature* **1995,** *373* (6514), 536-539.
22. Bemis, G. W.; Murcko, M. A., The Properties of Known Drugs. 1. Molecular Frameworks. *J. Med. Chem.* **1996,** *39* (15), 2887-2893.
23. Sicheri, F.; Kuriyan, J., Structures of Src-family tyrosine kinases. *Curr. Opin. Struct. Biol.* **1997,** *7* (6), 777-785.
24. Colicelli, J., ABL Tyrosine Kinases: Evolution of Function, Regulation, and Specificity. *Sci. Signal.* **2010,** *3* (139), re6-.
25. Musumeci, F.; Schenone, S.; Brullo, C.; Botta, M., An update on dual Src/Abl inhibitors. *Future Med. Chem.* **2012,** *4* (6), 799-822.
26. Martin, B. L.; Wu, D. L.; Jakes, S.; Graves, D. J., Chemical Influences on the Specificity of Tyrosine Phosphorylation. *J. Biol. Chem.* **1990,** *265* (13), 7108-7111.
27. Wang, Q.; Cahill, S. M.; Blumenstein, M.; Lawrence, D. S., Self-Reporting Fluorescent Substrates of Protein Tyrosine Kinases. *J. Am. Chem. Soc.* **2006,** *128* (6), 1808-1809.
28. Wells, J. A.; McClendon, C. L., Reaching for high-hanging fruit in drug discovery at protein-protein interfaces. *Nature* **2007,** *450* (7172), 1001-1009.
29. Bamborough, P., System-based drug discovery within the human kinome. *Expert Opinion on Drug Discovery* **2012,** *7* (11), 1053-1070.
30. Valsasina, B.; Kalisz, H. M.; Isacchi, A., Kinase selectivity profiling by inhibitor affinity chromatography. *Expert Review of Proteomics* **2004,** *1* (3), 303-315.
31. Brandvold, K. R.; Steffey, M. E.; Fox, C. C.; Soellner, M. B., Development of a Highly Selective c-Src Kinase Inhibitor. *ACS Chem. Biol.* **2012,** *7* (8), 1393-1398.
32. Hanke, J. H.; Gardner, J. P.; Dow, R. L.; Changelian, P. S.; Brissette, W. H.; Weringer, E. J.; Pollok, B. A.; Connelly, P. A., Discovery of a Novel, Potent, and Src Family-selective Tyrosine Kinase Inhibitor: Study of Lck- and FynT-Dependent T Cell Activation. *J. Biol. Chem.* **1996,** *271* (2), 695-701.
33. Davis, M. I.; Hunt, J. P.; Herrgard, S.; Ciceri, P.; Wodicka, L. M.; Pallares, G.; Hocker, M.; Treiber, D. K.; Zarrinkar, P. P., Comprehensive analysis of kinase inhibitor selectivity. *Nat. Biotechnol.* **2011,** *29* (11), 1046-U124.
34. Sherman, W.; Day, T.; Jacobson, M. P.; Friesner, R. A.; Farid, R., Novel procedure for modeling ligand/receptor induced fit effects. *J. Med. Chem.* **2006,** *49* (2), 534-553.
35. Zheng, X.; Resnick, R. J.; Shalloway, D., Apoptosis of estrogen-receptor negative breast cancer and colon cancer cell lines by PTP alpha and Src RNAi. *Int. J. Cancer* **2008,** *122* (9), 1999-2007.
36. Fallahi-Sichani, M.; Honarnejad, S.; Heiser, L. M.; Gray, J. W.; Sorger, P. K., Metrics other than potency reveal systematic variation in responses to cancer drugs. *Nat. Chem. Biol.* **2013,** *9* (11), 708-+.
37. Park, B. J.; Whichard, Z. L.; Corey, S. J., Dasatinib synergizes with both cytotoxic and signal transduction inhibitors in heterogeneous breast cancer cell lines - Lessons for design of combination targeted therapy. *Cancer Lett.* **2012,** *320* (1), 104-110.
38. Yoshizumi, M.; Abe, J.-i.; Haendeler, J.; Huang, Q.; Berk, B. C., Src and Cas Mediate JNK Activation but Not ERK1/2 and p38 Kinases by Reactive Oxygen Species. *J. Biol. Chem.* **2000,** *275* (16), 11706-11712.

39. Garcia, R.; Bowman, T. L.; Niu, G.; Yu, H.; Minton, S.; Muro-Cacho, C. A.; Cox, C. E.; Falcone, R.; Fairclough, R.; Parsons, S.; Laudano, A.; Gazit, A.; Levitzki, A.; Kraker, A.; Jove, R., Constitutive activation of Stat3 by the Src and JAK tyrosine kinases participates in growth regulation of human breast carcinoma cells. *Oncogene* **2001,** *20* (20), 2499-2513.
40. Auerbach, T.; Mermershtain, I.; Davidovich, C.; Bastian, A.; Belousoff, M.; Wekselman, I.; Zimmerman, E.; Xiong, L.; Klepacki, D.; Arakawa, K.; Kinashi, H.; Mankin, A. S.; Yonath, A., The Structure of Ribosome-Lankacidin Complex Reveals Ribosomal Sites for Synergistic Antibiotics. *Proceedings of the National Academy of Sciences of the United States of America* **2010,** *107* (5), 1983-1988.
41. Belousoff, M. J.; Shapira, T.; Bashan, A.; Zimmerman, E.; Rozenberg, H.; Arakawa, K.; Kinashi, H.; Yonath, A., Crystal structure of the synergistic antibiotic pair, lankamycin and lankacidin, in complex with the large ribosomal subunit. *Proceedings of the National Academy of Sciences of the United States of America* **2011,** *108* (7), 2717-2722.
42. Radzio, J.; Sluis-Cremer, N., Efavirenz Accelerates HIV-1 Reverse Transcriptase Ribonuclease H Cleavage, Leading to Diminished Zidovudine Excision. *Molecular Pharmacology* **2008,** *73* (2), 601-606.
43. Cruchaga, C.; Odriozola, L.; Andréola, M.; Tarrago-Litvak, L.; Martínez-Irujo, J. J., Inhibition of Phosphorolysis Catalyzed by HIV-1 Reverse Transcriptase Is Responsible for the Synergy Found in Combinations of 3‘-Azido-3‘-deoxythymidine with Nonnucleoside Inhibitors†. *Biochemistry* **2005,** *44* (9), 3535-3546.
44. Lipka, D. B.; Hoffmann, L. S.; Heidel, F.; Markova, B.; Blum, M.-C.; Breitenbuecher, F.; Kasper, S.; Kindler, T.; Levine, R. L.; Huber, C.; Fischer, T., LS104, a non-ATP-competitive small-molecule inhibitor of JAK2, is potently inducing apoptosis in JAK2V617F-positive cells. *Molecular Cancer Therapeutics* **2008,** *7* (5), 1176-1184.
45. Zhang, J.; Adrian, F. J.; Jahnke, W.; Cowan-Jacob, S. W.; Li, A. G.; Iacob, R. E.; Sim, T.; Powers, J.; Dierks, C.; Sun, F.; Guo, G.-R.; Ding, Q.; Okram, B.; Choi, Y.; Wojciechowski, A.; Deng, X.; Liu, G.; Fendrich, G.; Strauss, A.; Vajpai, N.; Grzesiek, S.; Tuntland, T.; Liu, Y.; Bursulaya, B.; Azam, M.; Manley, P. W.; Engen, J. R.; Daley, G. Q.; Warmuth, M.; Gray, N. S., Targeting Bcr-Abl by combining allosteric with ATP-binding-site inhibitors. *Nature* **2010,** *463* (7280), 501-506.
46. Dar, A. C.; Lopez, M. S.; Shokat, K. M., Small Molecule Recognition of c-Src via the lmatinib-Binding Conformation. *Chemistry & Biology* **2008,** *15* (10), 1015-1022.
47. Berenbaum, M. C., Criteria for Analyzing Interactions Between Biologically-Active Agents. *Adv.Cancer Res.* **1981,** *35*, 269-335.
48. Dhanasekarana, N.; Premkumar Reddy, E., Signaling by dual specificity kinases *Oncogene* **1998,** *17* (11), 1447.
49. Lindberg, R. A.; Quinn, A. M.; Hunter, T., Dual-specificity protein kinases: will any hydroxyl do? *Trends in Biochemical Sciences* **1992,** *17* (3), 114-119.
50. Maiti, D.; Buchwald, S. L., Orthogonal Cu- and Pd-Based Catalyst Systems for the O- and N-Arylation of Aminophenols. *J. Am. Chem. Soc.* **2009,** *131* (47), 17423-17429.
51. Seeliger, M. A.; Young, M.; Henderson, M. N.; Pellicena, P.; King, D. S.; Falick, A. M.; Kuriyan, J., High yield bacterial expression of active c-Abl and c-Src tyrosine kinases. *Protein Science* **2005,** *14* (12), 3135-3139.

52. Carna Biosciences, Kinase Profiling Book, http://www.carnabio.com/output/pdf/ProfilingProfilingBook_en.pdf.
53. Kwarcinski, F. E.; Fox, C. C.; Steffey, M. E.; Soellner, M. B., Irreversible Inhibitors of c-Src Kinase That Target a Nonconserved Cysteine. *ACS Chem. Biol.* **2012,** *7* (11), 1910-1917.

CHAPTER IV

Progress Towards Non-Peptidic Bisubstrate Kinase Inhibitors

Abstract

Bisubstrate kinase inhibitors that target both the substrate and the ATP binding sites are highly sought after as they can combine the potency of ATP-competitive inhibitors with the selectivity of substrate-competitive inhibitors. However, the peptidic nature of current bisubstrate inhibitors has limited their use as biological probes, and the limited number of reported small molecule ligands for kinase substrate sites has prevented the rational design of nonpeptidic bisubstrate inhibitors. We have applied small molecule substrates identified through SAS in **Chapter III** to the design of nonpeptidic bisubstrate inhibitors. Initial inhibitors which linked substrates to ATP-competitive inhibitors through the location of the substrate hydroxyl group showed poor potency, likely due to loss of hydrogen bonding contacts in the substrate site. A second generation of inhibitors that retained the substrate hydroxyl group showed increased potency. The second generation inhibitors used an unoptimized substrate scaffold, and therefore it is predicted that future bisubstrate inhibitors that use optimized substrate scaffolds should have increased potency. Results from this study will aid in the design of future bisubstrate inhibitors.

Introduction

Bivalent inhibitors link two inhibitors targeting unique binding sites on a kinase to generate a single molecule that can inhibit both binding sites at once. Most bivalent kinase inhibitors link an ATP-competitive inhibitor to a ligand that binds outside of the ATP binding site, such as the substrate binding site or binding sites in regulatory domains.[1-3] Bivalent inhibitors are a sought after class of kinase inhibitors because targeting two sites simultaneously enables combining the high potency of ATP-competitive inhibitors with the increased selectivity of ligands binding outside the highly

conserved ATP pocket. The potency of the bivalent inhibitors can be described as $\Delta G^{\circ}_{AB} = \Delta G^{i}_{A} + \Delta G^{i}_{B} + \Delta G^{s}$, where the ΔG^{i} terms are the intrinsic binding energies of each piece of the bivalent inhibitor and ΔG^{s} is the "connection Gibbs energy".[4] Assuming ideal binding of both pieces, no negative cooperativity between the binding sites, and no negative binding effects due to the linker, binding potency greater than the sum of the individual pieces can be achieved due to a reduction in entropy described by ΔG^{s}. As a result of this, combining an ATP-competitive inhibitor with even a weak inhibitor of a second binding site can result in drastic increases in potency. The potency of a bivalent inhibitor combined with the increased selectivity can drastically limit off-target effects, which makes bivalent inhibitors attractive for use as biological probes.

Most reported bivalent inhibitors for kinases are bisubstrate inhibitors that simultaneously target the ATP and substrate binding sites. The general strategy that has been previously employed for the design of bisubstrate inhibitors has been to covalently attach peptides to ATP or an ATP-competitive inhibitor. However, the poor pharmacokinetic properties associated with most peptides and nucleotides limits the use of many of these compounds as effective probes *in vivo*. In contrast, a bisubstrate inhibitor comprised of a non-nucleotide ATP-competitive inhibitor and a nonpeptidic substrate-competitive inhibitor should overcome these obstacles. While there are now many ATP-competitive inhibitors that can be utilized, the limited knowledge of small molecule scaffolds that bind in the substrate site has complicated the development of nonpeptidic bisubstrate inhibitors.[5] A small number of bisubstrate inhibitors have been described that use a single phenyl ring as a tyrosine pharmacophore for the substrate competitive portion; however, these inhibitors suffer from poor potency (micromolar).[6-8]

Our lab has previously developed one of the most potent bisubstrate inhibitors of c-Src reported to date.[9] As shown in **Scheme 4.1**, bisubstrate inhibitor **4.1** combines an optimal c-Src substrate peptide sequence and an analogue of the ATP-competitive inhibitor **PP2**. Inhibitor **4.1** showed excellent potency against c-Src (IC_{50} <5 nM, K_d = 187 pM) and exceptional selectivity for c-Src over other kinases in a panel of over 200 diverse kinases. However, despite the favorable biochemical profile of **4.1** it showed no efficacy *in cellulo*, and an Arg_9 tagged analogue was found to only weakly inhibit HT29

colon adenocarcinoma cell proliferation (GI_{50} = 36 μM). This is likely a result of poor permeability due to the peptidic nature of the substrate-competitive portion.

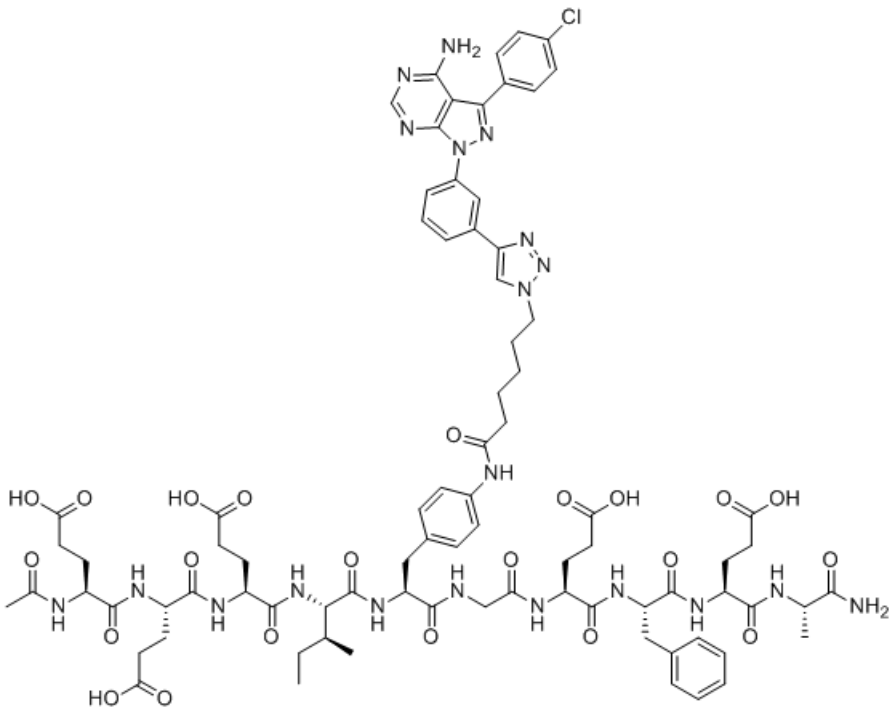

Scheme 4.1. A peptidic bisubstrate inhibitor of c-Src.

Inhibitor **4.1** clearly illustrates how the poor pharmacokinetic properties of even the most potent peptidic bisubstrate inhibitors limit their application as biological probes. To remedy the problems associated with current bisubstrate inhibitors, we aimed to develop nonpeptidic bisubstrate inhibitors using the small molecule c-Src substrates identified through SAS (see **Chapter III**) in place of peptidic substrates.[10] We hypothesized that this would generate potent bisubstrate inhibitors with increased permeability compared to peptidic bisubstrate inhibitors. Furthermore, a kinase profiling service could be used to profile the nonpeptidic bisubstrate inhibitors against a broad panel of diverse kinases. This analysis would give us additional insight into the selectivity of the substrate scaffolds identified through SAS by comparing the selectivity of the bisubstrate inhibitors

to the selectivity of **PP2**. Lead nonpeptidic bisubstrate inhibitors with high potency and selectivity could serve as useful biological probes for studying kinase activity.

A modular approach was used to design nonpeptidic bisubstrate inhibitors (**Scheme 4.2**). Similar to the design strategy for peptidic bisubstrate inhibitors **4.1**, an analogue of **PP2** modified to contain a phenyl alkyne (**PP2-alkyne**) was used for the ATP-competitive portion.[11] A small molecule substrate analogue (identified through SAS) modified to contain a primary amine was used for the substrate-competitive portion. The substrate was coupled though the amine to an azido acid linker of variable length via an amide coupling. Finally, a copper or ruthenium catalyzed click reaction was used to join the ATP-competitive portion and the linker via a 1,4-disubstitituted-1,2,3-triazole or 1,5-disubstitituted-1,2,3-triazole, respectively. This design strategy enabled the substrate scaffold, the linker length, and the triazole geometry to be easily modified for the generation of different libraries.

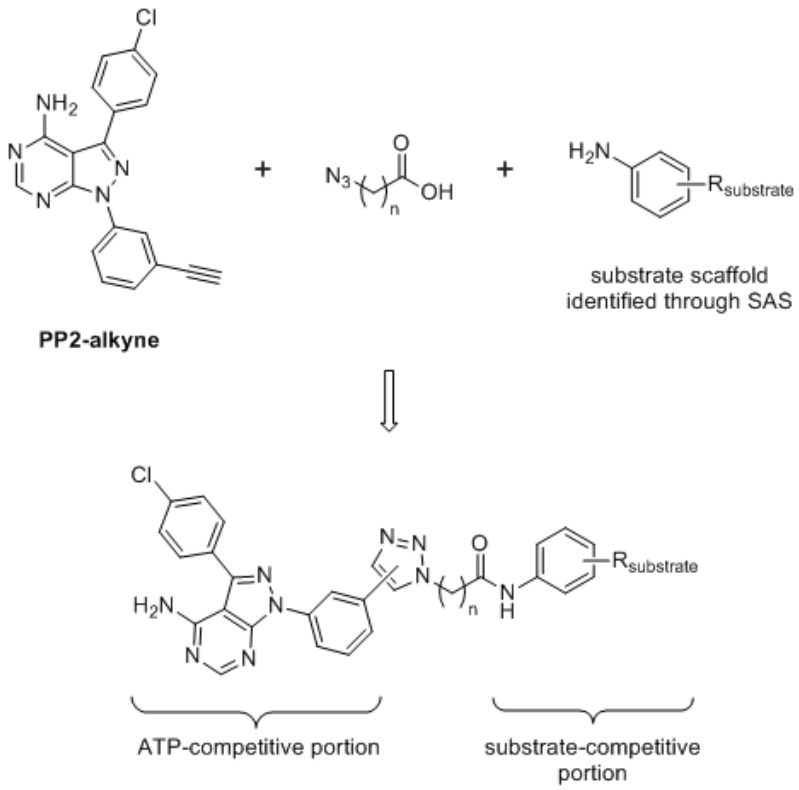

Scheme 4.2. A modular approach for the preparation of nonpeptidic bisubstrate inhibitors.

Evaluation of First Generation Inhibitors

We initially used the previously described pyrene peptide assay to evaluate two compounds with five methylene linkers similar to the peptidic bisubstrate inhibitor **4.1** (**Scheme 4.3**).[12] Both compounds **4.2** and **4.3** use an amine analogue of the diphenylamine scaffold **3.5** identified through SAS as the substrate competitive portion. Both the 1,4-trizole **4.2** and the 1,5-triazole **4.3** were found to be poor inhibitors of c-Src (IC_{50} > 250 μM). We hypothesized that this could be due to the lower binding potency of the substrate-competitive portion used (K_M = 122 μM). The K_M for kinase substrates overestimates binding affinity ($K_M < K_d$), and this coupled with the loss of interactions made by the substrate hydroxyl group due to incorporation of the linker has likely resulted in a poor K_d for the substrate competitive portion.[13-15] This led us to explore compounds which would utilize a more potent substrate-competitive fragment. Two small libraries of compounds with the general structures shown in **Scheme 4.4** were designed using an amine analogue of the optimized substrate-competitive inhibitor **3.12** and evaluated in the pyrene peptide assay.

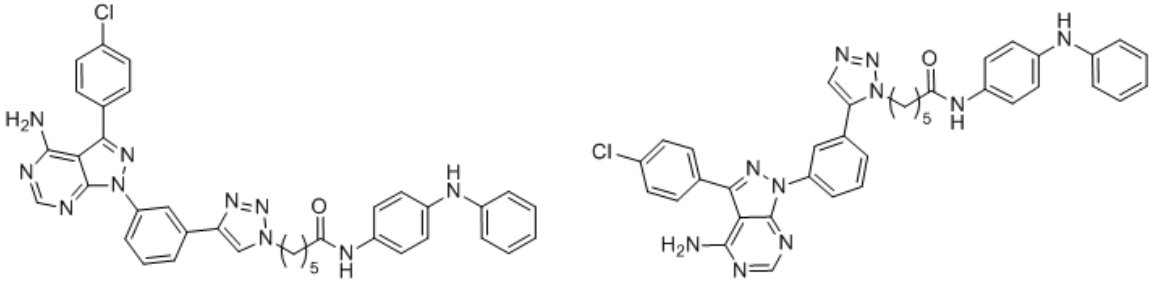

Scheme 4.3. Nonpeptidic bisubstrate inhibitors containing a substrate scaffold identified through SAS.

We initially explored linkage via a 1,4-triazole since these better resembled the peptidic bisubstrate inhibitor **4.1**. Inhibitor **4.4** used the same five methylene linker that was used in **4.1**, but it showed only modest potency (IC_{50} = 75 μM). We hypothesized that the small molecule substrates could be binding in a slightly different conformation

compared to the peptide in **4.1**, so inhibitors with shorter and longer linkers were also prepared. Compound **4.5** had poor potency (IC_{50} > 125 μM), but inhibitor **4.6**, which had a shorter 3 methylene linker, had improved potency (IC_{50} = 4 μM). However, despite the increased potency relative to the initial inhibitors, the potency of inhibitor **4.6** was still far lower than expected. In fact, the bisubstrate inhibitors are less potent than both the ATP-competitive inhibitor **PP2** (IC_{50} = 80 nM) and the precursor used in the synthesis of the bisubstrate inhibitors, **PP2-alkyne** (IC_{50} = 1 μM).[11] We expected the bisubstrate inhibitors to have sub-micromolar potency based on the potency of **PP2** and **PP2-alkyne**.

We next examined the inhibitors with 1,5-triazole linkages and the optimized substrate fragment (**Scheme 4.4**). The inhibitors with a five methylene linker **4.7** and a six methylene linker **4.8** were both poor inhibitors of c-Src (IC_{50} > 125 μM). Increasing the linker length to seven methylenes as in inhibitor **4.9** gave the best inhibition (IC_{50} = 1 μM), and further increasing the length of the linker to eight carbons in inhibitor **4.10** resulted in decreased potency (IC_{50} = 48 μM). While inhibitor **4.9** was the most potent inhibitor evaluated, the potency was still worse than expected.

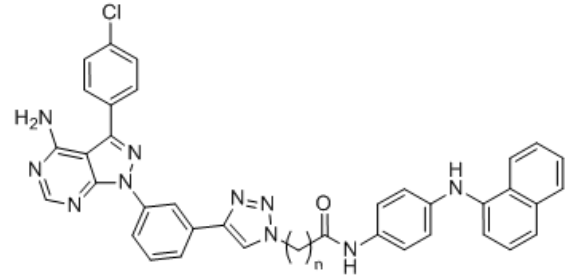

4.4: n = 5, c-Src IC_{50} = 75 ± 16 μM
4.5: n = 7, c-Src IC_{50} > 125 μM
4.6: n = 3, c-Src IC_{50} = 4 ± 2 μM

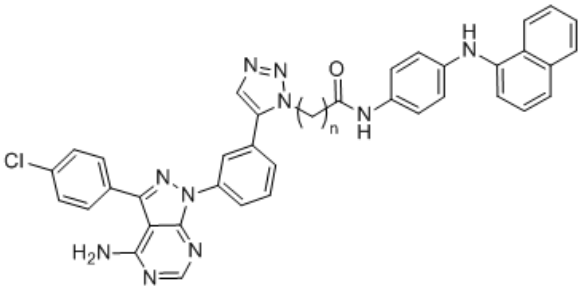

4.7: n = 5, c-Src IC_{50} > 125 μM
4.8: n = 6, c-Src IC_{50} > 125 μM
4.9: n = 7, c-Src IC_{50} = 1.1 ± 0.4 μM
4.10: n = 8, c-Src IC_{50} = 48 ± 14 μM

Scheme 4.4. Nonpeptidic bisubstrate inhibitors containing an optimized substrate scaffold.

To gain more insight into the binding of the bisubstrate inhibitors, we also prepared and evaluated two analogues of **4.9** that used different substrate-competitive fragments (**Scheme 4.5**). Inhibitor **4.11** used the unoptimized diphenylamine scaffold **3.5** (K_M = 122 μM), and as expected a decrease in potency was observed (IC_{50} = 53 μM). We also examined an inhibitor that used a different small molecule c-Src substrate scaffold identified through SAS. Compound **4.12** used an analogue of substrate **3.1** (K_M = 52 μM), which was one of the better small molecule substrates identified, and the potency of **4.12** (IC_{50} = 2 μM) was similar to that observed with **4.9**. While no improvements in potency were observed, we were pleased to see that the potency of the bisubstrate inhibitors tracked well with the relative affinity of the substrate scaffolds. This suggested that the substrate-competitive portion was binding similar to the substrates within the substrate binding site.

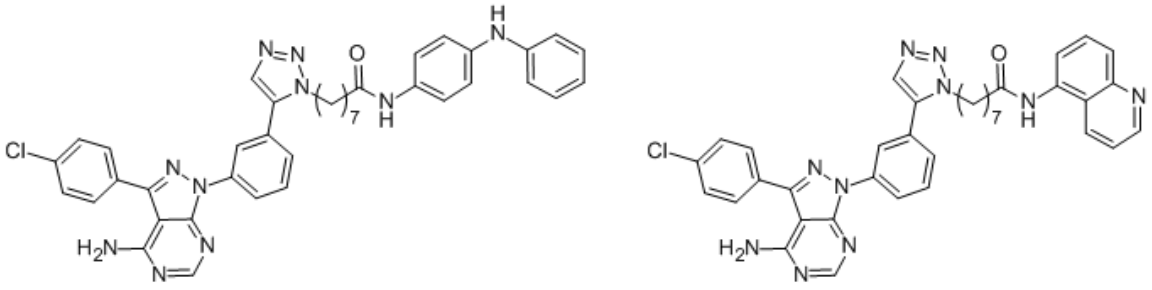

4.11
c-Src IC_{50} = 57 ± 8 μM

4.12
c-Src IC_{50} = 2.0 ± 0.2 μM

Scheme 4.5. Analogues of the nonpeptidic bisubstrate inhibitor **4.9** containing the unoptimized diphenylamine scaffold and a quinoline scaffold identified through SAS.

As a whole, the potencies of the bisubstrate inhibitors were much lower than the submicromolar potency we expected. One reason for this could be that the linker makes unfavorable interactions with c-Src. We found it unlikely that this was the sole reason for the low potency because these compounds contain the same linker used in the peptidic bisubstrate inhibitor **4.1**, and inhibitor **4.1** saw a large increase in potency relative to the ATP-competitive and substrate-competitive portions alone. In order to better understand

the poor potency of the nonpeptidic bisubstrate inhibitors, the affinity of each part of the bisubstrate inhibitor **4.9** was evaluated using compounds **4.13** and **4.14**, which separated **4.9** into an ATP-competitive and substrate-competitive halves, respectively (**Scheme 4.6**). The ATP-competitive portion **4.13** had increased potency (IC_{50} = 272 nM) relative to the bisubstrate inhibitors and the precursor ATP-competitive fragment **PP2-alkyne**. This increase in potency was not due to interactions with the substrate binding site, as the IC_{50} value was found to be unaffected when the substrate peptide concentration was increased 10-fold (IC_{50} = 295 nM). In contrast, the substrate competitive portion **4.14** was found to be a very poor inhibitor of c-Src (IC_{50} > 250 μM). This justifies why a large increase in potency was not seen with the nonpeptidic bisubstrate inhibitors. Because the substrate fragments are attached to the linker through the location of the substrate hydroxyl group, the poor potency of the substrate-competitive fragment is likely due to the loss of hydrogen bonds between the substrate hydroxyl group and the substrate binding site.

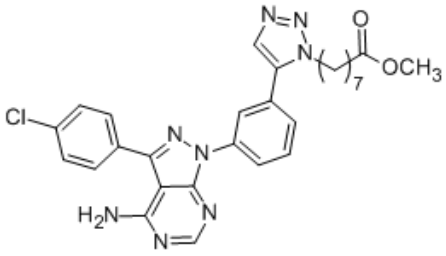

4.13
c-Src IC_{50} = 272 ± 53 nM

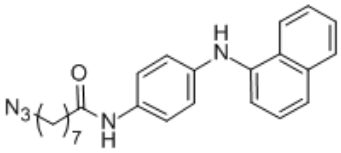

4.14
c-Src IC_{50} > 250 μM

Scheme 4.6. The nonpeptidic bisubstrate inhibitor **4.9** separated into its ATP-competitive (**4.13**) and substrate-competitive (**4.14**) components.

Taken together, these experiments raised the possibility that the substrate scaffold portion may not be binding in the substrate site as predicted. To test this, inhibitor **4.9** was evaluated under conditions where the pyrene peptide substrate concentration was increased to 500 μM and was found to have IC_{50} = 2 μM. Despite a 10-fold increase in peptide substrate concentration, the IC_{50} value was identical the value obtained under the

standard assay conditions. We saw two possible reasons for not observing a change in the IC_{50} value with increasing substrate concentration. First, an effect on the IC_{50} may not be noticeable because the substrate fragment binds weakly (as demonstrated by compound **4.14**) and does not contribute much to the overall potency of the bisubstrate inhibitor compared to the ATP-competitive portion. Alternatively, the substrate fragments may bind outside of the substrate site, or may not bind to c-Src at all, once incorporated into the bisubstrate inhibitor. The differences in potency observed for bisubstrate inhibitors **4.9**, **4.11**, and **4.12** that tracked with the differences in the relative affinities of the substrate scaffolds support that the substrate-competitive portion is binding weakly within the substrate binding site. In either case, it is clear that alteration of the substrate hydroxyl group in order to provide a point of attachment for the linker was not well tolerated and resulted in a significant loss in substrate fragment binding. Performing Lineweaver-Burk analysis would likely clarify if the bisubstrate compounds are substrate-competitive; however, these experiments were not performed as they are resource and time intensive, and the compounds are unlikely to be utilized further due to their low potencies.

Evaluation of Second Generation Inhibitors

While we were disappointed with the results from our initial inhibitors, the data are consistent with our previous studies that have shown that maintaining the hydrogen bonds formed by the substrate hydroxyl group are important for binding of small molecules to the substrate binding site. As such, we hypothesized bisubstrate inhibitors that maintained the hydroxyl group within the substrate fragment would have better potency due to increased interactions within the substrate binding site. To investigate this, nonpeptidic bisubstrate inhibitors using 2-aminophenol as the substrate-competitive fragment were prepared and evaluated using the pyrene peptide assay. As shown in **Scheme 4.7**, the substrate portion was attached to the linker via an amide as was done previously, and a 1,4-disubstituted-1,2,3-triazole was used to join the ATP-competitive portion and the linker. The 1,4-triazole was chosen because it was the linkage used in the peptidic bisubstrate inhibitor **4.1**. Since the linker was now attached to the "side" of the substrate instead of through the location of the substrate hydroxyl group, we

hypothesized that a longer linker would be necessary. We initially examined compounds with 8 and 9 methylene linkers.

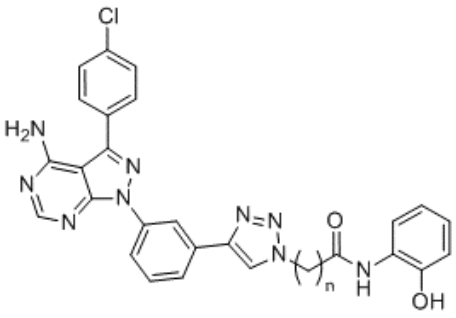

4.15: n = 8, c-Src IC_{50} = 5 ± 2 μM
4.16: n = 9, c-Src IC_{50} = 4 ± 1 μM

Scheme 4.7. Nonpeptidic bisubstrate inhibitors which retain a hydroxyl group in the substrate scaffold.

Results from the evaluation of the second generation bisubstrate inhibitors were promising. Both inhibitors **4.15** and **4.16** were nearly equivalent to the most potent compounds identified from the first generation inhibitors (IC_{50} = 5 μM and 4 μM, respectively). It should be stressed that these second generation inhibitors used an unoptimized substrate scaffold. In fact, 2-aminophenol was a poor substrate of c-Src when evaluated in the SAS study (see **Appendix C**, compound **P-S42**). Thus, using an optimized c-Src substrate scaffold that retains its hydroxyl group as the substrate-competitive fragment will likely further increase the potency of bisubstrate inhibitors. The results from these initial second generation inhibitors support that the poor potency observed with the first generation bisubstrate inhibitors was due to loss of important hydrogen bonds made by the substrate hydroxyl group. This further highlights the importance of these contacts for potent binding of ligands to the substrate binding site.

Conclusions

Bisubstrate inhibitors that target both the substrate and the ATP binding sites are highly sought after as they can combine the potency of ATP-competitive inhibitors with

the selectivity of substrate-competitive inhibitors. However, the lack of compounds which bind to the substrate site has limited the ability to design bisubstrate kinase inhibitors, and most reported bisubstrate inhibitors utilize peptides or a single phenyl ring as the substrate-competitive fragment. To remedy the problems associated with current bisubstrate inhibitors, we aimed to develop nonpeptidic bisubstrate inhibitors by replacing the peptidic portion of a bisubstrate inhibitor previously developed in our lab with small molecule c-Src substrates identified through SAS.

The initial library of inhibitors used substrate-competitive scaffolds which were attached to the ATP-competitive portion via an amide at the location of the reactive hydroxyl group. Despite our expectations of submicromolar potency, the best inhibitor (**4.9**) was found to have only low micromolar potency (IC_{50} = 1 μM). Further analysis of each "half" of inhibitor **4.9** showed that while the ATP-competitive portion was a nanomolar inhibitor of c-Src (**4.13**, IC_{50} = 272 nM), the substrate-competitive half was not a competent inhibitor (**4.14**, IC_{50} > 250 μM). The data from the initial set of bisubstrate inhibitors are consistent with our previous studies which have shown that maintaining the hydrogen bonds formed by the substrate hydroxyl group is important for binding of small molecules to the substrate site.

The importance of the hydroxyl group was supported by evaluation of two nonpeptidic bisubstrate inhibitors using 2-aminophenol as the substrate-competitive portion. Despite using a poor substrate scaffold, the potencies of inhibitors **4.15** and **4.16** (IC_{50} = 5 μM and 4 μM, respectively) were on par with the best inhibitors from the first library. While the initial study supports that incorporation of the linker *ortho* to the hydroxyl group is tolerated in this example, it should be cautioned that this has not been extensively examined and may not hold for other scaffolds beyond this simple case. Additionally, many of the previously identified small molecule substrates do not already contain a handle for straight forward attachment of the linker at the *ortho* position, and altering the scaffolds to incorporate a linker at this position may alter how the substrate binds. As such, evaluation of phenols that contain reactive handles at this position as c-Src substrates may prove useful. This SAR could potentially be combined with the previous SAR to generate optimal scaffolds for attachment to the linker.

Overall, while no potent nonpeptidic bisubstrate inhibitors were identified, we have gleaned important SAR that can be applied to the design of future bisubstrate inhibitors. In particular, we have once again seen that interactions made by the substrate hydroxyl group are critical for the binding of small molecules to the substrate site. We anticipate that future nonpeptidic bisubstrate inhibitors that contain optimized substrate scaffolds which retain the substrate hydroxyl group will show increased potency, and these inhibitors may prove to be useful biological probes for studying kinase signaling.

Materials and Methods

General Synthetic Methods

Unless otherwise noted, all reagents were obtained via commercial sources and used without further purification. ^{1}H NMR spectra were measured with a Varian MR400 or Inova 500 spectrometer.

Synthetic Protocols

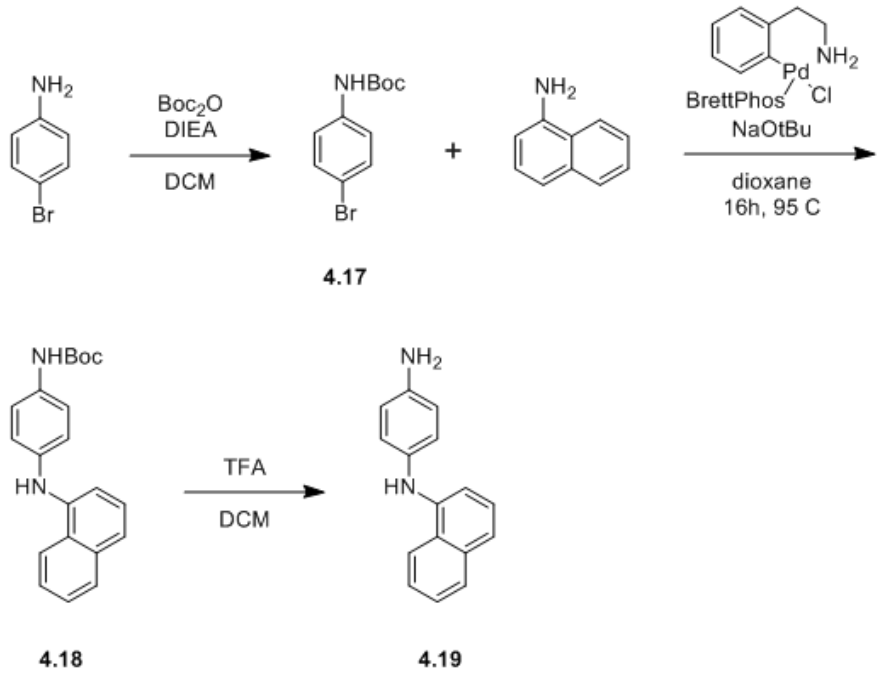

Scheme 4.8. Synthesis of compound **4.19**.

Tert-butyl (4-bromophenyl)carbamate (**4.17**). In a 250 mL round bottom flask, *p*-bromoaniline (2.0 g) was dissolved in 40 mL anhydrous CH_2Cl_2. Boc anhydride (2.8 g)

was added followed by DIEA (2.0 mL). The reaction was stirred at room temperature for 24 h. The reaction was washed with 10% aq. citric acid (1 x 30 mL) and the organic layer was dried over $MgSO_4$, filtered, and concentrated under reduced pressure. Purification by automated silica gel chromatography using a linear 2 → 20% EtOAc in hexanes gradient yielded the product as a white crystalline solid (2.3 g, 74% yield). ^{1}H NMR (500 MHz, Chloroform-*d*) δ 7.37 (d, *J* = 8.8 Hz, 2H), 7.24 (d, *J* = 8.8 Hz, 2H), 6.43 (s, 1H), 1.49 (s, 9H).

Tert-butyl (4-(naphthalen-1-ylamino)phenyl)carbamate (**4.18**). Compound **4.18** was prepared following the method of Maiti and Buchwald.[16] To an oven-dried 4 mL conical vial was added aryl bromide **4.17** (136 mg), 1-naphthylamine (86 mg), anhydrous sodium tert-butoxide (120 mg), and catalyst (0.8 mg). The vial was flushed with N_2, and then 2 mL anhydrous dioxane was added. The reaction was heated at 95 C for 16 h. The reaction was cooled to room temperature, diluted with 20 mL H_2O, and extracted with EtOAc (3 x 15 mL). The combined organic extracts were washed with 10% aq. citric acid (1 x 30 mL), dried over $MgSO_4$, filtered, and concentrated under reduced pressure. Purification by automated silica gel chromatography using a linear 5 → 40% EtOAc in hexanes gradient yielded the product as a purple crystalline solid (86 mg, 51% yield). ^{1}H NMR (400 MHz, Chloroform-*d*) δ 8.01 – 7.94 (m, 1H), 7.87 – 7.79 (m, 1H), 7.52 – 7.40 (m, 3H), 7.33 (t, *J* = 7.8 Hz, 1H), 7.28 – 7.18 (m, 2H), 7.02 – 6.94 (m, 3H), 6.34 (s, 1H), 5.87 (s, 1H), 1.50 (s, 9H).

N^1-(naphthalen-1-yl)benzene-1,4-diamine (**4.19**). In a 25 mL round bottom flask, the Boc-protected amine **4.18** (80 mg) was dissolved in 4.5 mL CH_2Cl_2. Trifluoroacetic acid (0.5 mL) was added and the reaction was stirred at room temperature overnight. The reaction was diluted with 10 mL H_2O and the pH was adjusted to ~12 with 1 M NaOH. The reaction was extracted with CH_2Cl_2 (3 x 15 mL) and EtOAc (2 x 15 mL). The combined organic extracts were dried over MgSO4, filtered, and concentrated under reduced pressure. Purification by automated silica gel chromatography using a linear 12 → 100% EtOAc in hexanes gradient yielded the product as a brown crystalline solid (45 mg, 84% yield). ^{1}H NMR (400 MHz, Chloroform-*d*) δ 8.01 – 7.92 (m, 1H), 7.86 – 7.77

(m, 1H), 7.51 – 7.40 (m, 2H), 7.37 (d, *J* = 8.2 Hz, 1H), 7.28 (t, *J* = 7.8 Hz, 1H), 7.03 – 6.93 (m, 3H), 6.73 – 6.64 (m, 2H), 5.81 (s, 1H), 3.60 (s, 2H).

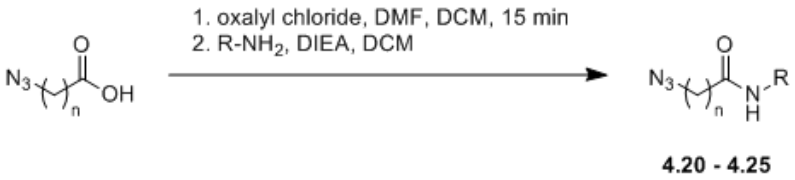

Scheme 4.9. Synthesis of substrate scaffolds attached to an azide linker.

General procedure for coupling of substrate scaffolds to azido acid linkers. Azido acids were prepared as previously described.[17] In an oven-dried round bottom flask under N_2, the appropriate azido acid (1.0 eq) was dissolved in anhydrous CH_2Cl_2. Oxalyl chloride (1.4 eq) was added followed by 1 drop of anhydrous DMF. The reaction began to effervesce. The reaction was stirred at room temperature for 15 minutes, and then the solvent was removed under reduced pressure. The resulting oil was dissolved in anhydrous CH_2Cl_2 in a round bottom flask under N_2. The appropriate amine (1.0 eq) was dissolved in minimal anhydrous CH_2Cl_2 and was added to the reaction followed by DIEA (2.0 eq). The reaction was stirred at room temperature under N_2 for 24h. The reaction was diluted with H_2O and extracted three times with CH_2Cl_2. The combined organic extracts were washed with 10% aqueous citric acid and brine. The organic layer was dried over MgSO4, filtered, and the solvent was removed under reduced pressure. The crude products were purified by automated silica gel chromatography. An analogous methyl ester (n = 7) was prepared in a similar manner as described above using anhydrous methanol in place of the amine in step 2 (compound provided by Kristin Ko).

6-azido-*N*-(4-(phenylamino)phenyl)hexanamide (**4.20**). ^{1}H NMR (400 MHz, Chloroform-*d*) δ 7.38 (dd, *J* = 9.1, 2.9 Hz, 2H), 7.28 – 7.18 (m, 2H), 7.08 – 6.96 (m, 5H), 6.89 (m, 1H), 5.63 (s, 1H), 3.32-3.25 (m, 2H), 2.38-2.30 (m, 2H), 1.80-1.70 (m, 2H), 1.69-1.59 (m, 2H), 1.51 – 1.40 (m, 2H).

8-azido-*N*-(4-(phenylamino)phenyl)octanamide (**4.21**). ^{1}H NMR (400 MHz, Chloroform-*d*) δ 7.41 – 7.33 (m, 2H), 7.25 – 7.18 (m, 2H), 7.11 – 6.95 (m, 5H), 6.88 (t, *J* = 7.3 Hz, 1H), 5.66 (s, 1H), 3.24 (t, *J* = 6.9 Hz, 2H), 2.36 – 2.28 (m, 2H), 1.76 – 1.67 (m, 2H), 1.64-1.50 (m, 2H), 1.43-1.30 (m, 6H).

4-azido-*N*-(4-(naphthalen-1-ylamino)phenyl)butanamide (**4.22**). ^{1}H NMR (500 MHz, Chloroform-*d*) δ 8.75 (s, 1H), 7.98 (d, *J* = 8.0 Hz, 2H), 7.84 (t, *J* = 7.1 Hz, 2H), 7.60 – 7.42 (m, 5H), 7.42 – 7.26 (m, 6H), 7.07 (s, 1H), 6.96 (dd, *J* = 8.7, 1.9 Hz, 4H), 5.93 (d, *J* = 23.7 Hz, 2H), 3.42 (t, *J* = 6.6 Hz, 2H), 2.47 – 2.40 (m, 2H), 2.04 – 1.97 (m, 2H).

6-azido-*N*-(4-(naphthalen-1-ylamino)phenyl)hexanamide (**4.23**). ^{1}H NMR (400 MHz, Chloroform-*d*) δ 8.01 – 7.94 (m, 1H), 7.87 – 7.81 (m, 1H), 7.54 – 7.42 (m, 3H), 7.40 – 7.33 (m, 3H), 7.28 – 7.25 (m, 1H), 7.01 (s, 1H), 6.98 – 6.94 (m, 2H), 5.90 (s, 1H), 3.28 (t, *J* = 6.8 Hz, 2H), 2.34 (t, *J* = 7.4 Hz, 2H), 1.80 – 1.71 (m, 2H), 1.68-1.59 (m, 2H), 1.52 – 1.41 (m, 2H).

7-azido-*N*-(4-(naphthalen-1-ylamino)phenyl)heptanamide (**4.24**). ^{1}H NMR (500 MHz, Chloroform-*d*) δ 7.98 (d, *J* = 8.1 Hz, 1H), 7.84 (d, *J* = 7.7 Hz, 1H), 7.54 – 7.41 (m, 3H), 7.40 – 7.32 (m, 3H), 7.27 (d, *J* = 8.3 Hz, 1H), 7.04 (s, 1H), 6.96 (d, *J* = 8.6 Hz, 2H), 5.91 (s, 1H), 3.25 (t, *J* = 6.9 Hz, 2H), 2.33 (t, *J* = 7.4 Hz, 2H), 1.76-1.70 (m, 2H), 1.63-1.59 (m, 2H), 1.46 – 1.35 (m, 4H).

8-azido-*N*-(4-(naphthalen-1-ylamino)phenyl)octanamide (**4.14**). ^{1}H NMR (400 MHz, Chloroform-*d*) δ 7.99-7.95 (m, 1H), 7.85-7.82 (m, 1H), 7.55 – 7.40 (m, 3H), 7.42 – 7.31 (m, 3H), 7.27 (d, 1H), 7.01 (s, 1H), 6.98 – 6.93 (m, 2H), 5.90 (s, 1H), 3.24 (t, *J* = 7.5 Hz, 2H), 2.32 (t, *J* = 7.5 Hz, 2H), 1.75-1.68 (m, 2H), 1.63-1.55 (m, 2H), 1.42-1.33 (m, 6H).

9-azido-*N*-(4-(naphthalen-1-ylamino)phenyl)nonanamide (**4.25**). ^{1}H NMR (500 MHz, Chloroform-*d*) δ 7.98 (d, *J* = 7.9 Hz, 1H), 7.84 (d, *J* = 8.1 Hz, 1H), 7.54 – 7.41 (m, 3H), 7.41 – 7.32 (m, 3H), 7.27 (d, *J* = 8.1 Hz, 1H), 7.02 (s, 1H), 6.96 (d, *J* = 8.2 Hz, 2H), 5.90

(s, 1H), 3.24 (t, *J* = 7.0 Hz, 2H), 2.32 (t, *J* = 7.5 Hz, 2H), 1.71 (t, *J* = 7.3 Hz, 2H), 1.40 – 1.30 (m, 10H).

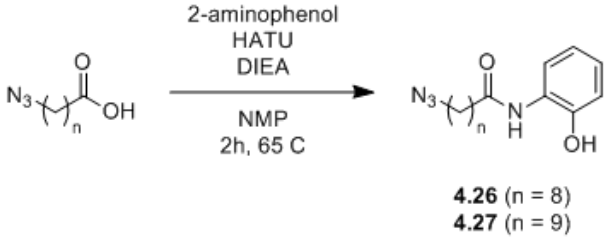

4.26 (n = 8)
4.27 (n = 9)

Scheme 4.10. Synthesis of phenol substrates attached to azido linkers.

General procedure for coupling of 2-aminophenol to azido acid linkers. Azido acids were prepared as previously described.[17] In a scintillation vial, 2-aminophenol (1.0 eq), HATU (1.0 eq), and DIEA (1.0 eq) were dissolved in NMP and were stirred at room temperature for 15 min. The appropriate azido acid (1.0 eq) was added and the reaction was stirred at 65 C for 2 h. The reaction was cooled to room temperature, diluted with EtOAc, and washed three times with H_2O. The organic layer was dried over $MgSO_4$, filtered, and the solvent was removed under reduced pressure. The crude products were purified by automated silica gel chromatography using a linear 6 → 50% EtOAc in hexanes gradient.

9-azido-*N*-(2-hydroxyphenyl)nonanamide (**4.26**). ^{1}H NMR (500 MHz, Chloroform-*d*) δ 8.81 (s, 1H), 7.50 (s, 1H), 7.10 (ddd, *J* = 8.6, 7.3, 1.6 Hz, 1H), 6.99 (ddd, *J* = 9.6, 8.0, 1.5 Hz, 2H), 6.84 (td, J = 7.6, 1.5 Hz, 1H), 3.24 (t, *J* = 6.9 Hz, 2H), 2.43 (t, *J* = 7.5 Hz, 2H), 1.73 (p, *J* = 7.5 Hz, 2H), 1.58 – 1.53 (m, 2H), 1.41 – 1.26 (m, 8H).

10-azido-*N*-(2-hydroxyphenyl)decanamide (**4.27**). ^{1}H NMR (500 MHz, Chloroform-*d*) δ 8.80 (s, 1H), 7.42 (s, 1H), 7.10 (t, *J* = 7.6 Hz, 1H), 7.01 (d, *J* = 8.0 Hz, 1H), 6.98 (d, *J* = 8.0 Hz, 1H), 6.84 (t, *J* = 7.5 Hz, 1H), 3.24 (t, *J* = 7.0 Hz, 2H), 2.44 (t, *J* = 7.5 Hz, 2H), 1.72 (q, *J* = 7.1 Hz, 2H), 1.62 – 1.52 (m, 2H), 1.40 – 1.25 (m, 10H).

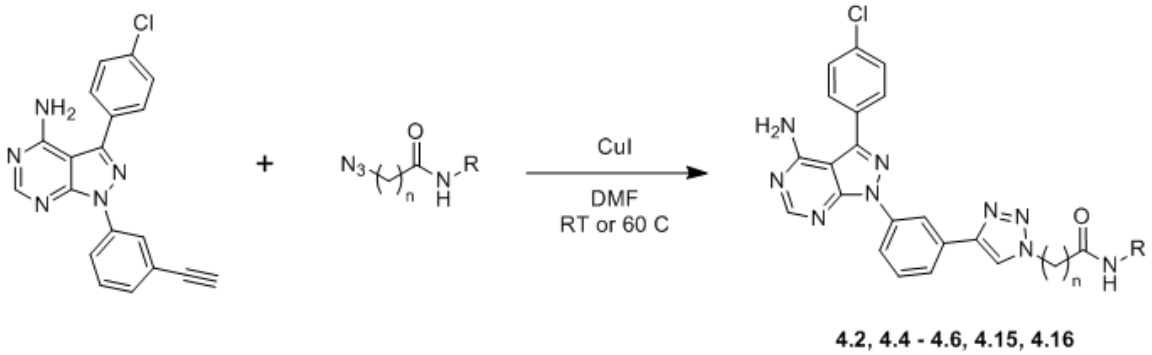

Scheme 4.11. Synthesis of 1,4-disubstituted-1,2,3-triazoles.

General synthesis of 1,4-disubstituted-1,2,3-triazoles. PP2-alkyne was prepared following a published protocol.[11] In an oven-dried flask under N_2, PP2-alkyne (1.0 eq), the appropriate azide (1.0 eq), and CuI (0.1 eq) were dissolved in anhydrous DMF. The reaction was stirred at room temperature or 60 C overnight. The reaction was diluted with H_2O and extracted with EtOAc. The combined organic extracts were concentrated under reduced pressure. The resulting residue was purified by reverse phase HPLC using a linear 30 → 90% ACN in H_2O gradient.

6-(4-(3-(4-amino-3-(4-chlorophenyl)-1*H*-pyrazolo[3,4-*d*]pyrimidin-1-yl)phenyl)-1*H*-1,2,3-triazol-1-yl)-*N*-(4-(phenylamino)phenyl)hexanamide (**4.2**). ^{1}H NMR (400 MHz, DMSO-d_6) δ 9.68 (s, 1H), 8.71 (s, 1H), 8.69 (t, *J* = 1.9 Hz, 1H), 8.40 (s, 1H), 8.27 – 8.20 (m, 1H), 7.97 (s, 1H), 7.79 (d, *J* = 8.4 Hz, 3H), 7.68 – 7.58 (m, 3H), 7.42 (d, *J* = 8.8 Hz, 2H), 7.16 (t, *J* = 7.9 Hz, 2H), 6.97 (m, 4H), 6.73 (t, *J* = 7.3 Hz, 1H), 4.43 (t, *J* = 7.0 Hz, 2H), 2.26 (t, *J* = 7.3 Hz, 2H), 1.96 – 1.87 (m, 2H), 1.67-1.59 (m, 2H), 1.35-1.22 (m, 2H).

6-(4-(3-(4-amino-3-(4-chlorophenyl)-1*H*-pyrazolo[3,4-*d*]pyrimidin-1-yl)phenyl)-1*H*-1,2,3-triazol-1-yl)-*N*-(4-(naphthalen-1-ylamino)phenyl)hexanamide (**4.4**). ^{1}H NMR (500 MHz, DMSO-d_6) δ 9.70 (s, 1H), 8.71 (s, 1H), 8.69 (t, *J* = 2.0 Hz, 1H), 8.40 (s, 1H), 8.26 – 8.20 (m, 1H), 8.17 (d, *J* = 8.2 Hz, 1H), 8.06 (s, 1H), 7.84 (dd, *J* = 7.9, 1.7 Hz, 1H), 7.82 – 7.75 (m, 3H), 7.67 – 7.58 (m, 3H), 7.52 – 7.38 (m, 5H), 7.32 (t, *J* = 7.8 Hz, 1H), 7.15 (d, *J* = 7.5 Hz, 1H), 7.00 (d, *J* = 8.9 Hz, 2H), 4.43 (t, *J* = 7.0 Hz, 2H), 2.27 (t, *J* = 7.3 Hz, 2H), 1.95 – 1.88 (m, 2H), 1.67 – 1.60 (m, 2H), 1.34 – 1.27 (m, 2H).

7-(4-(3-(4-amino-3-(4-chlorophenyl)-1*H*-pyrazolo[3,4-*d*]pyrimidin-1-yl)phenyl)-1*H*-1,2,3-triazol-1-yl)-*N*-(4-(naphthalen-1-ylamino)phenyl)octanamide (**4.5**). ^{1}H NMR (500 MHz, DMSO-d_6) δ 9.69 (s, 1H), 8.70 (s, 1H), 8.68 (t, *J* = 1.9 Hz, 1H), 8.40 (s, 1H), 8.23 (dd, *J* = 8.2, 2.2 Hz, 1H), 8.17 (d, *J* = 8.3 Hz, 1H), 8.06 (s, 1H), 7.83 (d, *J* = 7.6 Hz, 1H), 7.82-7.76 (m, 3H), 7.69 – 7.58 (m, 3H), 7.52 – 7.38 (m, 5H), 7.32 (t, *J* = 7.8 Hz, 1H), 7.15 (d, *J* = 7.5 Hz, 1H), 7.01 (d, *J* = 8.8 Hz, 2H), 4.41 (t, *J* = 7.1 Hz, 2H), 2.25 (t, *J* = 7.4 Hz, 2H), 1.92-1.84 (m, 2H), 1.60 – 1.53 (m, 2H), 1.37 – 1.26 (m, 6H).

4-(4-(3-(4-amino-3-(4-chlorophenyl)-1*H*-pyrazolo[3,4-*d*]pyrimidin-1-yl)phenyl)-1*H*-1,2,3-triazol-1-yl)-*N*-(4-(naphthalen-1-ylamino)phenyl)butanamide (**4.6**). ^{1}H NMR (500 MHz, DMSO-d_6) δ 9.78 (s, 1H), 8.72 (m, 2H), 8.41 (s, 1H), 8.24 (dd, *J* = 8.1, 2.2 Hz, 1H), 8.17 (d, *J* = 8.1 Hz, 1H), 8.07 (s¸1H), 7.87 – 7.76 (m, 4H), 7.65-7.62 (m, 3H), 7.50-7.41 (m, 5H), 7.32 (t, *J* = 7.8 Hz, 1H), 7.16 (d, *J* = 7.5 Hz, 1H), 7.02 (d, *J* = 8.6 Hz, 2H), 4.50 (t, *J* = 6.9 Hz, 2H), 2.34 (t, *J* = 7.4 Hz, 2H), 2.20 (p, *J* = 7.2 Hz, 2H).

9-(4-(3-(4-amino-3-(4-chlorophenyl)-1*H*-pyrazolo[3,4-*d*]pyrimidin-1-yl)phenyl)-1*H*-1,2,3-triazol-1-yl)-*N*-(2-hydroxyphenyl)nonanamide (**4.15**). ^{1}H NMR (500 MHz, DMSO-d_6) δ 9.71 (s, 1H), 9.22 (s, 1H), 8.70 (s, 1H), 8.68 (t, *J* = 2.0 Hz, 1H), 8.40 (s, 1H), 8.27 – 8.20 (m, 1H), 7.79 (dd, *J* = 8.7, 2.2 Hz, 3H), 7.67 – 7.59 (m, 4H), 6.91 (t, *J* = 7.7 Hz, 1H), 6.82 (d, *J* = 8.0 Hz, 1H), 6.73 (t, *J* = 7.6 Hz, 1H), 4.40 (t, *J* = 7.1 Hz, 2H), 2.35 (t, *J* = 7.4 Hz, 2H), 1.87 (p, *J* = 7.1 Hz, 2H), 1.59 – 1.52 (m, 2H), 1.31 – 1.20 (m, 8H).

10-(4-(3-(4-amino-3-(4-chlorophenyl)-1*H*-pyrazolo[3,4-*d*]pyrimidin-1-yl)phenyl)-1*H*-1,2,3-triazol-1-yl)-*N*-(2-hydroxyphenyl)decanamide (**4.16**). ^{1}H NMR (500 MHz, DMSO-d_6) δ 9.22 (s, 1H), 8.70 (s, 1H), 8.68 (t, *J* = 1.7 Hz, 1H), 8.40 (s, 1H), 8.23 (dd, *J* = 8.2, 2.2 Hz, 1H), 7.79 (d, *J* = 8.7, 3H), 7.67 – 7.60 (m, 4H), 6.91 (t, *J* = 7.7, 1H), 6.83 (d, *J* = 8.0 Hz, 1H), 6.73 (t, *J* = 7.6 Hz, 1H), 4.40 (t, *J* = 7.1 Hz, 2H), 2.35 (t, *J* = 7.4 Hz, 2H), 1.87 (p, *J* = 7.0 Hz, 2H), 1.55 (t, *J* = 7.3 Hz, 2H), 1.30-1.20 (m, 10H).

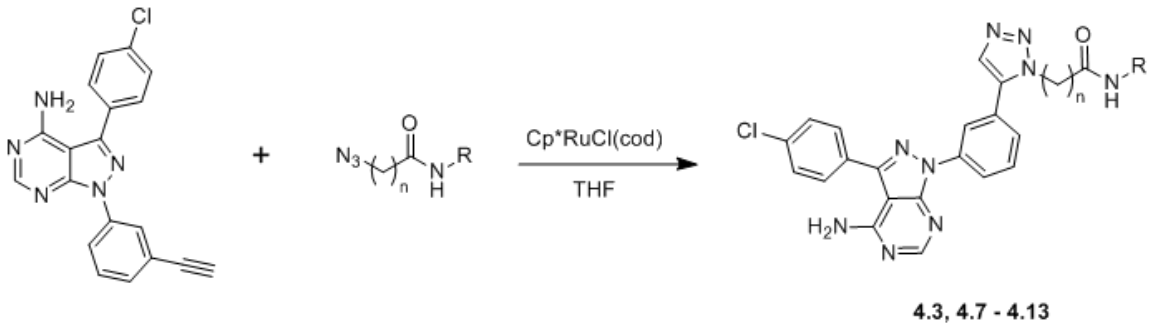

Scheme 4.12. Synthesis of 1,5-disubstituted-1,2,3-triazoles.

General synthesis of 1,5-disubstituted-1,2,3-triazoles. PP2-alkyne was prepared following a published protocol.[11] In a flame-dried flask under N_2, PP2-alkyne (1.0 eq) and Cp*RuCl(COD) (0.1 eq) were dissolved anhydrous THF. The appropriate azide (1.0 eq) was added and the reaction was stirred at room temperature overnight. The solvent was removed under reduced pressure. The resulting residue was purified by reverse phase HPLC using a linear 30 → 90% ACN in H_2O gradient.

6-(5-(3-(4-amino-3-(4-chlorophenyl)-1*H*-pyrazolo[3,4-*d*]pyrimidin-1-yl)phenyl)-1*H*-1,2,3-triazol-1-yl)-*N*-(4-(phenylamino)phenyl)hexanamide (**4.3**). ^{1}H NMR (500 MHz, DMSO-d_6) δ 9.63 (s, 1H), 8.45 (s, 1H), 8.39 (s, 1H), 8.34 (dd, *J* = 8.1, 2.2 Hz, 2H), 7.98 (s, 2H), 7.80 – 7.74 (m, 2H), 7.71 (t, *J* = 8.0 Hz, 2H), 7.65 – 7.57 (m, 2H), 7.53 (d, *J* = 7.7 Hz, 1H), 7.40 (dd, *J* = 9.2, 3.0 Hz, 2H), 7.17 (t, *J* = 7.7 Hz, 2H), 6.97 (dd, *J* = 8.3, 5.2 Hz, 4H), 6.73 (t, *J* = 7.3 Hz, 1H), 4.48 (t, *J* = 7.2 Hz, 2H), 2.17 (t, *J* = 7.4 Hz, 2H), 1.86 – 1.79 (m, 2H), 1.56 – 1.47 (m, 2H), 1.30 – 1.20 (m, 2H).

6-(5-(3-(4-amino-3-(4-chlorophenyl)-1*H*-pyrazolo[3,4-*d*]pyrimidin-1-yl)phenyl)-1*H*-1,2,3-triazol-1-yl)-*N*-(4-(naphthalen-1-ylamino)phenyl)hexanamide (**4.7**). ^{1}H NMR (500 MHz, DMSO-d_6) δ 9.65 (s, 1H), 8.46 (s, 1H), 8.41 – 8.32 (m, 2H), 8.17 (d, *J* = 8.3 Hz, 1H), 8.06 (s, 1H), 7.98 (s, 1H), 7.85 (d, *J* = 8.0 Hz, 1H), 7.77 (d, *J* = 8.2 Hz, 3H), 7.71 (t, *J* = 7.9 Hz, 1H), 7.62 (dd, *J* = 8.0, 5.5 Hz, 3H), 7.57 – 7.43 (m, 2H), 7.41 (d, *J* = 8.2 Hz, 2H), 7.35-7.29 (m, 1H), 7.15 (d, *J* = 7.5 Hz, 1H), 7.00 (d, *J* = 8.4 Hz, 2H), 4.48 (t, *J* = 7.1 Hz, 2H), 2.18 (t, *J* = 7.5 Hz, 2H), 1.85-1.78 (m, 2H), 1.57-1.48 (m, 2H), 1.30 – 1.25 (m, 2H).

7-(5-(3-(4-amino-3-(4-chlorophenyl)-1*H*-pyrazolo[3,4-*d*]pyrimidin-1-yl)phenyl)-1*H*-1,2,3-triazol-1-yl)-*N*-(4-(naphthalen-1-ylamino)phenyl)heptanamide (**4.8**). ^{1}H NMR (500 MHz, DMSO-d_6) δ 9.64 (s, 1H), 8.45 (t, *J* = 2.0 Hz, 1H), 8.39 (s, 1H), 8.35 (dd, *J* = 8.3, 2.1 Hz, 1H), 8.17 (d, *J* = 8.3 Hz, 1H), 7.98 (s, 1H), 7.84 (d, *J* = 7.2 Hz, 1H), 7.77 (d, *J* = 8.4 Hz, 2H), 7.72 (t, *J* = 8.0 Hz, 1H), 7.62 (d, *J* = 8.5 Hz, 2H), 7.54 (d, *J* = 7.6 Hz, 1H), 7.51 – 7.39 (m, 5H), 7.32 (t, *J* = 7.8 Hz, 1H), 7.15 (d, *J* = 7.5 Hz, 1H), 7.00 (d, *J* = 8.8 Hz, 2H), 4.47 (t, *J* = 7.2 Hz, 2H), 2.16 (t, *J* = 7.4 Hz, 2H), 1.83 – 1.76 (m, 2H), 1.49-1.44 (m, 2H), 1.25-1.19 (m, 4H).

7-(5-(3-(4-amino-3-(4-chlorophenyl)-1*H*-pyrazolo[3,4-*d*]pyrimidin-1-yl)phenyl)-1*H*-1,2,3-triazol-1-yl)-*N*-(4-(naphthalen-1-ylamino)phenyl)octanamide (**4.9**). ^{1}H NMR (500 MHz, DMSO-d_6) δ 9.65 (s, 1H), 8.45 (t, *J* = 2.0 Hz, 1H), 8.38 (s, 1H), 8.36 (dd, *J* = 8.2, 2.1 Hz, 1H), 8.18 (d, *J* = 8.1 Hz, 1H), 7.98 (s, 1H), 7.87 – 7.82 (m, 1H), 7.81 – 7.69 (m, 3H), 7.62 (d, *J* = 8.4 Hz, 2H), 7.54 (d, *J* = 7.7 Hz, 1H), 7.51-7.38 (m, 5H), 7.32 (t, *J* = 7.8 Hz, 1H), 7.15 (d, *J* = 7.5 Hz, 1H), 7.01 (d, *J* = 8.8 Hz, 2H), 4.47 (t, *J* = 7.2 Hz, 2H), 2.17 (t, *J* = 7.4 Hz, 2H), 1.82-1.74 (m, 2H), 1.49 – 1.42 (m, 2H), 1.28 – 1.18 (m, 6H).

9-(5-(3-(4-amino-3-(4-chlorophenyl)-1*H*-pyrazolo[3,4-*d*]pyrimidin-1-yl)phenyl)-1*H*-1,2,3-triazol-1-yl)-*N*-(4-(naphthalen-1-ylamino)phenyl)nonanamide (**4.10**). ^{1}H NMR (500 MHz, DMSO-d_6) δ 9.65 (s, 1H), 8.46 (t, *J* = 2.0 Hz, 1H), 8.41 – 8.34 (m, 2H), 8.18 (d, *J* = 8.3 Hz, 1H), 8.07 (s, 1H), 7.98 (s, 1H), 7.85 (d, *J* = 8.3 Hz, 1H), 7.81 – 7.72 (m, 3H), 7.63 (m, 2H), 7.57 – 7.39 (m, 6H), 7.33 (t, *J* = 7.9 Hz, 1H), 7.16 (d, *J* = 7.5 Hz, 1H), 7.02 (d, *J* = 8.8 Hz, 2H), 4.47 (t, *J* = 7.2 Hz, 2H), 2.18 (t, *J* = 7.5 Hz, 2H), 1.79 (p, *J* = 7.2 Hz, 2H), 1.47 (t, *J* = 7.1 Hz, 2H), 1.17 (m, *8*H).

8-(5-(3-(4-amino-3-(4-chlorophenyl)-1*H*-pyrazolo[3,4-*d*]pyrimidin-1-yl)phenyl)-1*H*-1,2,3-triazol-1-yl)-*N*-(4-(phenylamino)phenyl)octanamide (**4.11**). ^{1}H NMR (500 MHz, DMSO-d_6) δ 9.63 (s, 1H), 8.45 (s, 1H), 8.40 – 8.33 (m, 2H), 8.00 – 7.95 (m, 2H), 7.80 – 7.69 (m, 3H), 7.62 (dd, *J* = 8.5, 2.1 Hz, 2H), 7.53 (d, *J* = 7.7 Hz, 1H), 7.44 – 7.38 (m, 2H), 7.23 – 7.13 (m, 2H), 7.08 – 7.02 (m, 1H), 7.00 – 6.93 (m, 3H), 6.73 (t, *J* = 7.3 Hz,

1H), 4.46 (t, *J* = 7.1 Hz, 2H), 2.15 (t, *J* = 7.3 Hz, 2H), 1.81 – 1.74 (m, 2H), 1.48 – 1.40 (m, 2H), 1.24 – 1.12 (m, 6H).

8-(5-(3-(4-amino-3-(4-chlorophenyl)-1*H*-pyrazolo[3,4-*d*]pyrimidin-1-yl)phenyl)-1*H*-1,2,3-triazol-1-yl)-*N*-(quinolin-5-yl)octanamide (**4.12**). ^{1}H NMR (500 MHz, DMSO-d_6) δ 9.98 (s, 1H), 8.48 – 8.32 (m, 5H), 7.99 (s, 1H), 7.85 – 7.67 (m, 7H), 7.62 (d, *J* = 7.6 Hz, 2H), 7.57 – 7.50 (m, 2H), 4.49 (t, *J* = 7.2 Hz, 2H), 3.03 – 2.97 (m, 2H), 2.43 – 2.35 (m, 2H), 1.85 – 1.75 (m, 2H), 1.30 – 1.16 (m, 6H).

Methyl 8-(5-(3-(4-amino-3-(4-chlorophenyl)-1*H*-pyrazolo[3,4-*d*]pyrimidin-1-yl)phenyl)-1*H*-1,2,3-triazol-1-yl)octanoate (**4.13**). ^{1}H NMR (500 MHz, DMSO-d_6) δ 8.45 (s, 1H), 8.38 (m, 2H), 7.98 (s, 1H), 7.78 (d, *J* = 8.4 Hz, 2H), 7.74 (t, *J* = 8.0 Hz, 1H), 7.64 (d, *J* = 8.3 Hz, 2H), 7.54 (d, *J* = 7.7 Hz, 1H), 4.46 (t, *J* = 7.2 Hz, 2H), 3.52 (s, 3H), 2.15 (t, *J* = 7.4 Hz, 2H), 1.79-1.74 (m, 2H), 1.39 – 1.32 (m, 2H), 1.23-1.08 (m, 6H).

Spectral Data

Spectral data (^{1}H NMR) for compounds **4.2** – **4.27** is shown in **Appendix C**.

General Biochemical Methods

Black, opaque-bottom 96 well plates were used for fluorescence assays and were purchased from Nunc. c-Src was expressed by Christel Fox in *E. coli* using previously published procedures.[18] Data was obtained using a Biotek Synergy 4 plate reader. Curve fitting was performed using GraphPad Prism 4 software unless otherwise noted.

Determination of Inhibitor IC_{50}

A previously reported continuous fluorescence assay was used to determine inhibitor IC_{50} values.[12] Reaction volumes of 100 µL were used in 96-well plates. 85 µL of enzyme in buffer mix was added to each well followed by 2.5 µL of the appropriate inhibitor dilution (typically 5000, 2500, 1250, 625, 313, 156, 78, and 39 µM in DMSO) and 2.5 µL of a substrate peptide solution ("compound 3" as described in Wang *et al.*, typically 1.8 mM in DMSO). The reaction was initiated with 10 µL of ATP (1 mM in water), and reaction progress was immediately monitored at 405 nm (ex. 340 nm) for 10 minutes. Reactions had final concentrations of 30 nM c-Src, 45 µM "substrate 3", 1 mM

ATP, 100 μM Na_3VO_4, 100mM Tris buffer (pH 8), 10 mM $MgCl_2$, and 0.01% Triton X-100. To evaluate if inhibitors were substrate-competitive, the assay was carried out as described above with the final concentration of "substrate 3" increased to 500 μM.

The initial rate data collected was used for determination of IC_{50} values. The IC_{50} values were obtained directly from nonlinear regression of substrate-velocity curves in the presence of various concentrations of the inhibitor. The IC_{50} value for each inhibitor was determined using ≥3 independent experiments (unless otherwise noted) which were averaged to give an average IC_{50} value ± standard deviation. For analytical data see **Appendix C**.

References

1. Gower, C. M.; Chang, M. E. K.; Maly, D. J., Bivalent inhibitors of protein kinases. *Critical Reviews in Biochemistry and Molecular Biology* **2014,** *49* (2), 102-115.
2. Lamba, V.; Ghosh, I., New Directions in Targeting Protein Kinases: Focusing Upon True Allosteric and Bivalent Inhibitors. *Current Pharmaceutical Design* **2012,** *18* (20), 2936-2945.
3. Lavogina, D.; Enkvist, E.; Uri, A., Bisubstrate Inhibitors of Protein Kinases: from Principle to Practical Applications. *ChemMedChem* **2010,** *5* (1), 23-34.
4. Jencks, W. P., On the attribution and additivity of binding energies. *Proceedings of the National Academy of Sciences* **1981,** *78* (7), 4046-4050.
5. Han, K.-C.; Kim, S. Y.; Yang, E. G., Recent Advances in Designing Substrate-Competitive Protein Kinase Inhibitors *Current Pharmaceutical Design* **2012,** *18* (20), 2875-2882.
6. Kalesh, K. A.; Liu, K.; Yao, S. Q., Rapid synthesis of Abelson tyrosine kinase inhibitors using click chemistry. *Organic & Biomolecular Chemistry* **2009,** *7* (24), 5129-5136.
7. Kruse, C. H.; Holden, K. G.; Pritchard, M. L.; Feild, J. A.; Rieman, D. J.; Greig, R. G.; Poste, G., Synthesis and evaluation of multisubstrate inhibitors of an oncogene-encoded tyrosine-specific protein kinase. 1. *J. Med. Chem.* **1988,** *31* (9), 1762-1767.
8. Parang, K.; Till, J. H.; Ablooglu, A. J.; Kohanski, R. A.; Hubbard, S. R.; Cole, P. A., Mechanism-based design of a protein kinase inhibitor. *Nat Struct Mol Biol* **2001,** *8* (1), 37-41.
9. Brandvold, K. R.; Soellner, M. B., manuscript in preparation. 2014.
10. Breen, M. E.; Steffey, M. E.; Lachacz, E. J.; Kwarcinski, F. E.; Fox, C. C.; Soellner, M. B., Substrate Activity Screening with Kinases: Discovery of Small-Molecule Substrate-Competitive c-Src Inhibitors. *Angewandte Chemie International Edition* **2014,** *53* (27), 7010-7013.
11. Brandvold, K. R.; Steffey, M. E.; Fox, C. C.; Soellner, M. B., Development of a Highly Selective c-Src Kinase Inhibitor. *ACS Chem. Biol.* **2012,** *7* (8), 1393-1398.

12. Wang, Q.; Cahill, S. M.; Blumenstein, M.; Lawrence, D. S., Self-Reporting Fluorescent Substrates of Protein Tyrosine Kinases. *J. Am. Chem. Soc.* **2006,** *128* (6), 1808-1809.
13. Wang, C.; Lee, T. R.; Lawrence, D. S.; Adams, J. A., Rate-Determining Steps for Tyrosine Phosphorylation by the Kinase Domain of v-fps†. *Biochemistry* **1996,** *35* (5), 1533-1539.
14. Adams, J. A.; Taylor, S. S., Energetic limits of phosphotransfer in the catalytic subunit of cAMP-dependent protein kinase as measured by viscosity experiments. *Biochemistry* **1992,** *31* (36), 8516-8522.
15. Hubbard, S. R., *Crystal structure of the activated insulin receptor tyrosine kinase in complex with peptide substrate and ATP analog*. 1997; Vol. 16, p 5572-5581.
16. Maiti, D.; Buchwald, S. L., Orthogonal Cu- and Pd-Based Catalyst Systems for the O- and N-Arylation of Aminophenols. *J. Am. Chem. Soc.* **2009,** *131* (47), 17423-17429.
17. David, O.; Meester, W. J. N.; Bieräugel, H.; Schoemaker, H. E.; Hiemstra, H.; van Maarseveen, J. H., Intramolecular Staudinger Ligation: A Powerful Ring-Closure Method To Form Medium-Sized Lactams. *Angewandte Chemie International Edition* **2003,** *42* (36), 4373-4375.
18. Seeliger, M. A.; Young, M.; Henderson, M. N.; Pellicena, P.; King, D. S.; Falick, A. M.; Kuriyan, J., High yield bacterial expression of active c-Abl and c-Src tyrosine kinases. *Protein Science* **2005,** *14* (12), 3135-3139.

CHAPTER V
Conclusions

Abstract

Studies presented in this dissertation have focused on the discovery of substrate-competitive inhibitors of c-Src kinase, including peptidic inhibitors, small molecule inhibitors, and non-peptidic bisubstrate inhibitors. Results from all three studies have stressed the importance of maintaining key hydrogen bonds formed by the tyrosine hydroxyl group within the substrate binding site. Overall, these studies have added to our understanding of how to best discover substrate-competitive tyrosine kinase inhibitors through both screening and rational design. This knowledge will enable the development of additional potent substrate-competitive inhibitors for c-Src and other kinases of interest.

Discovery of Substrate-Competitive Kinase Inhibitors

Despite the interest in substrate-competitive inhibitors, greater than 99% of reported kinase inhibitors are ATP-competitive inhibitors. This is largely due to the difficulty associated with identifying substrate-competitive inhibitors. Compared to the ATP binding site, which is located in a deep hydrophobic cleft, the substrate-binding site is shallow and largely solvent exposed which makes it challenging to target with small molecules. Furthermore, high throughput screening libraries are highly biased towards heterocyclic compounds that are more likely to act as ATP mimics. Taken together, this has hindered the discovery of substrate-competitive inhibitors.

Few methods have been reported that can reliably identify substrate-competitive inhibitors, and all of the methods suffer from significant flaws. Peptidic substrate-competitive inhibitors have been rationally designed by replacing the phosphorylated residue by nonphosphorylatable residues, and also have been discovered from screens of peptide libraries using phage display and one-bead-one-compound techniques. However,

these inhibitors often have poor potency and poor pharmacokinetic properties which limits their use *in vivo*. Recently, reports of the discovery of small molecule ATP-noncompetitive inhibitors identified using a variety of approaches has increased. Some of these approaches such as virtual screening or structure based drug design required structural data, and this will limit their application, especially to new or understudied targets. Other methods such as biased activity assays, competitive binding assays, and NMR screens using ATP-competitive paramagnetic probes can be applied without requiring structural knowledge of the target, but these methods still have shortcomings. While biased competitive assays have the potential to identify substrate-competitive inhibitors, the conditions also favor the discovery of allosteric inhibitors or highly potent ATP-competitive inhibitors, and thus far no substrate-competitive inhibitors have been reported that were identified from a biased activity assay. NMR screening using spin-labeled ATP-competitive probes can identify substrate-competitive inhibitors, but these methods can also identify allosteric inhibitors. Competitive binding assays using substrate-competitive probes currently hold the most promise for the exclusive identification of substrate-competitive inhibitors, but the modest affinity of most substrate-competitive ligands has prevent the development of the required probes. Potent bisubstrate probes composed of ATP-competitive and substrate-competitive inhibitors address this issue; however, these probes will also identify ATP-competitive inhibitors, and thus a counter screen will be required.

As a whole, there is still a great need for the development of new methods for the identification of small molecule substrate-competitive inhibitors. The work presented in this dissertation aimed to remedy this problem by developing new methods methodologies for the discovery of small-molecule substrate-competitive tyrosine kinase inhibitors. Substrate-competitive small molecules were also applied to the design of nonpeptidic bisubstrate inhibitors.

Peptidic Inhibitors of c-Src Kinase for Pharmacophore Identification

Work for this dissertation began with the development of peptidic inhibitors of c-Src kinase. The aim of the study was to identify new tyrosine pharmacophores for c-Src using a library of peptides. We anticipated that potent peptidic inhibitors discovered

from this study could then be fluorescently labeled and used to develop a competitive binding fluorescence polarization assay to screen for small molecule substrate-competitive inhibitors. SAR for the tyrosine pharmacophores could also be applied later to the design of small molecule substate-competitive inhibitors. While peptidic inhibitors of c-Src with substituted phenylalanine pharmacophores have been previously reported, the study was limited to pharmacophores with *para*-substitutions (with the exception of pentafluorophenylalanine).[1] We have expanded the substituents explored at the *para* position, as well as examined the effects of substitutions at the *ortho* and *meta* positions. We also evaluated natural amino acids other than phenylalanine or alanine as pharmacophores.

In general, for two libraries of peptides based on the c-Src substrate Ac-AIYAA-NH_2, poor inhibition was observed upon replacement of the reactive tyrosine residue (all $K_i \geq 200$ μM). While no mono-substitutions at the *meta* position were found to increase potency, an *ortho*-fluorine group increased potency and could later be combined with optimal *para* substituents to increase potency. The best *para* substituents were halogens, and inhibitor potency increased with increasing halogen size. Potency also increased with increasing number of halogen substituents. Because other non-halogen substitutions that increased hydrophobicity were poor inhibitors, we hypothesize pharmacophores must increase the hydrophobic surface area and decrease the electron density within the phenylalanine ring in order to produce c-Src inhibition.

The poor potency of the Ac-AIXAA-NH_2 library prompted us to also reexamine three peptides reported in the literature to be potent inhibitors of c-Src.[2-4] Only peptide **2.51** was found to be a c-Src inhibitor (K_i = 70 μM). An AMCA-labeled analogue of this peptide (**2.52**) was evaluated as well, but it was still less potent than required for FP assay development (K_i = 49 μM).

While no peptides potent enough for developing an FP screen were identified from these libraries, we did gain valuable insight into the SAR of tyrosine pharmacophores. Our results also support the long-held belief that the tyrosine hydroxyl group makes important hydrogen bonding contacts within the substrate binding site, and thus removal of this hydroxyl group greatly reduces potency. Combined with our pharmacophore analysis, this suggests that an ideal pharmacophore would maintain these hydrogen

bonding contacts, have increased hydrophobic surface area, and have decreased electron density. The development of such pharmacophores may enable the design of peptidic inhibitors with the low micromolar potency required for developing a substrate-competitive FP probe.

Substrate Activity Screening for Protein Tyrosine Kinases

Although a competitive binding assay using a peptidic substrate-competitive c-Src ligand would be useful for the identification of substrate-competitive inhibitors of c-Src, the probe would not be widely applicable to any kinase and new probes would need to be developed for other kinases of interest. Thus, we also wanted to develop general screening methodology that could be applied to any tyrosine kinase of interest to identify substrate-competitive inhibitors. Substrate activity screening (SAS) is a screening method pioneered by the Ellman lab that identifies substrates of an enzyme instead of inhibitors.[5] We thought SAS would be an excellent strategy for the identification of substrate-competitive inhibitors of tyrosine kinases because substrates converted into inhibitors should inherently be substrate-competitive.

Using an ADP detection assay, we have reported the first small molecule substrates of a protein kinase. Several of the small molecule substrates have K_M values better than that of a known peptide substrate. Using knowledge gained from the pharmacophore library and literature, one of the identified substrates (**3.5**, K_M = 122 μM) was then successfully converted into an inhibitor of c-Src (**3.7**, K_i = 257 μM) by replacing the phenol with tetrafluorophenol. Two previously unreported pharmacophores, pyridine N-oxide and hydroxypyridine, were also evaluated but were found to be less potent and less selective than tetrafluorophenol. Through a focused library of analogues, lead inhibitor **3.12** (K_i = 16 μM) was identified. Extensive kinetics analysis, modeling, and mutagenesis studies support that lead inhibitor **3.12** has a substrate-competitive, ATP-noncompetitive binding mode as hypothesized.

Biochemical evaluation showed that inhibitor **3.12** has greater than 66-fold selectivity against the highly similar non-Src family kinase c-Abl, as well as selectivity against other Src family kinases including Yes. We have also conclusively demonstrated

for the first time that a substrate-competitive kinase inhibitor can be combined with ATP-competitive inhibitors to produce synergistic inhibition of the target.

The non-peptidic nature of **3.12** also enabled us to explore its activity *in cellulo*. Inhibitor **3.12** inhibits the growth of c-Src dependent cancer cell lines with low micromolar GI_{50} values that are comparable to the most potent ATP-competitive c-Src inhibitors known. In contrast to the ATP-competitive c-Src inhibitor **PP2**, which is often used as a c-Src biological probe, **3.12** only inhibits the activation of c-Src dependent signaling pathways. The biochemical and cellular evaluation of **3.12** clearly demonstrated the improved features of substrate-competitive inhibitors compared to ATP-competitive inhibitors.

While other methods have been reported for the discovery of substrate-competitive kinase inhibitors, the SAS method described here is the only general screening method for the exclusive identification of small molecule substrate-competitive kinase inhibitors. Our SAS method should be applicable to any tyrosine kinase of interest, and could likely be modified for screening non-tyrosine kinases.

Progress Towards Nonpeptidic Bisubstrate Kinase Inhibitors

In addition to substrate-competitive kinase inhibitors, bisubstrate inhibitors that target both the substrate and the ATP binding sites are also highly sought after as they can combine the potency of ATP-competitive inhibitors with the selectivity of substrate-competitive inhibitors. However, the lack of compounds which bind to the substrate site has limited the ability to design bisubstrate kinase inhibitors. Most reported bisubstrate inhibitors utilize peptides as the substrate-competitive fragment, and this has prevented their use as biological probes. A small number of bisubstrate inhibitors which use a single phenyl ring as a tyrosine pharmacophore for the substrate competitive portion have been reported, but these bisubstrate inhibitors suffer from poor potency. To remedy the problems associated with current bisubstrate inhibitors, we aimed to develop nonpeptidic bisubstrate inhibitors by replacing the peptidic portion of a bisubstrate inhibitor previously developed in our lab with small molecule c-Src substrates identified through SAS.

The initial library of inhibitors used substrate-competitive scaffolds identified from SAS that were attached to the ATP-competitive portion via an amide at the location of the reactive hydroxyl group. While submicromolar potency was expected based on the potency of similar ATP-competitive inhibitors, the best inhibitors were found to have only low micromolar potency (**4.9**, IC_{50} = 1 μM). Further analysis of each "half" of inhibitor **4.9** showed that while the ATP-competitive portion was a nanomolar inhibitor of c-Src (**4.13**, IC_{50} = 272 nM), the substrate-competitive half was not a competent inhibitor (**4.14**, IC_{50} > 250 μM). We also found that the differences in potency for bisubstrate inhibitors utilizing different substrate-competitive portions tracked well with the differences in the relative affinities of the substrate-competitive scaffolds. This supports that the substrate-competitive portion is binding weakly within the substrate binding site.

The data from the initial set of bisubstrate inhibitors is consistent with our previous studies which have shown that maintaining the hydrogen bonds formed by the substrate hydroxyl group is important for binding of small molecules to the substrate site. We then evaluated two inhibitors that contained a hydroxyl group in the substrate-competitive portion. It was encouraging to see that despite using a poor substrate scaffold the potencies of inhibitors **4.15** (IC_{50} = 5 μM) and **4.16** (IC_{50} = 4 μM) were on par with the best inhibitors from the first library. Because the first library used an optimized substrate scaffold, we anticipate that future bisubstrate inhibitors that use optimized substrate scaffolds which retain the substrate hydroxyl group will show increased potency. Although this study supports that incorporation of the linker *ortho* to the phenol is tolerated, one hurdle moving forward will be that the c-Src substrates previously identified do not already contain handles for attachment of the linker at the *ortho* position, and incorporating these handles may change how the substrates bind.

Conclusions

The studies presented in this dissertation have highlighted the difficulties facing the discovery of substrate-competitive kinase inhibitors, whether through the development of new screening methods or the rational design of inhibitors. We initially sought to identify potent peptidic inhibitors of c-Src that could be used to develop a fluorescence

polarization assay to screen for small molecule substrate-competitive inhibitors. Although this assay could have proved useful for the identification of new substrate-competitive c-Src inhibitors, the assay would not have been widely applicable to all kinases as the substrate site is not conserved across the kinome. While the low similarity between kinase substrate sites enables substrate-competitive inhibitors to be more selective than ATP-competitive inhibitors, an additional consequence of this is that probes targeting the substrate site will only bind to a small subset of kinases. This has complicated the development of new screening methods for substrate-competitive inhibitors since assays which rely on displacement of a probe bound to the substrate site will not be general. Therefore, a general screening method that can be applied to many kinases will be more useful. In contrast to other reported screening methods, the SAS method developed in this work is the only general screening method for the discovery of substrate-competitive tyrosine kinase inhibitors. Because the SAS method relies on monitoring the production of ADP, which is a byproduct of all kinase reactions, the method can be applied to any tyrosine kinase of interest. The method should also be applicable to dual specificity kinases, and modification of the screening library and pharmacophores may allow the method to be expanded to other kinases as well.

In particular, our studies have stressed the importance of maintaining key hydrogen bonds formed by the tyrosine hydroxyl group within the substrate binding site. It was clearly demonstrated throughout this work that loss of the hydrogen bonds formed with the substrate hydroxyl group negatively impacted inhibitor potency. In the first study, we were unable to find any peptides with low micromolar c-Src potency despite examining nearly 50 pharmacophores. Although the lack of potent inhibitors prevented us from using these peptides in the development of an FP assay to screen for small molecule substrate-competitive inhibitors, the SAR found in this study would prove useful for the conversion of small molecule c-Src substrates into inhibitors in the development of the SAS method for tyrosine kinases. From the peptidic inhibitor SAR, we concluded an ideal pharmacophore should maintain the hydrogen bonding contacts formed by the tyrosine hydroxyl group, have increased hydrophobic surface area, and have decreased electron density. We evaluated three pharmacophores which fit these criteria in the SAS

study and found that all three successfully converted the small molecule substrate into an inhibitor. This served as key step in the development of the SAS method.

The importance of the substrate hydroxyl group was also seen in the rational design of non-peptidic bisubstrate inhibitors. No potent bisubstrate inhibitors were identified in the first library, which linked the substrate scaffold to the ATP-competitive portion at the location of the hydroxyl group. Additionally, evaluation of the substrate-competitive "half" showed that it was a poor inhibitor of c-Src. However, a second set of inhibitors that used an unoptimized substrate scaffold but retained the substrate hydroxyl group were found to have potency equivalent to the best inhibitors in the first library. This further supports the importance of contacts made by the substrate hydroxyl group, and suggests that future non-peptidic bisubstrate inhibitors should maintain the substrate hydroxyl group.

Overall, these studies have added to our knowledge of how to best discover substrate-competitive tyrosine kinase inhibitors through both screening and rational design. We anticipate that the SAS method for tyrosine kinases will enable the discovery of substrate-competitive inhibitors for other kinases of interest. Additionally, better understanding of tyrosine pharmacophores and the importance of the hydroxyl group for inhibitor potency will help guide the rational design of future peptidic and nonpeptidic substrate-competitive inhibitors as well as nonpeptidic bisubstrate inhibitors. Improved inhibitors, especially small molecule substrate-competitive inhibitors and non-peptidic bisubstrate inhibitors, can serve as important biological tools for the study of kinase signaling and potential therapeutics.

References

1. Niu, J.; Lawrence, D. S., Nonphosphorylatable Tyrosine Surrogates: Implications for Protein Kinase Inhibitor Design. *J. Biol. Chem.* **1997,** *272* (3), 1493-1499.
2. Kamath, J. R.; Liu, R.; Enstrom, A. M.; Lou, Q.; Lam, K. S., Development and characterization of potent and specific peptide inhibitors of p60c-src protein tyrosine kinase using pseudosubstrate-based inhibitor design approach. *The Journal of Peptide Research* **2003,** *62* (6), 260-268.
3. Kumar, A.; Ye, G.; Wang, Y.; Lin, X.; Sun, G.; Parang, K., Synthesis and Structure−Activity Relationships of Linear and Conformationally Constrained Peptide Analogues of CIYKYY as Src Tyrosine Kinase Inhibitors. *J. Med. Chem.* **2006,** *49* (11), 3395-3401.

4. Hah, J.-M.; Sharma, V.; Li, H.; Lawrence, D. S., Acquisition of a "Group A"-Selective Src Kinase Inhibitor via a Global Targeting Strategy. *J. Am. Chem. Soc.* **2006,** *128* (18), 5996-5997.
5. Wood, W. J. L.; Patterson, A. W.; Tsuruoka, H.; Jain, R. K.; Ellman, J. A., Substrate activity screening: A fragment-based method for the rapid identification of nonpeptidic protease inhibitors. *J. Am. Chem. Soc.* **2005,** *127* (44), 15521-15527.

Appendix A
Analytical Data for Chapter II

Analytical Data for Determination of K_i for Peptidic Inhibitors

Ac-AIXAA-NH$_2$ Libraries:

2.1 (X = Tyr, c-Src) K_i > 1000 μM

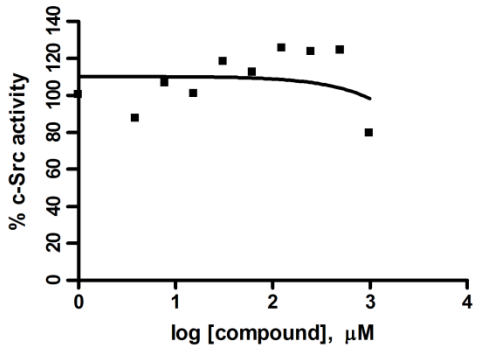

2.2 (X = D-Tyr) c-Src K_i > 1000 μM

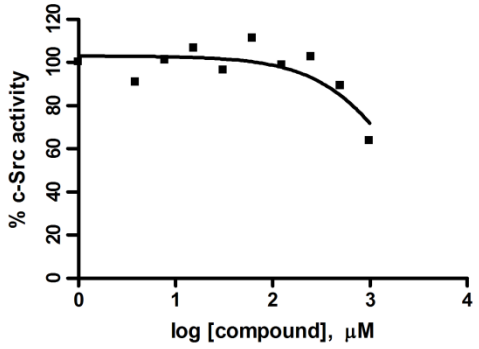

2.2 (X = D-Tyr) c-Abl K_i > 1000 μM

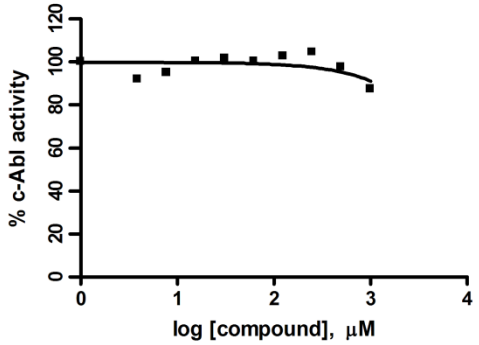

2.3 (Ac-aaiya-NH2) c-Src K_i > 1000 μM

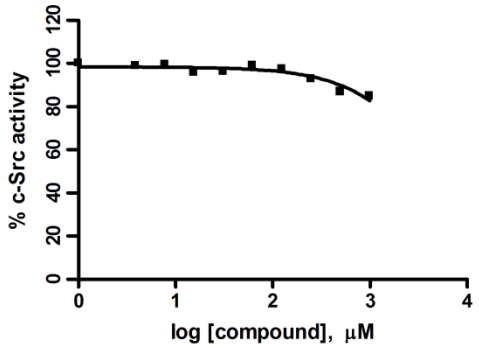

2.4 (X = Phe) c-Src K_i = 950 ± 55 μM

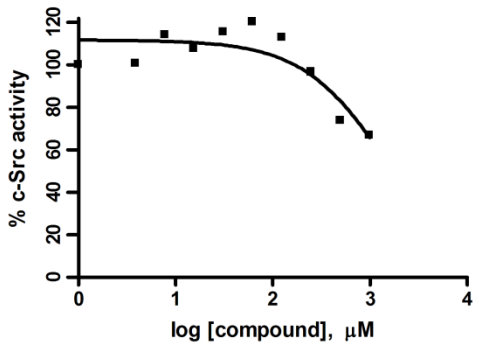

2.4 (X = Phe) c-Abl K_i = >500 μM

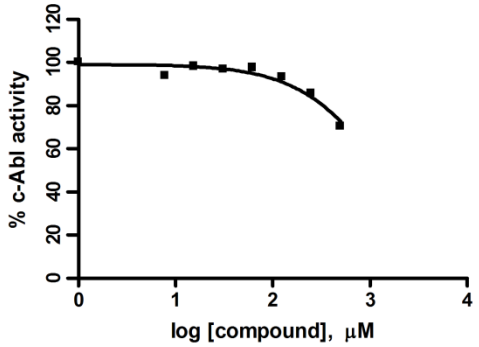

2.5 (X = Ala) c-Src K_i > 1000 μM

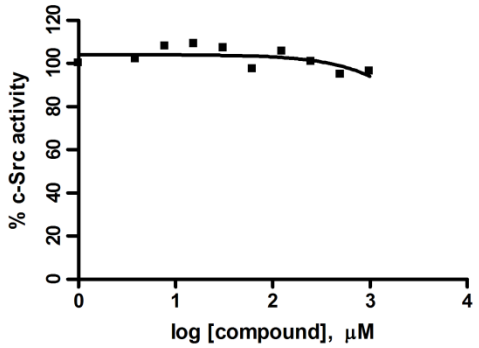

2.5 (X = Ala) c-Abl K_i > 1000 μM

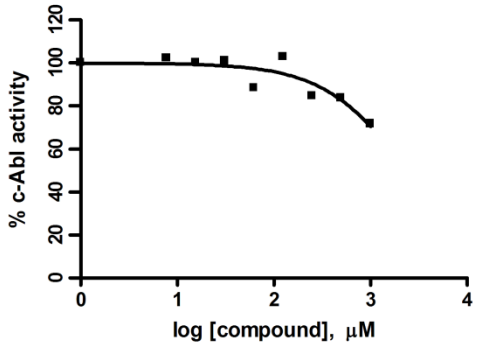

2.6 (X = Trp) c-Src K_i > 1000 μM

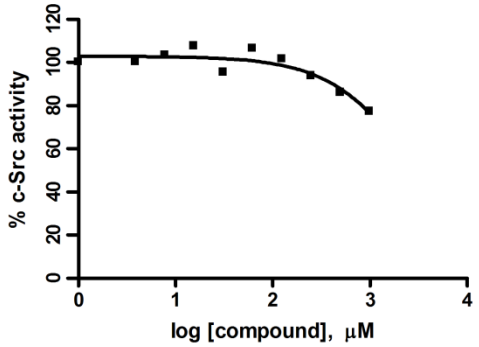

2.6 (X = Trp) c-Abl K_i > 1000 μM

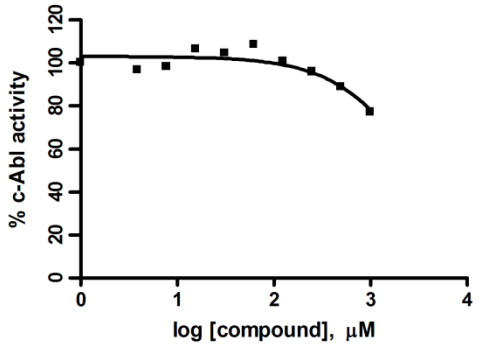

2.7 (X = His) c-Src K_i = 172 ± 11 μM

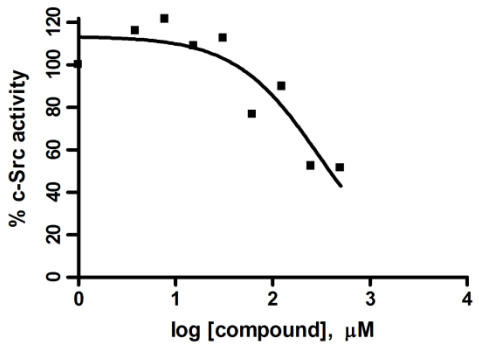

2.7 (X = His) c-Abl K_i > 1000 μM

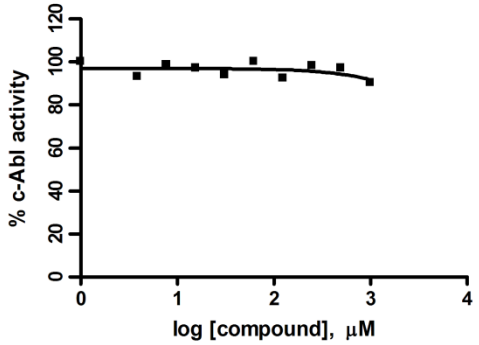

2.8 (X = 2-CH_3 Phe) c-Src K_i > 500 μM

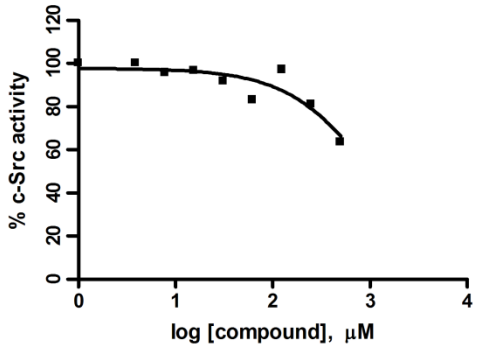

2.8 (X = 2-CH_3 Phe) c-Abl K_i > 1000 μM

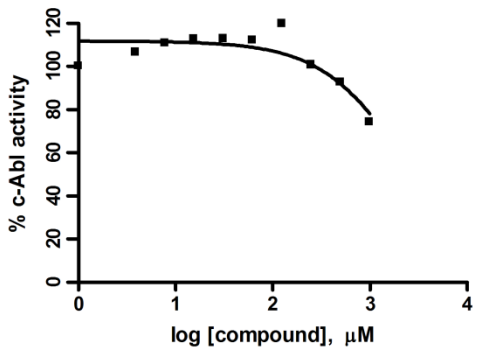

2.9 (X = 2-CF_3 Phe) c-Src K_i > 1000 μM

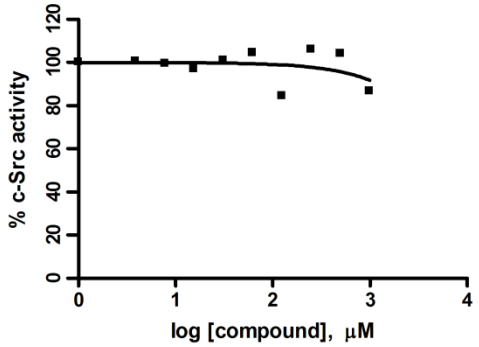

2.10 (X = 2-OCH_3 Phe) c-Src K_i > 1000 μM

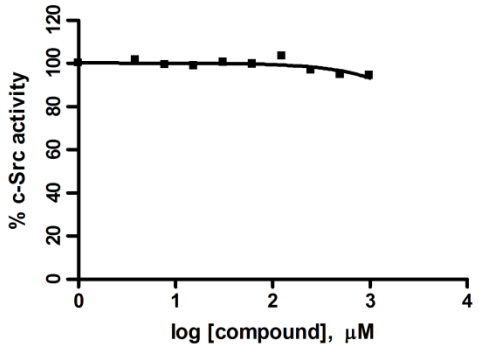

2.11 (X = 2-F Phe) c-Src K_i = 433 ± 48 μM

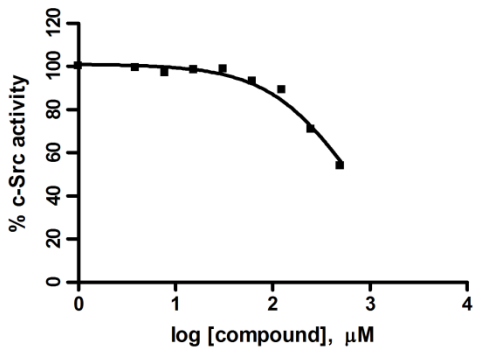

2.11 (X = 2-F Phe) c-Abl K_i > 1000 μM

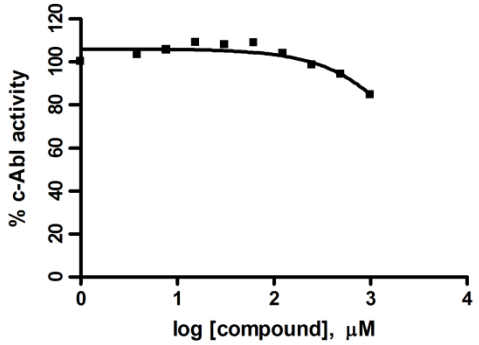

2.12 (X = 2-Cl Phe) c-Src K_i = 845 ± 186 μM

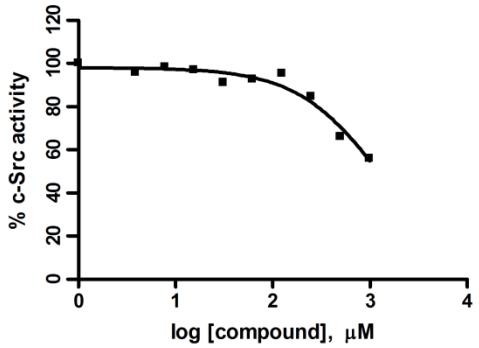

2.12 (X = 2-Cl Phe) c-Abl K_i > 1000 μM

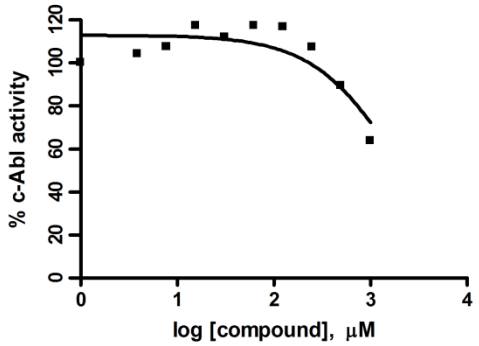

2.13 (X = 3-CH_3 Phe) c-Src K_i > 1000 μM

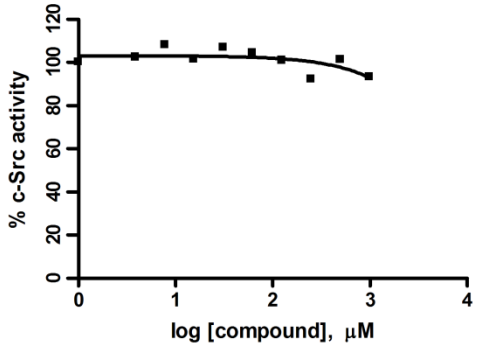

2.14 (X = 3-CF_3 Phe) c-Src K_i > 1000 μM

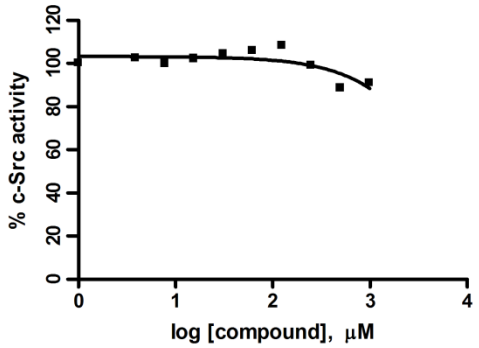

2.15 (X = 3-OCH_3 Phe) c-Src K_i > 1000 μM

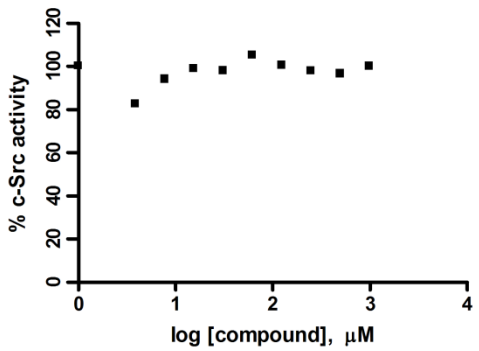

2.16 (X = 3-F Phe) c-Src K_i > 1000 μM

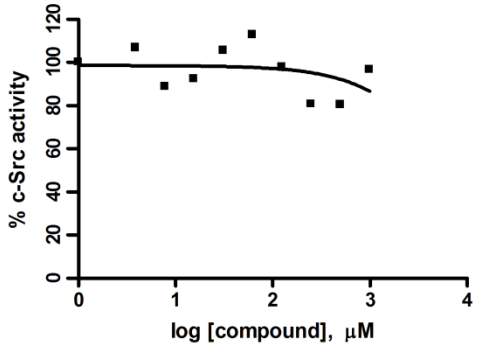

2.17 (X = 3-Cl Phe) c-Src K_i > 1000 μM

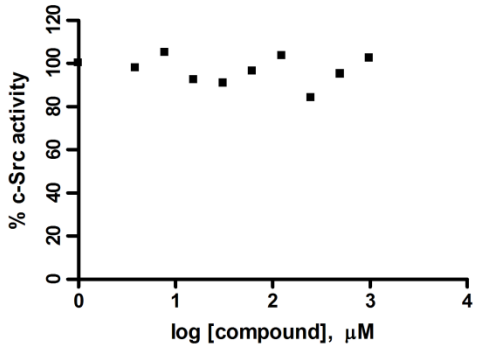

2.18 (X = 4-CH_3 Phe) c-Src K_i > 500 μM

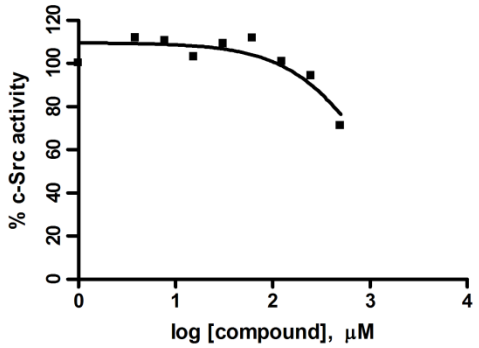

2.18 (X = 4-CH_3 Phe) c-Abl K_i > 1000 μM

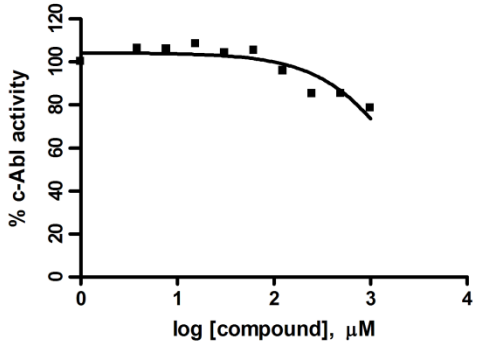

2.19 (X = 4-CF_3 Phe) c-Src K_i = 862 ± 159 μM

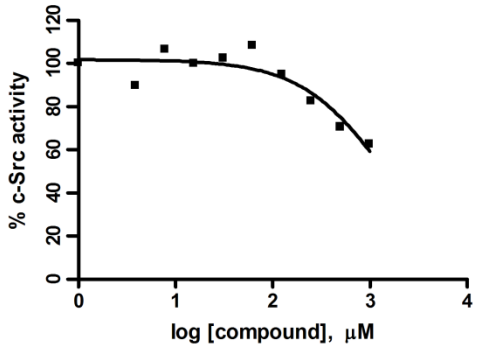

2.19 (X = 4-CF_3 Phe) c-Abl K_i > 1000 μM

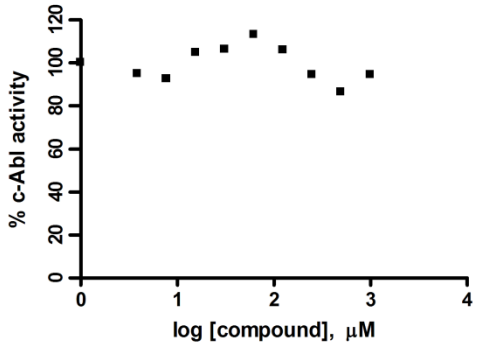

2.20 (X = 4-OCH_3 Phe) c-Src K_i > 1000 μM

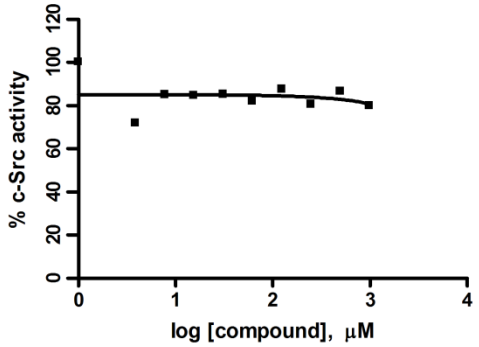

2.21 (X = 4-OCH_2CH_3 Phe) c-Src K_i > 1000 μM

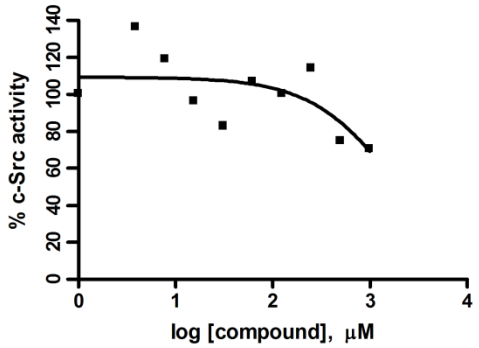

2.22 (X = 4-$OCHCH_2$ Phe) c-Src K_i > 1000 μM

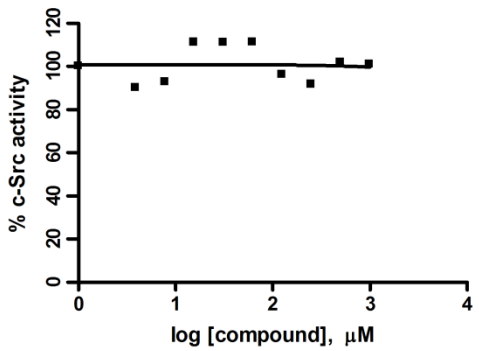

2.23 (X = 4-OPh Phe) c-Src K_i > 1000 μM

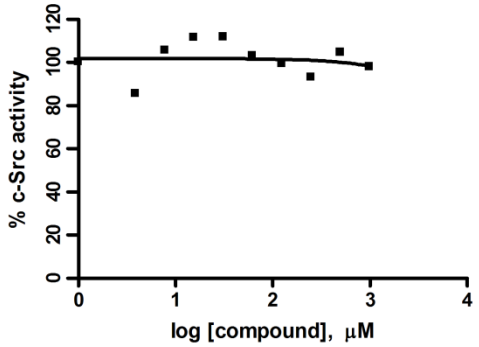

2.24 (X = 4-OBn Phe) c-Src K_i = 783 ± 156 μM

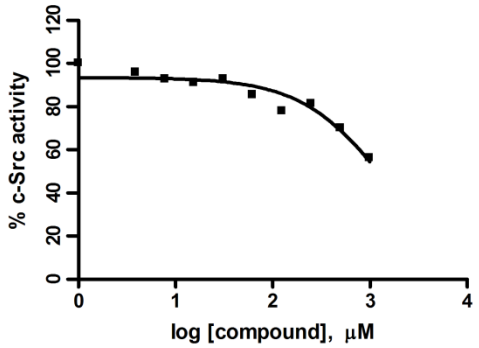

2.24 (X = 4-OBn Phe) c-Abl K_i > 1000 μM

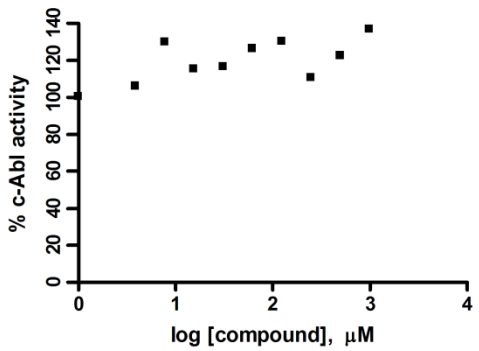

2.25 (X = 4-Bz Phe) c-Src K_i = 429 ± 91 μM

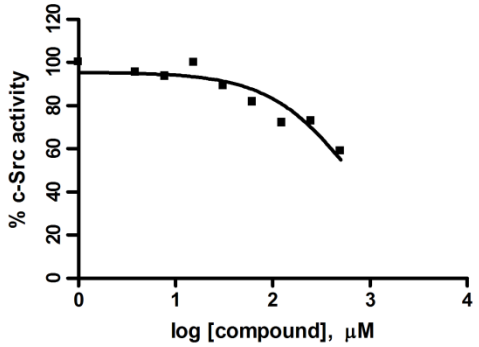

2.25 (X = 4-Bz Phe) c-Abl K_i > 1000 μM

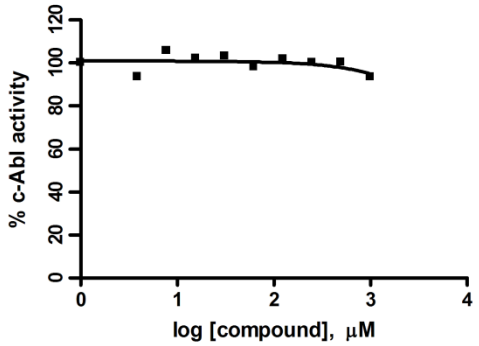

2.26 (X = 4-CO_2H Phe) c-Src K_i > 1000 μM

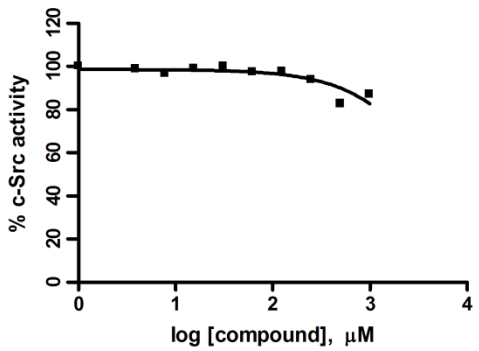

2.27 (X = 4-CN Phe) c-Src K_i > 1000 μM

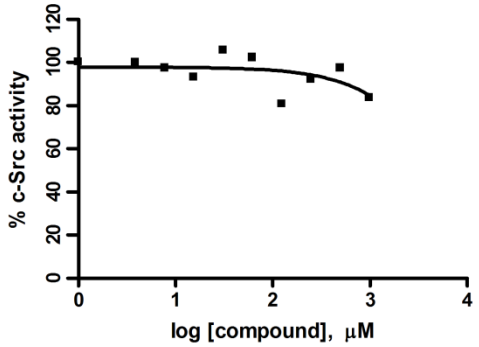

2.28 (X = 4-N_3 Phe) c-Src K_i = 831 ± 199 μM

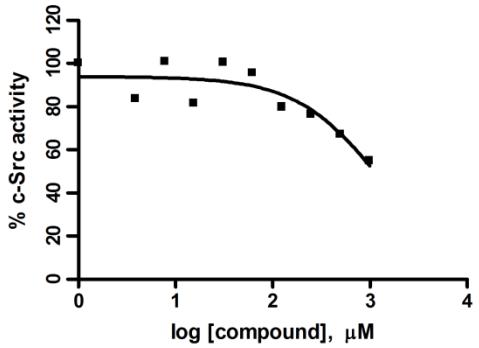

2.28 (X = 4-N_3 Phe) c-Abl K_i > 1000 μM

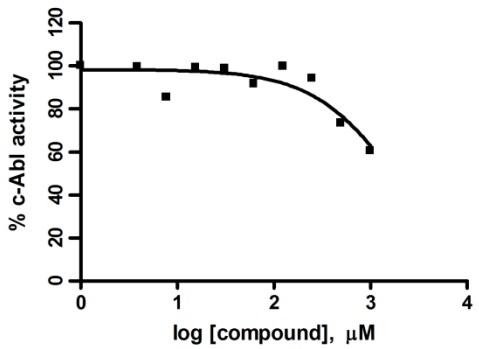

2.29 (X = 4-NH_2 Phe) c-Src K_i > 1000 μM

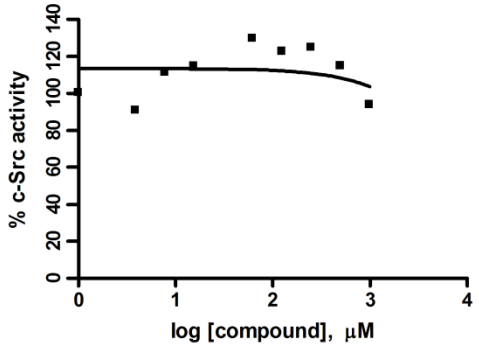

2.30 (X = 4-CH_2NH_2 Phe) c-Src K_i > 1000 μM

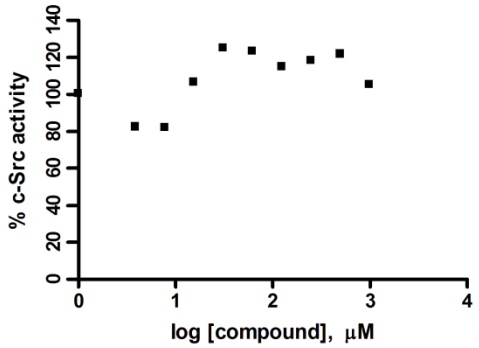

2.31 (X = 4-SO_2NH_2 Phe) c-Src K_i > 1000 μM

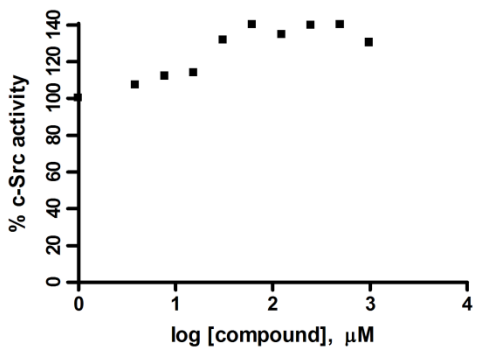

2.32 (X = 4-guanido Phe) c-Src K_i > 1000 μM

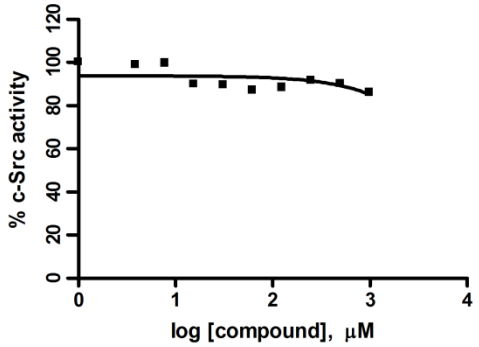

2.33 (X = 4-F Phe) c-Src K_i > 1000 μM

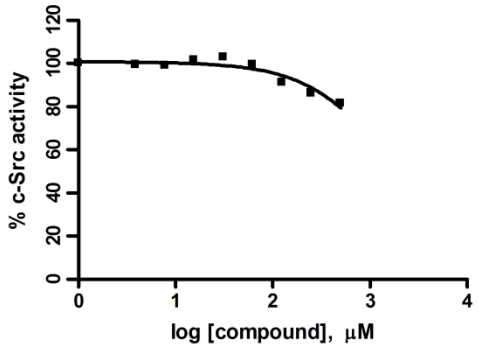

2.34 (X = 4-Cl Phe) c-Src K_i = 446 ± 70 μM

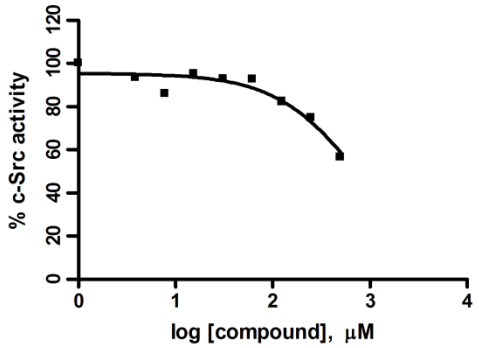

2.34 (X = 4-Cl Phe) c-Abl K_i > 1000 μM

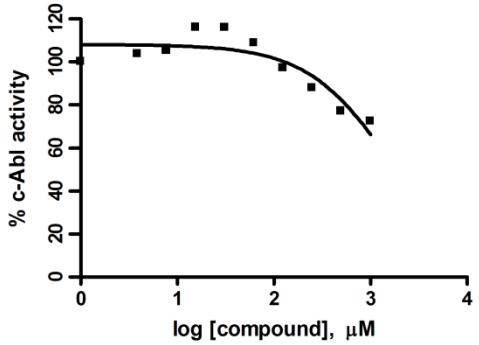

2.35 (X = 4-Br Phe) c-Src K_i = 392 ± 97 μM

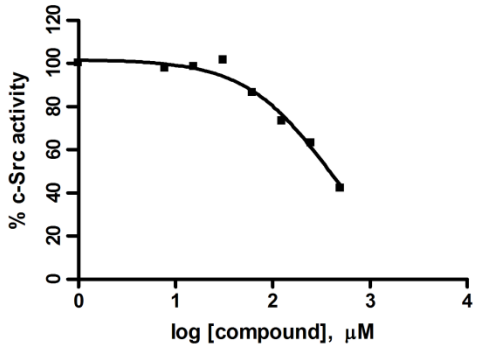

2.35 (X = 4-Br Phe) c-Abl K_i > 500 μM

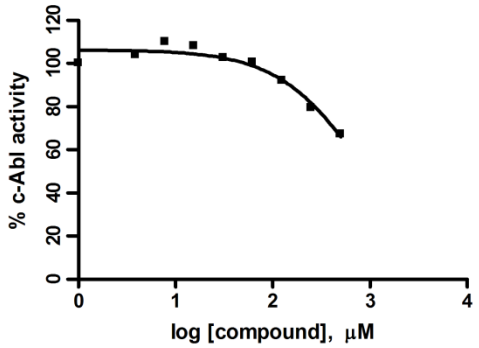

2.36 (X = 4-I Phe) c-Src K_i = 242 ± 31 μM

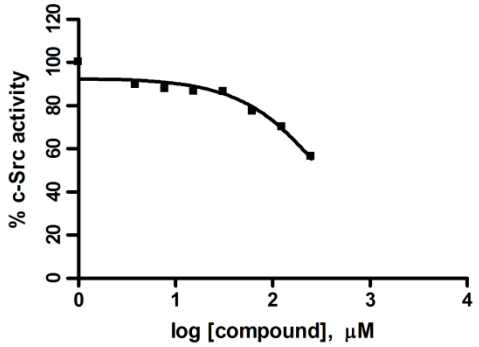

2.36 (X = 4-I Phe) c-Abl K_i = 827 ± 81 μM

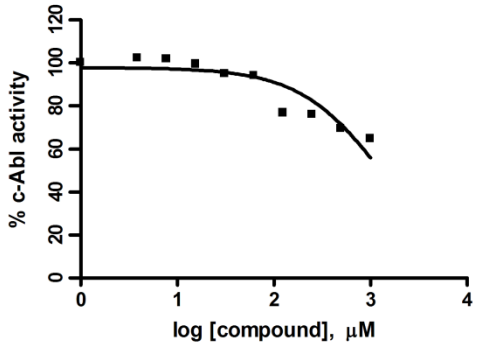

2.37 (X = 4-NO_2 Phe) c-Src K_i > 1000 μM

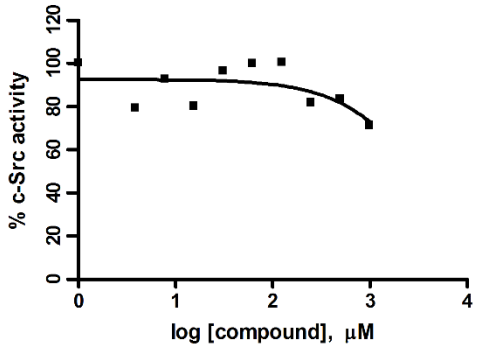

2.38 (X = 3,4-OCH_3 Phe) c-Src K_i > 1000 μM

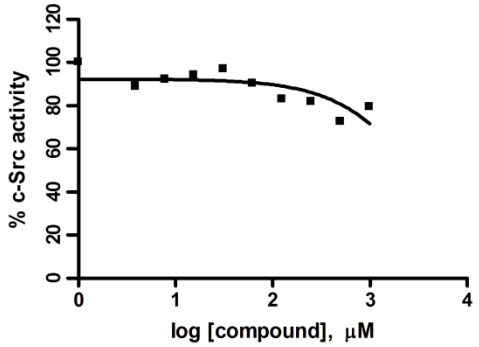

2.39 (X = 3-NO_2, 4-OAc Phe) c-Src K_i > 789 ± 102 μM

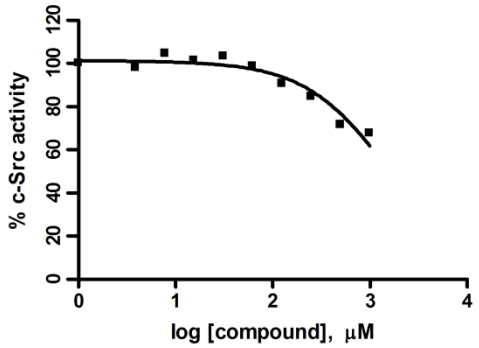

2.39 (X = 3-NO_2, 4-OAc Phe) c-Abl K_i > 1000 μM

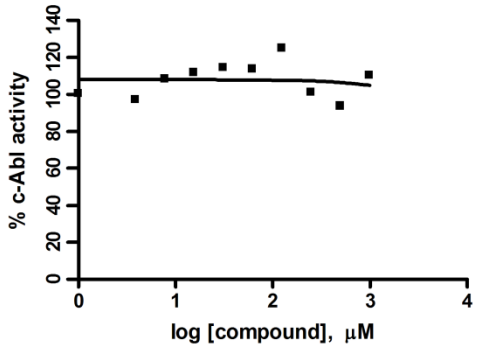

2.40 (X = 3,4-F Phe) c-Src K_i = 379 ± 68 μM

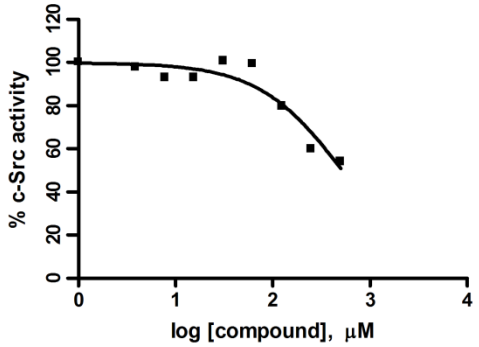

2.40 (X = 3,4-F Phe) c-Abl K_i > 500 μM

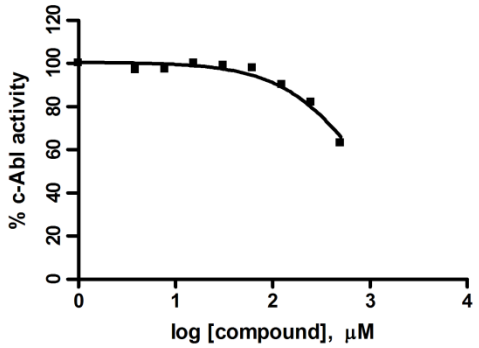

2.41 (X = 3,5-F Phe) c-Src K_i = 545 ± 37 μM

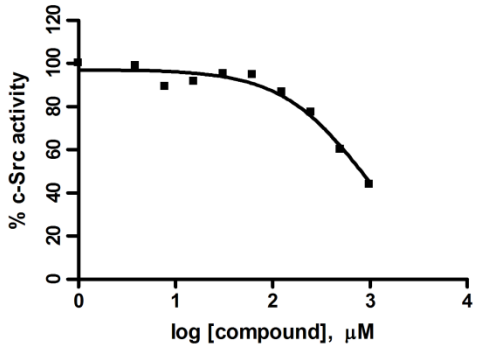

2.41 (X = 3,5-F Phe) c-Abl K_i = 912 ± 267 μM

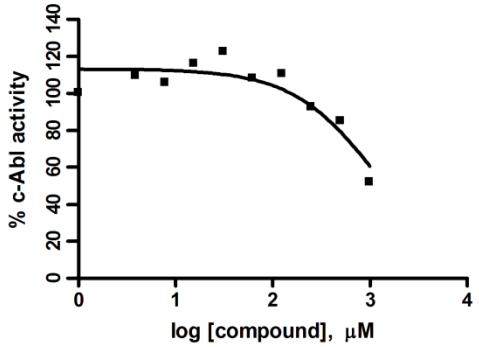

2.42 (X = 3,4,5-F Phe) c-Src K_i > 1000 μM

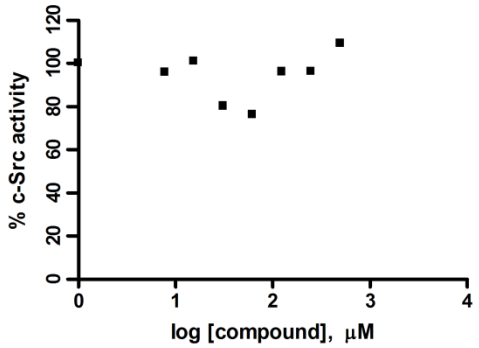

2.43 (X = 2,3,4,5,6-F Phe) c-Src K_i = 205 ± 56 μM

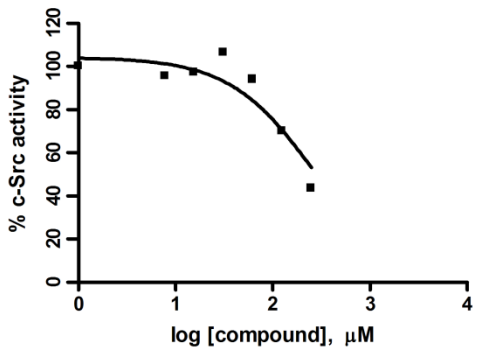

2.43 (X = 2,3,4,5,6-F Phe) c-Abl K_i > 250 μM

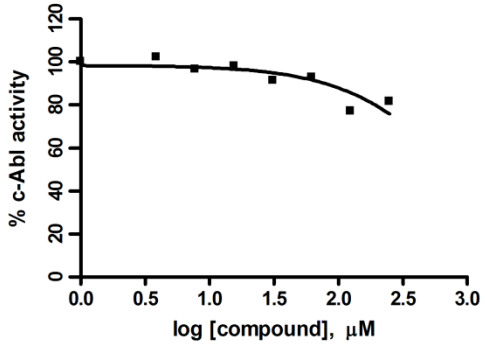

2.44 (X = 1-naphthyl Ala) c-Src K_i > 1000 μM

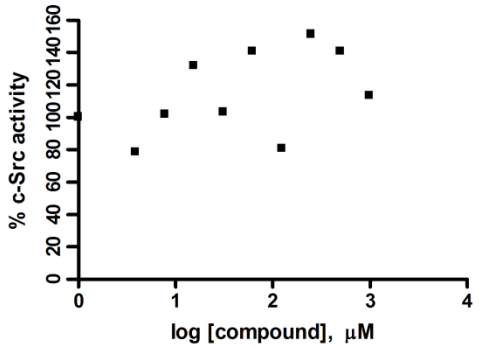

2.45 (X = 2-naphthyl Ala) c-Src K_i > 1000 μM

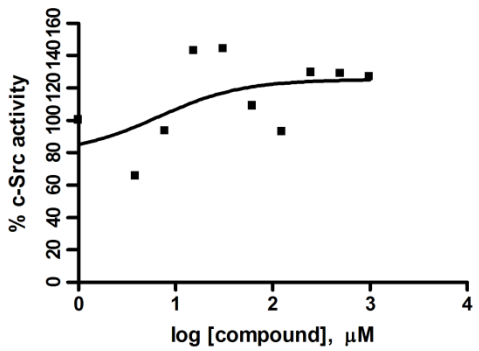

2.46 (X = 4-Ph Phe) c-Src K_i > 1000 μM

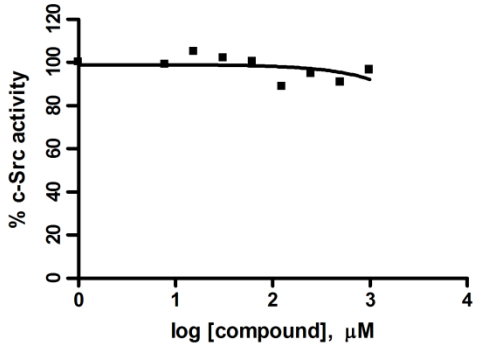

2.47 (X = 3-pyridyl Ala) c-Src K_i > 1000 μM

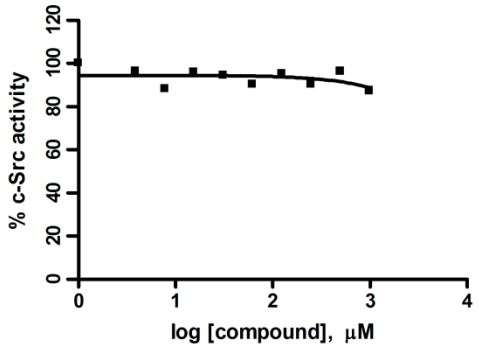

Literature Peptides and Analogues:

2.48 c-Src K_i > 1000 μM

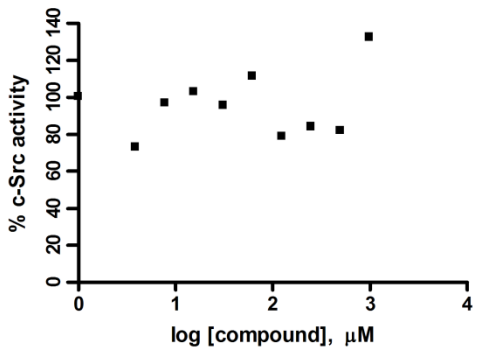

2.49 c-Src K_i > 1000 μM

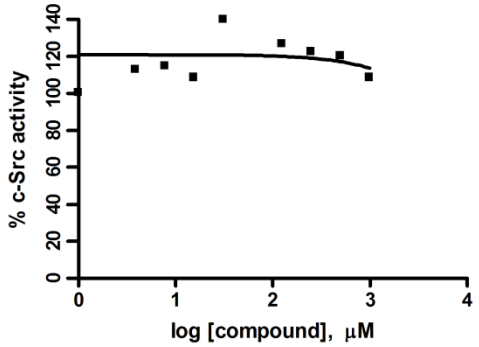

2.51 c-Src K_i = 70 ± 16 μM

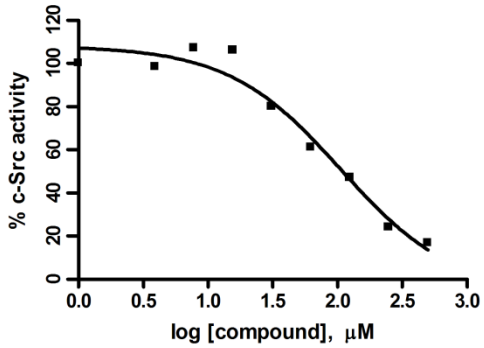

2.52 c-Src K_i = 49 μM (n = 2)

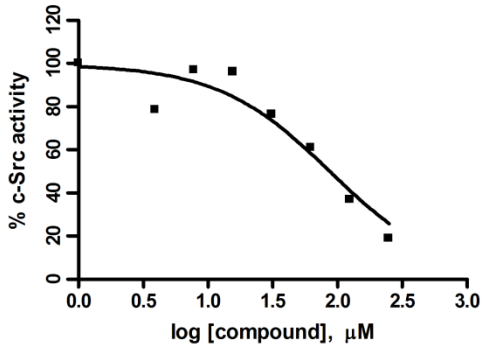

Analytical Data for Determination of Peptide Substrate "Substrate 3" K_M

c-Src K_M = 61 ± 4 µM

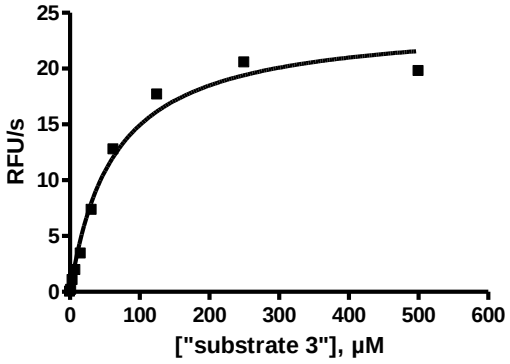

c-Abl K_M = 90 ± 7 µM

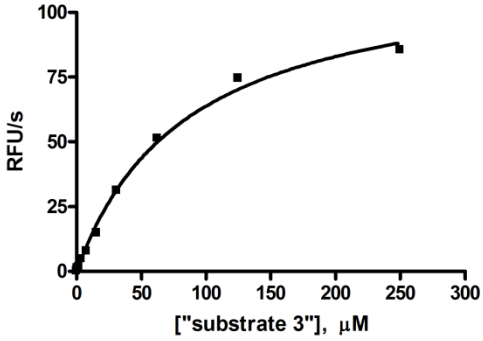

Appendix B

Analytical Data and Supplemental Information for Chapter III

Spectral Data for Compounds 3.7-3.12

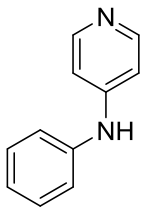

3.13

^{1}H:

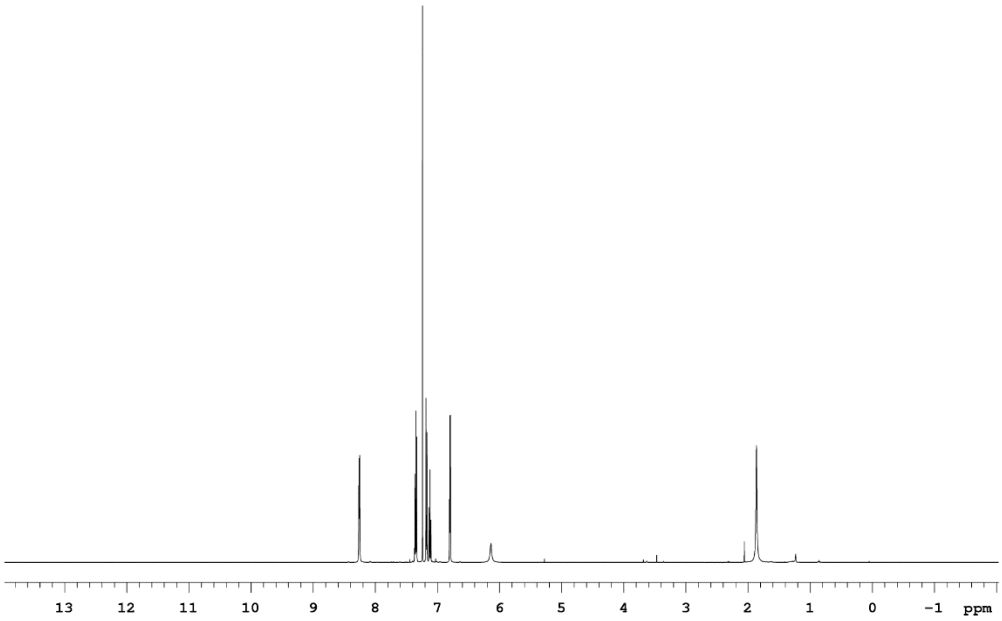

^{13}C:

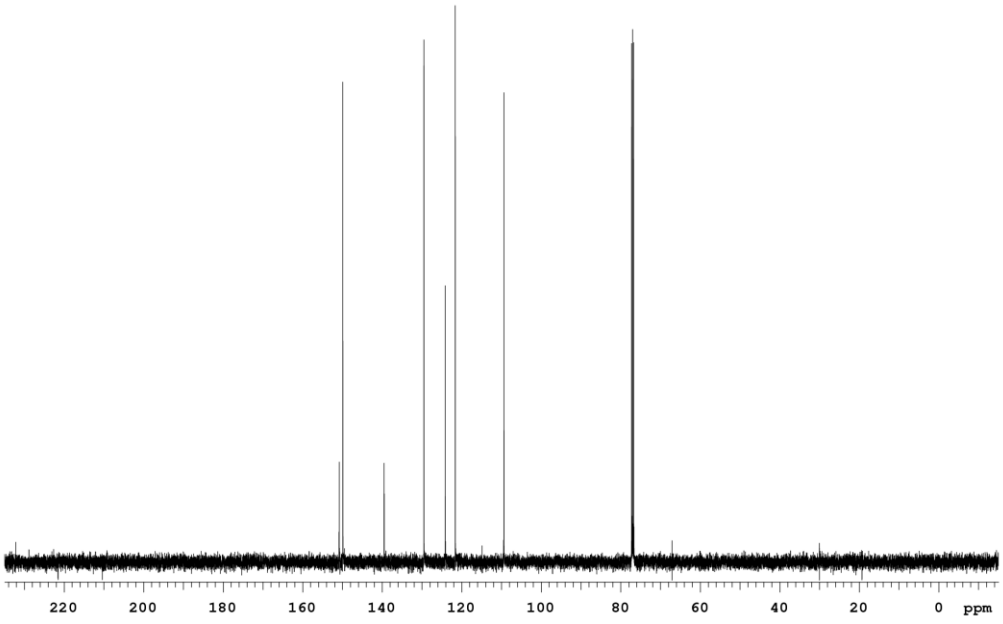

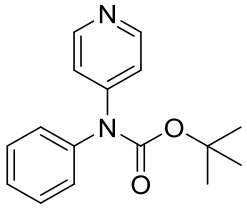
N
N
O
O

3.14

^{1}H:

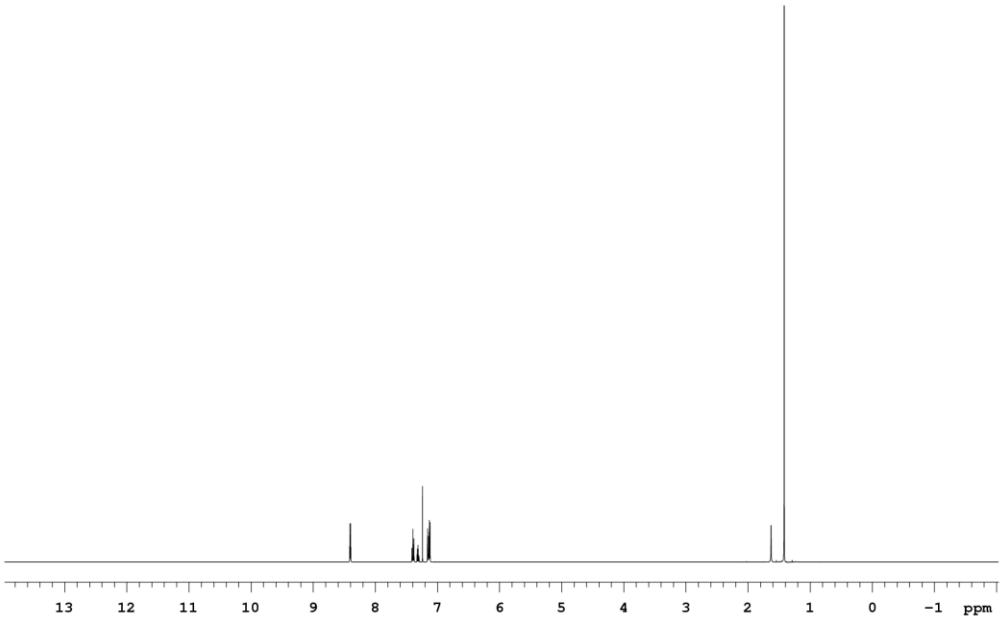
13
12
11
10
9
8
7
6
5
4
3
2
1
0
−1
ppm

^{13}C:

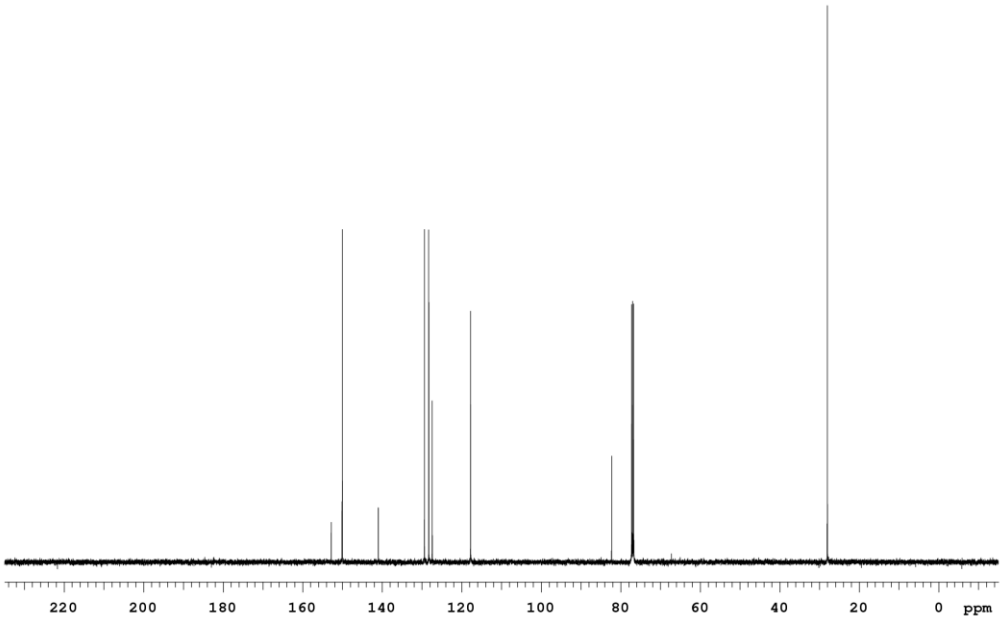
220
200
180
160
140
120
100
80
60
40
20
0
ppm

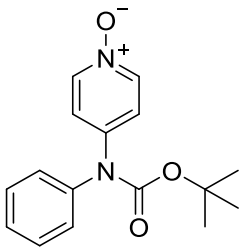

3.15

^{1}H:

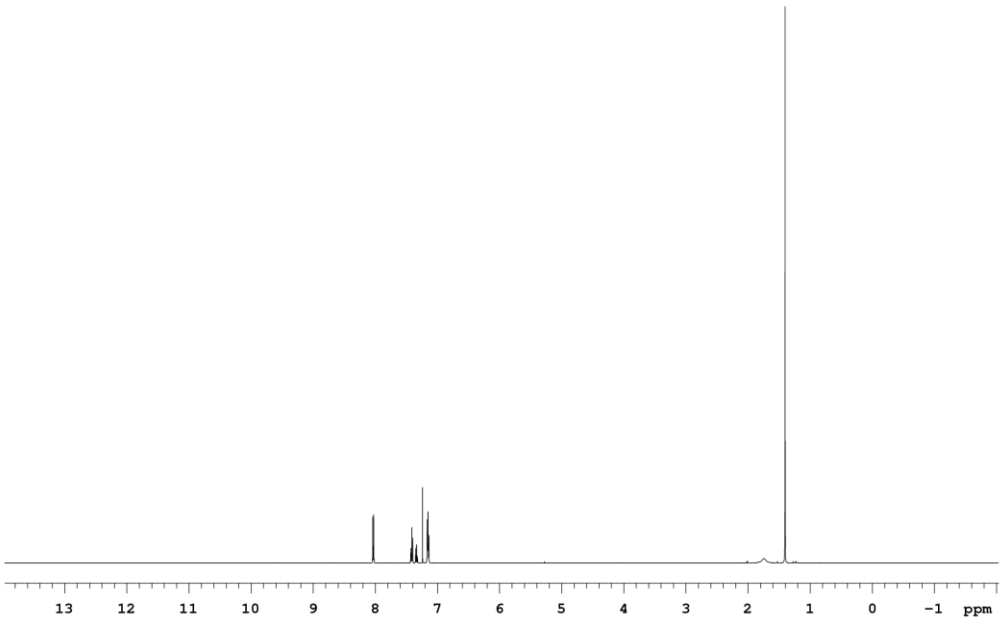
13
12
11
10
9
8
7
6
5
4
3
2
1
0
−1
ppm

^{13}C:

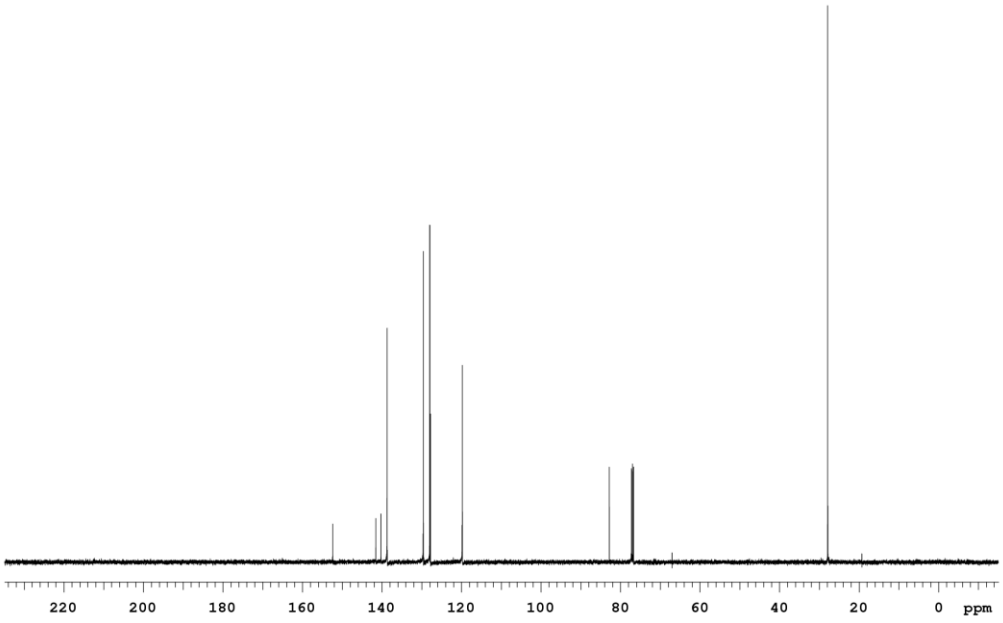
220
200
180
160
140
120
100
80
60
40
20
0
ppm

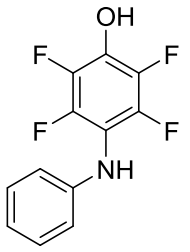

3.7

^{1}H:

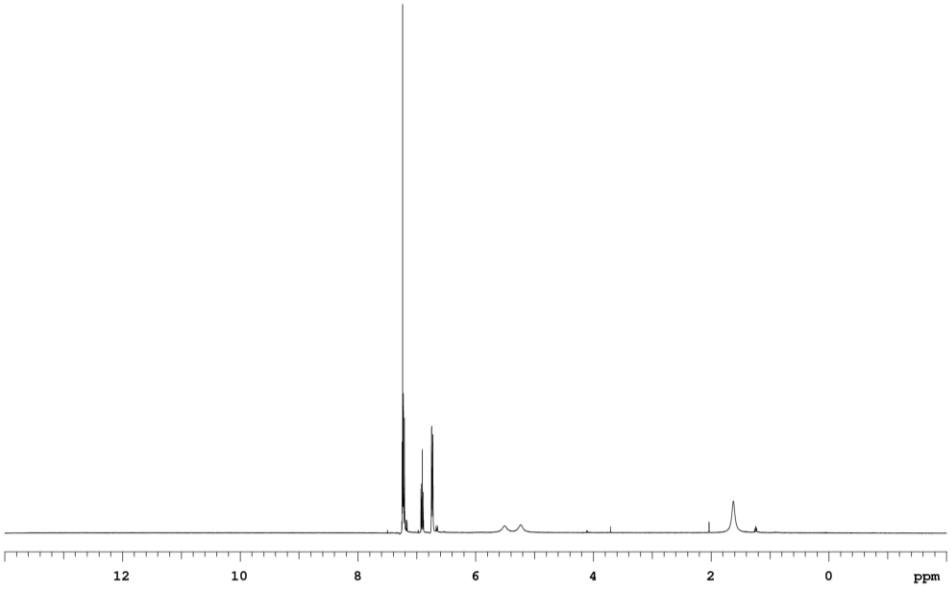

^{19}F:

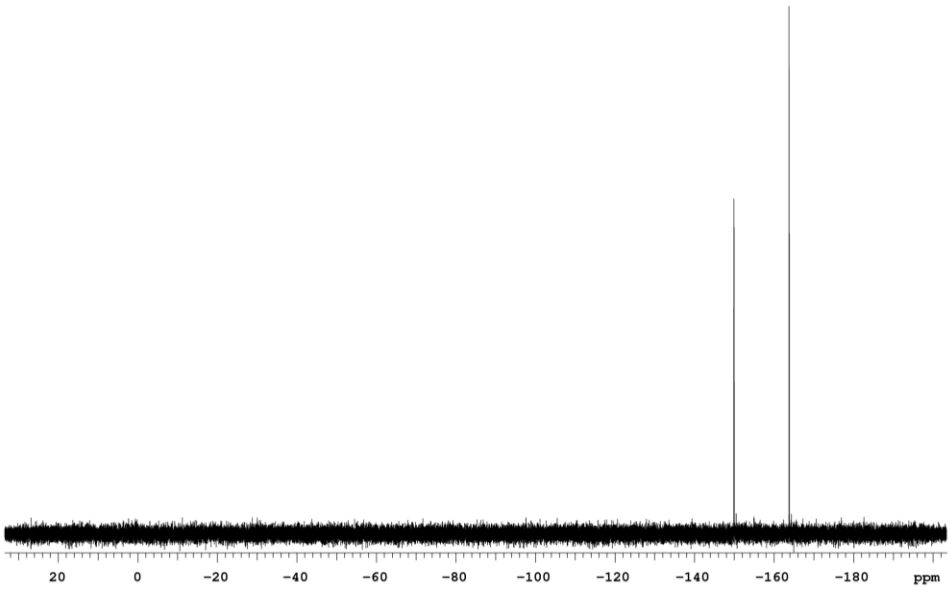

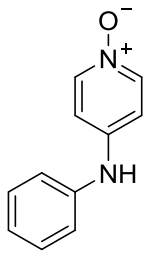
O
N+
NH

3.8

^{1}H:

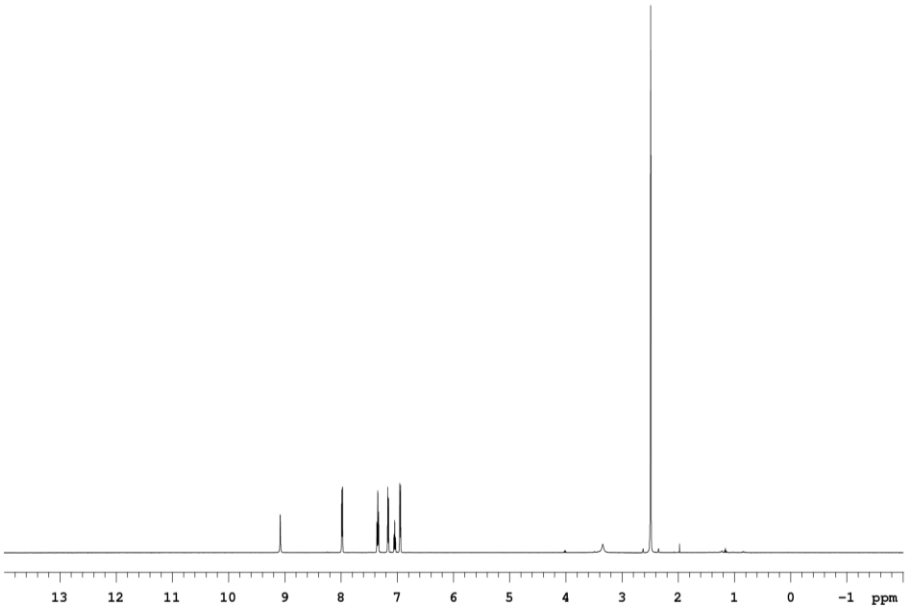
13
12
11
10
9
8
7
6
5
4
3
2
1
0
−1
ppm

^{13}C:

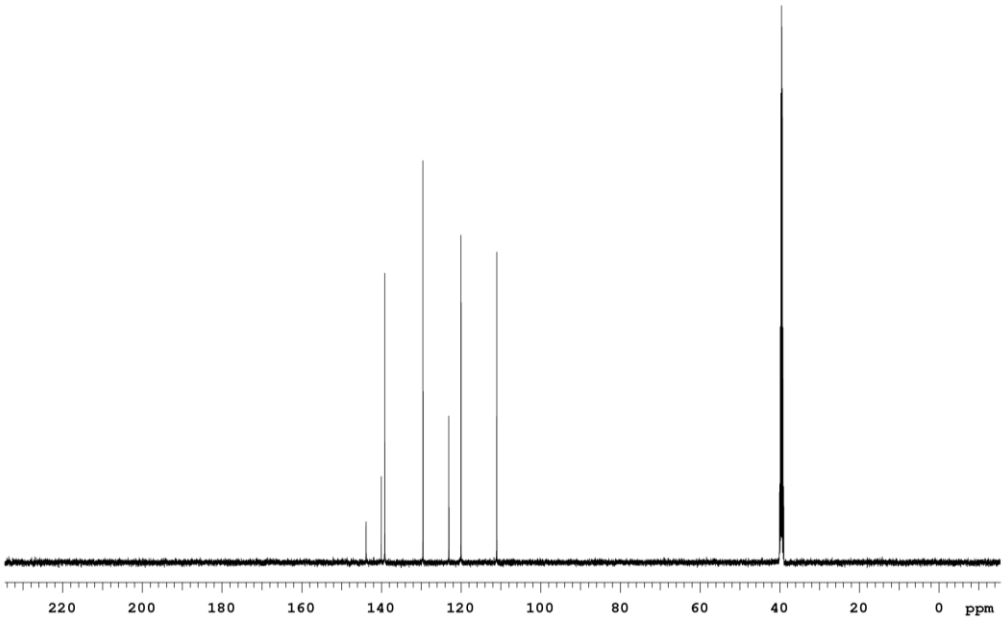
220
200
180
160
140
120
100
80
60
40
20
0
ppm

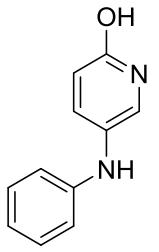
OH
N
NH

3.9

^{1}H:

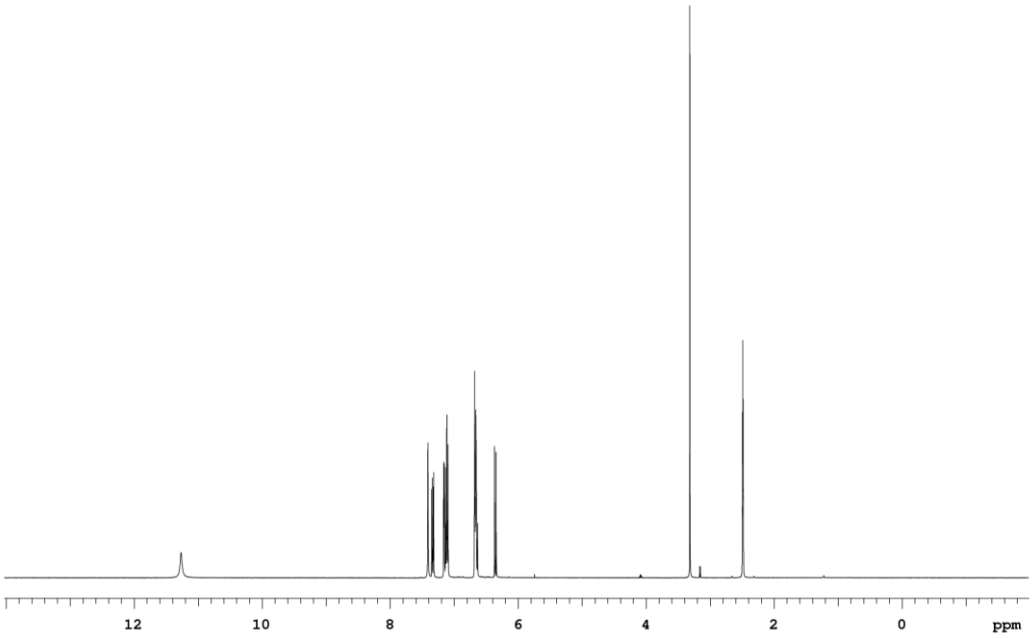
12
10
8
6
4
2
0
ppm

^{13}C:

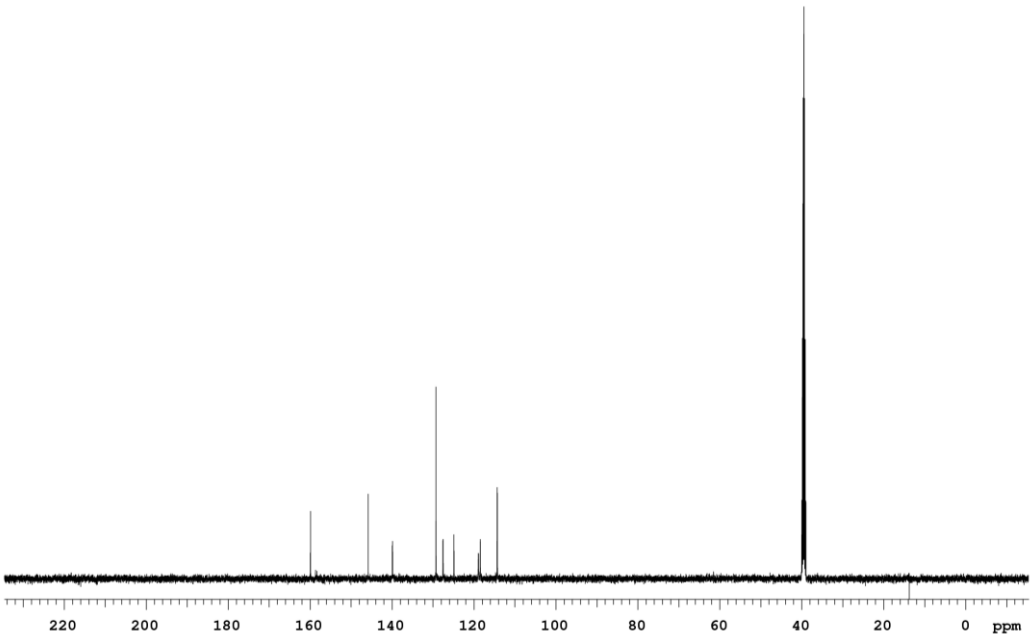
220
200
180
160
140
120
100
80
60
40
20
0
ppm

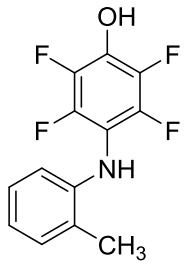
OH
F
F
F
F
NH
CH3

3.10

^{1}H:

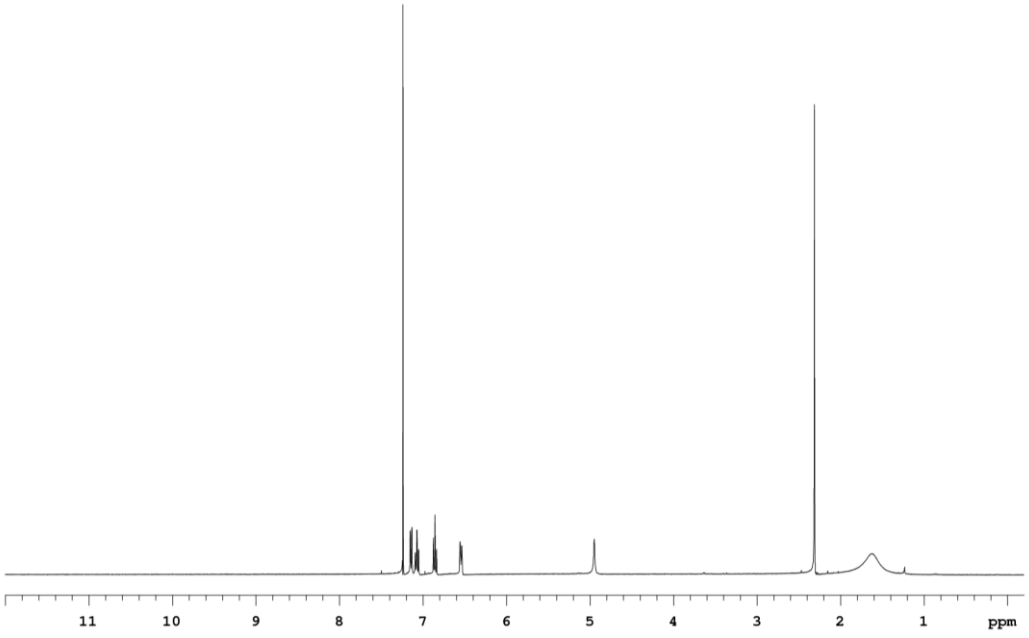
11
10
9
8
7
6
5
4
3
2
1
ppm

^{19}F:

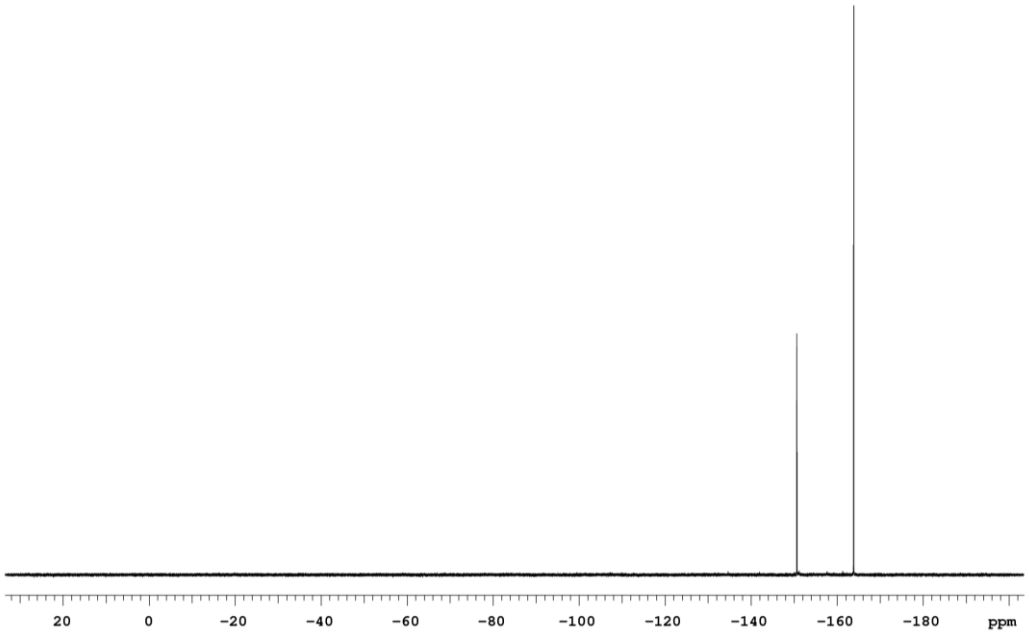
20
0
-20
-40
-60
-80
-100
-120
-140
-160
-180
ppm

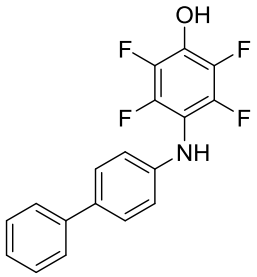
OH
F
F
F
F
NH

3.11

^{1}H:

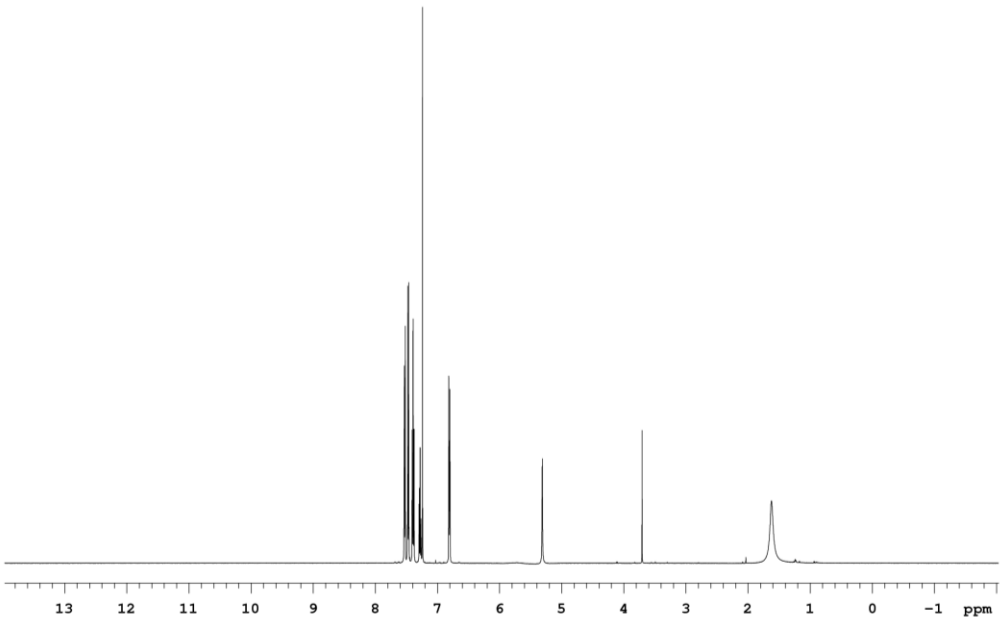
13
12
11
10
9
8
7
6
5
4
3
2
1
0
−1
ppm

^{19}F:

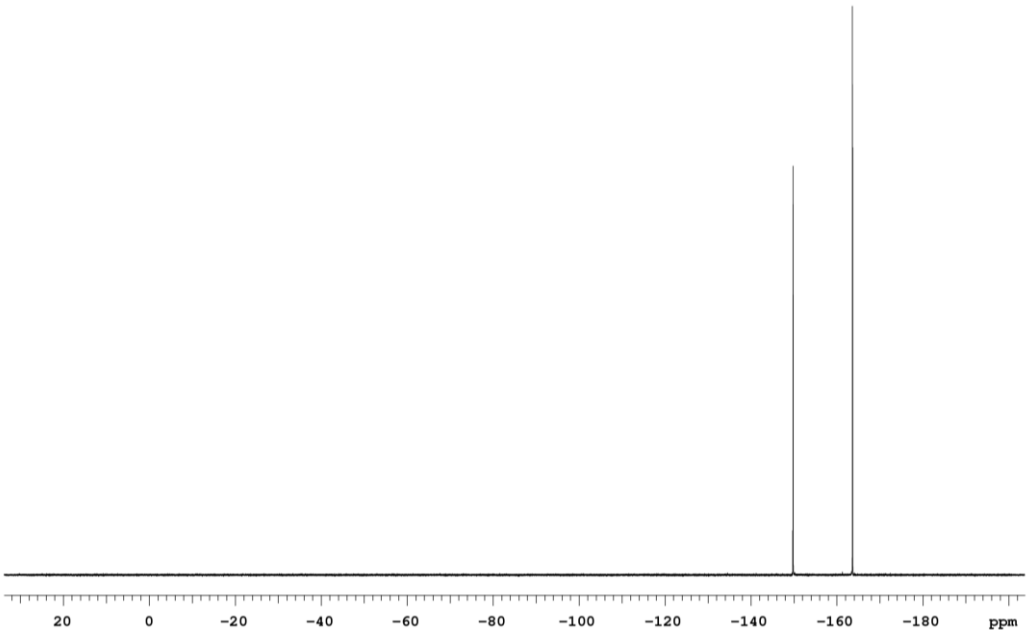
20
0
−20
−40
−60
−80
−100
−120
−140
−160
−180
ppm

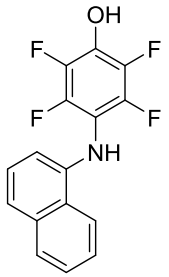

3.12

^{1}H:

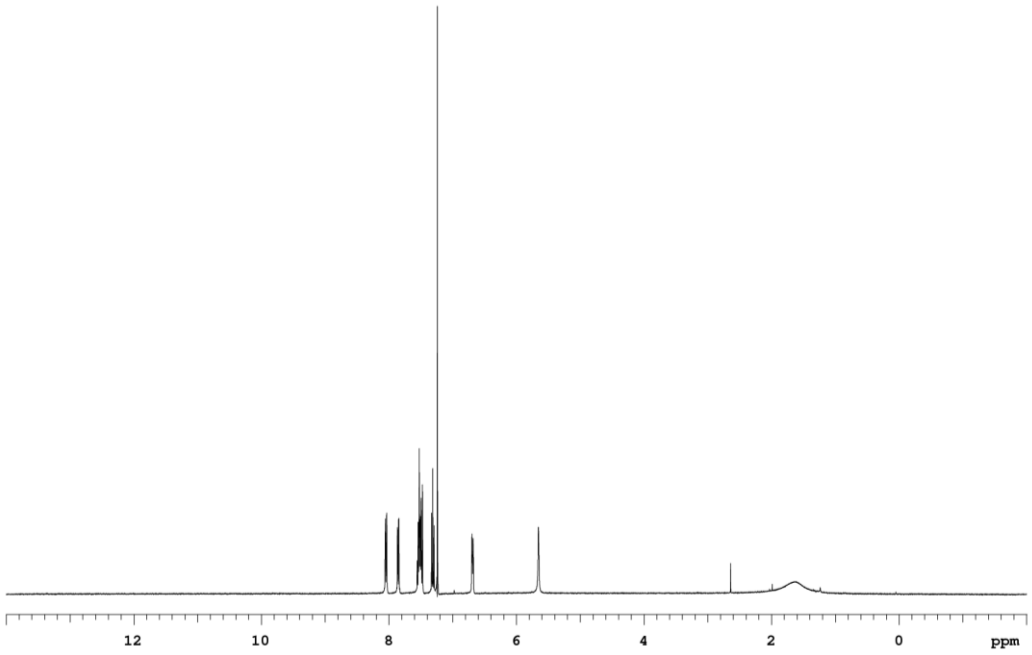

^{19}F:

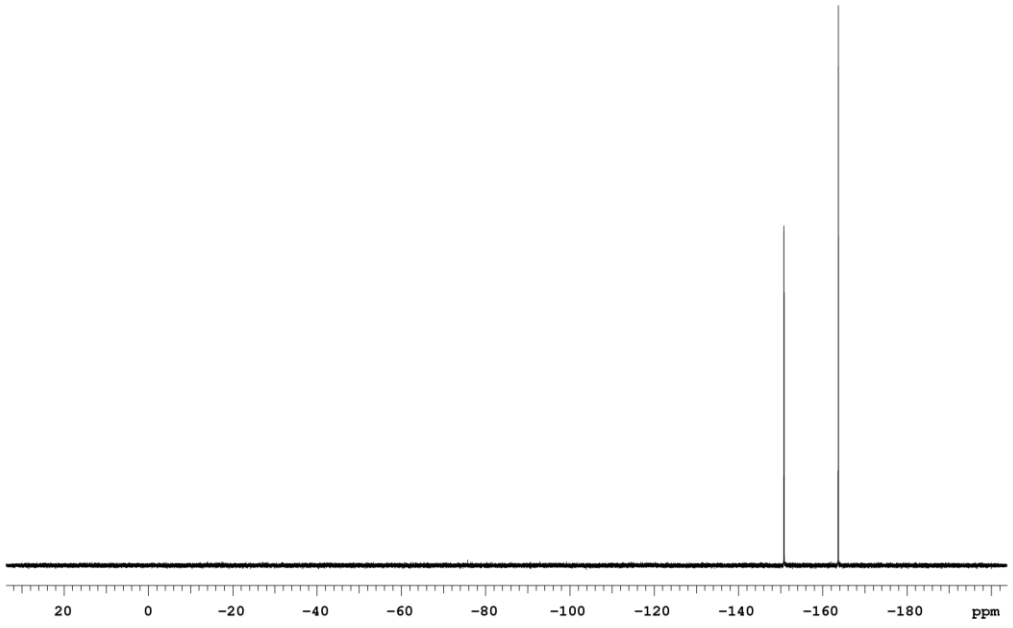

Gas Chromatography Traces of Compounds 3.7-3.12

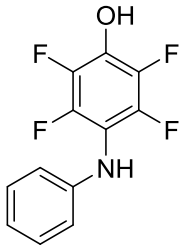

3.7

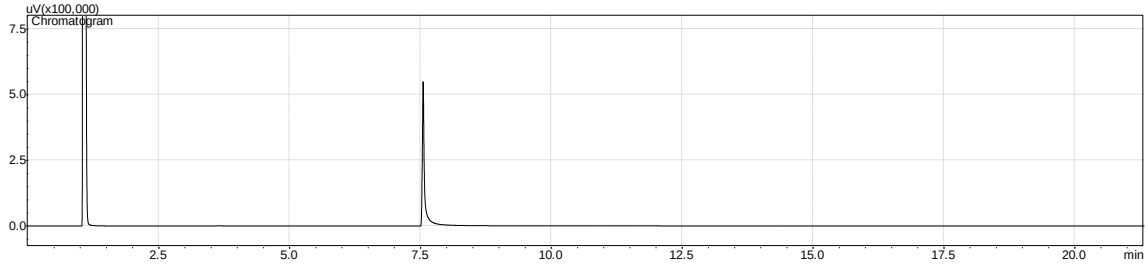

Peak	Retention Time	Area	% Area
1	3.636	513.3	0.3
2	7.550	1672609.0	99.7

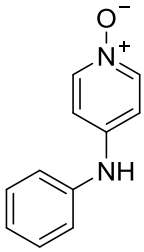

3.8

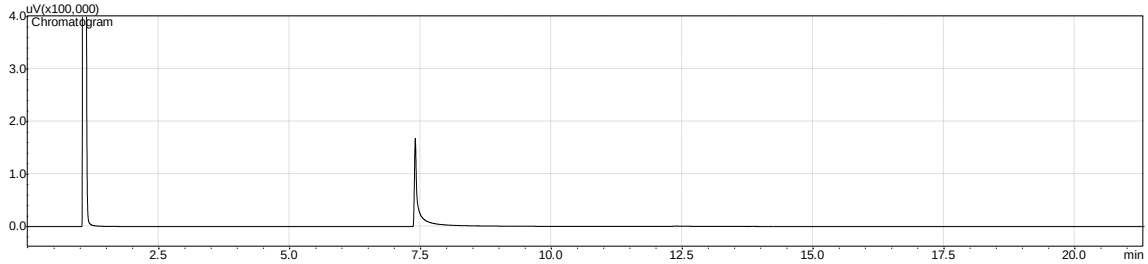

Peak	Retention Time	Area	% Area
1	7.399	835686.0	99.6
2	12.400	3050.1	0.4

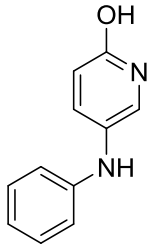

3.9

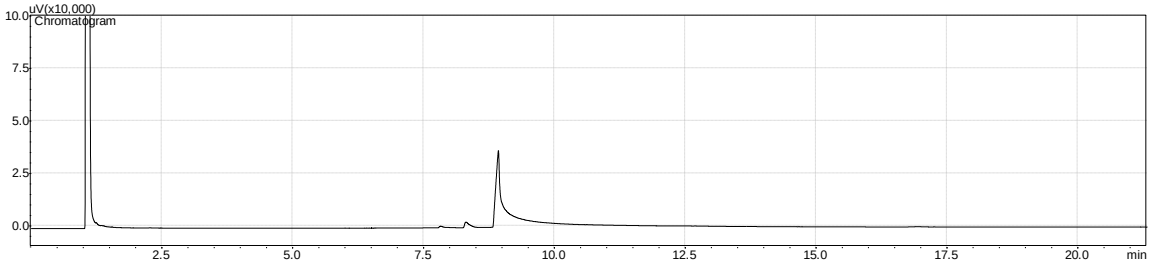

Peak	Retention Time	Area	% Area
1	7.826	3767.6	0.8
2	8.311	18333.3	4.0
3	8.929	440013.5	95.2

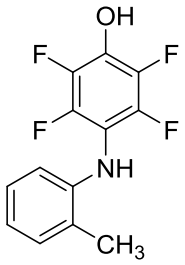

3.10

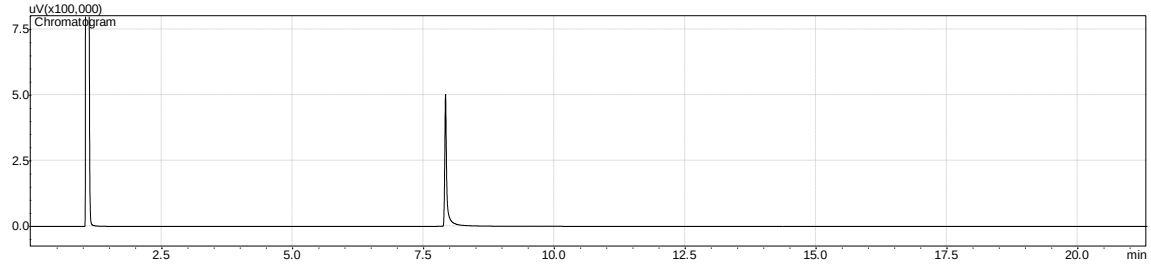

Peak	Retention Time	Area	% Area
1	7.920	1454029.6	100.0

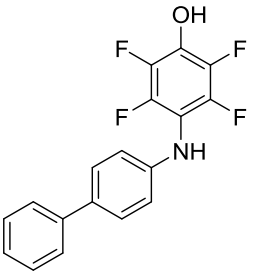

3.11

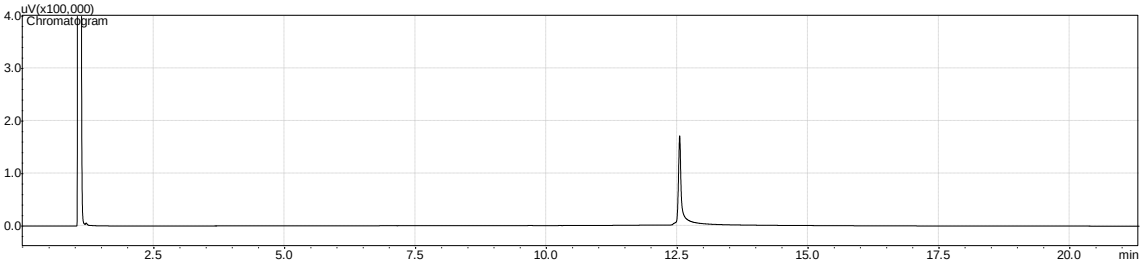

Peak	Retention Time	Area	% Area
1	6.927	1071.8	0.1
2	9.672	1024.6	0.1
3	12.546	789498.5	99.7

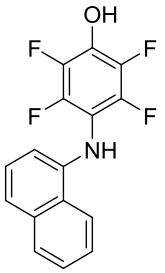

3.12

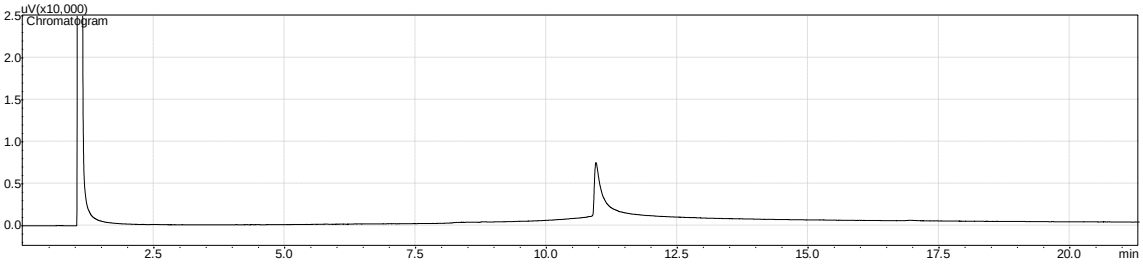

Peak	Retention Time	Area	% Area
1	10.945	71352.0	100.0

Analytical Data and Supplemental Information for Biochemical Substrate Identification Assays

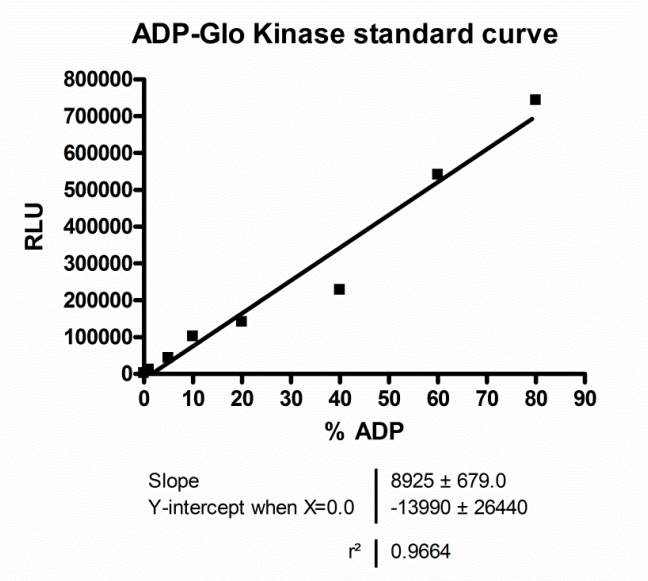

Table B.1. Evaluation of a library of small molecule phenols as substrates of c-Src.

Name	Structure	% ADP (100 µM)
Positive Control	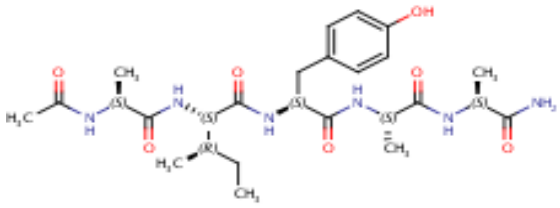	12.8 ± 5.2 (n=16)
P-S1 (**3.1**)	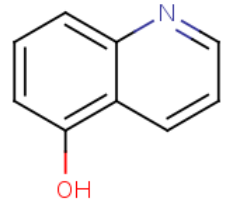	7.6 ± 4.1 (n=3)
P-S2 (**3.2**)	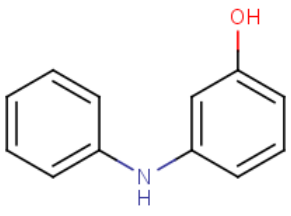	5.0 ± 3.4 (n=3)

P-S3 (**3.3**)	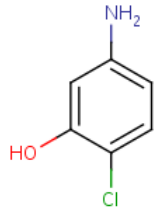	4.6 ± 4.8 (n=4)
P-S4	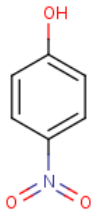	4.4 ± 6.2 (n=2)
P-S5 (**3.4**)	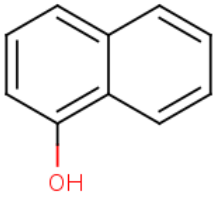	4.3 ± 2.5 (n=3)
P-S6	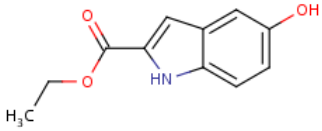	3.6 ± 5.6 (n=4)
P-S7	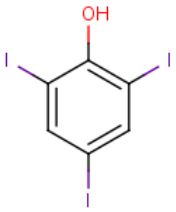	2.8 ± 1.6 (n=2)
P-S8 (**3.5**)	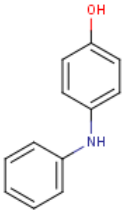	2.6 ± 4.8 (n=3)
P-S9 (**3.6**)	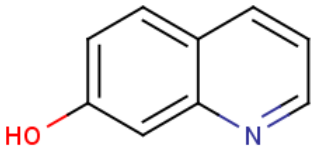	2.5 ± 5.5 (n=4)

P-S10	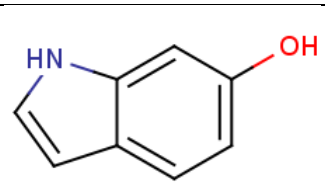	1.4 ± 2.6 (n=2)
P-S11		1.3 ± 1.7 (n=2)
P-S12	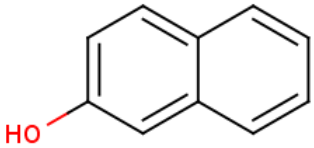	1.0 ± 4.1 (n=3)
P-S13	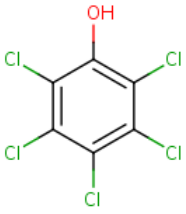	1.0 ± 0.2 (n=2)
P-S14	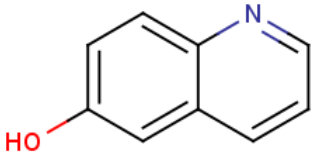	0.8 ± 2.3 (n=2)
P-S15	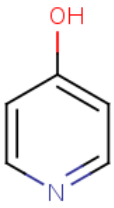	0.4 ± 1.5 (n=2)
P-S16	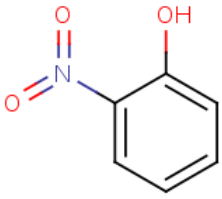	0.1 ± 0.7 (n=2)

P-S17	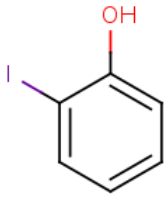	0.0 ± 0.4 (n=2)
P-S18	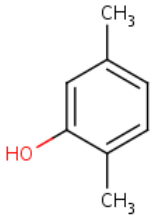	-0.2 ± 0.2 (n=2)
P-S19	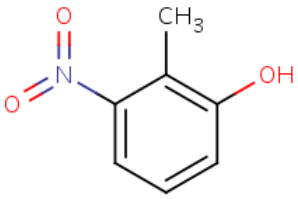	-0.2 ± 0.6 (n=2)
P-S20	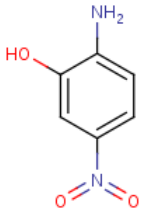	-0.2 ± 0.6 (n=2)
P-S21	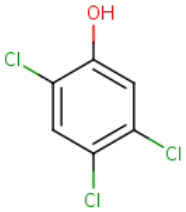	-0.2 ± 0.2 (n=2)
P-S22	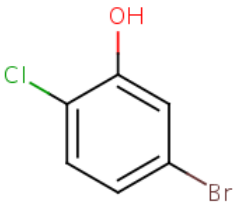	-0.3 ± 0.3 (n=2)
P-S23	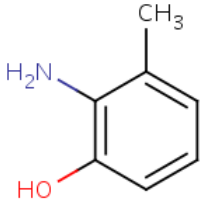	-0.4 ± 1.5 (n=2)

P-S24	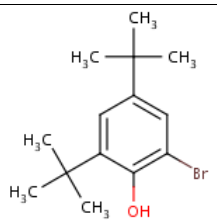	-0.4 ± 1.0 (n=2)
P-S25	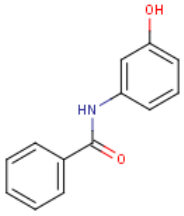	-0.5 ± 1.0 (n=2)
P-S26	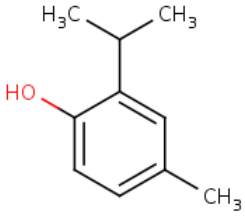	-0.6 ± 0.7 (n=2)
P-S27	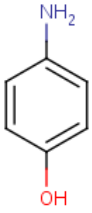	-0.6 ± 0.2 (n=2)
P-S28	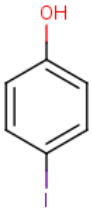	-0.7 ± 0.2 (n=2)
P-S29	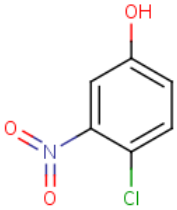	-0.8 ± 1.1 (n=2)
P-S30	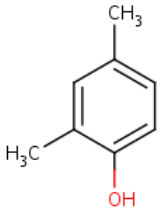	-0.9 ± 0.4 (n=2)

P-S31	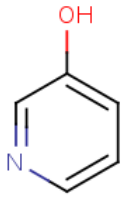	-0.9 ± 0.1 (n=2)
P-S32	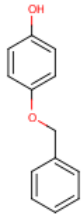	-0.9 ± 0.5 (n=2)
P-S33	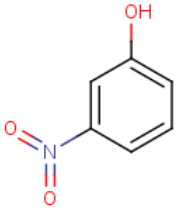	-1.0 ± 0.4 (n=2)
P-S34	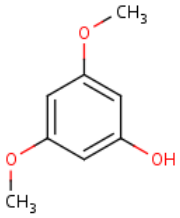	-1.0 ± 1.6 (n=2)
P-S35	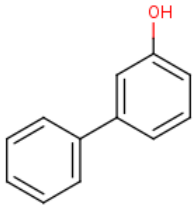	-1.0 ± 0.3 (n=2)
P-S36	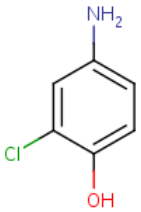	-1.0 ± 1.0 (n=2)
P-S37	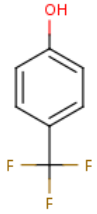	-1.1 ± 0.3 (n=2)

P-S38	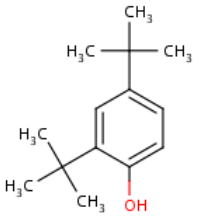	-1.1 ± 0.5 (n=2)
P-S39	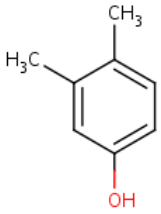	-1.2 ± 1.3 (n=2)
P-S40	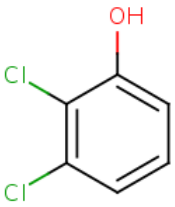	-1.2 ± 1.3 (n=2)
P-S41	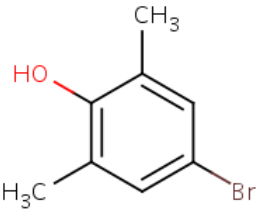	-1.2 ± 0.5 (n=2)
P-S42	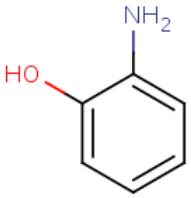	-1.3 ± 0.2 (n=2)
P-S43	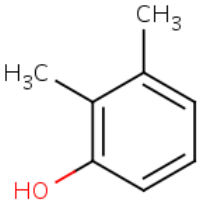	-1.3 ± 1.3 (n=2)
P-S44	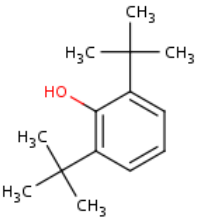	-1.3 ± 0.7 (n=2)

P-S45	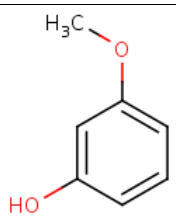	-1.3 ± 1.5 (n=2)
P-S46	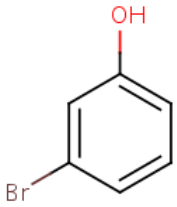	-1.4 ± 0.3 (n=2)
P-S47	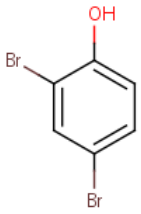	-1.4 ± 0.0 (n=2)
P-S48	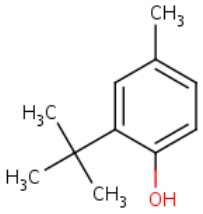	-1.4 ± 0.5 (n=2)
P-S49	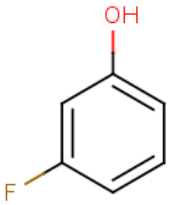	-1.4 ± 0.9 (n=2)
P-S50	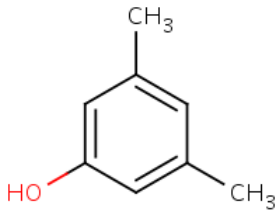	-1.5 ± 0.2 (n=2)
P-S51	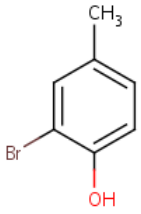	-1.6 ± 0.3 (n=4)

P-S52	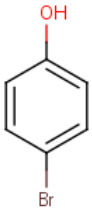	-1.6 ± 1.1 (n=2)
P-S53	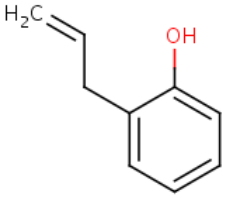	-1.7 ± 0.7 (n=2)
P-S54	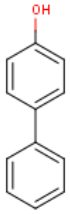	-1.9 ± 0.2 (n=2)
P-S55	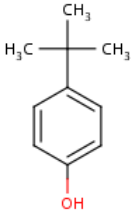	-1.9 ± 0.5 (n=2)
P-S56	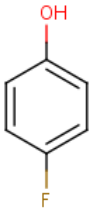	-1.9 ± 0.3 (n=2)
P-S57	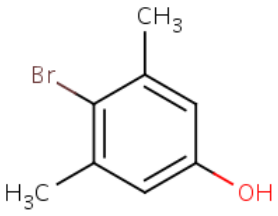	-1.9 ± 1.3 (n=2)
P-S58	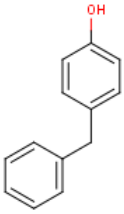	-2.0 ± 1.0 (n=2)

P-S59	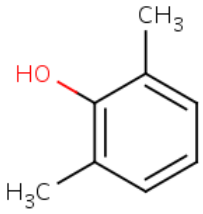	-2.0 ± 1.2 (n=2)
P-S60	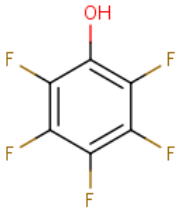	-2.1 ± 0.8 (n=2)
P-S61	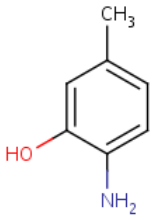	-2.2 ± 0.2 (n=2)
P-S62	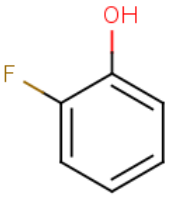	-2.2 ± 0.4 (n=2)
P-S63	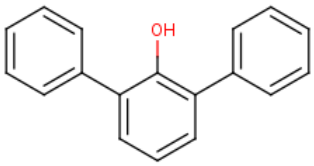	-2.3 ± 0.3 (n=2)
P-S64	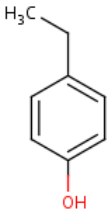	-2.3 ± 0.8 (n=2)
P-S65	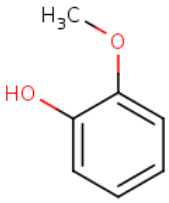	-2.4 ± 0.2 (n=2)

P-S66	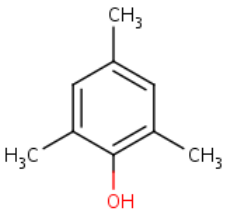	-2.5 ± 0.3 (n=2)
P-S67	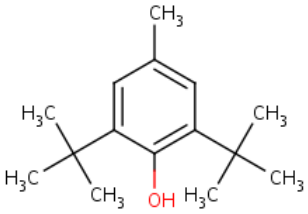	-2.5 ± 0.4 (n=2)
P-S68	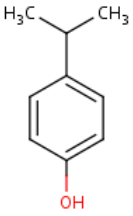	-2.6 ± 0.0 (n=2)
P-S69	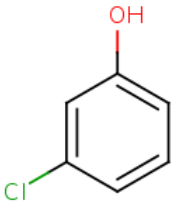	-2.7 ± 0.7 (n=2)
P-S70	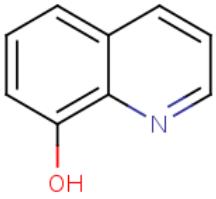	-2.6 ± 0.6 (n=2)
P-S71	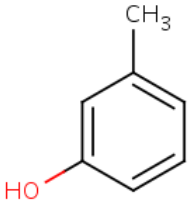	-2.7 ± 0.2 (n=2)
P-S72	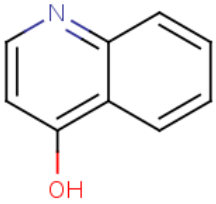	-2.7 ± 0.0 (n=2)

P-S73	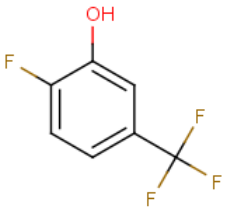	-2.7 ± 0.7 (n=2)
P-S74	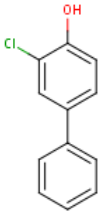	-2.8 ± 0.6 (n=2)
P-S75	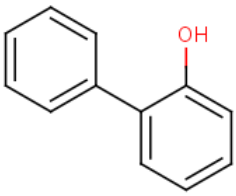	-2.8 ± 0.1 (n=2)
P-S76	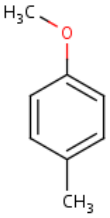	-2.8 ± 1.3 (n=2)
P-S77	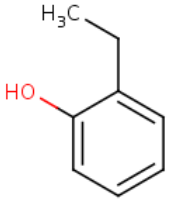	-2.8 ± 0.5 (n=2)
P-S78	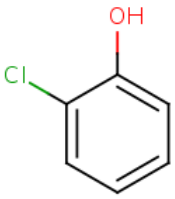	-2.8 ± 0.6 (n=2)
P-S79	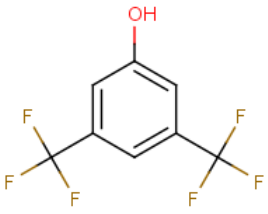	-2.9 ± 0.7 (n=2)

P-S80	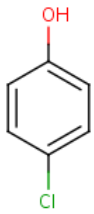	-2.9 ± 1.8 (n=2)
P-S81	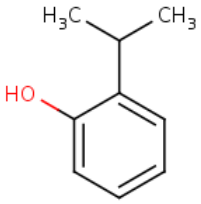	-2.9 ± 0.6 (n=2)
P-S82	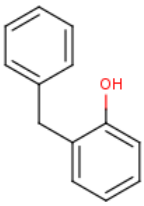	-3.0 ± 1.5 (n=2)
P-S83	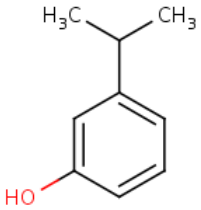	-3.0 ± 0.6 (n=2)
P-S84	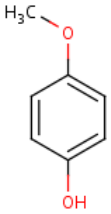	-3.1 ± 0.3 (n=2)
P-S85	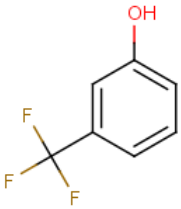	-3.1 ± 0.3 (n=2)
P-S86	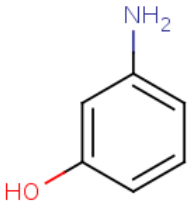	-3.1 ± 0.2 (n=2)

P-S87	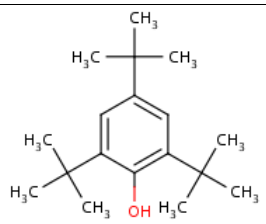	-3.3 ± 0.9 (n=2)
P-S88	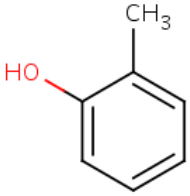	-3.3 ± 0.8 (n=2)

Analytical Data and Supplemental Information for Determination of K_M for Phenolic Substrates

Table B.2. Kinetic parameters for phenolic substrates of c-Src. Select compounds were also evaluated as substrates of Hck and c-Abl.

Name	Structure	K_M c-Src	V_{max} c-Src (%ADP)	K_M Hck	K_M c-Abl
Positive Control	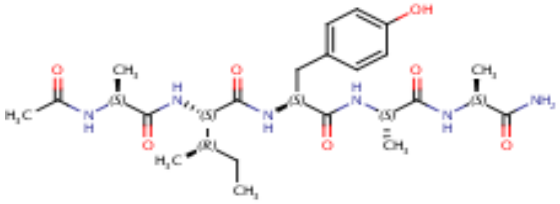	60 µM	29	ND[a]	ND
P-S1 (**3.1**)	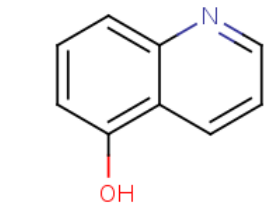	52 µM	15	124 µM	>1 mM
P-S2 (**3.2**)	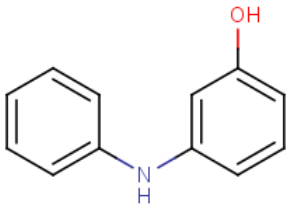	370 µM	6.5	316 µM	>1 mM

P-S3 (**3.3**)	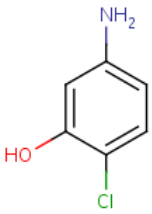	15 µM	10	ND	ND
P-S4	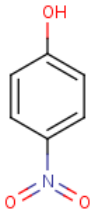	56 µM	3.2	>1 mM	>1 mM
P-S5 (**3.4**)	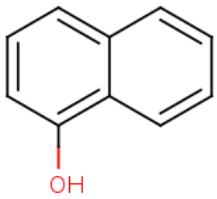	522 µM	19	169 µM	>1 mM
P-S6	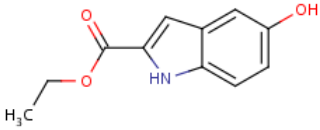	>10 mM	ND	ND	ND
P-S7	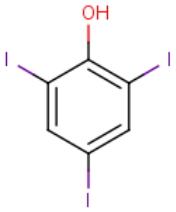	32 µM	2.5	>1 mM	>1 mM
P-S8 (**3.5**)	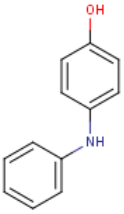	120 µM	7.3	137 µM	>1 mM
P-S9 (**3.6**)	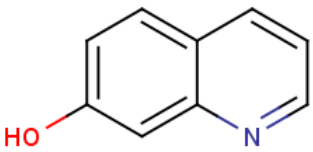	33 µM	14	ND	ND

3.12	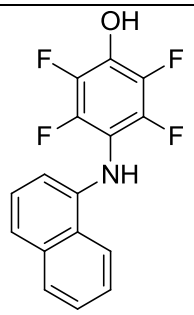	>1 mM	0	ND	ND

[a] Not determined

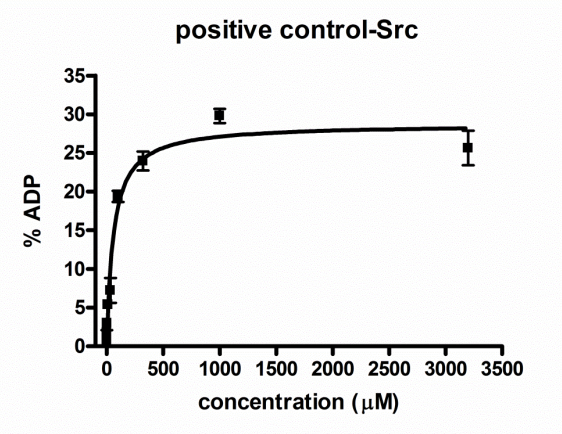

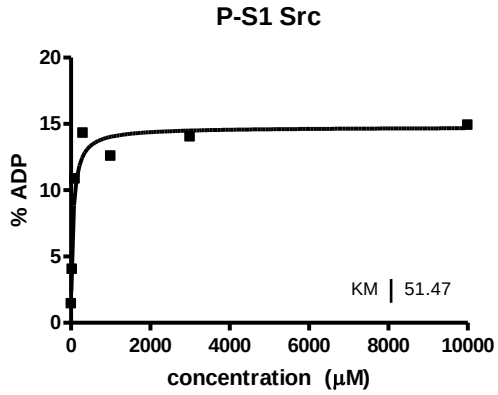

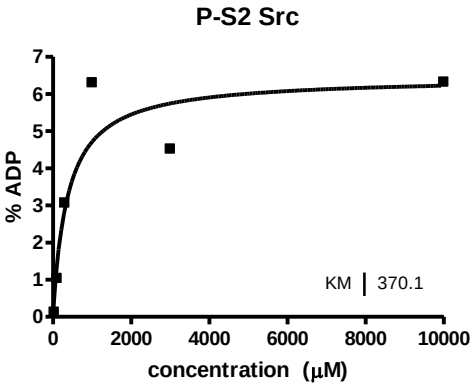

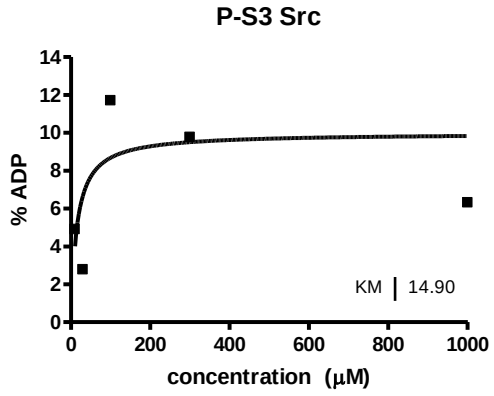

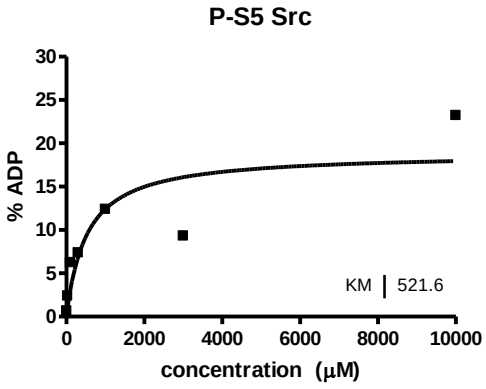
P-S5 Src
% ADP
concentration (μM)
KM | 521.6

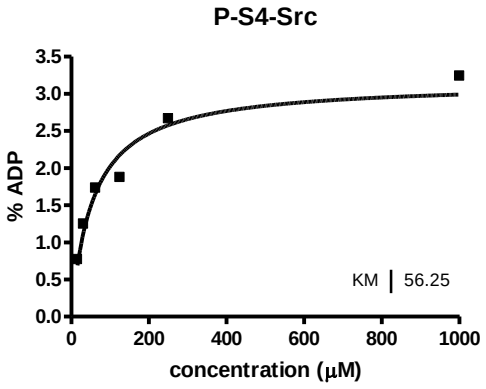
P-S4-Src
% ADP
concentration (μM)
KM | 56.25

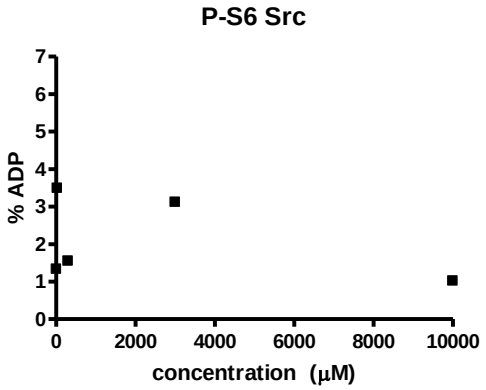
P-S6 Src
% ADP
concentration (μM)

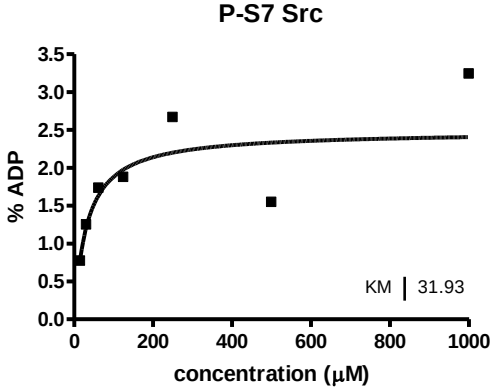
P-S7 Src
% ADP
concentration (μM)
KM | 31.93

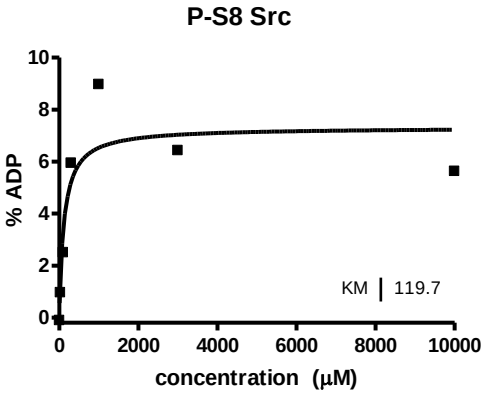
P-S8 Src
% ADP
concentration (μM)
KM | 119.7

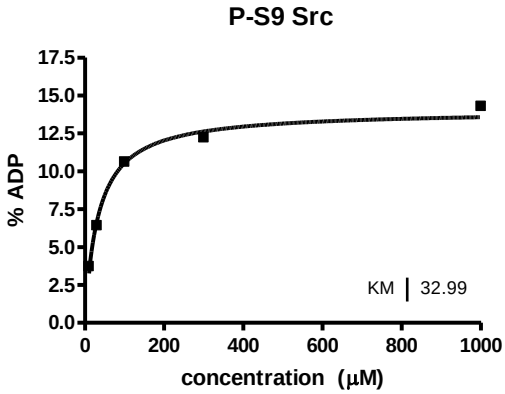
P-S9 Src
% ADP
concentration (μM)
KM | 32.99

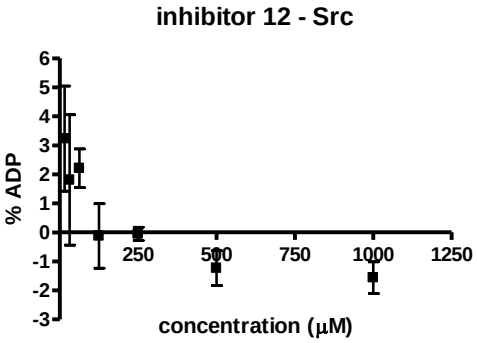
inhibitor 12 - Src
% ADP
concentration (μM)

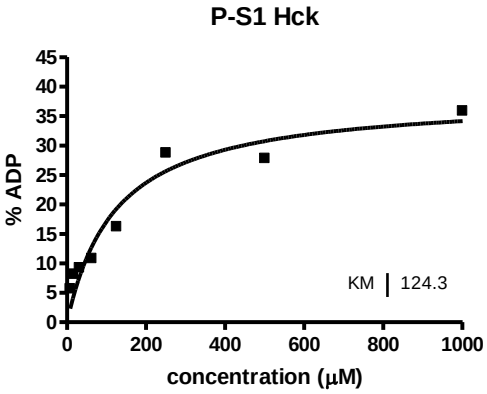
P-S1 Hck
% ADP
KM | 124.3
concentration (μM)

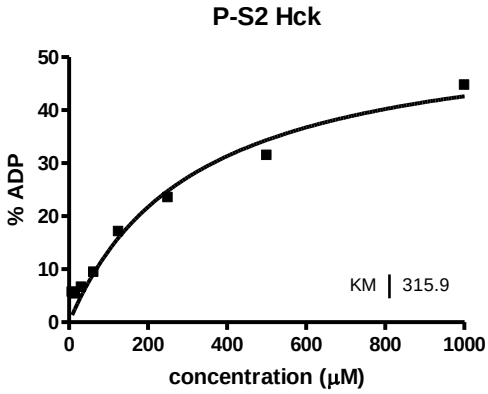
P-S2 Hck
% ADP
KM | 315.9
concentration (μM)

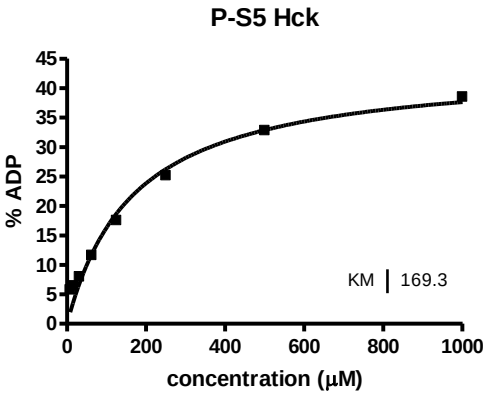
P-S5 Hck
% ADP
KM | 169.3
concentration (μM)

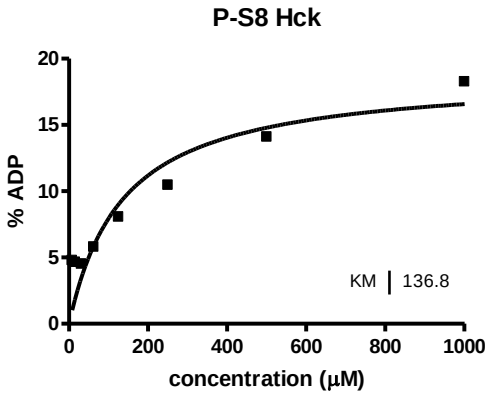
P-S8 Hck
% ADP
KM | 136.8
concentration (μM)

Analytical Data for Determination of K_i for Inhibitors

	Structure	c-Src K_i (μM)
S4	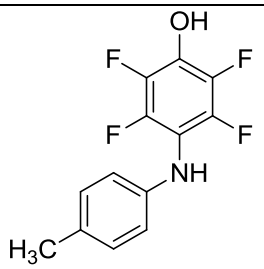	549 ± 57
S5	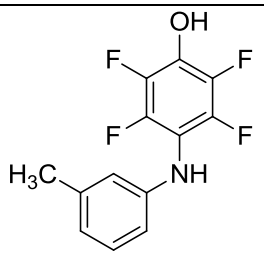	406 ± 67
3.10	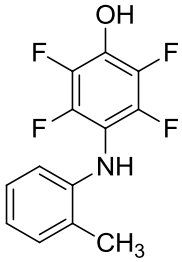	127 ± 11
S6	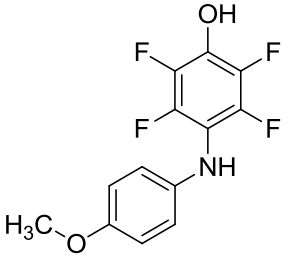	229 ± 49
S7	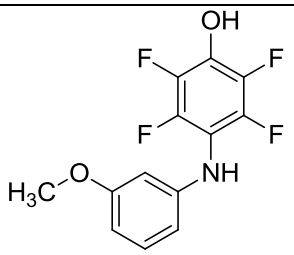	399 ± 92
S8	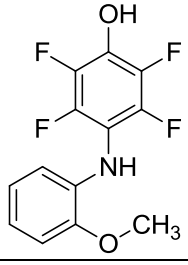	443 ± 13

S9	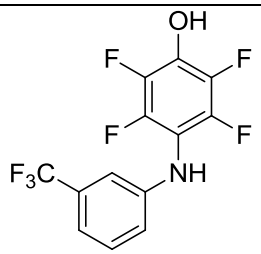	318 ± 16
3.11	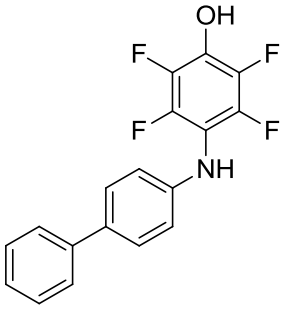	80 ± 6
S10	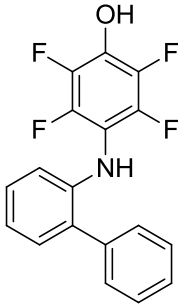	257 ± 8
3.12	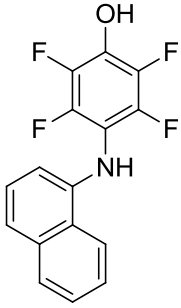	16 ± 1

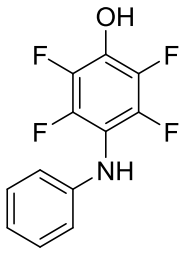

3.7

c-Src K_i = 257 ± 28 µM

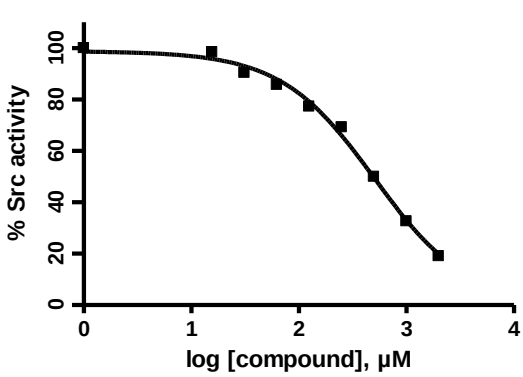

Hck K_i = 1015 ± 165 µM

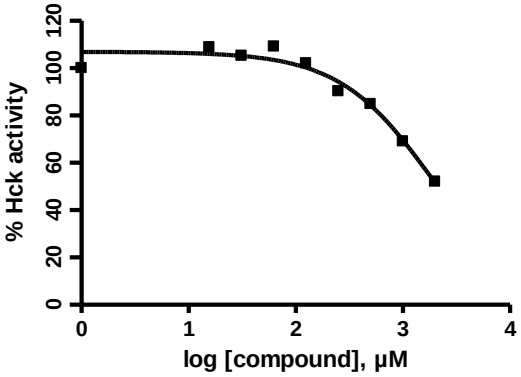

c-Abl K_i >1170 µM

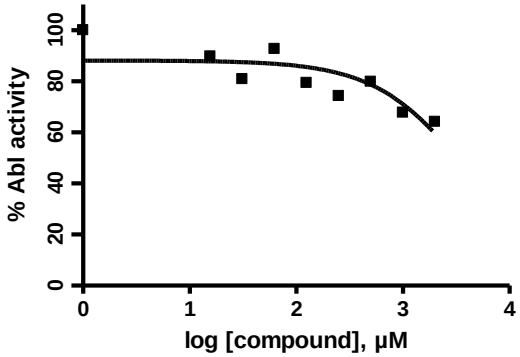

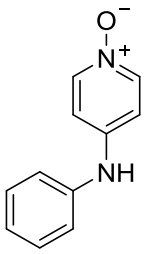

3.8

c-Src K_i = 478 ± 82 µM

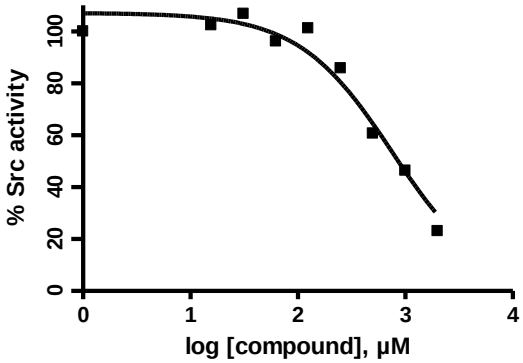

Hck K_i = 517 ± 32 µM

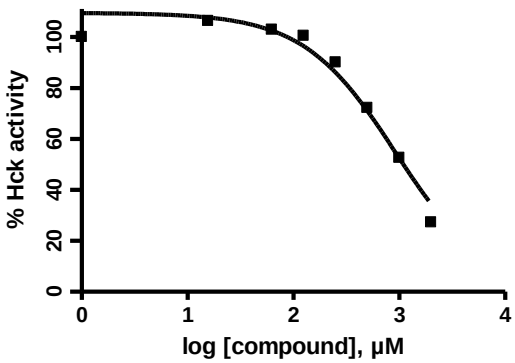

c-Abl K_i >1170 µM

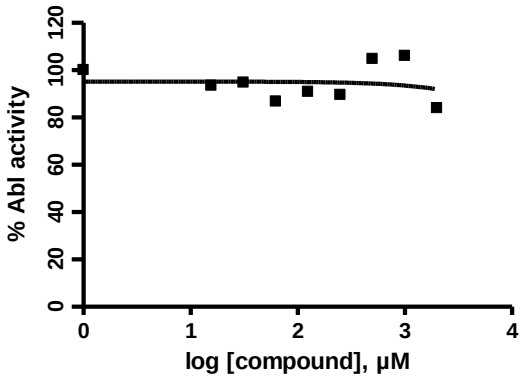

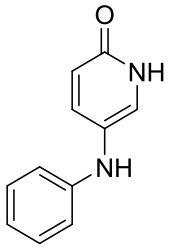

3.9

c-Src K_i = 552 ± 9 µM

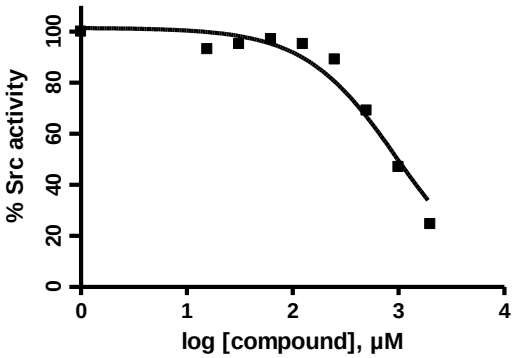

Hck K_i = 318 ± 17 µM

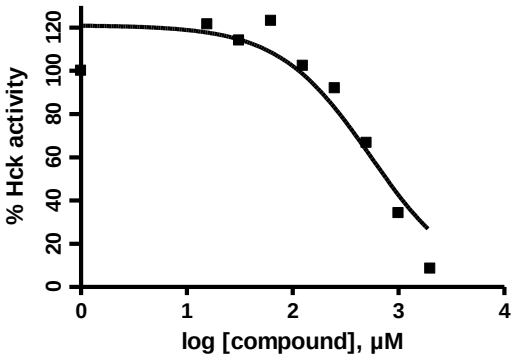

c-Abl K_i = 1046 ± 176 µM

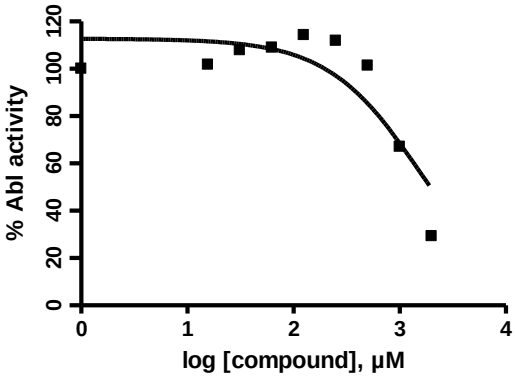

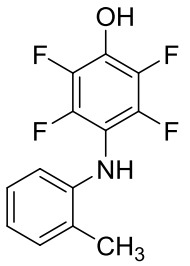

3.10

c-Src K_i = 127 ± 11 µM

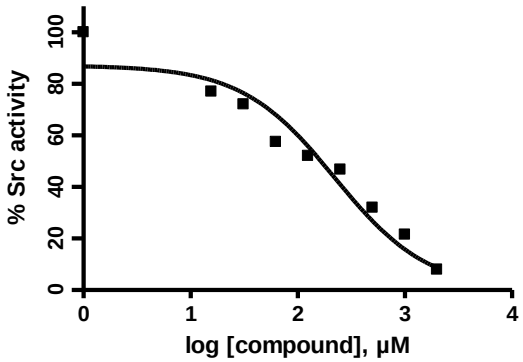

Hck K_i >1080 µM

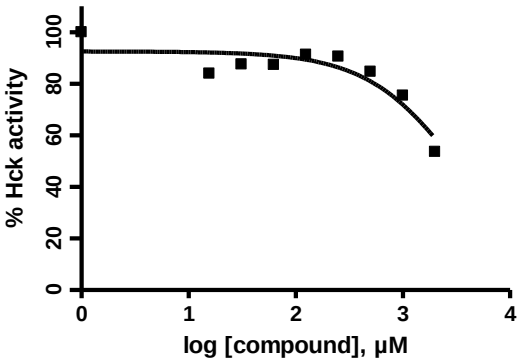

c-Abl K_i >1170 µM

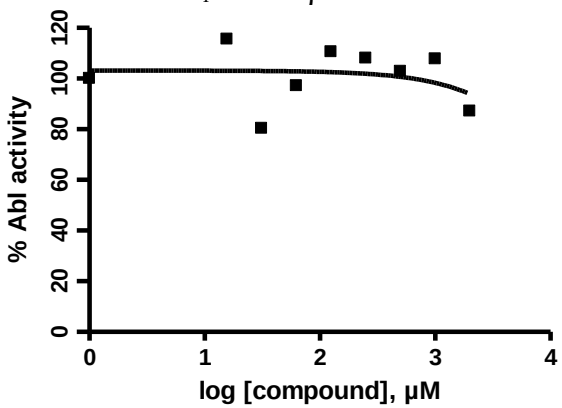

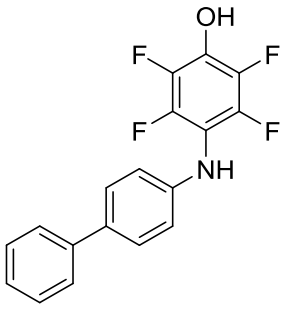

3.11

c-Src K_i = 80 ± 6 µM

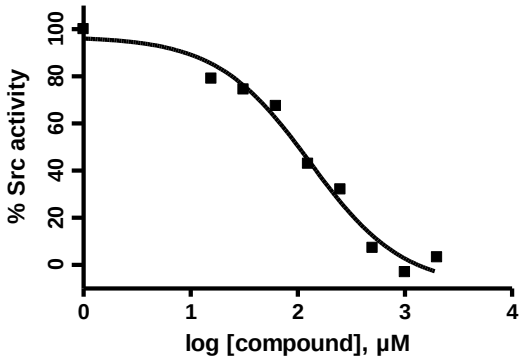

Hck K_i = 149 ± 6 µM

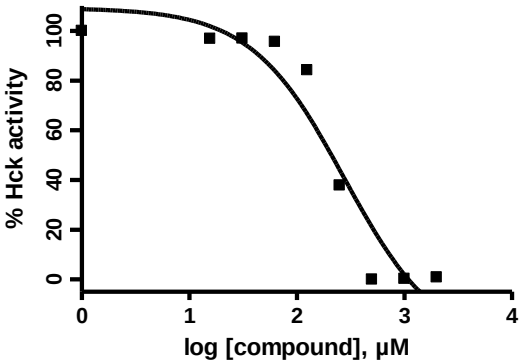

c-Abl K_i = 549 ± 138 µM

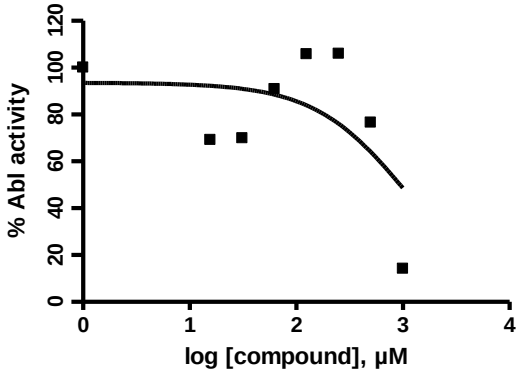

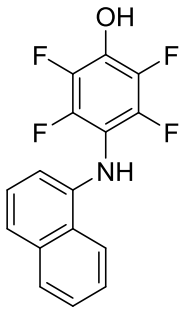

3.12

c-Src K_i = 16 ± 1 µM

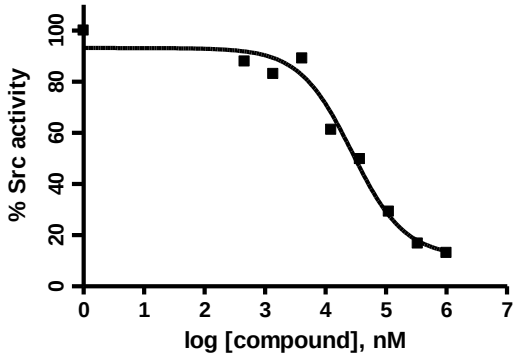

Hck K_i = 325 ± 30 µM

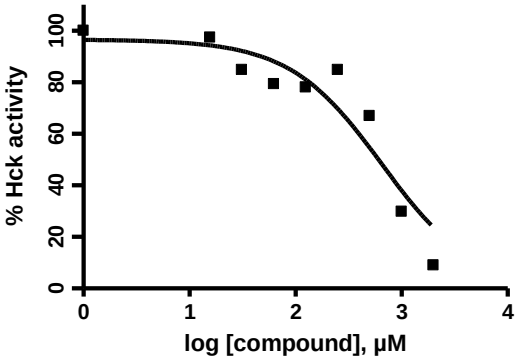

c-Abl K_i = 1067 ± 385 µM

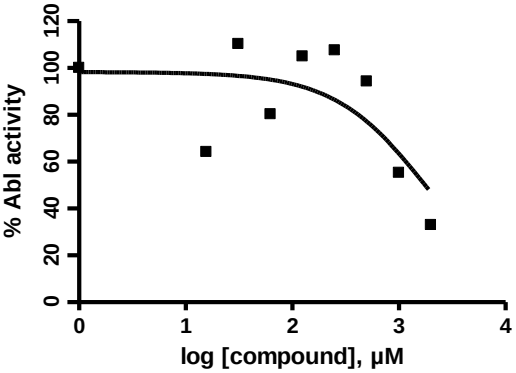

3D c-Src K_i = 36 ± 5 µM

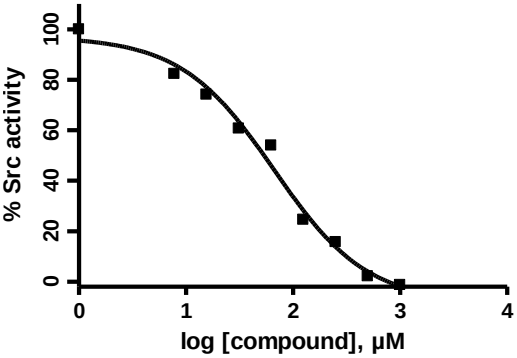

pY416 c-Src K_i = 73 ± 9 µM

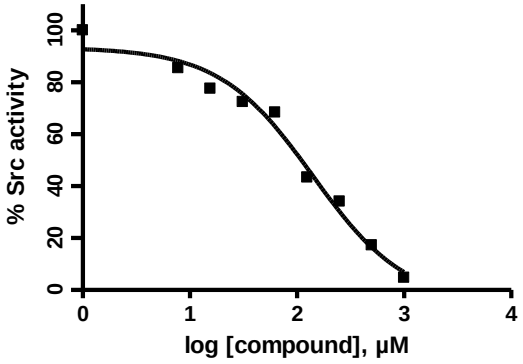

T338M c-Src K_i = 75 ± 15 µM

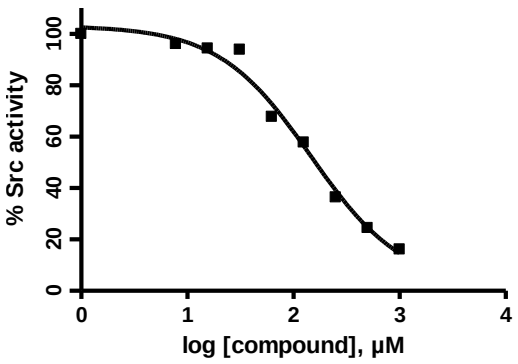

R388A/A390R c-Src K_i = 184 ± 53 µM

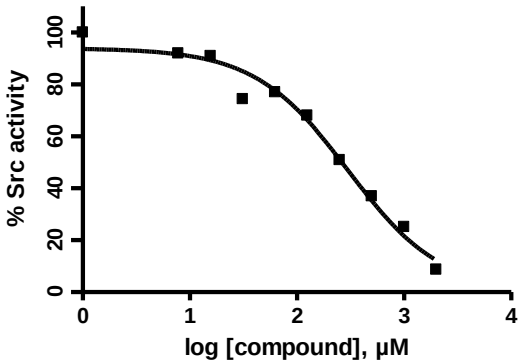

Yes K_i = 82 ± 16 µM

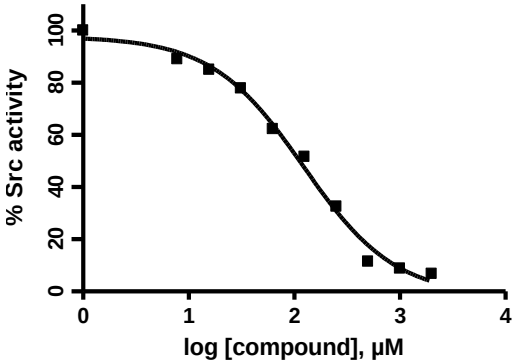

Blk K_i = 52 µM (n = 1)

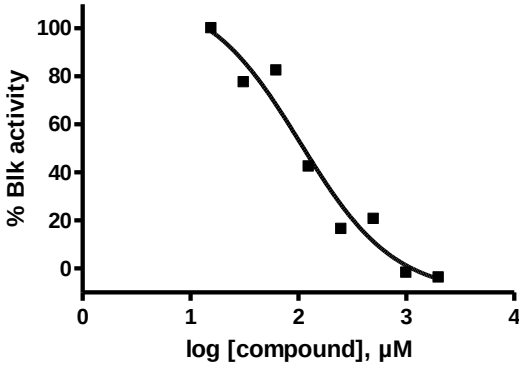

Fgr K_i = 51 µM (n = 1)

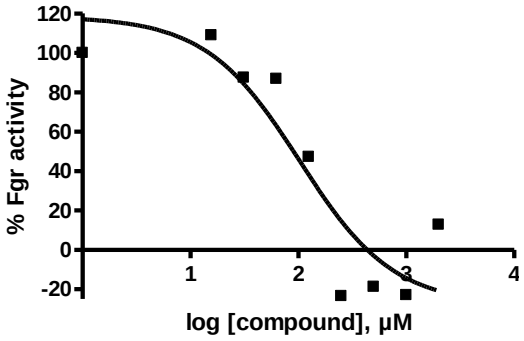

Frk K_i = 83 µM (n = 1)

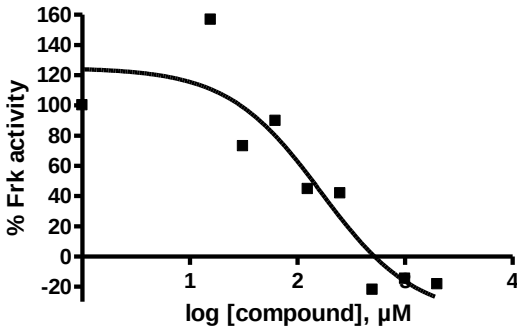

Fyn A K_i = 61 µM (n = 1)

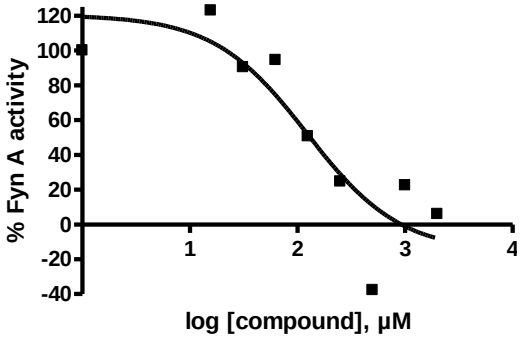

Lck K_i = 63 µM (n = 1)

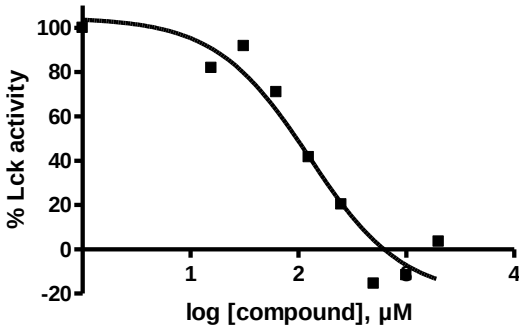

Lyn A K_i = 60 µM (n = 1)

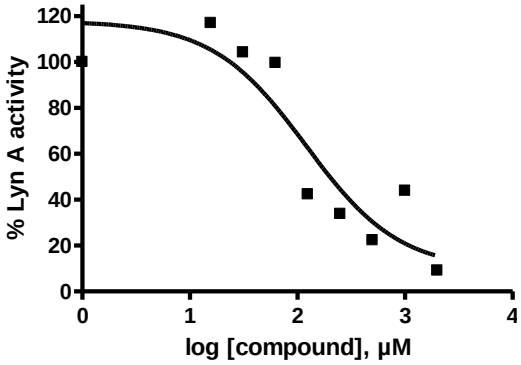

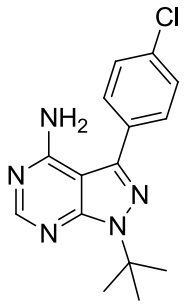

PP2

c-Src K_i = 45 ± 1 nM

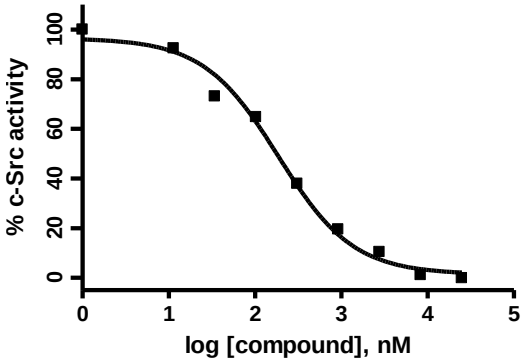

Hck K_i = 88 ± 5 nM

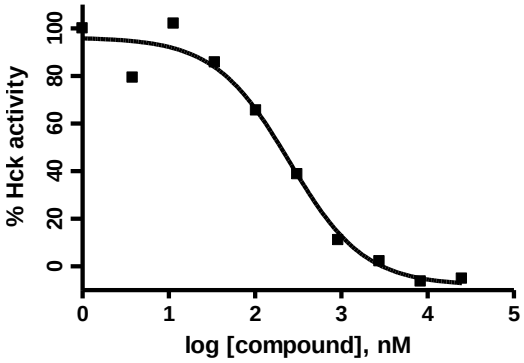

c-Abl K_i = 387 ± 17 nM

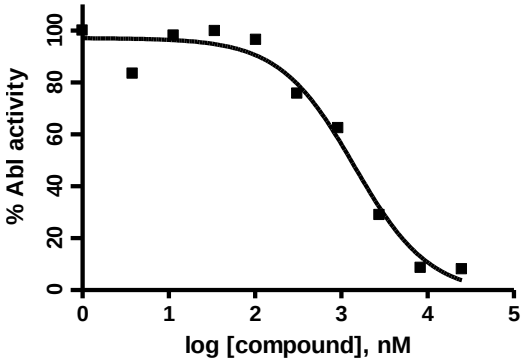

Yes K_i = 46 ± 11 nM

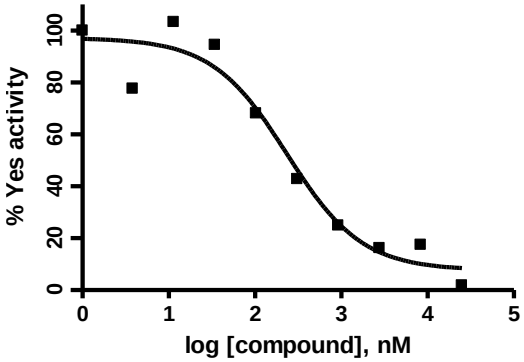

Blk K_i = 67 nM (n = 1)

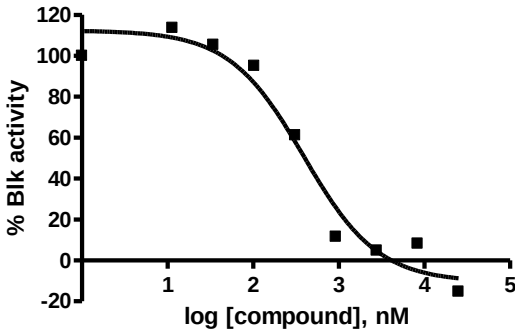

Fgr K_i = 25 nM (n = 1)

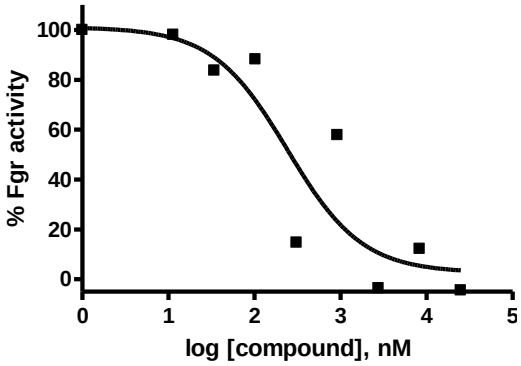

Frk K_i = 20 nM (n = 1)

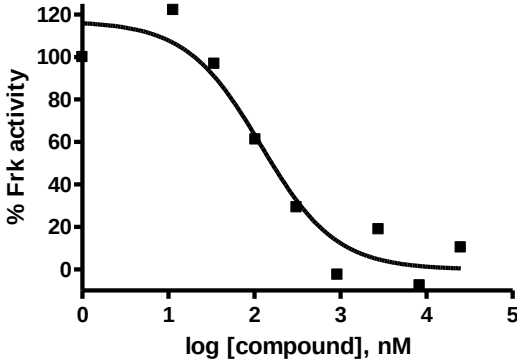

Fyn A K_i = 20 nM (n = 1)

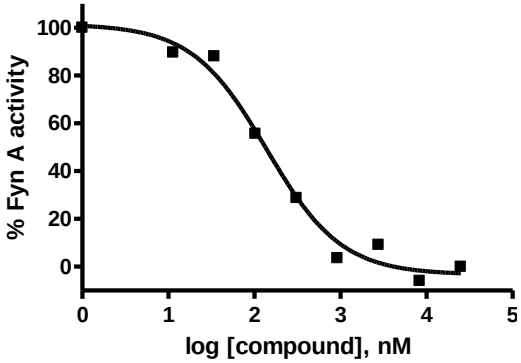

Lck K_i = 9 nM (n = 1)

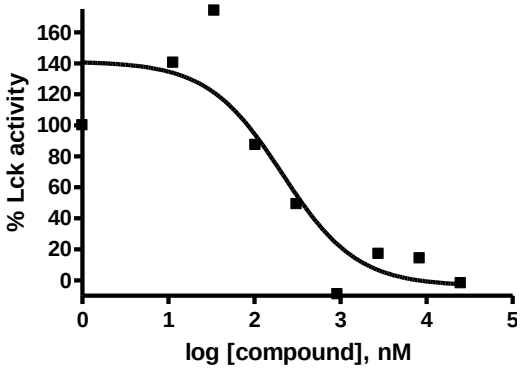

Lyn A K_i = 16 nM (n = 1)

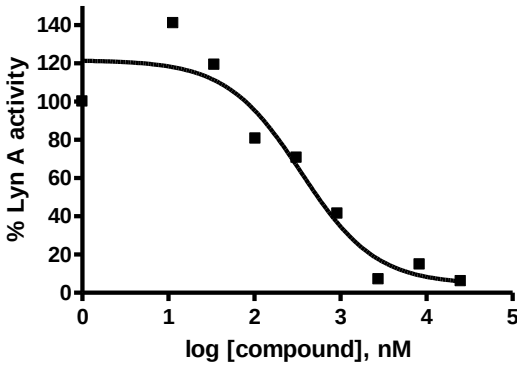

Analytical Data for Determination of Peptide Substrate "Substrate 3" K_M

c-Src K_M = 61 ± 4 µM

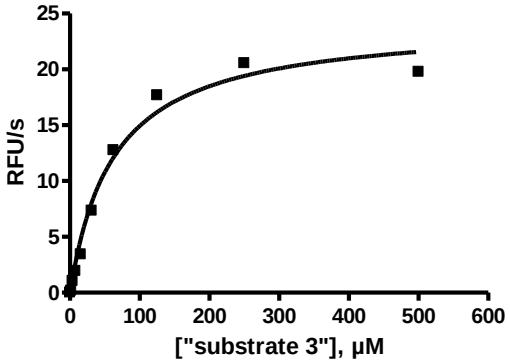

Hck K_M = 53 ± 2 µM

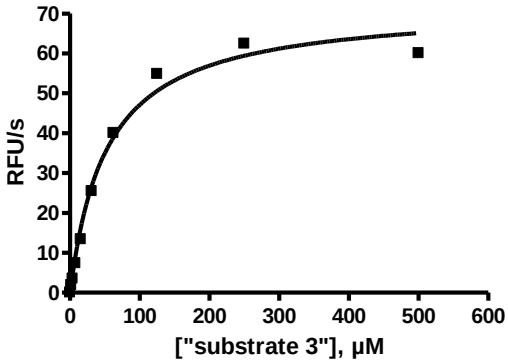

c-Abl K_M = 168 ± 19 µM

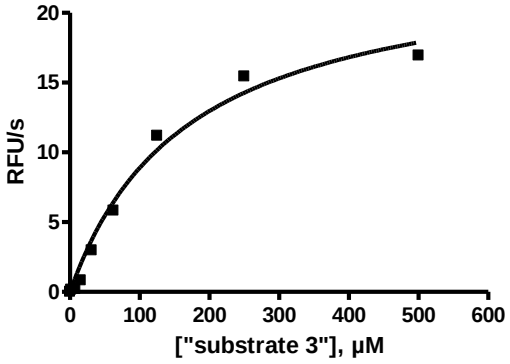

R388A/A390R c-Src K_M = 70 ± 17 µM

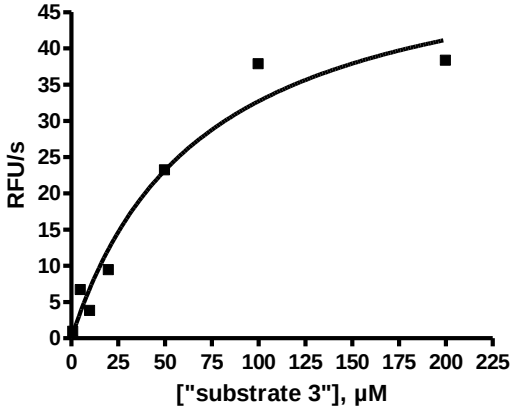

T338M c-Src K_M = 26 ± 8 µM

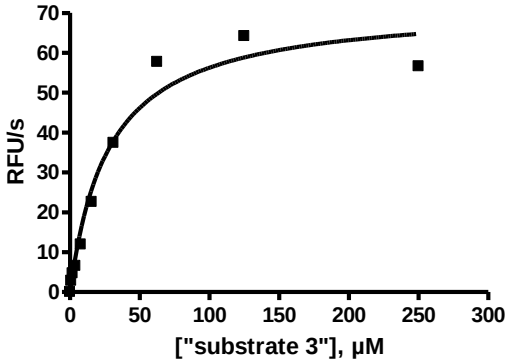

3D c-Src K_M = 64 ± 4 µM

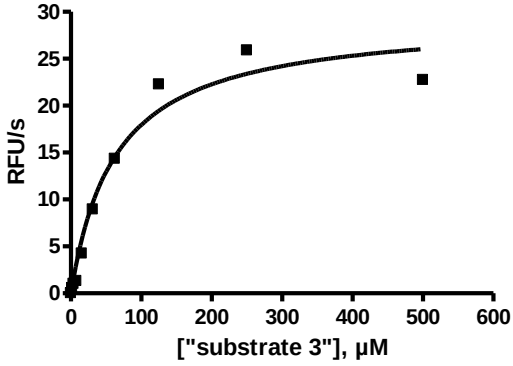

pY416 Src K_M = 43 ± 3 µM

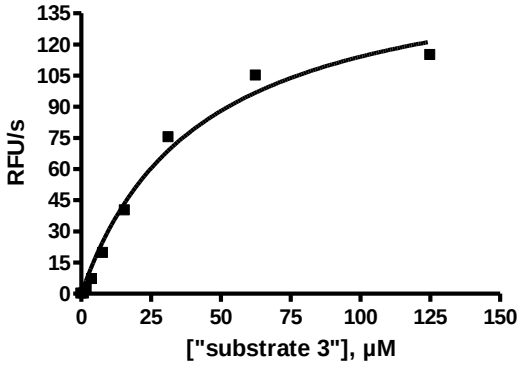

Yes K_M = 62 ± 6 µM

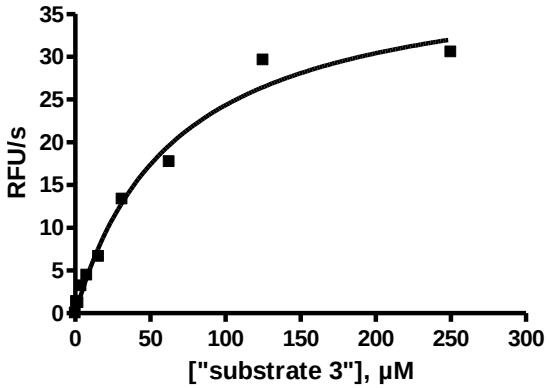

Blk K_M = 85 µM (n = 1)

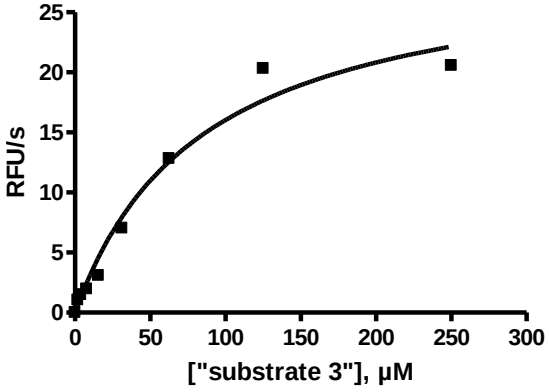

Frk K_M = 165 µM (n = 1)

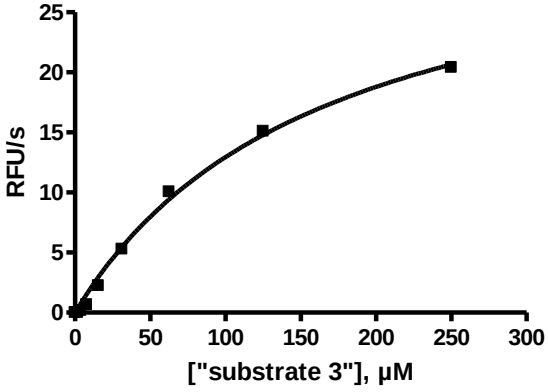

Analytical Data for Determination of ATP K_M

c-Abl K_M = 37 ± 6 µM

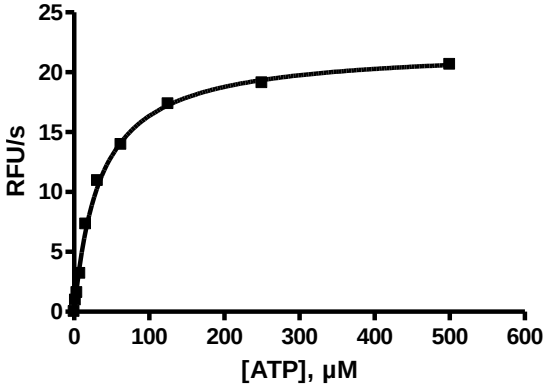

Hck K_M = 50 ± 3 µM

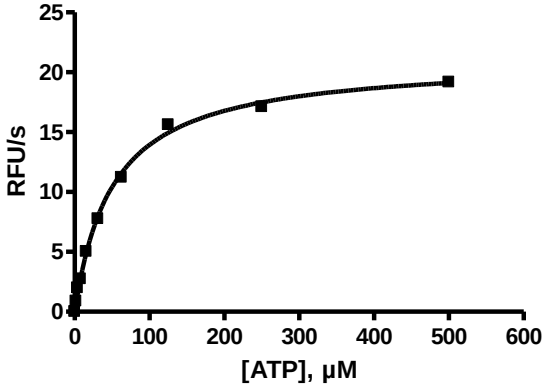

Yes K_M = 105 ± 21 µM

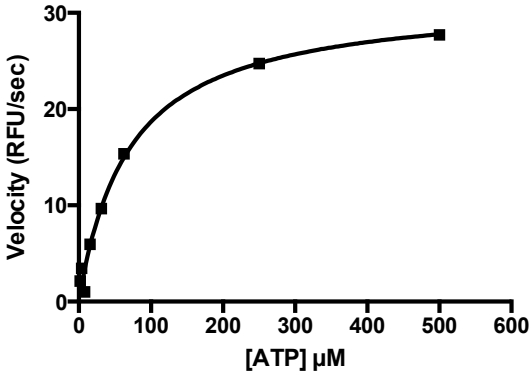

Analytical Data for Determination of Inhibitor IC_{50} at Variable ATP and Peptide Substrate Concentration

	IC_{50} under standard conditions
3.7	436 ± 60 µM
3.8	830 ± 143 µM
3.9	958 ± 16 µM
3.12	27 ± 2 µM

3.7 with high "substrate 3" conditions
IC_{50} > 2000 µM

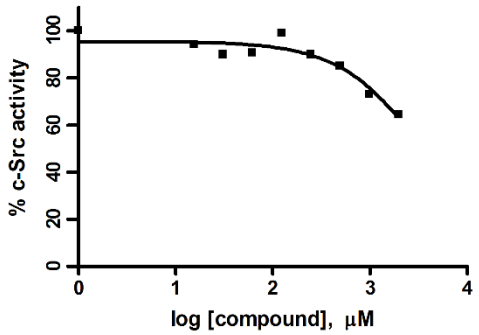

3.7 with low ATP conditions IC_{50}
IC_{50} = 253 ± 37 µM

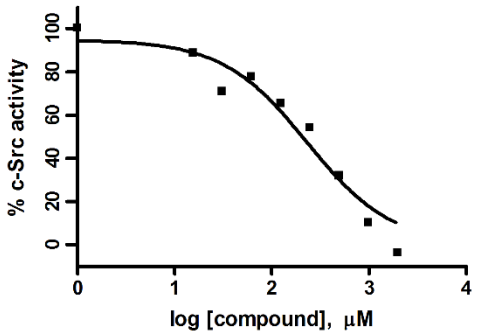

3.8 with high "substrate 3" conditions
IC_{50} = 1520 ± 440 µM

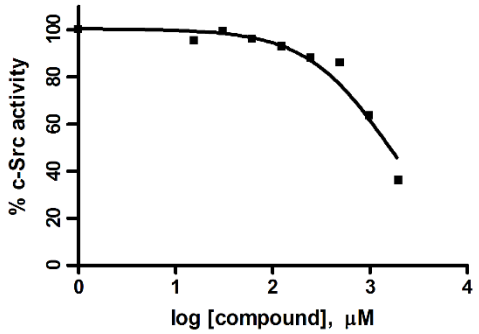

3.8 with low ATP conditions
IC_{50} = 444 ± 59 µM

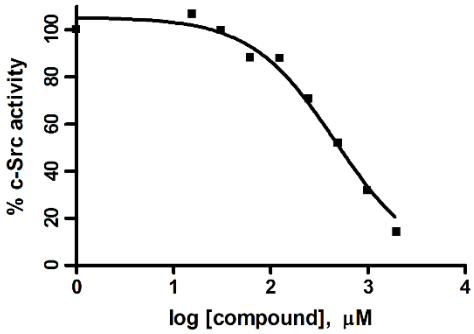

3.9 with high "substrate 3" conditions
IC_{50} = 1742 ± 614 µM

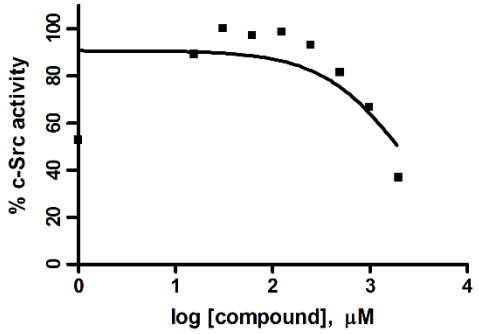

3.9 with low ATP conditions
IC_{50} = 665 ± 97µM

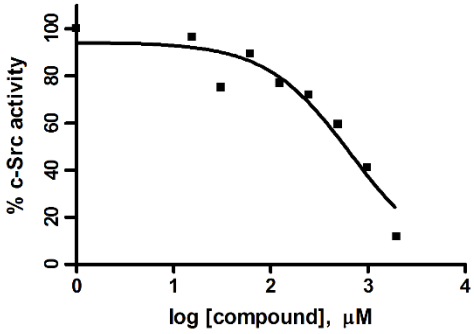

3.12 with high "substrate 3" conditions
IC_{50} = 557 ± 149 µM

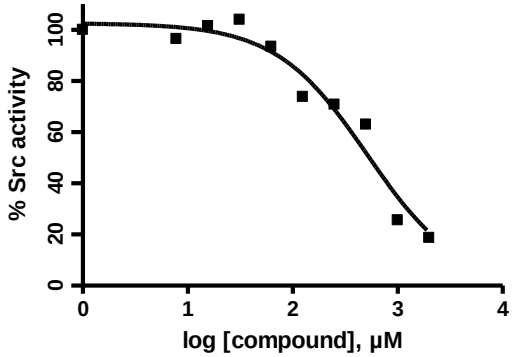

3.12 with low ATP conditions
IC_{50} = 44 ± 4 µM

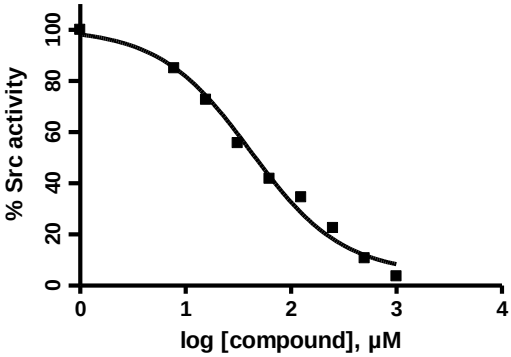

Analytical Data for Lineweaver-Burk Analysis of Compound 3.12

"Substrate 3" K_M and V_{max} at varied inhibitor concentrations:

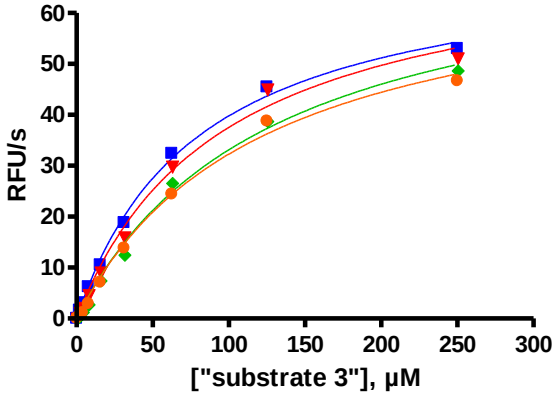

	0 µM 12	10 µM 12	30 µM 12	60 µM 12
Michaelis-Menten Best-fit values				
VMAX	71.69	73.57	75.22	71.18
KM	80.20	96.00	127.1	120.5

Global fit data for "substrate 3" K_M data:

	R^2
competitive	0.993
non-competitive	0.891
uncompetitive	0.888

ATP K_M and V_{max} at varied inhibitor concentrations:

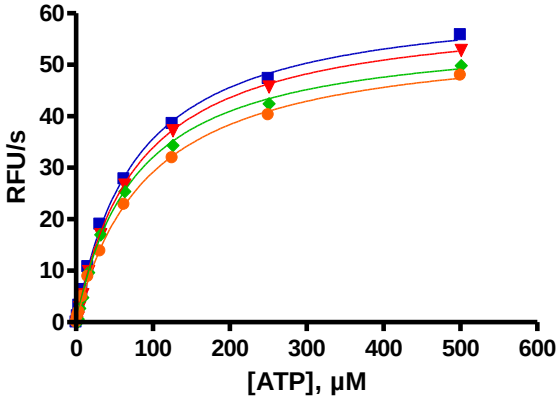

	0 µM 12	10 µM 12	30 µM 12	60 µM 12
Michaelis-Menten Best-fit values				
VMAX	63.41	61.14	56.82	56.20
KM	78.13	80.43	77.48	92.93

Global fit data for ATP K_M data:

	R^2
competitive	0.897
non-competitive	0.999
uncompetitive	0.897

Analytical Data for Combination Studies of Compound 3.12 with PP2 and PP5

Inhibitor **3.12** c-Src IC_{50} = 28 ± 14 µM

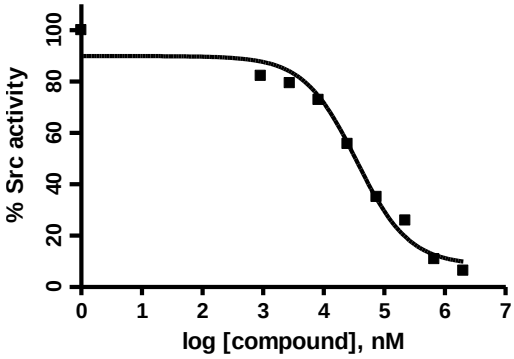

PP2 c-Src IC_{50} = 181 ± 6 nM

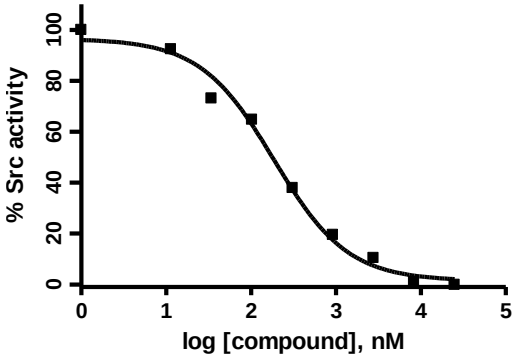

PP5 c-Src IC_{50} = 98 ± 17 nM

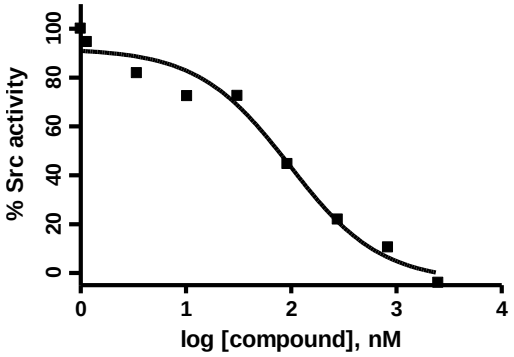

Inhibitor(s)	c-Src Inhibition (%)	Predicted Additivity (% inhibition)
100 nM PP2	34 ± 6	NA
50 nM PP5	32 ± 8	NA
20 µM 3.12	36 ± 10	NA
100 nM PP2 + 50 nM PP5	50 ± 3	55
100 nM PP2 + 20 µM 3.12	72 ± 6	58
50 nM PP5 + 20 µM 3.12	88 ± 5	56

Analytical Data for Inhibition of c-Src Autophosphorylation

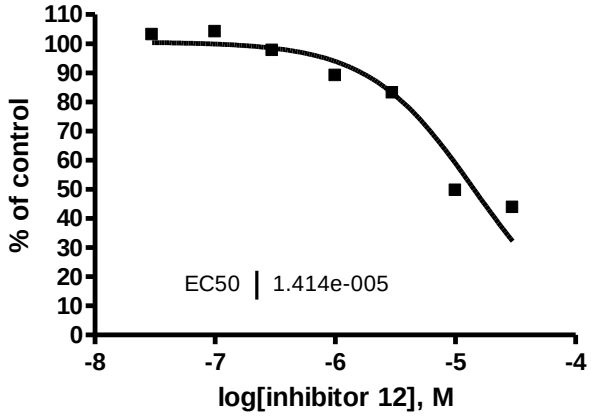

Analytical Data for Cancer Cell Growth Inhibition Assays

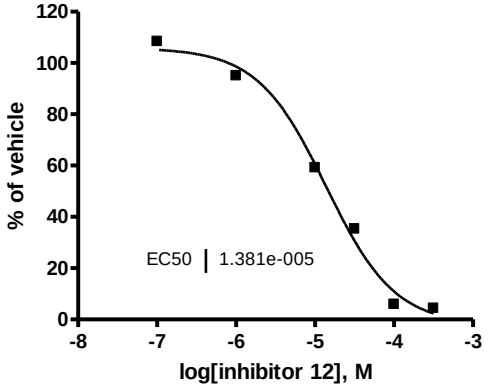

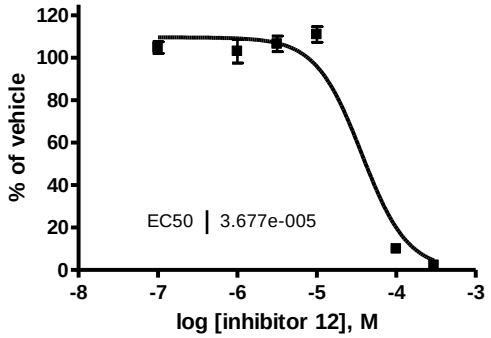

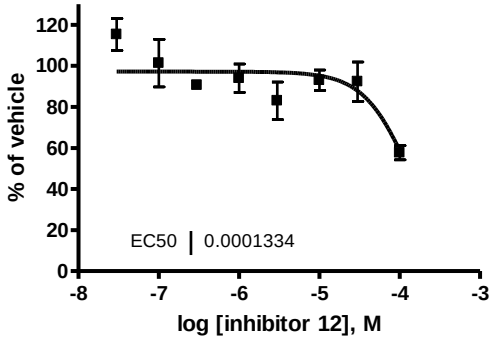

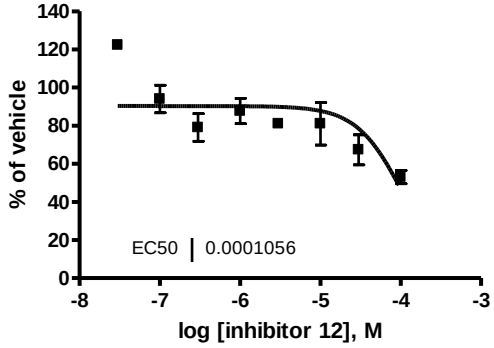

Appendix C
Analytical Data for Chapter IV

Spectral Data (^{1}H NMR) for Compounds 4.2-4.34

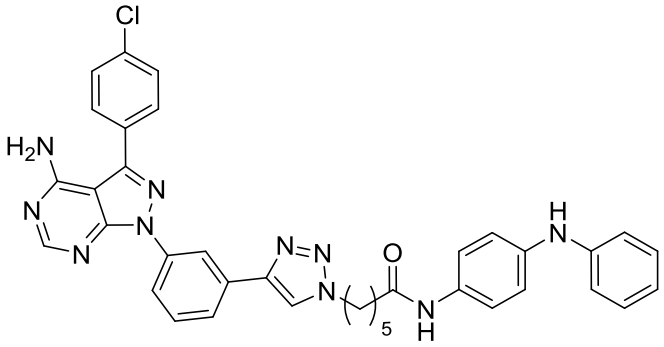

4.2

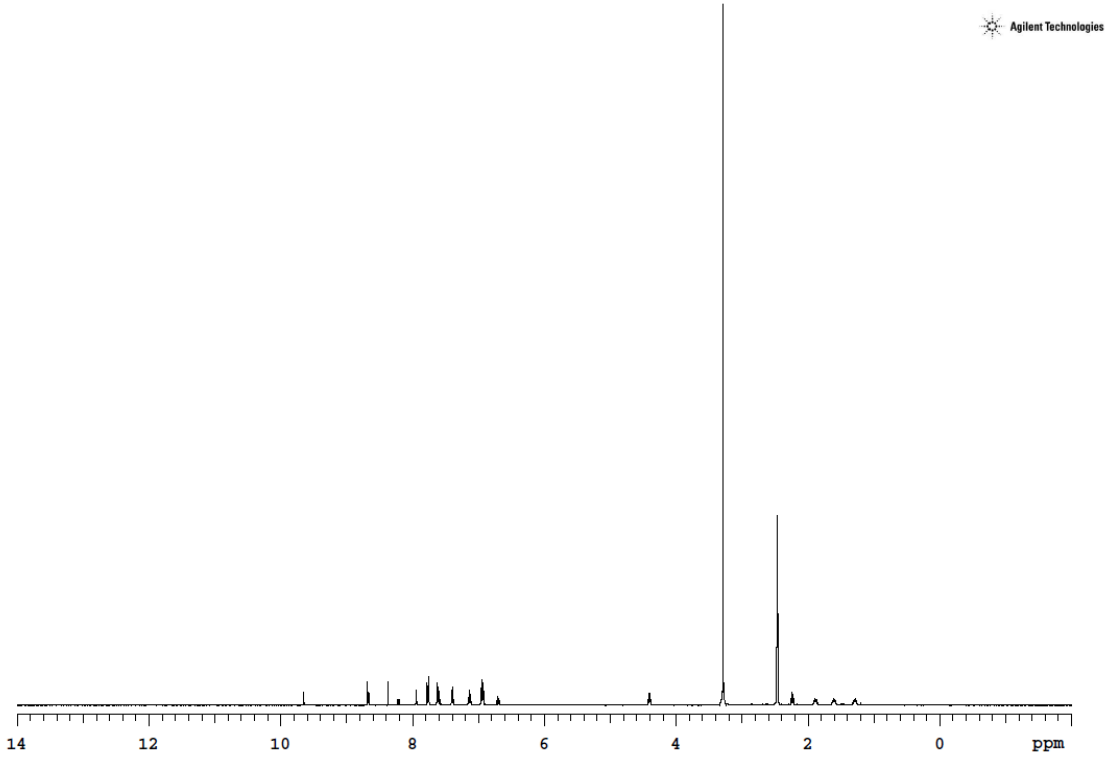

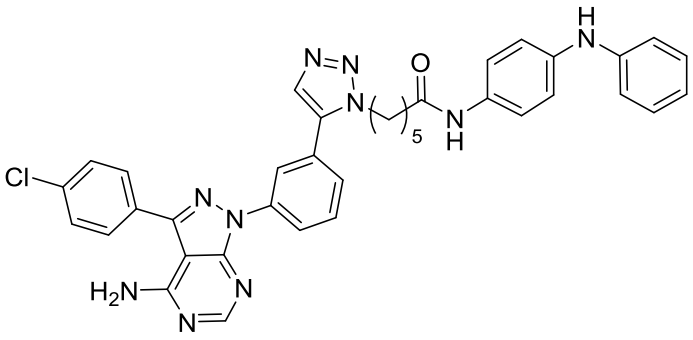

4.3

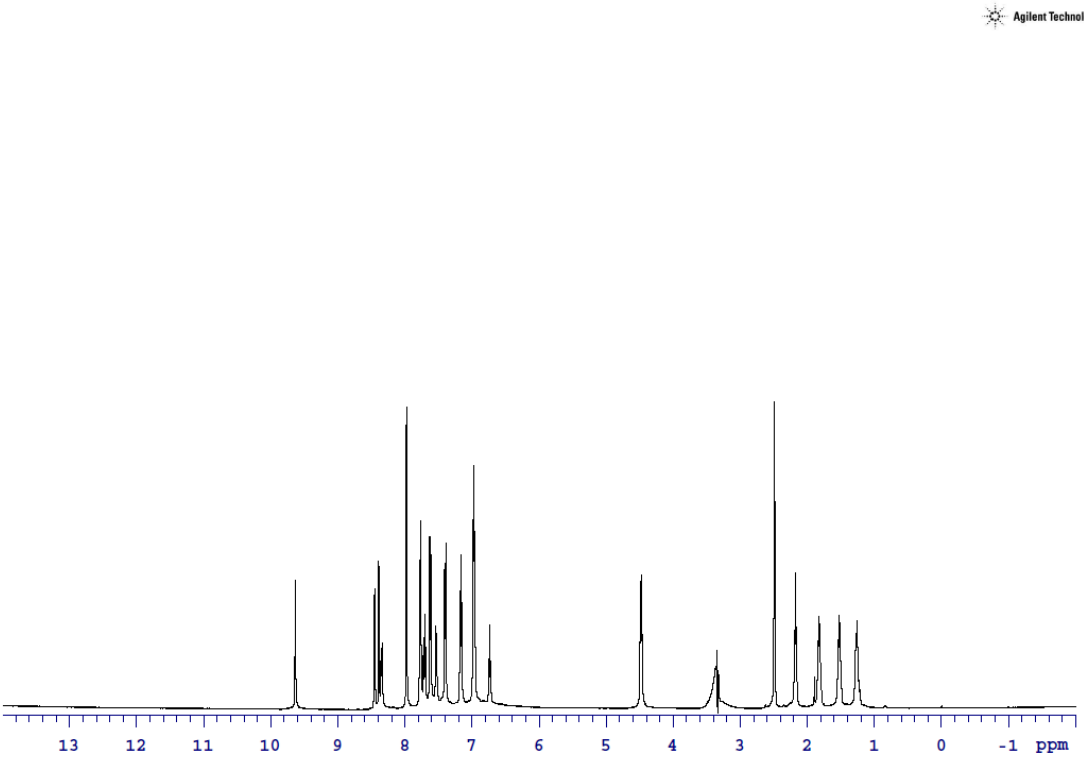

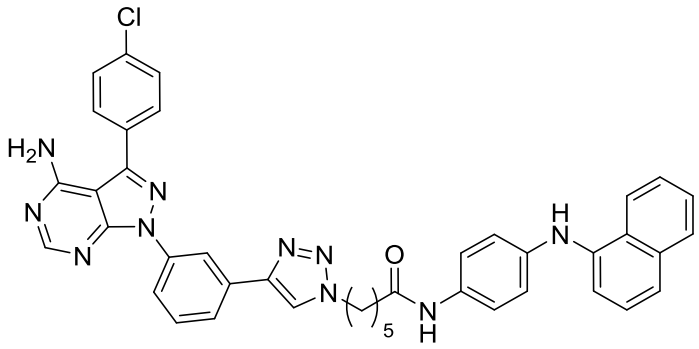
Cl
H2N
N
N
N
N
N=N
N
5
O
N
H
H
N

4.4

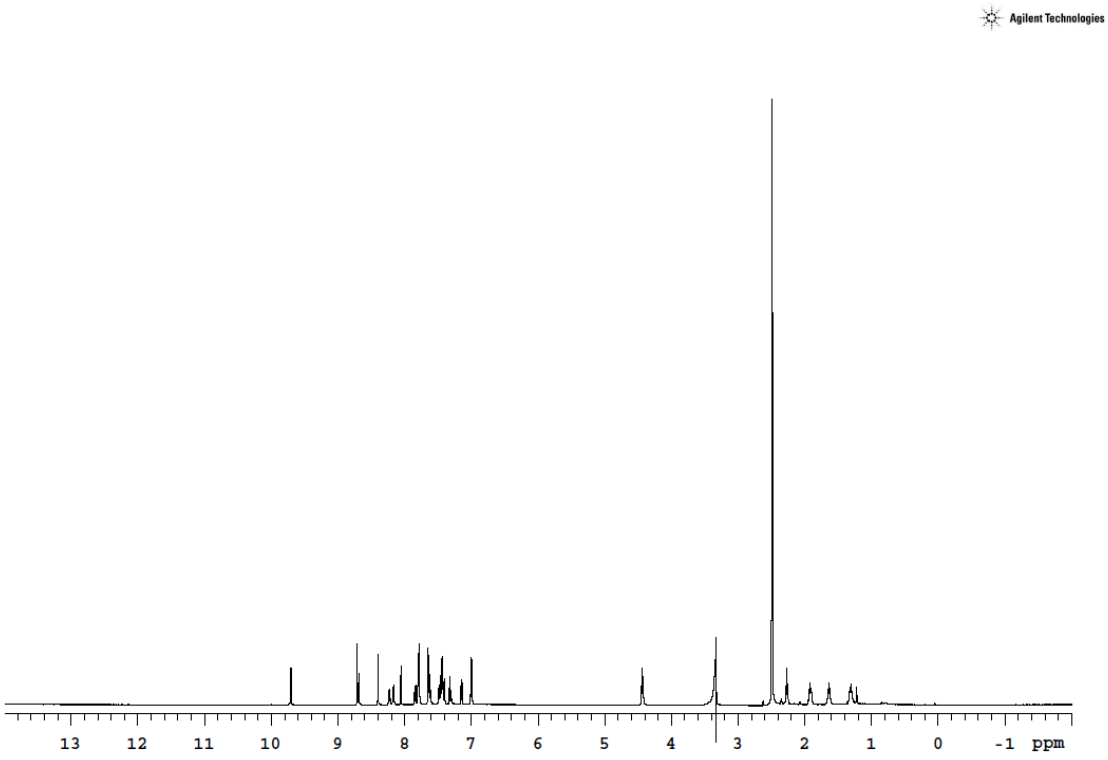
Agilent Technologies
13
12
11
10
9
8
7
6
5
4
3
2
1
0
-1
ppm

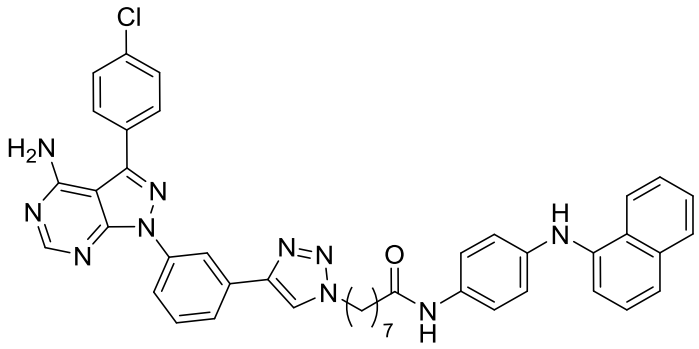
Cl
H2N
N
N
N
N
N
N
O
7
N
H
H
N

4.5

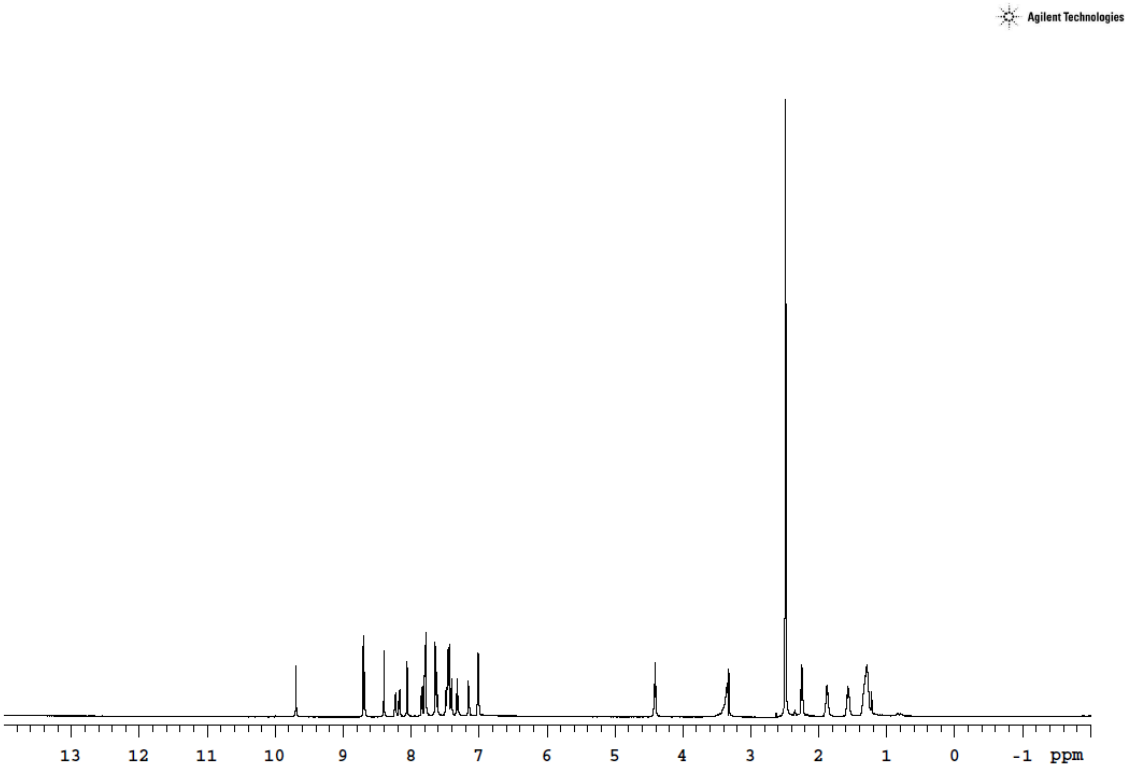
Agilent Technologies
13
12
11
10
9
8
7
6
5
4
3
2
1
0
-1
ppm

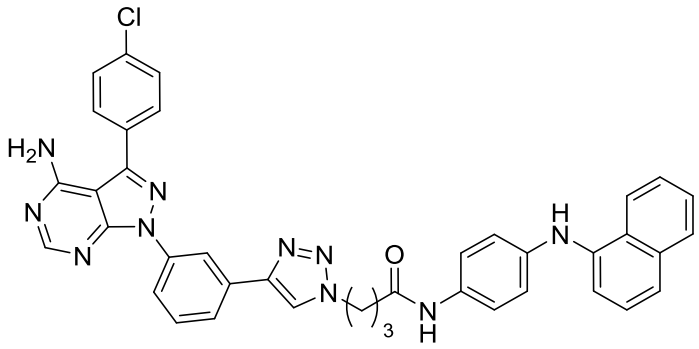

4.6

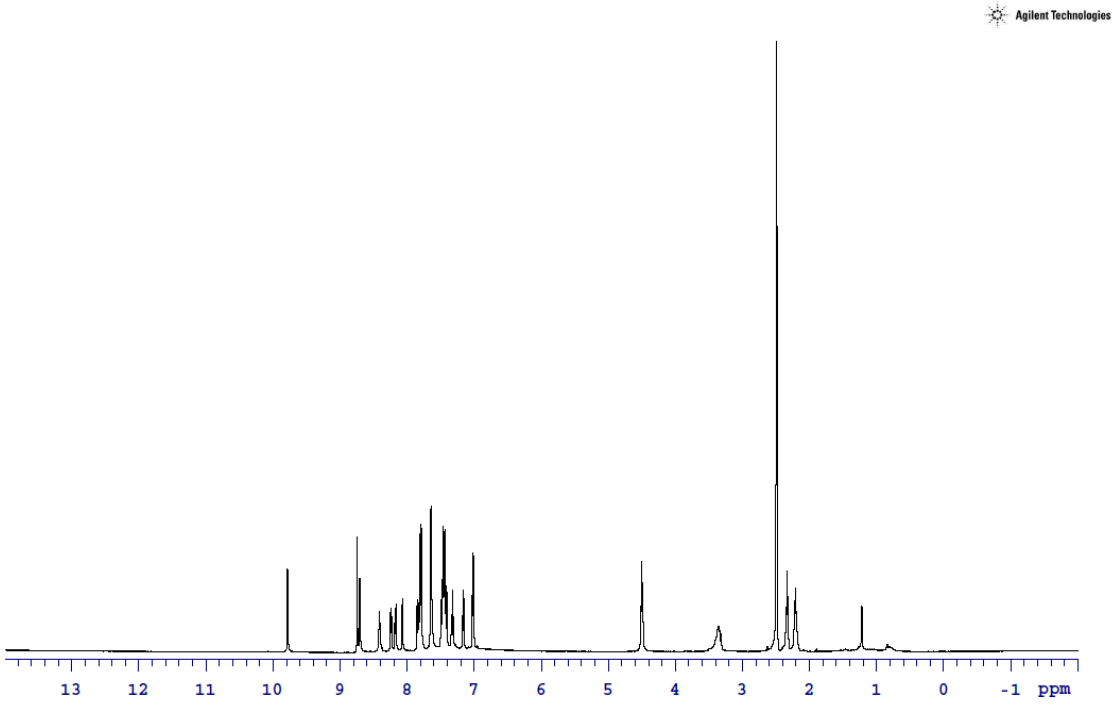

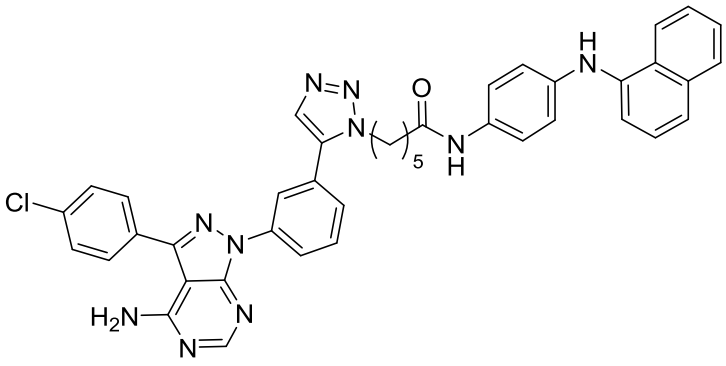

4.7

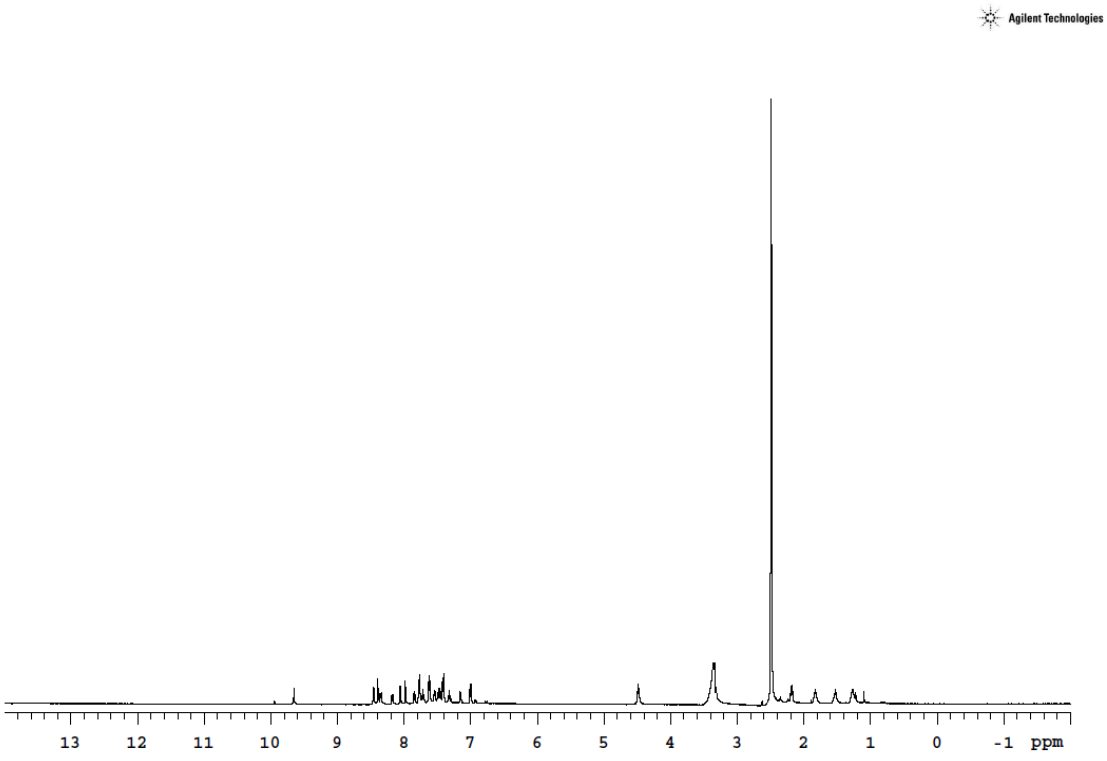

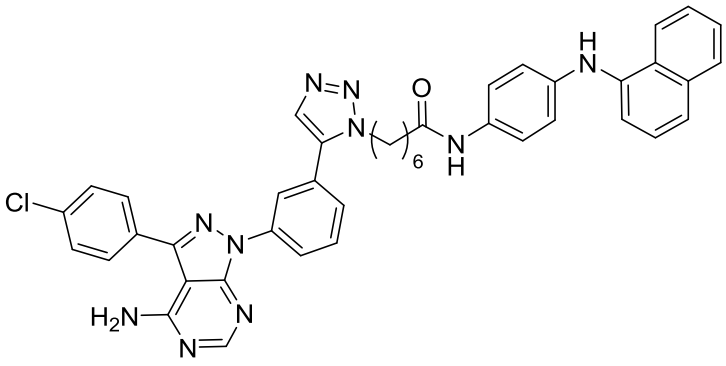

4.8

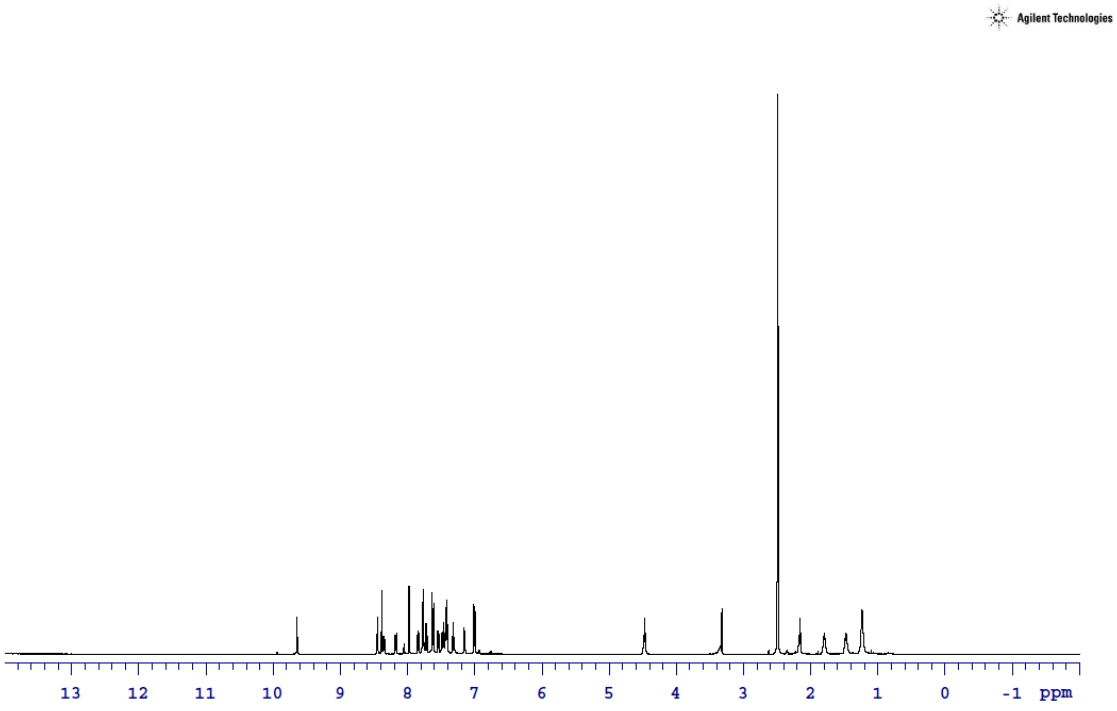

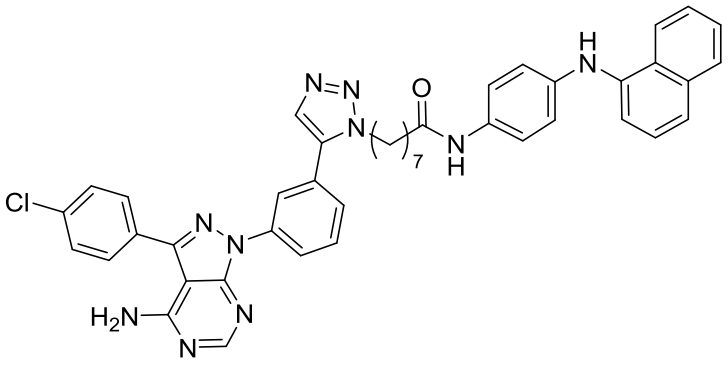

4.9

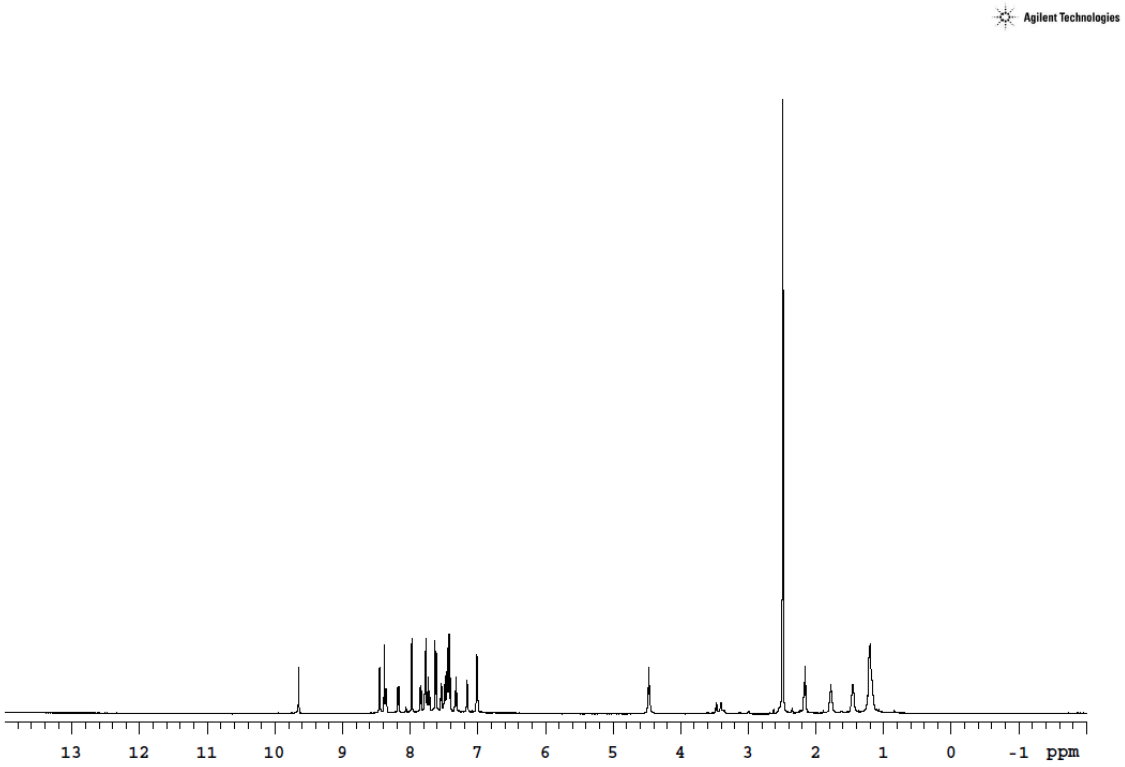

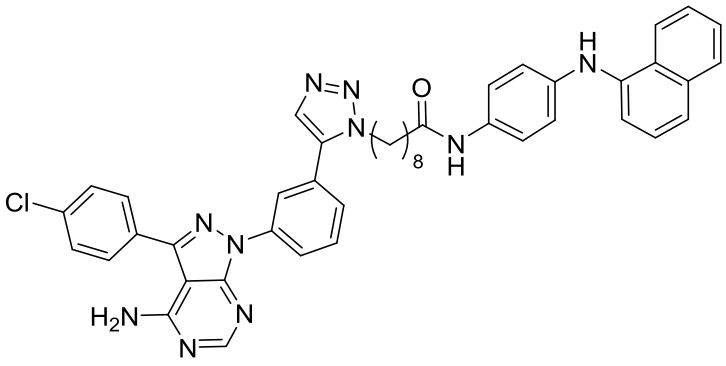

4.10

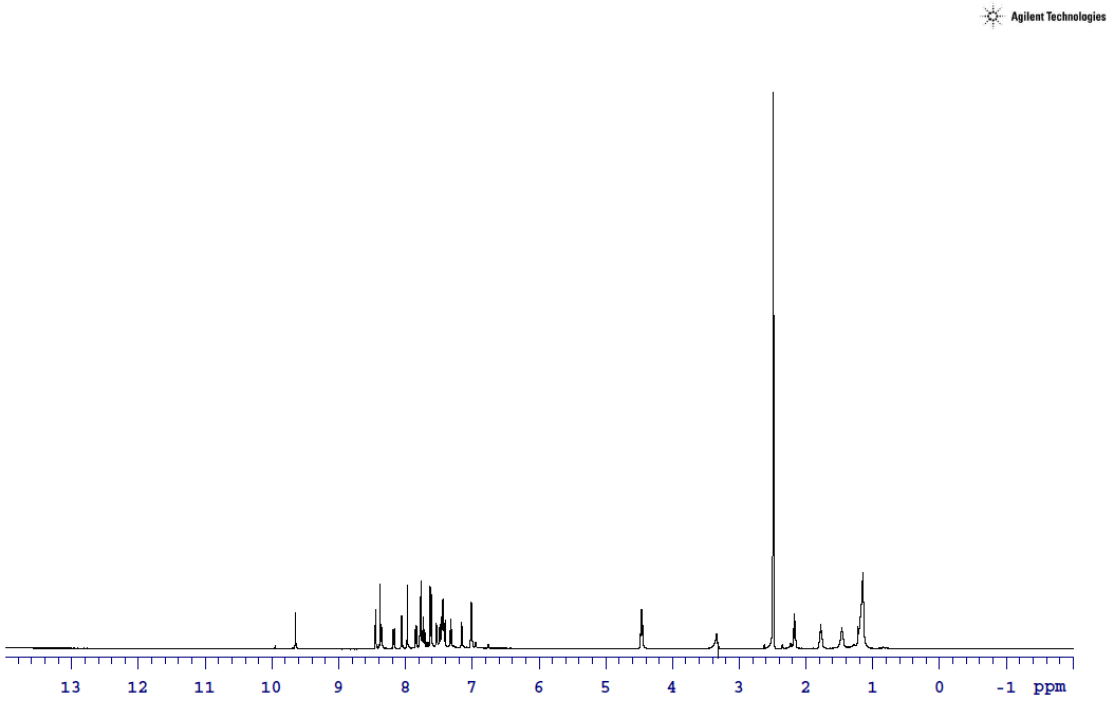

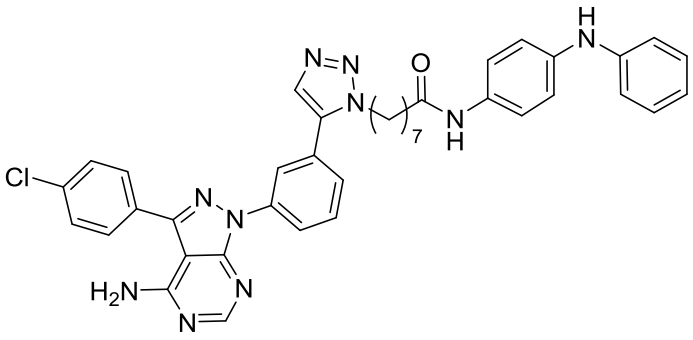

4.11

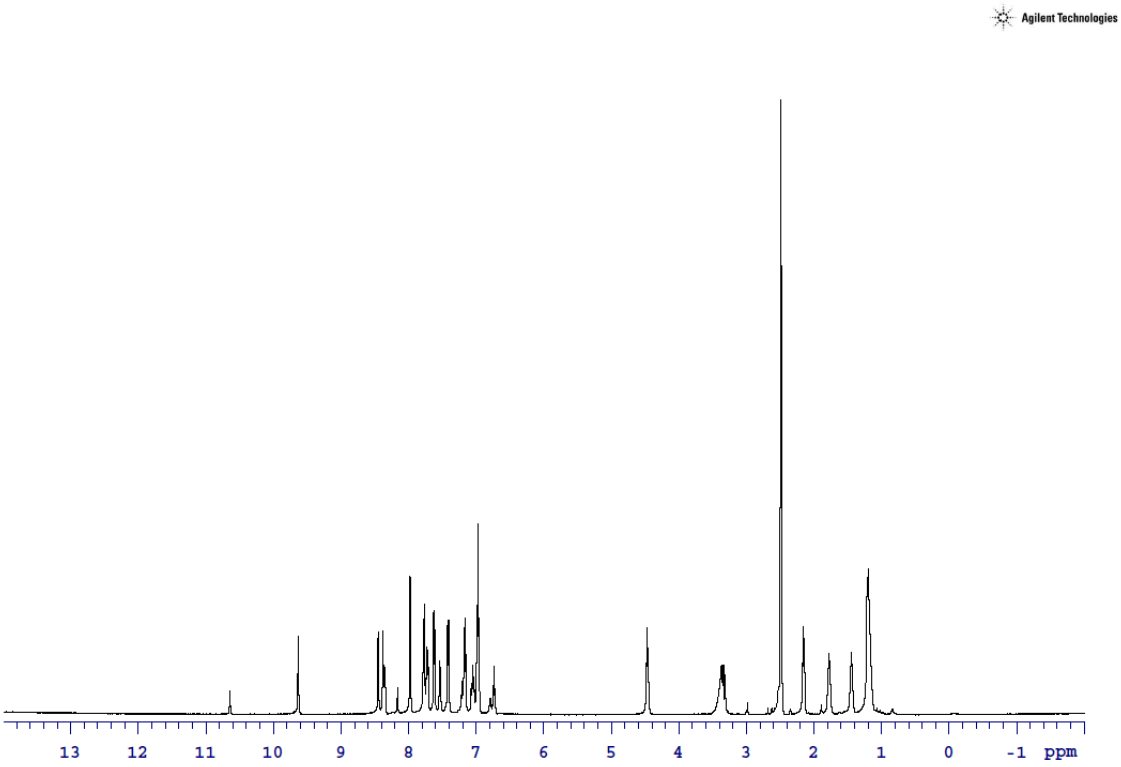

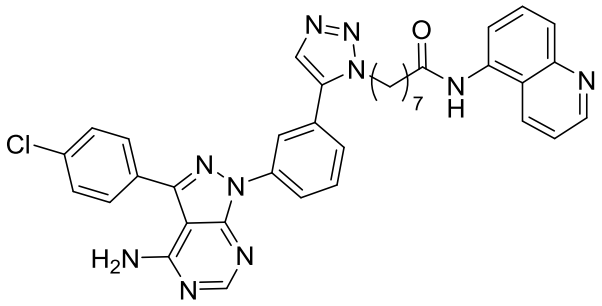

4.12

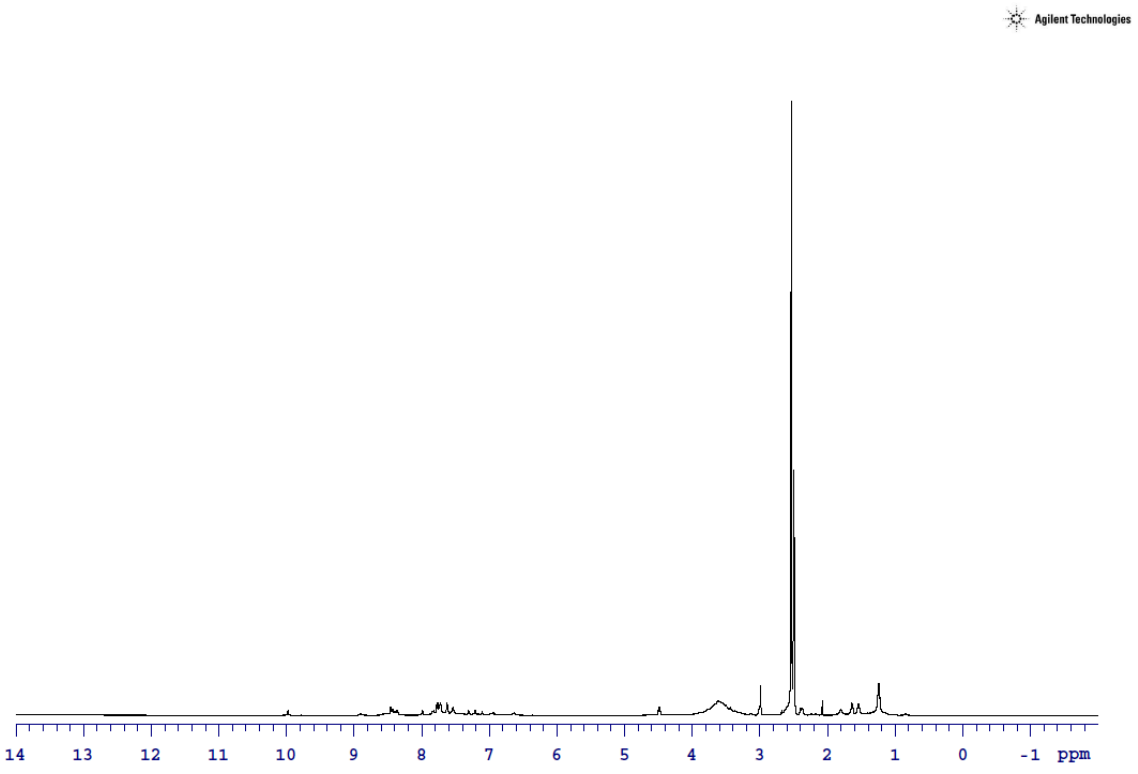

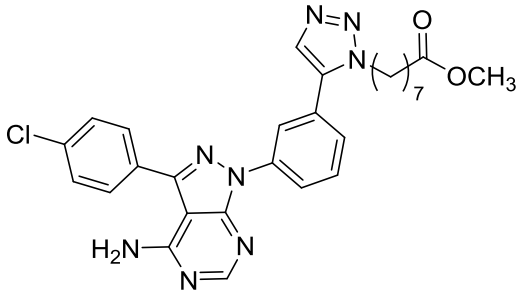
N=N
O
N
7
OCH3
Cl
N
N
H2N
N
N

4.13

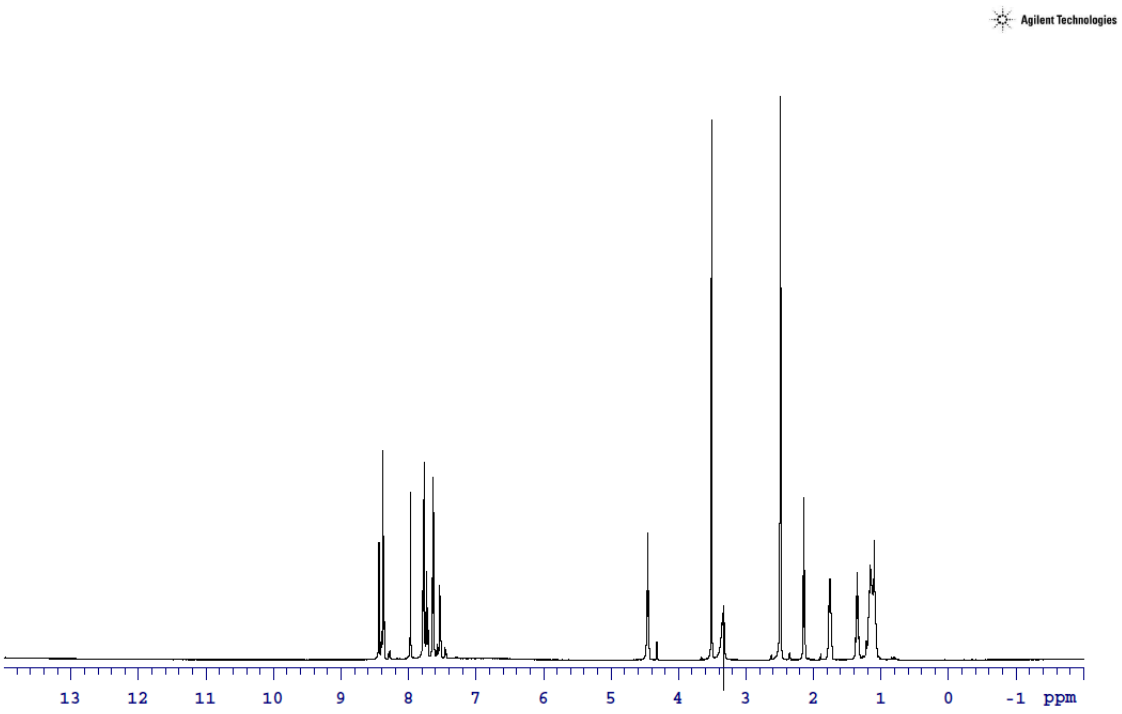
Agilent Technologies
13
12
11
10
9
8
7
6
5
4
3
2
1
0
-1
ppm

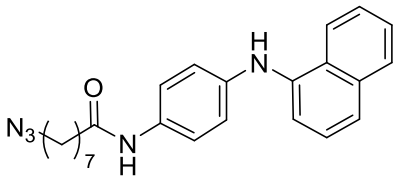

4.14

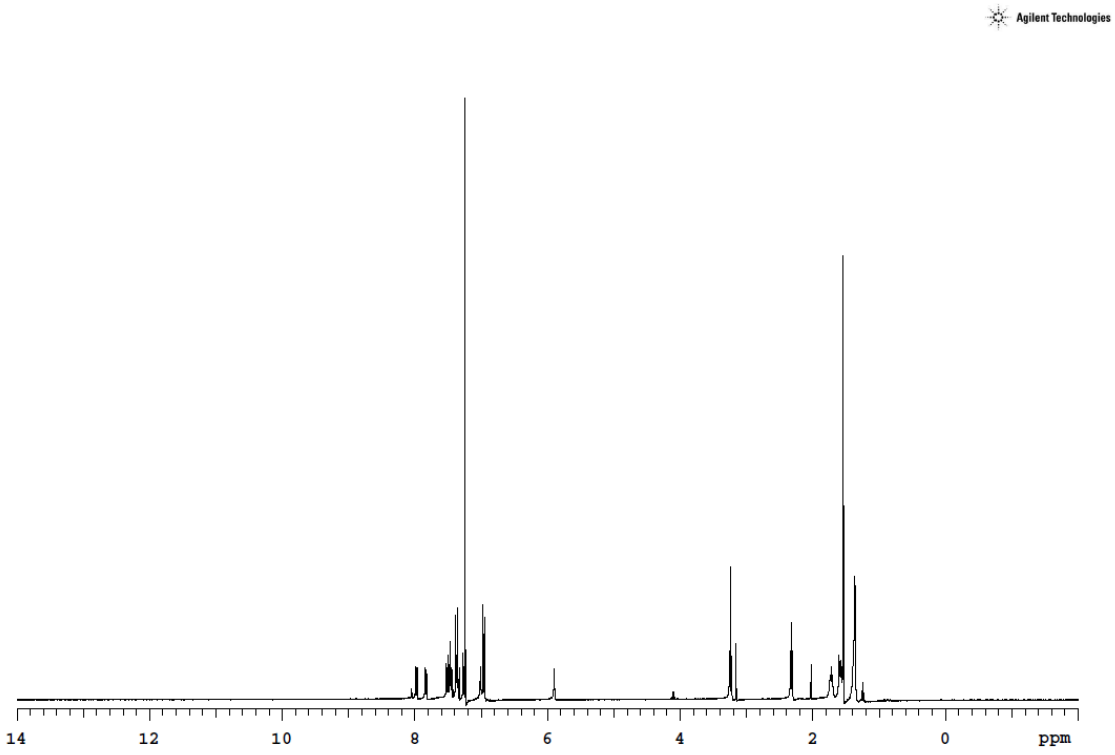

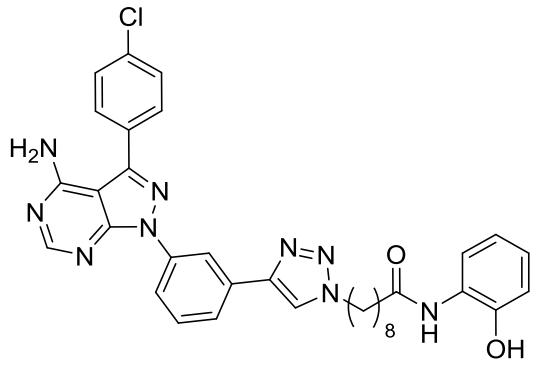
Cl
H2N
N
N
N
N
N=N
N
O
8
N
H
OH

4.15

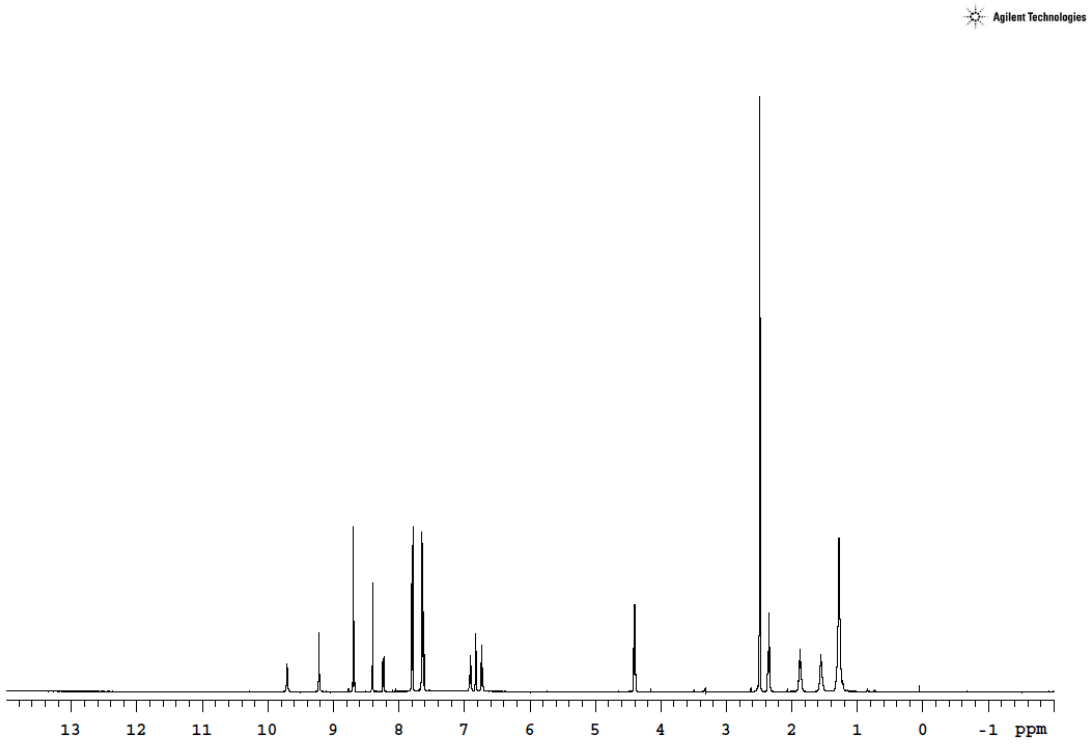
Agilent Technologies
13
12
11
10
9
8
7
6
5
4
3
2
1
0
-1
ppm

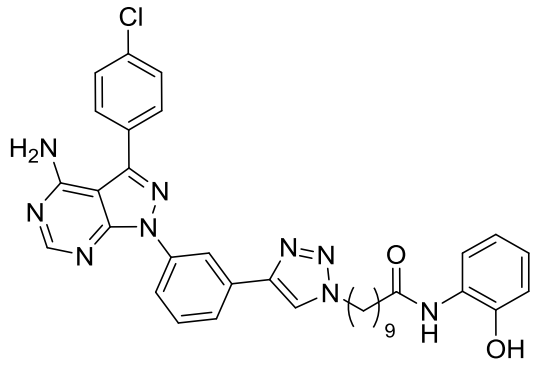
Cl
H2N
N
N
N
N
N
N
O
N
H
9
OH

4.16

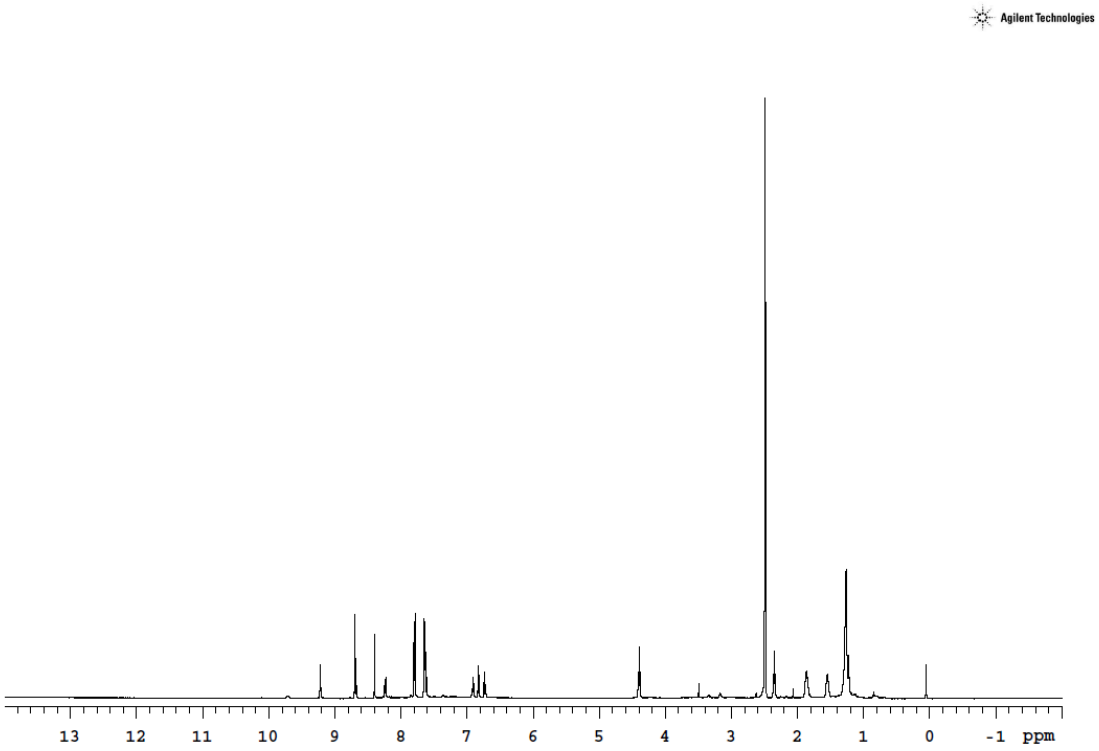
Agilent Technologies
13
12
11
10
9
8
7
6
5
4
3
2
1
0
-1
ppm

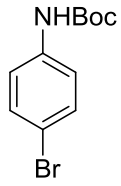

4.17

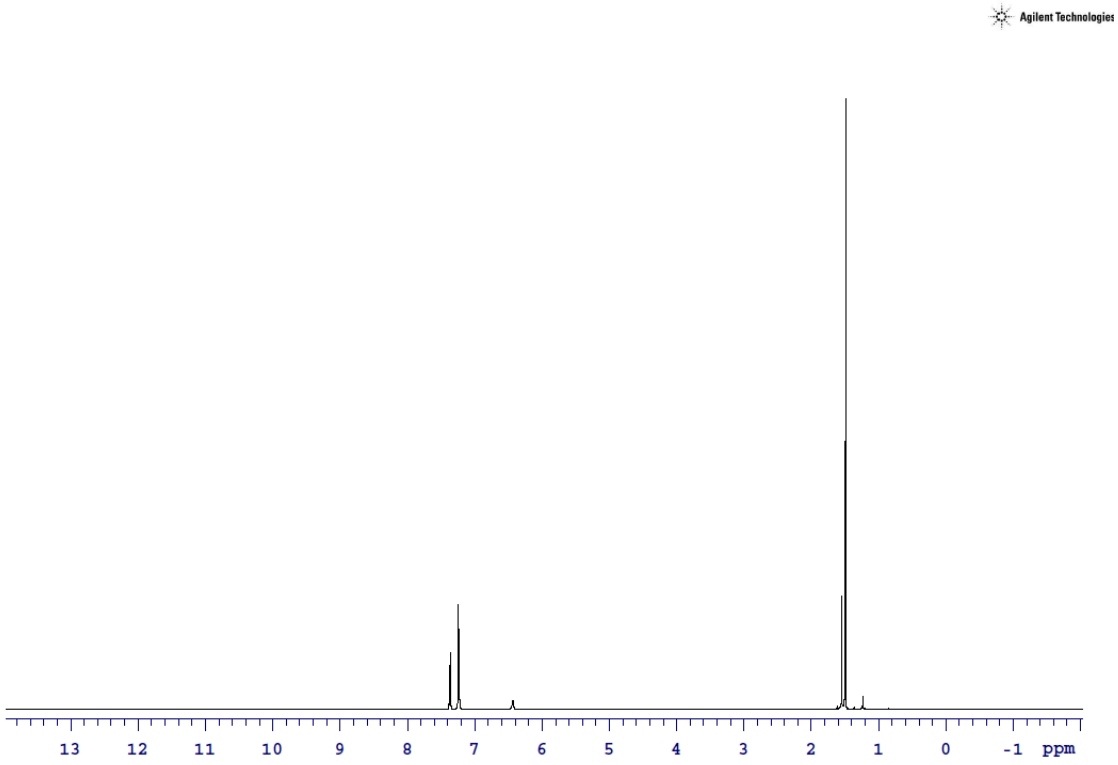

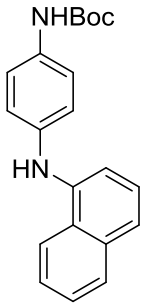

4.18

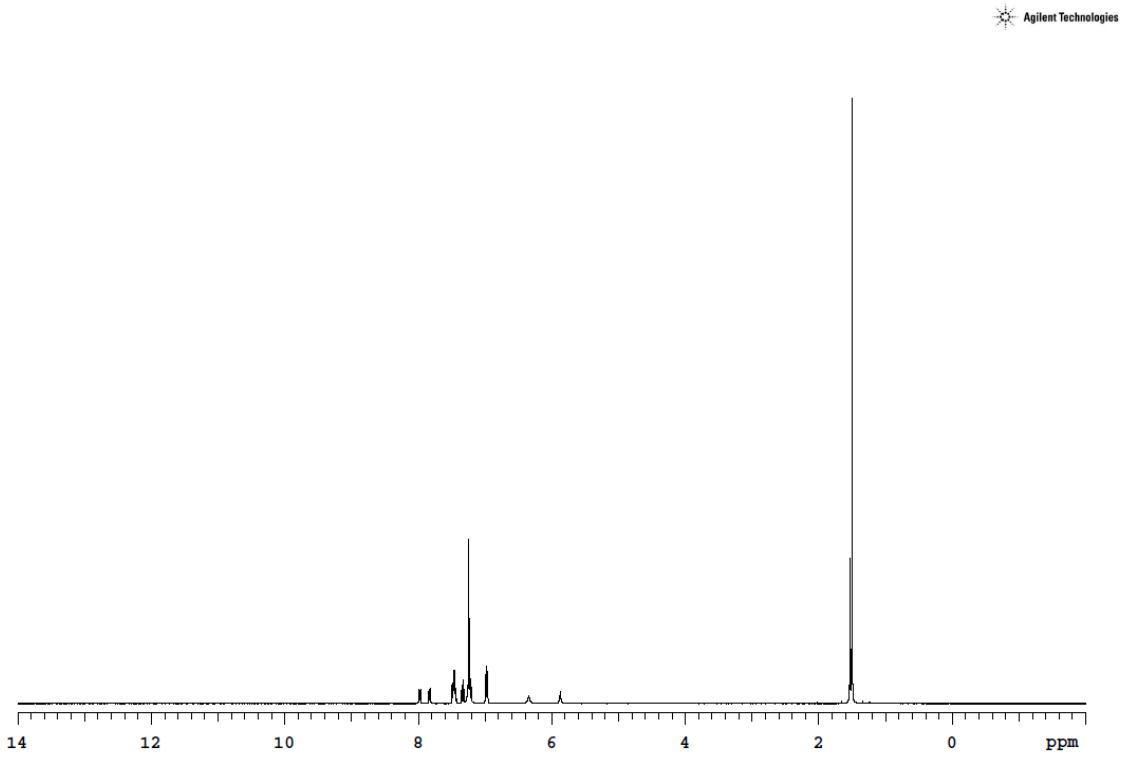

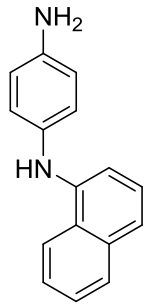

4.19

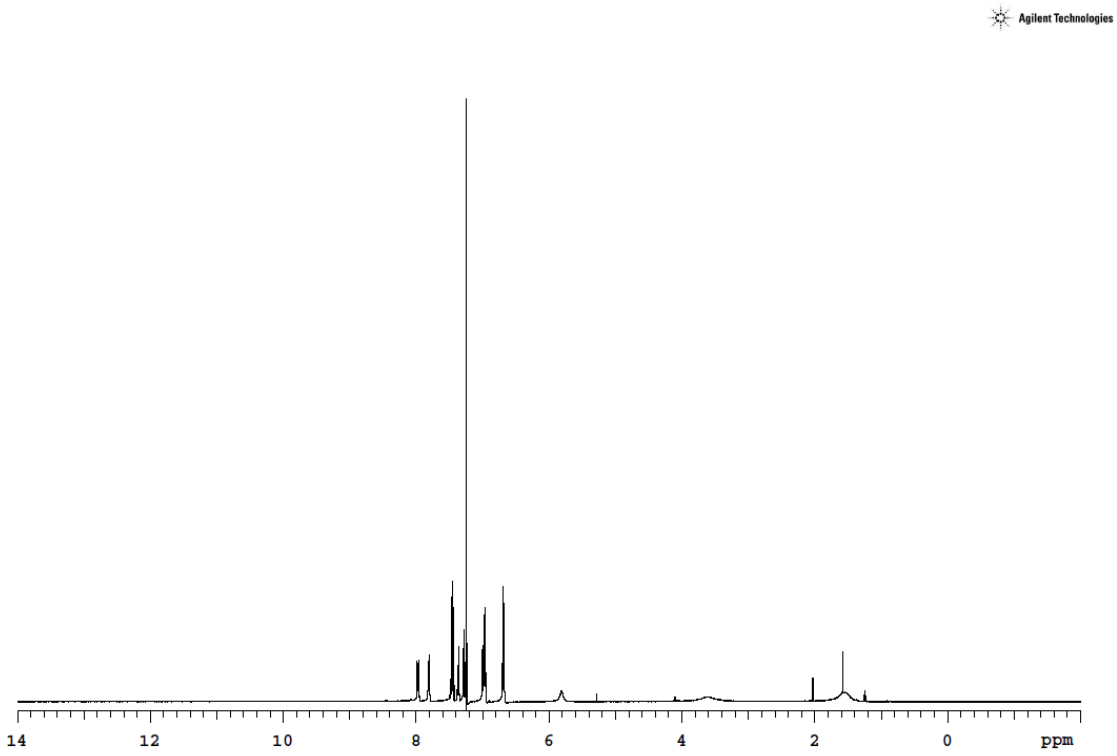

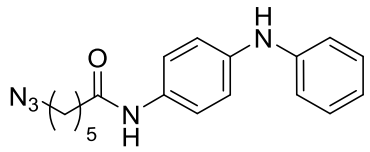

4.20

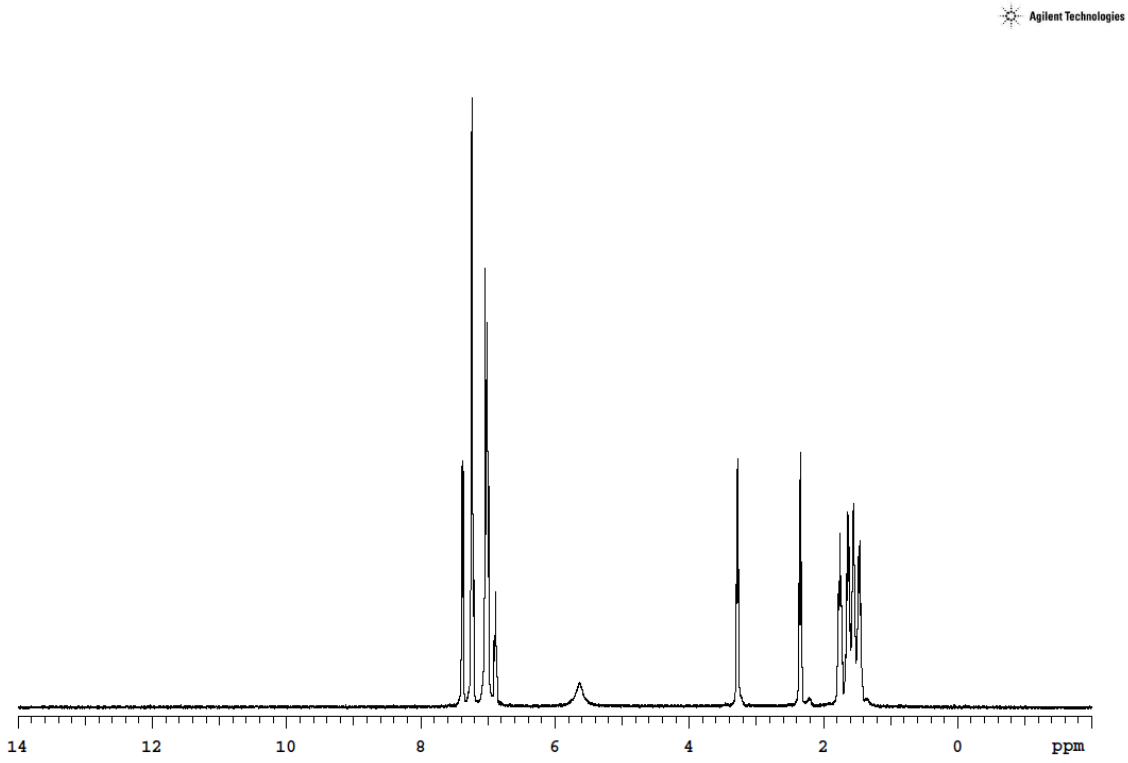

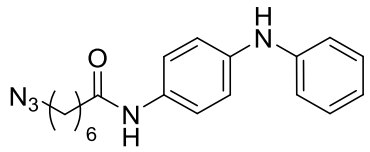

4.21

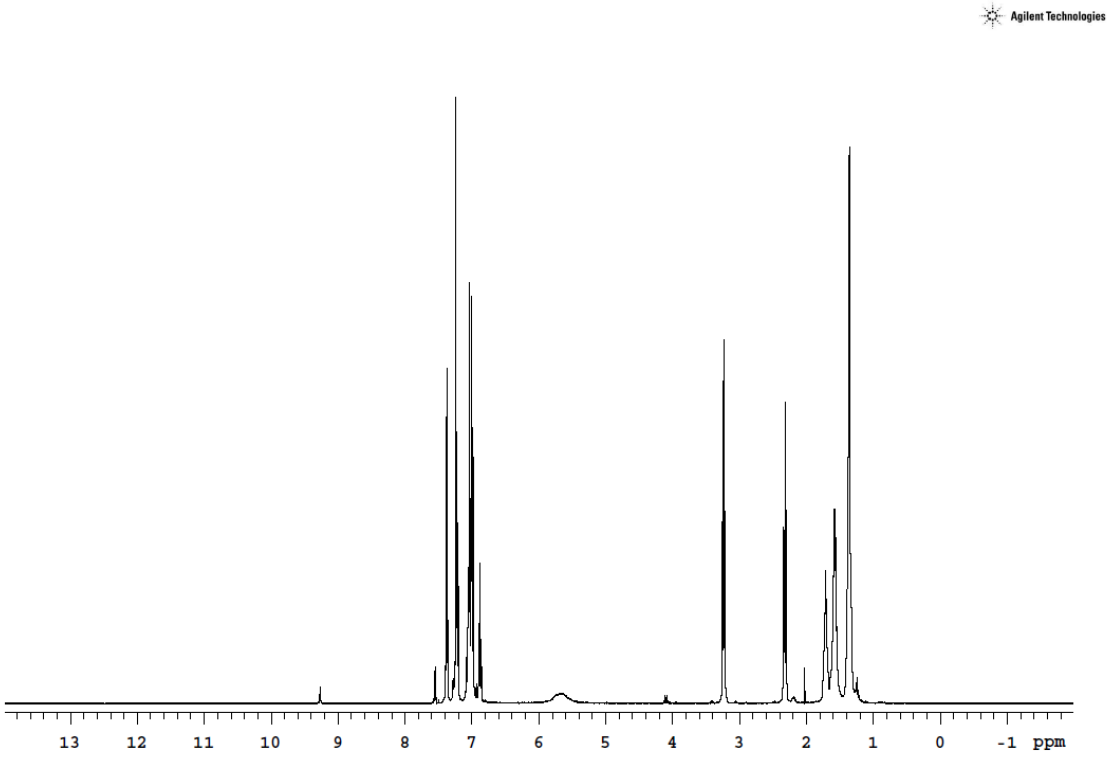

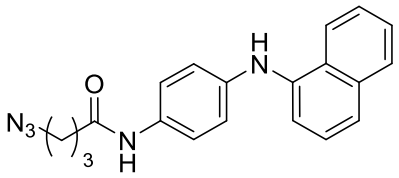

4.22

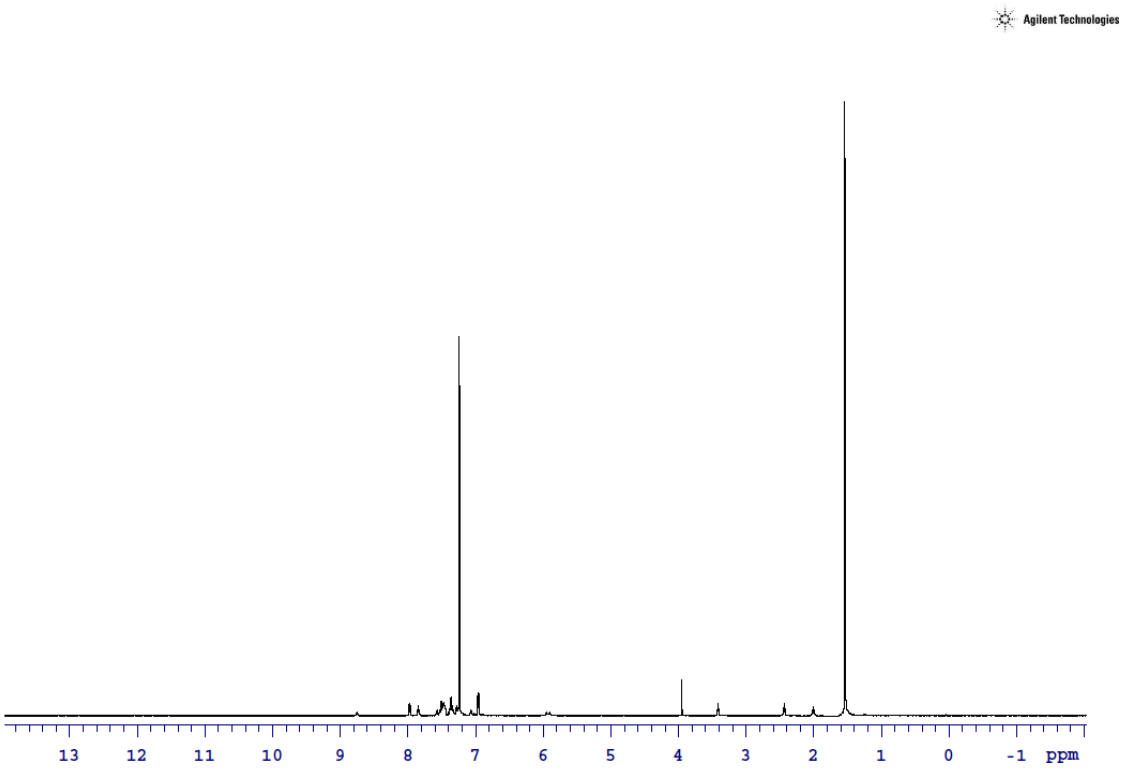

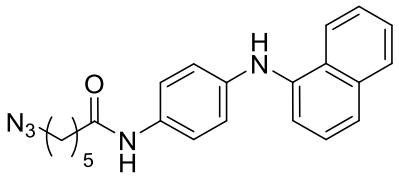

4.23

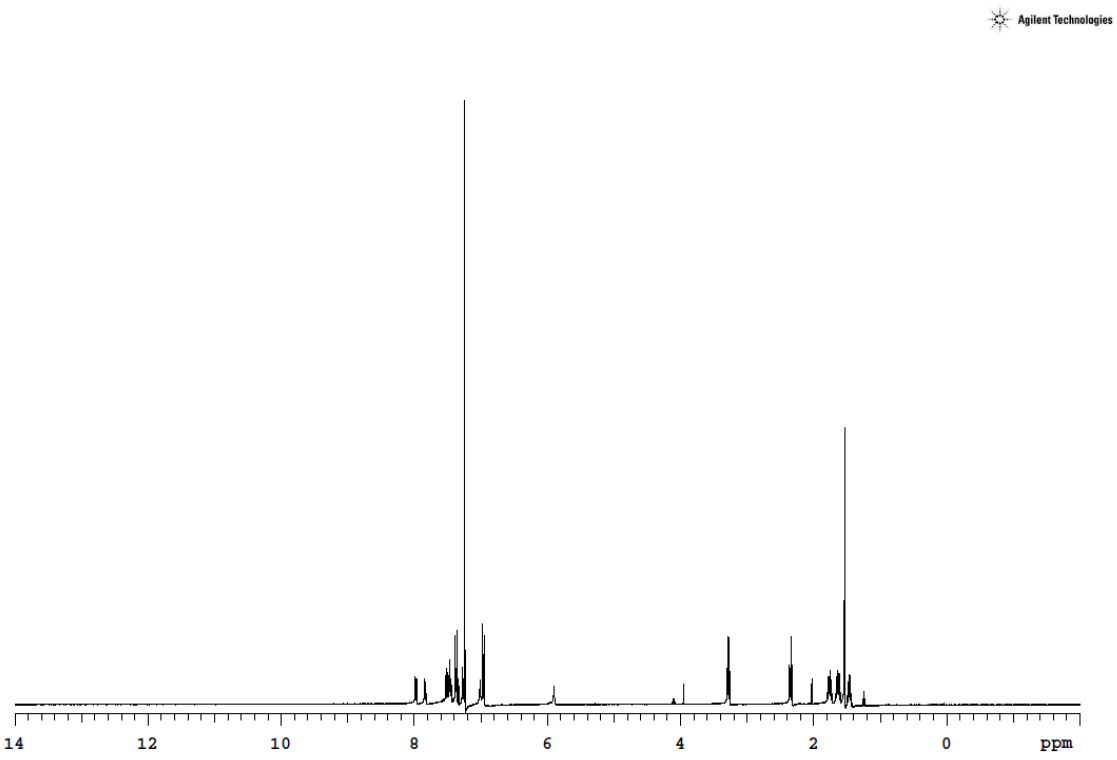

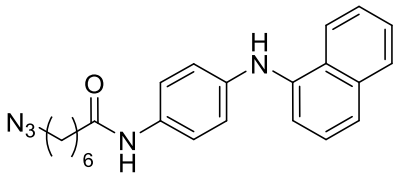

4.24

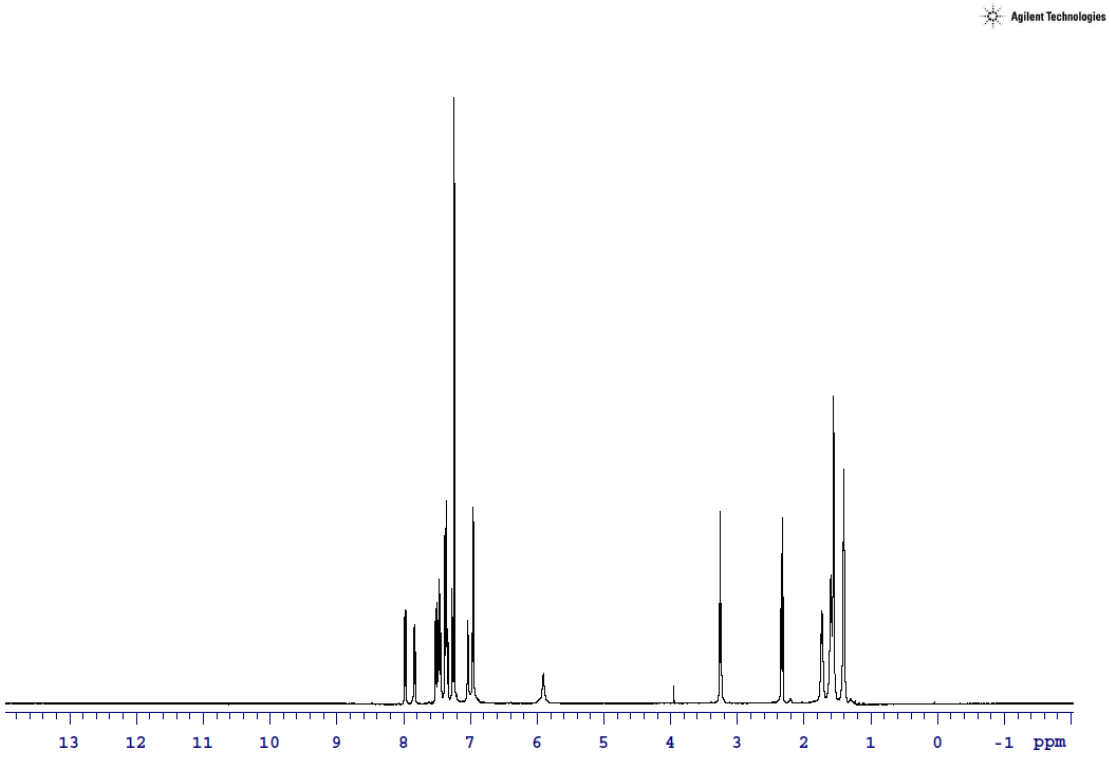

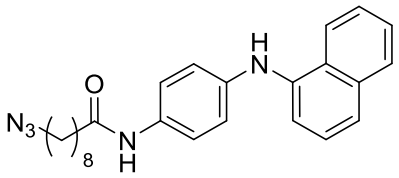

4.25

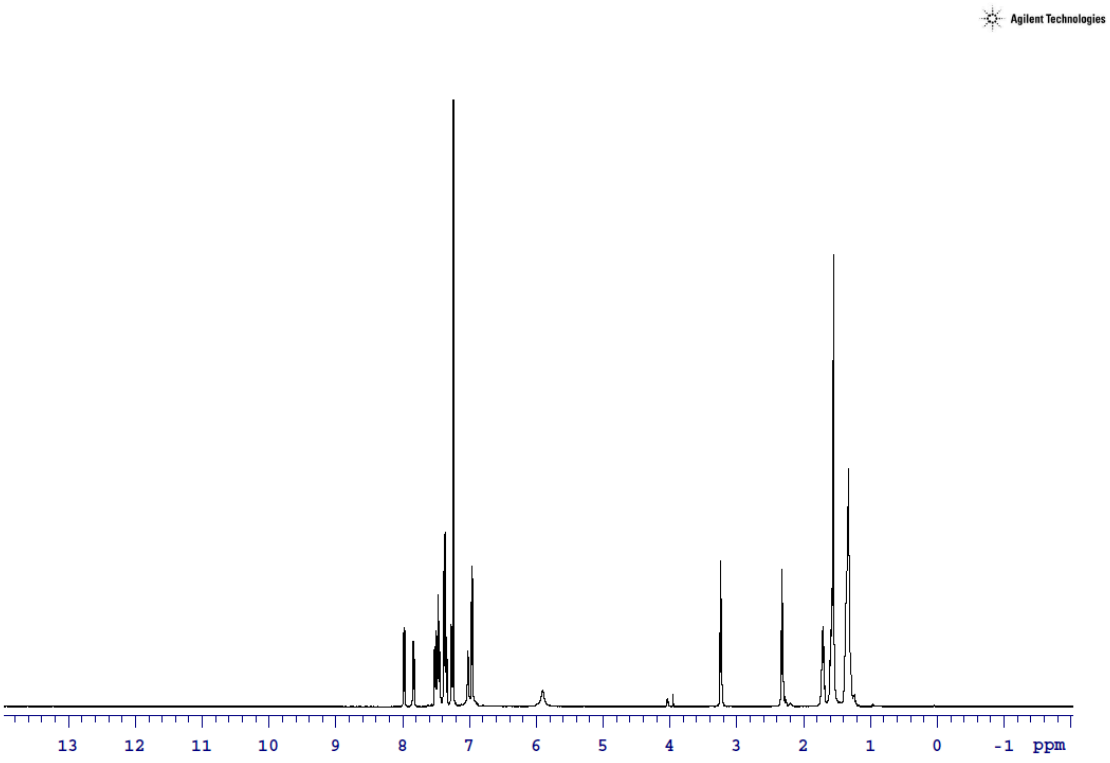

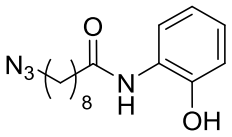

4.26

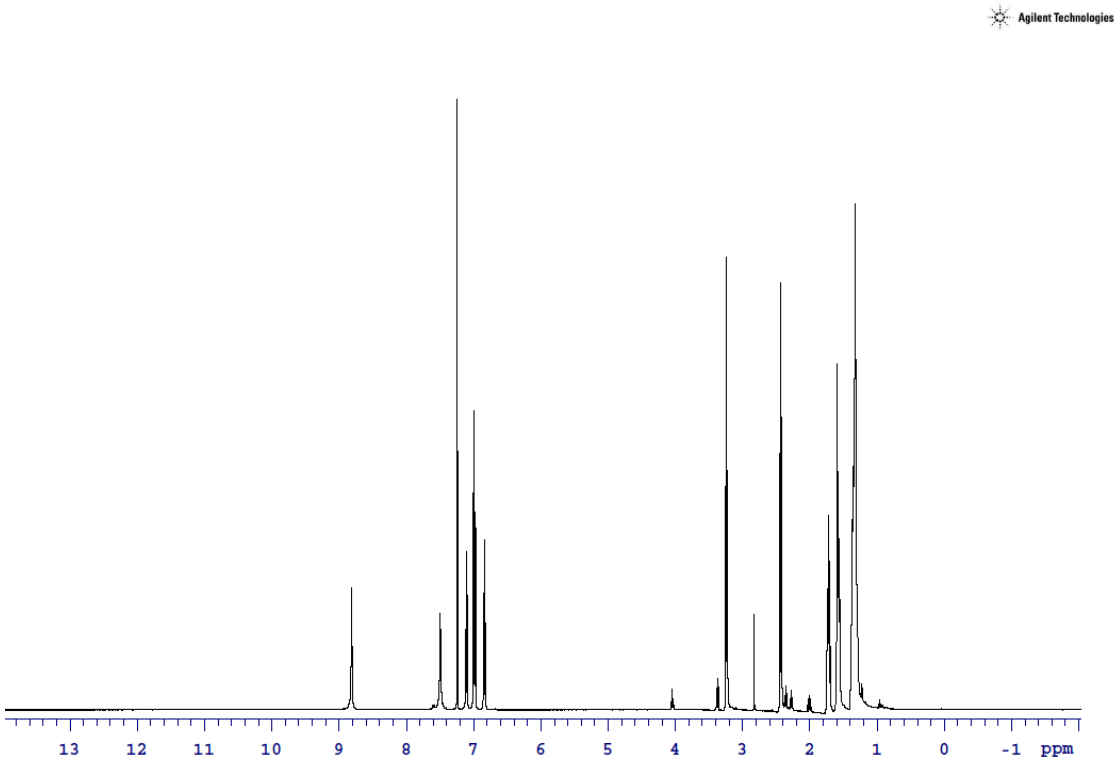

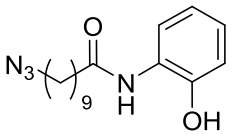

4.27

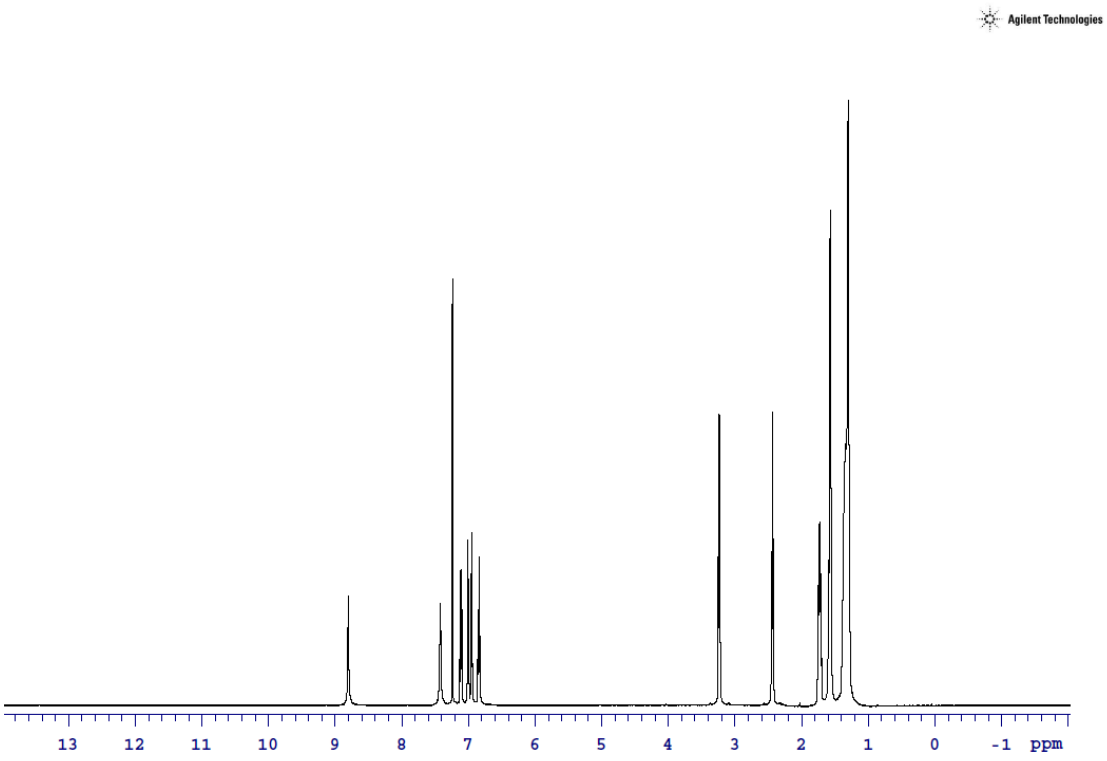

Analytical Data for Determination of IC_{50} for Bisubstrate Inhibitors

4.2 IC_{50} > 250 μM

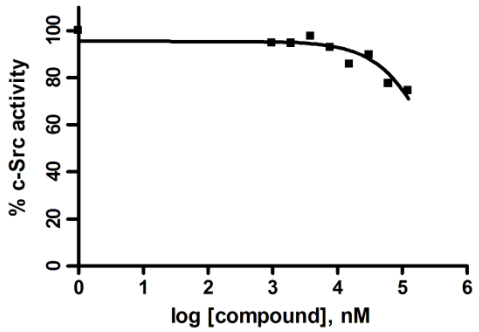

4.3 IC_{50} > 250 μM

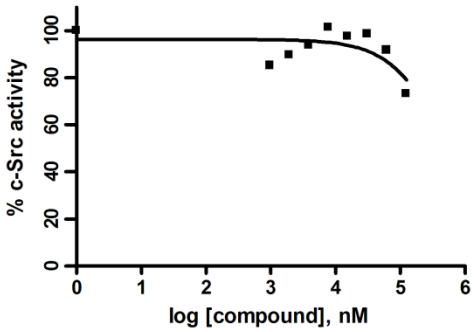

4.4 c-Src IC_{50} = 75 ± 16 μM

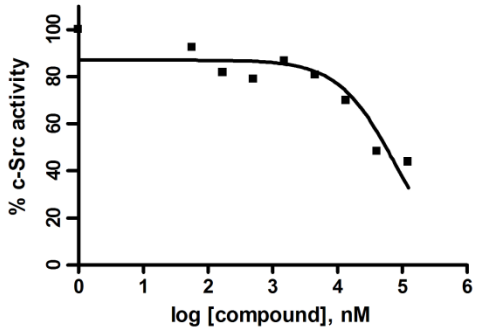

4.5 c-Src IC_{50} > 125 μM

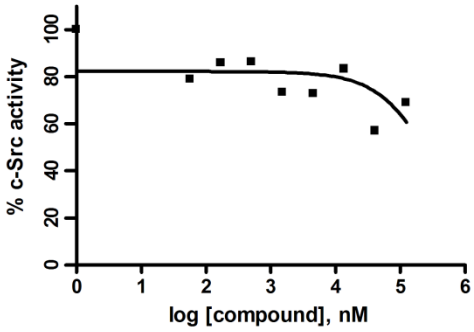

4.6 IC_{50} = 4 ± 2 μM

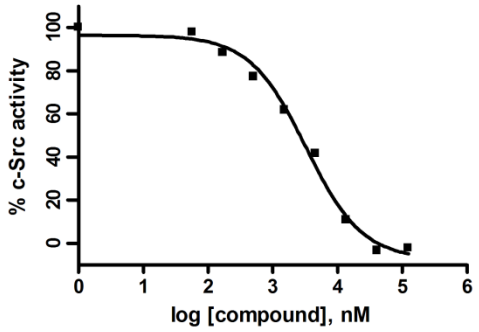

4.7 IC_{50} > 125 μM

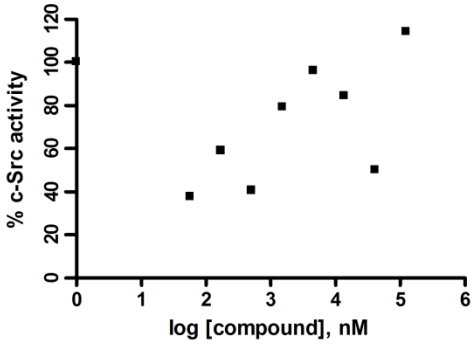

4.8 IC_{50} > 125 μM

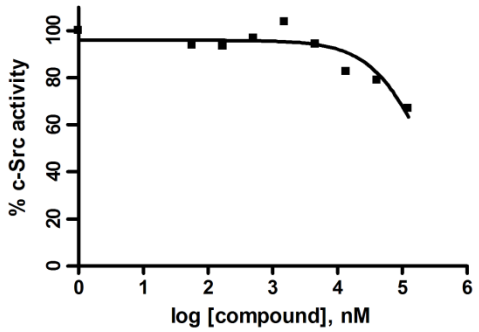

4.9 IC_{50} = 1.1 ± 0.4 μM

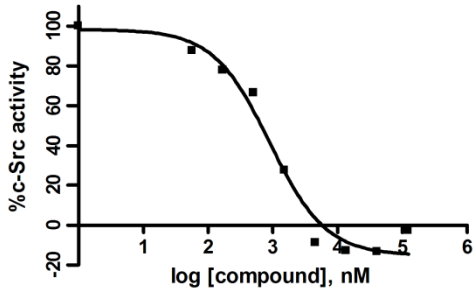

4.10 IC_{50} = 48 ± 14 μM

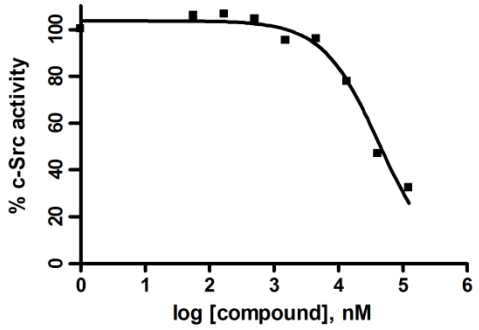

4.11 IC_{50} = 57 ± 8 μM

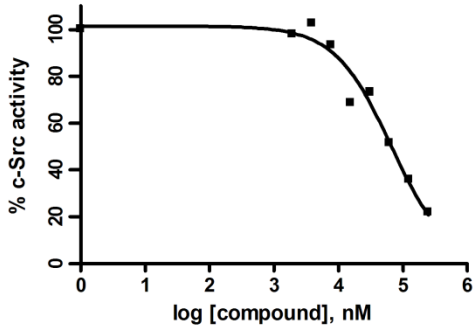

4.12 IC_{50} = 2.0 ± 0.2 μM

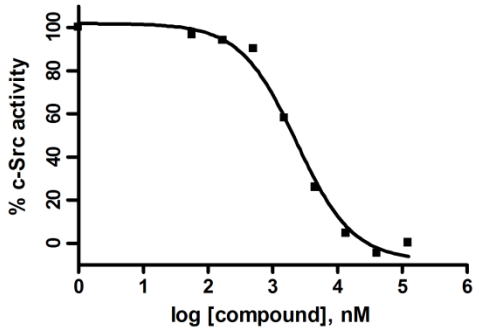

4.13 IC_{50} = 272 ± 53 nM

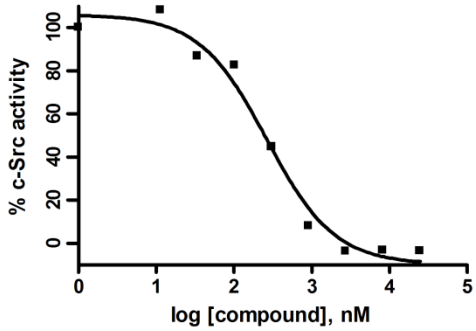

4.14 IC_{50} > 250 μM

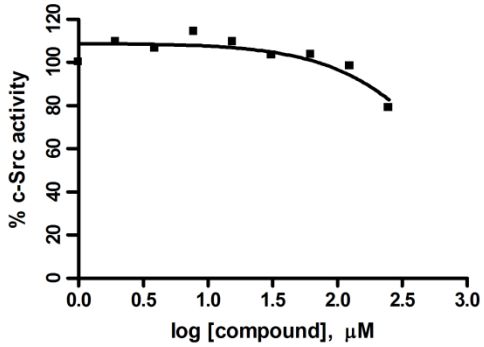

4.15 IC_{50} = 5 ± 2 μM

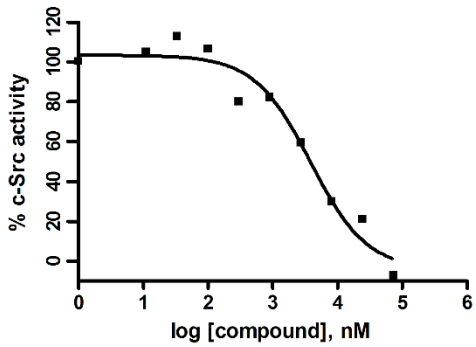

4.16 IC_{50} = 4 ± 1 μM

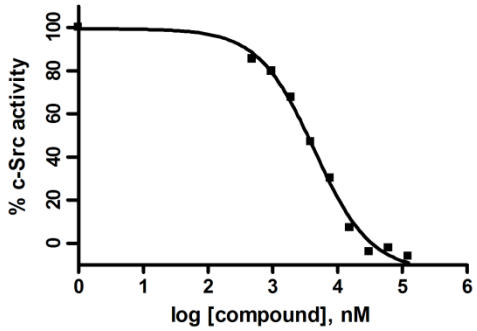

Analytical Data for Determination of IC_{50} for Inhibitors Under High "Substrate 3" Conditions

4.09 IC_{50} = 2.0 ± 0.1 μM

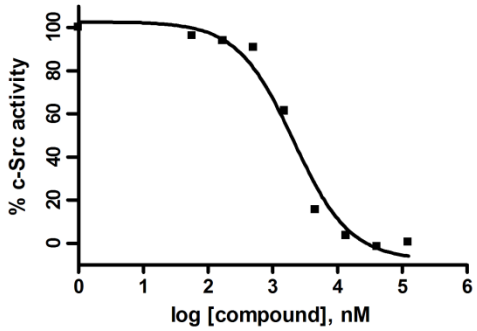
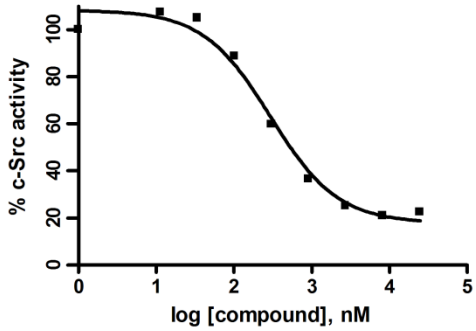
4.13 IC_{50} = 296 ± 1 nM